Development of nanovectors for the targeted drug delivery of antimalarials

Patricia Urbán

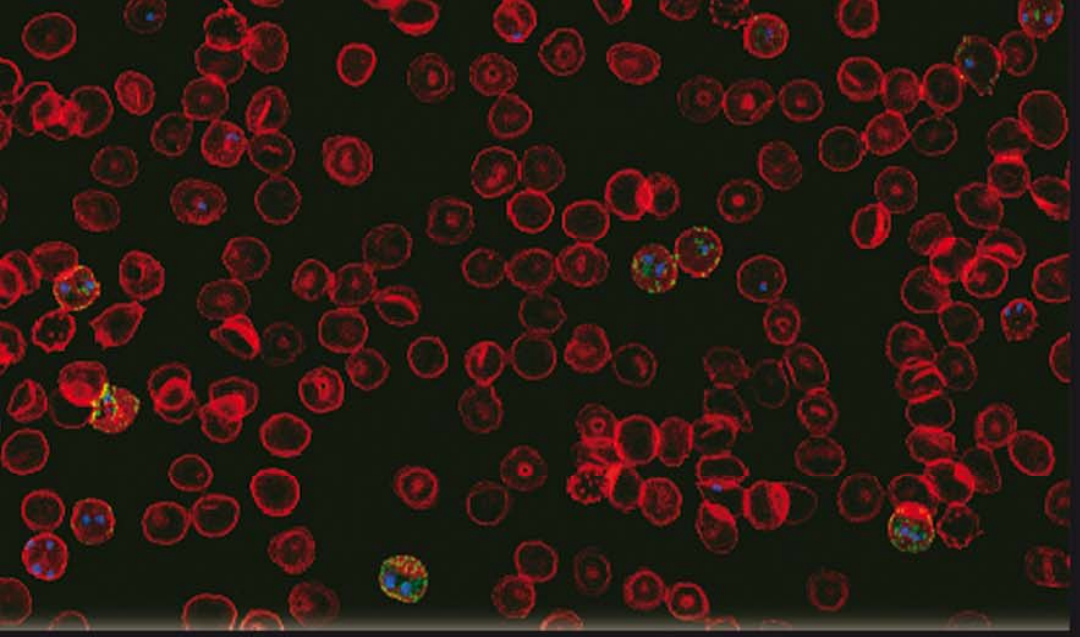

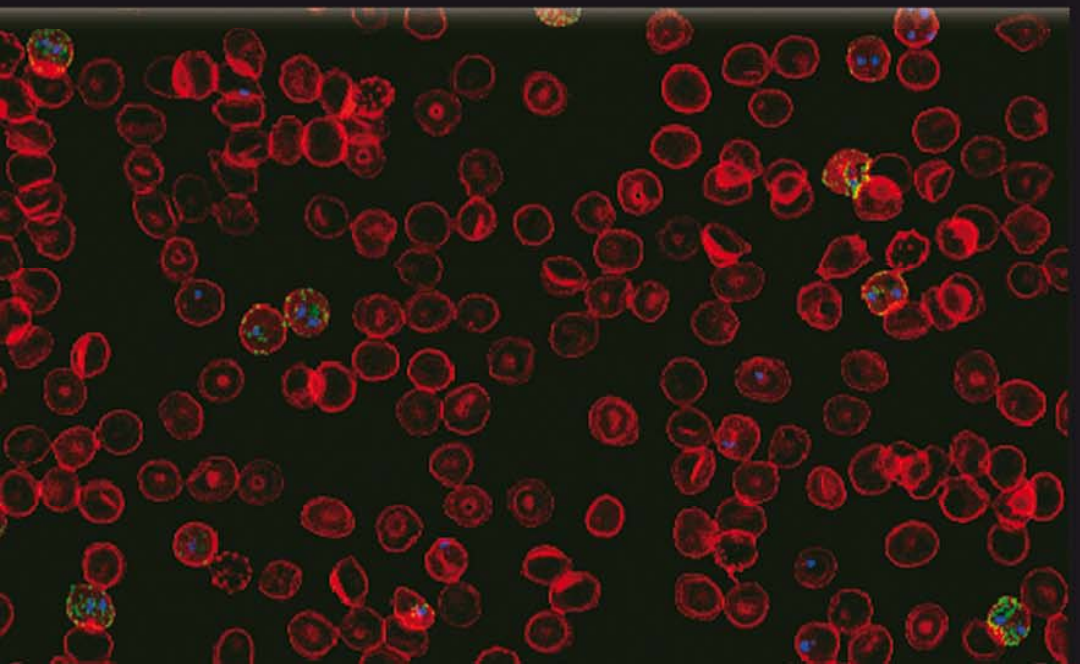

Patricia Urbán

DEVELOPMENT OF NANOVECTORS FOR THE TARGETED DRUG DELIVERY OF ANTIMALARIALS

2012

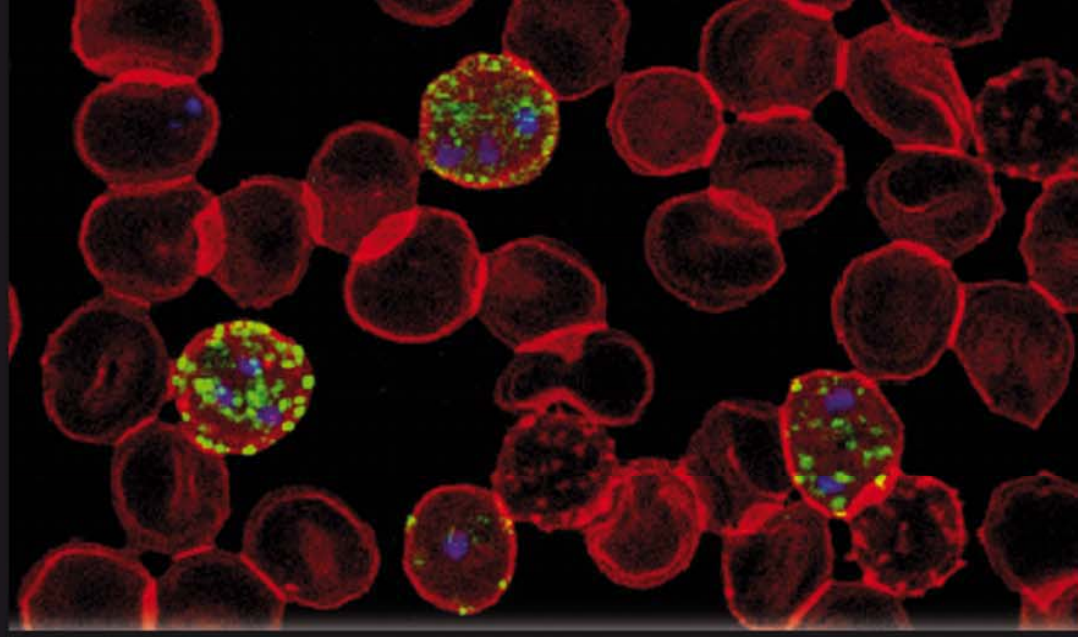

DEVELOPMENT OF NANOVECTORS FOR THE TARGETED DRUG DELIVERY OF ANTIMALARIALS

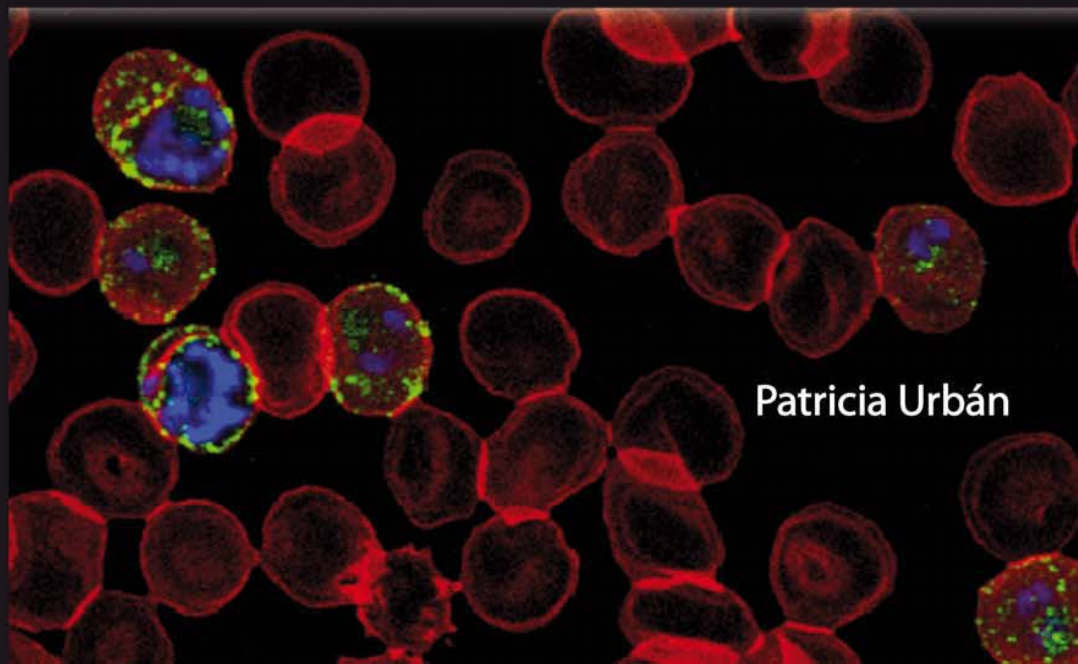

Patricia Urbán

DEVELOPMENT OF NANOVECTORS FOR THE TARGETED DRUG DELIVERY OF ANTIMALARIALS

Patricia Urbán

Departament de Físicoquímica

Facultat de Farmàcia

Universitat de Barcelona

2012

Programa de Doctorado de Biotecnología Molecular
Departament de Físicoquímica, Facultat de Farmàcia
Universitat de Barcelona

DEVELOPMENT OF NANOVECTORS FOR THE TARGETED DRUG DELIVERY OF ANTIMALARIALS

Memoria para optar al título de
Doctor por la Universitat de Barcelona

Los resultados experimentales de esta tesis han sido obtenidos en el Institut de Bioenginyeria de Catalunya y en el Centre de Salut Internacional de Barcelona

Patricia Urbán
Autora

Dr. Xavier Fernàndez-Busquets
Director

Dr. Joan Estelrich Latràs
Co-director

A mi familia,
la española y la italiana.

“Caminante no hay camino,
se hace camino al andar.”
Antonio Machado

TABLE OF CONTENTS

TABLE OF CONTENTS

LIST OF ABBREVIATIONS

ACTs	artemisin-based combination therapies
AFM	atomic force microscopy
AM	artemether
CQ	chloroquine
CS	chondroitin sulfate
DDT	dichloro-diphenyl-trichloroethane
ED	effective dose
G	generational growth
GAGs	glycosaminglycans
G6PD	glucose-6-phosphate dehydrogenase
GSK	GlaxoSmithKline
HMEC-1	human microvascular endothelial cell line
HPLC	high-performance liquid chromatography
HS	heparan sulfate
KAHRP	knob-associated histidine-rich protein
IEC	intraerythrocytic cycle
i.p.	intraperitoneal
i.v.	intravenous
MPA	bis(hydroxymethyl)propionic acid
NPs	nanoparticles
PAA	polyamidoamine (polymers)
PAMAM	polyamidoamine (dendrimers)
PEG	polyethylene glycol
PfEMP1	*P. falciparum* erythrocyte membrane protein 1
PLA	poly lactic acid
PPI	polypropylenimine
PQ	primaquine
pRBCs	*Plasmodium*-infected red blood cells

PV	parasitophorous vacuole
PVM	parasitophorous vacuole membrane
QN	quinine
RBC	red blood cells
RDTs	rapid diagnostic tests
rho	rhodamine
SEM	scanning electron microscopy
SLNs	solid lipid nanoparticles
SMFS	single molecule force spectroscopy
TEM	transmission electron microscopy
WHO	World Health Organization

INTRODUCTION

1. MALARIA

Malaria is a life-threatening infectious disease caused by parasites of the genus *Plasmodium* that are transmitted by infected *Anopheles* mosquitoes. Malaria remains a major cause of morbidity and mortality in tropical and subtropical regions of the world (Figure 1). Increased prevention and control measures have led to a reduction in malaria mortality rates by more than 25% globally since 2000. However, the World Health Organization (WHO) has estimated 216 million episodes of malaria in 2010 that resulted in 655,000 deaths. People living in the poorest countries are the most vulnerable and approximately 91% of malaria deaths were in the African Region, of which 86% were children under 5 years of age[1]. Early diagnosis and treatment of malaria reduce disease, incidence and transmission of the parasite, thus contributing to the reduction of death toll. Access to diagnostic testing and treatment should be seen not only as a component of malaria control but as a fundamental right for all populations at risk.

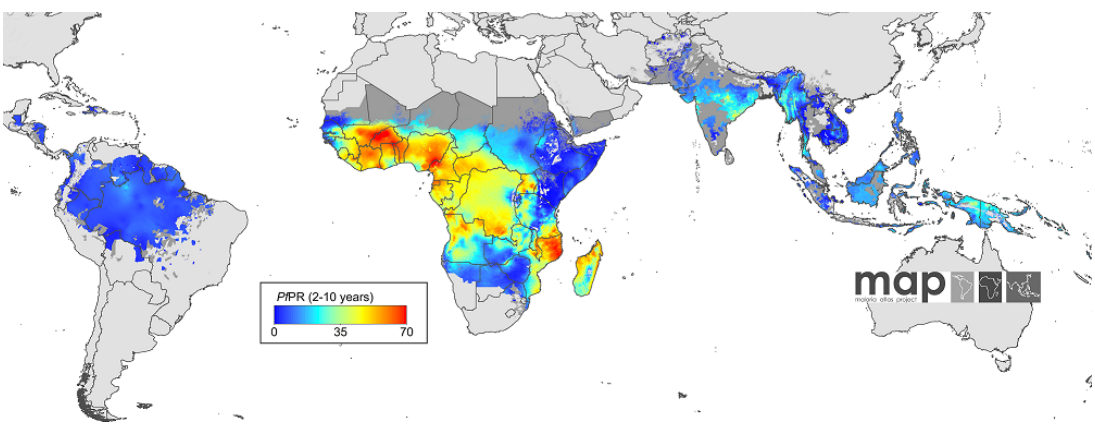

Figure 1. Geographical distribution of *P. falciparum* malaria endemicity, reproduced from[2]. The data mapped are the annual mean *P. falciparum* parasite rate (PfPR), which refers to the proportion of a sampled population that is confirmed positive for malaria parasites, in children between 2 and 10 years of age.

The five *Plasmodium* species affecting humans are: *P. falciparum*, *P. vivax*, *P. ovale*, *P. malariae* and *P. knowlesi. P. falciparum* causes the most deadly and severe cases, and it predominates in Africa. Children, naive adults, primigravid

women and their unborn children are particularly susceptible to *P. falciparum* infection. *P. vivax* produces less severe symptoms but it is more widespread[1], being located mainly in Asia and in South America, and can cause a relapsing form of malaria due to the reactivation of hypnozoites in the liver. Severity caused by *P. vivax* is increasing in some parts of the world and the development of drug resistance could result in an expansion of this debilitating and sometimes deadly infection[3,4]. The other species are found much less frequently, representing only 5% of total malaria cases.

Clinical manifestations of malaria usually appear between 10 and 15 days after the mosquito bite for non-inmune individuals, and consist in a wide range of flu-like symptoms including headache, nausea and cycles of fever. These symptoms are nonspecific and similar to the symptoms of a minor systemic viral illness. Complications of *P. falciparum* malaria may lead to severe malaria that could result in coma (cerebral malaria), metabolic acidosis, severe anaemia, hypoglycaemia, renal failure, acute pulmonary oedema and multi-organ system failure. If not treated, severe malaria is fatal in the majority of cases, and pregnant women are at high risk of dying from complications of this form of the disease. Malaria is also a cause of spontaneous abortion, premature delivery, stillbirth, severe maternal anaemia and low birth-weight babies. In malaria endemic areas, persons may develop partial immunity, allowing asymptomatic infections to occur.

For both *P. vivax* and *P. ovale*, clinical relapses may occur weeks to months after the first infection, even if the patient has left the malarious area. These new episodes arise from dormant liver forms known as hypnozoites (absent in *P. falciparum* and *P. malariae*) and special treatment, targeted at these liver stages[5], is required for a complete cure.

2. *PLASMODIUM FALCIPARUM*

2.1 Cellular structure of *Plasmodium falciparum*

Plasmodia are apicomplexan protists with a complex life cycle in two hosts: an asexual stage that occurs in human liver and red blood cells (RBCs), and a sexual stage in the vector, the female of certain *Anopheles* mosquito species. *Plasmodium* species share many morphological features, although, structural differences exist among them and common and distinct patterns of ultrastructure features are exhibited in the various stages of malaria parasites. In this section, the ultrastructure and main features of the erythrocytic stages of *P. falciparum (*merozoite, ring, trophozoite and schizont stages) will be described[6,7] (Figure 2). Like most apicomplexa, malaria parasites possess a plastid (the apicoplast), which is an evolutionary homologue of the chloroplasts of plant and algal cells. The apicoplast arose by secondary endosymbiosis and is non-photosynthetic but indispensable for the parasite, being involved in the synthesis of lipids and several other essential molecules. It provides an attractive target for antimalarial drug development, particularly in light of the emergence of parasites resistant to chloroquine and other existing antimalarial agents.

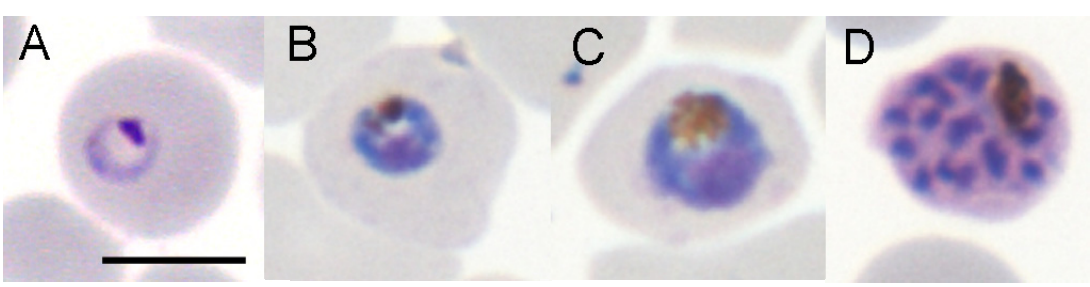

Figure 2 Giemsa staining of *Plasmodium*-infected RBCs at (A) ring, (B) young trophozoite, (C) mature trophozoite and (D) schizont stages. Size bar: 5 µm.

The erythrocytic merozoite has an elliptical shape with about 1.5 μm in length and 1 μm in diameter and despite this size, contains all the equipment needed to escape from its host RBC, find and attach a new one and invade it in order to restart the asexual cycle. It is surrounded by a plasma membrane and two inner membranes, where just beneath are located microtubules which are involved in motility. The nucleus is located at the posterior end of the parasite, ribosomes are abbundant in the cytoplasm and a mitochondrion is situated in the central portion of the merozoite. The apical end of the parasite presents two rhoptries, several micronemes and dense granules, which play an important role in the entry of the parasite in host RBCs and converge onto the apical prominence. The rhoptries are twin pear-shaped densely stained granules that contain a mix of many proteins and micronemes are ellipsoidal organelles which are observed adjacent to the rhoptries. The secretions of both organules might be vital for invasion and rhoptry proteins seem to be incorporated into the invaginating parasitophorous vacuole membrane (PVM), inside which the parasite proliferates, or RBC membrane. After the invasion, dense granules move to the surface of the parasite and release their contents into the parasitophorous vacuole (PV), facilitating the change in shape of the parasite to that of the ring stage.

In the early ring stage (Figure 3), the central region of the parasite is thinner than the peripheral region, which contains the nucleus and other organelles (mitochrondrion, apicoplast, most of the ribosomes and endoplasmic reticulum), giving the cell its characteristic “ring” appearance when smears are stained with Giemsa (Figure 2), although nuclear shape varies, ranging from a sausage-like form to a disc. By the mid-ring stage, (10-15 h post-invasion) the parasite begins endocyting the host cytoplasm via a process of micropinocytosis, creating a small food vacuole within the parasite cytoplasm. In the food vacuole takes place the digestion of hemoglobin and released hematin products are sequestered into a crystalline form, hemozoin, throughout the erythrocytic phase of the life cycle. As the parasite grows, the area of the PVM surrounding it also increases, and the ring eventually changes shape to a trophozoite.

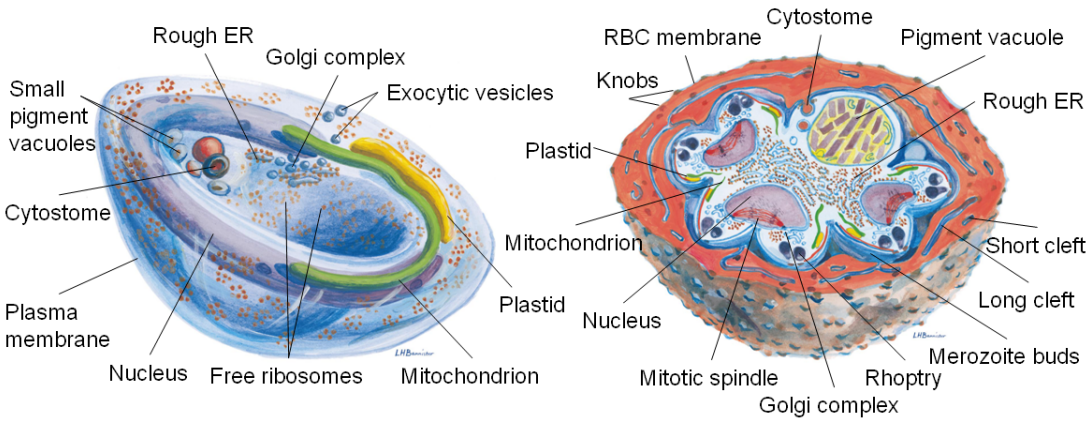

Figure 3. Three-dimensional organization of a *Plasmodium falciparum* early ring stage (left) and late schizont (right), reproduced from[6].

The trophozoite (20-38 h post-invasion) is the metabollically most active stage (Figure 2), and as the parasite matures, it initiates modifications to its host RBC that both facilitate access to nutrients and cause adhesion of the infected RBC (pRBC) to the vascular endothelium. The properties of the RBC membrane are modified by proteins that are secreted from the parasite (including kinases, lipases, adhesins, proteases and chaperon-like proteins) using a complex system of trafficking[8]. As a consequence of malaria infection, the pRBC membrane is less flexible, this fact may contribute to disease severity[9]. The parasite grows its organelles needed for metabolism (nucleus, endomembrane system, mithocondria and apicoplast) and develops novel organelles, including a modified lysosome (digestive vacuole), and a novel system for transporting malaria proteins beyond its own plasma membrane (Maurer's clefts and the tubovesicular complex).

A schizont (38-48h post-invasion) is an intraerythrocytic parasite that is undergoing or has undergone repetitive nuclear division (Figure 2). During this stage cytoplasmic organelles change and reappear merozoite organelles (rhoptries, micronemes and dense granules), that first appear within the schizont cytoplasm (Figure 3). The final stage of the life cycle generates merozoites that are capable of invading new RBCs. Rupture of pRBCs to release merozoites

liberates parasite toxins that are the ultimate cause of the fever and incapacitation associated with malaria. Thus, resident parasites inside pRBCs are the main target for chemotherapeutic approaches[10].

2.2. *Plasmodium* life cycle

Malaria infection (Figure 4) starts when a parasitized female *Anopheles*, during a blood meal, releases sporozoites that migrate through the skin into the circulation and then to the liver. Sporozoites invade hepatocytes in a few minutes, and each parasite will develop and replicate into thousands of new merozoites[11]. These are released into the circulation to infect RBCs, where they will undergo several cycles of asexual replication. Each asexual intraerythrocytic cycle lasts approximately 48 hours (for *P. falciparum*) and is responsible for the clinical symptoms of malaria. Inside RBCs, merozoites develop into ring, trophozoite and schizont stages, replicating to produce from 16 to 32 daughter merozoites that are released during egression. Free merozoites are then able to invade other erythrocytes to perpetuate the asexual blood-stage cycle, leading to an exponential increase in parasitemia. Occasionally, some parasites differentiate into sexual erythrocytic stages, female or male gametocytes that, after a subsequent blood meal, reach the mosquito's midgut. Here, fertilization of gametes occurs forming ookinetes which transform into oocysts from which sporozoites are released and migrate to the mosquito salivary glands to restart the cycle at the next blood meal.

There are several important features of *P. falciparum* biology that make it a successful parasite and contribute to *Plasmodium* survival and transmission within an ever-changing host environment, such as its high asexual multiplication rate, an efficient evasion of host immunity through sequestration in the peripheral circulation, its elevated antigenic variation[12] and the redundancy in erythrocyte invasion pathways. *P. falciparum* invasion involves the interaction of several parasite ligands with receptors that line the RBC surface. The malaria parasite is capable not only of using a number of these receptors but also of varying the

primary route used and adapting to variation in RBC surface receptors and still successfully infect the human host. Despite the substantial impact of this pathogen on human health, much of its basic biology is poorly understood[13]. Whilst each stage of the parasite lifecycle is the subject of intensive research, the centrality of blood stage infection to disease pathology has led to extensive effort towards understanding some of its core biological processes.

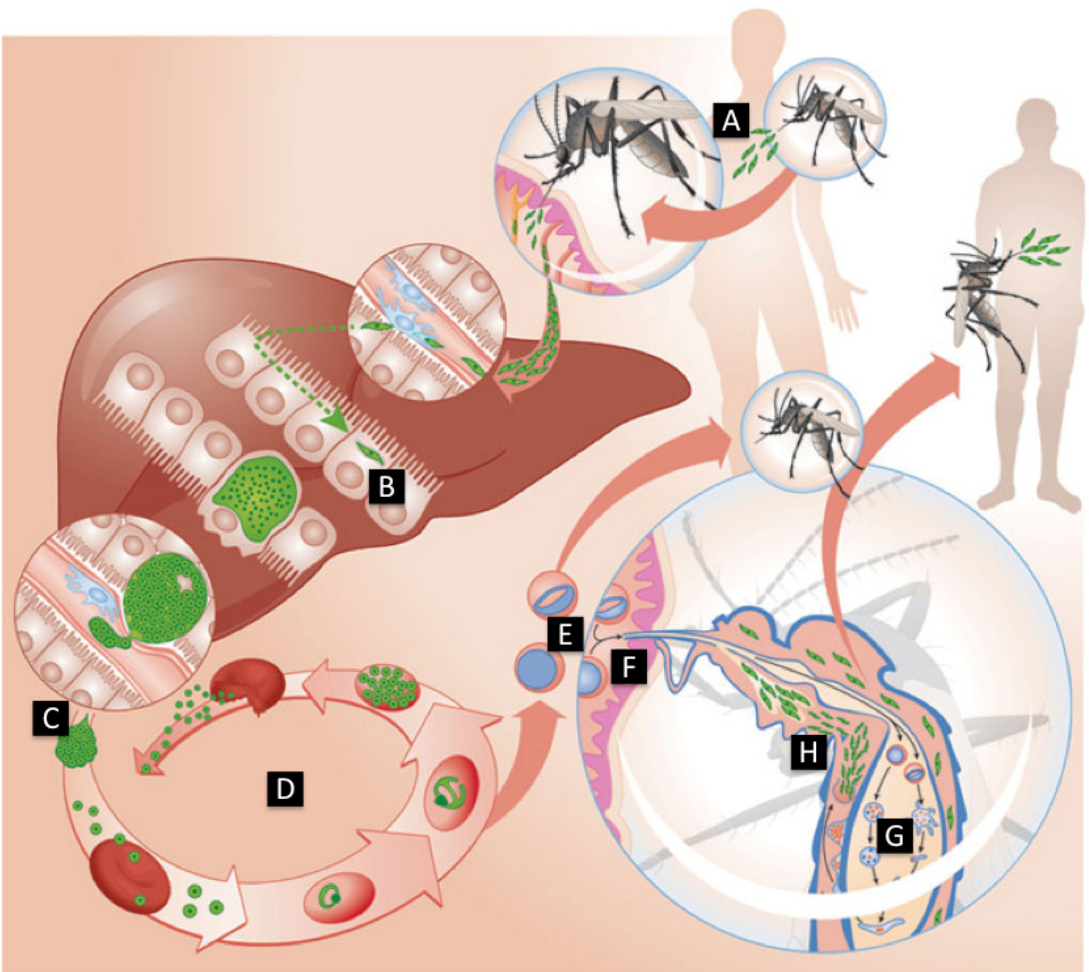

Figure 4. *Plasmodium* life cycle. (A) Injection of sporozoites, (B) migration to the liver, (C) release of merozoites into the bloodstream, (D) invasion of RBCs and asexual replication, (E) generation of gametocytes, (F) ingestion of gametocytes by the mosquito, (G) fertilization of gametes and (H) migration of sporozoites to the salivary glands and release during the next blood meal. Reproduced from[14]

2.3. *Plasmodium*-infected red blood cells

Merozoite invasion is a multistep process that involves the molecular interaction of numerous host receptors and parasite ligands (Figure 5). Parasite molecules implicated in invasion are usually discharged from its apical secretory organelles (micronemes, rhoptries and dense granules). The initial contact between the merozoite and the erythrocyte is a crucial step where the parasite identifies RBCs competent for invasion. Merozoite invasion begins with a low affinity attachment of the parasite to the erythrocyte which is followed by its reorientation to appose its apical end with the erythrocyte membrane. A tight junction involving high-affinity interactions is formed between the parasite and the host membrane. This junction moves from the apical to the posterior end of the merozoite in a complex series of events by the action of its actin-myosin motor[15].

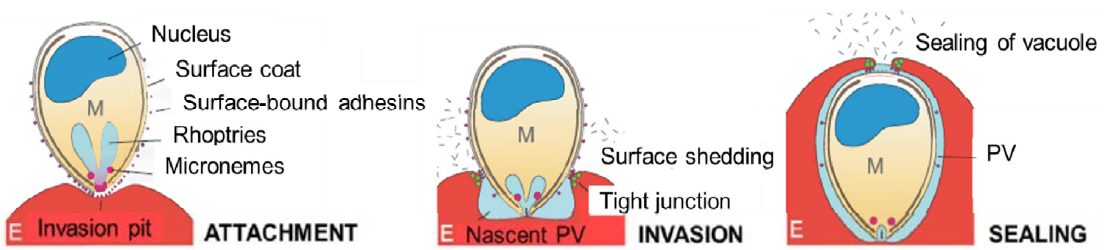

Figure 5. Merozoite invasion of RBCs, modified from[16].

During the invasion process, the parasite creates the parasitophorous vacuole inside which it proliferates[16]. The PVM, which remains closely associated with the parasite plasma membrane, is composed of lipids that are derived from both the erythrocyte and the merozoite. The entire process is completed in less than a minute.

Once inside a human RBC the parasite immediately begins remodelling the host cell, particularly its membrane and cytoskeleton, in order to meet its needs for growth and multiplication. These modifications are directed at solving two problems: membrane transport processes and evasion from the immune system of the host. Although hemoglobin provides a source of protein building blocks,

Plasmodium has evolved a machinery for the obtainment of other nutrients as well as for the detoxification of hemoglobin breakdown products[17]. Hemoglobin digestion releases toxic free heme-derived products, which are metabolized into innocuous hemozoin crystals, which can be easily observed under the microscope.

The RBC is unable to process and present antigens, so it can provide protection from the host's immune system. However, the intraerythrocytic parasite needs to avoid passage through the spleen where resident macrophages recognize and remove RBCs with altered deformability. Mature stage parasites avoid spleen clearance by promoting adhesion of the pRBCs to the vascular endothelium, or sequestration, through knob-like protusions of the host membrane (Figure 6). Knobs are formed by self association of the knob-associated histidin-rich protein and act as platforms for presentation of the major adhesion protein on the RBC membrane, *P. falciparum* erythrocyte membrane protein 1 (PfEMP1). Effective presentation of adhesins is needed for parasite virulence, and knobs are found in all field strains of the parasite. PfEMP1 also mediates a process called rosetting, the attachment of uninfected RBCs to parasitized erythrocytes, via an interaction with several different receptors on uninfected erythrocytes, a phenotype that may be associated with severe malaria[18,19].

Plasmodium has acquired the ability to vary the proteins exported to the host cell membrane by switching expression between members of a multigene family. An individual parasite expresses only a single form of PfEMP1 at a time, with simultaneous silencing of all other family members[20,21]. PfEMP1 is also a key antigenic molecule, being exposed to the host immune system which readily makes antibodies against it. Before an infection has been successfully cleared, a subpopulation emerges that has switched to express a distinct PfEMP1 that is no longer recognized by host immunity[22]. Rifins and rosettins, which are parasite-derived proteins from the surface of pRBCs, are also clonally antigenically variable[9]. This antigenic variation leads to waves of parasitemia and persistent infections despite antibody-mediated immune pressure in non-naive individuals[23].

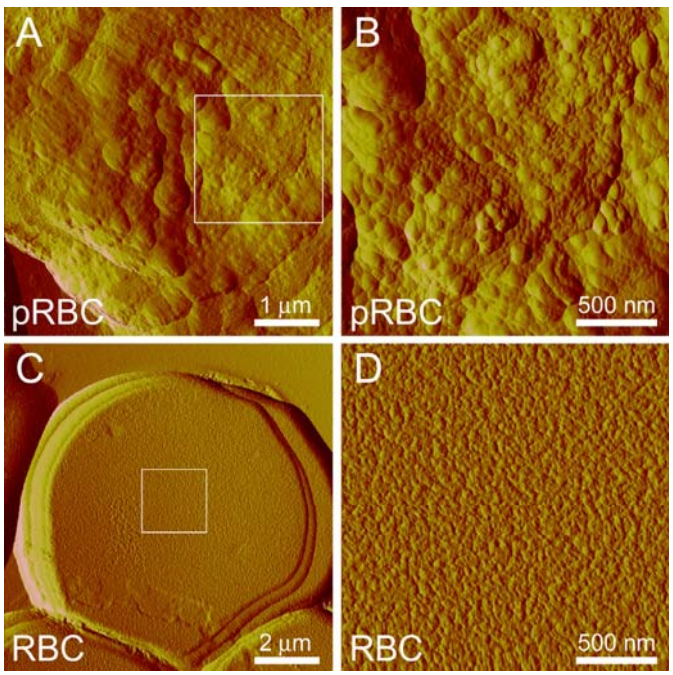

Figure 6. High resolution images of infected and non-infected red blood cells[24]. AFM images of a pRBC (A, B) and a RBC (C, D). B) and D) are magnified images of the square areas framed in A) and C), respectively. The small round bumps in A) and B) correspond to knobs on the pRBC membrane which are not present on the smoother RBC membrane (C, D).

3. FIGHTING AGAINST MALARIA

Currently, three major tools are used to fight malaria: control of mosquitoes and reduction of human-vector contact, vaccines, and drugs for the prevention and treatment of the disease.

3.1. Malaria control, elimination and eradication

Malaria control[25] is an organised attempt to prevent malaria mortality and to reduce morbidity to a locally acceptable level using the preventive and curative tools available today in endemic countries through the progressive improvement and strengthening of local and national capabilities. Control relies on effective

prevention and case management; prevention with vector control interventions aims at reducing transmission and thus decrease the incidence and prevalence of parasite infection and clinical malaria. Early and effective case management of malaria will shorten its duration and restrict complications and most deaths from malaria and by scaling up appropriate interventions for all populations at risk and then sustaining control over time until proceeding to elimination, control can be achieved.

Elimination[26] aims at reducing to zero all locally-acquired infections in a specific geographic area through deliberate efforts, which is epidemiologically feasible in more settings than previously thought, specifically in areas of unstable transmission, where over a billion people are at risk of malaria infection. Some countries are currently engaging in elimination and more will soon reach this phase. However, in high transmission settings complete interruption of malaria transmission will require additional, new control tools.

Eradication, or reducing the global incidence of malaria to zero with continued measures in place to prevent re-establishment of transmission, is the long-term goal that will be achieved through progressive elimination where feasible. The malaria eradication strategy is based on three principles[27]:

1. Elimination of infection and transmission in areas of low or moderate endemicity, primarily in countries “at the margins” of heavy transmission areas, with *P.falciparum* elimination as a priority.
2. Aggressive control in the areas with high transmission.
3. Research and development to improve existing diagnosis tools. New, better and safer drugs, vector control and personal protection tools, immunological (vaccine) interventions and new delivery mechanisms will be needed to progressively eliminate malaria and maintain a malaria-free status in each country until global elimination is achieved.

Progress in shrinking the geographical range of endemic malaria has been remarkable. Since the WHO-led Global Malaria Eradication Campaign was started in 1955 with the aim of worldwide malaria eradication, 79 countries have eliminated malaria and the proportion of the world's population living in malaria-endemic countries has decreased more than 50%[28]. Sub-Saharan Africa was not included in the first global programmes due to its intensity of transmission and its poor healh infrastructure. Dichloro-diphenyl-trichloroethane (DDT) was used as an effective and safe insecticide, chloroquine and quinine were administered for treatment and prevention, and primaquine was being introduced to prevent relapses[26]. Efforts were gradually abandoned from 1969 to 1976 due to the realization that the objective of malaria eradication was unlikely to be easily achieved. Although large areas of the world were successful in controlling the disease, this was not the case for many developing countries. The resistance of the vector to DDT and the evolution of *P. falciparum* strains insensitive to chloroquine severely impaired the WHO program[29].

During the late 1970s and early 1980s the strategy was more focused on control in high transmission areas, since the priority was reduction of malaria mortality in young children with an adequate treatment. In the 1990s malaria research and control strategies were accelerated[30] trough the creation of several research and public health coalitions, such as the Multilateral Initiative on Malaria, the Global Fund to Fight AIDS, Tuberculosis and Malaria, The U.S. President's Malaria Initiative and the Roll Back Malaria partnership, which should serve as a model for developing consensus on elimination.

Malaria pathophysiology is too complex and the disease is too widespread to be fought with a single weapon. However, it is generally accepted that to achieve a reasonable level of success against malaria, a well-designed attack will be necessary using a combination of strategies, which include the improvement of existing weapons and the development of new ones[31], whereas drug therapy remains the mainstay of treatment and prevention of this disease[32]. Of particular interest are drugs suitable for mass administration that can be delivered in a single

encounter at infrequent intervals, and that result in radical cure of all parasite stages (the so-called SERCAP: Single Encounter Radical Cure And Prophylaxis).

3.2. Vector control

The most effective vector control strategies in use nowadays rely on insecticide interventions like indoor residual insecticide sprays and long-lasting insecticide-treated nets that reduce vector daily survival rates[33]. In malaria-endemic regions these tools can make substantial contributions to malaria control and may be sufficient for local malaria elimination, unless high rates of transmission occur[34].

The massive use of DDT in the 1940s brought a radical change in malaria control strategies since it appeared to be effective everywhere and required only semestral or annual applications. However, its widespread application led to the first appearance of mosquito strains resistant to DDT ten years later[35]. In the last decade, the emergence of resistance to common classes of insecticides in populations of *Anopheles* has been reported in many African countries. Current methods of malaria control are highly dependent on a single class of chemicals, the pyrethroids, which are the only insecticides currently used on treated nets and are the most predominant in indoor residual insecticide sprays in terms of spray area covered. Unfortunately, resistance to them has already been reported in many countries[36].

Because of the large number of vector species and the potential resistance mechanisms, choosing the correct vector control strategy is a complex problem[34]. New vector control strategies will be needed in the short- and mid-term as the current tools will be inadequate for malaria eradication in most settings.

3.3. Vaccines

The global agenda for malaria eradication would benefit from the development of a vaccine that protects against disease and interrupts transmission of *Plasmodium*[37]. However, the extraordinary antigenic variability and complex life cycle of the malaria parasite, and the possibility that *Plasmodium* develops resistance, complicate the obtention of a permanent malaria vaccine reaching 100% efficacy.

There are two major findings that support the feasibility of a malaria vaccine. First, radiation-attenuated sporozoites, which must remain "viable" and capable of invading hepatocytes, have been proved to induce protection against malaria pre-erythrocytic stages, although this protective immunity lasts only several months[38]. Second, after many years of exposure in malaria endemic areas, indivuals develop naturally acquired immunity. Host age plays a determinant role in this protection against clinical manifestations of the disease[39], since it is known that after a brief period of apparently uniform heavy exposure among age groups, adults are resistant to infection, while children remain susceptible[40].

Attempts to develop a malaria vaccine[41] began more than 50 years ago, with some promising results[42,43], such as the candidate vaccine developed by Manuel Patarroyo in Colombia, Spf66. Nevertheless, a lack of consistency with other trials[44], the failure to prevent malaria in infants[45], and difficulties in product availability and reproducibility halted further development of this vaccine[46,47]. The most succesful vaccine in development is RTS,S, which is directed against the sporozoite and has attained around 40% efficacy[48] being currently in Phase III clinical trials. Although this vaccine has a partially protective effect against malaria, it is not likely to significantly impact on transmission, and new improved versions will be needed that contain other antigens from different stages of the parasite lifecycle to improve its efficacy and longevity.

However, to achieve a highly effective vaccine that impacts on transmission in all life stages, antigens from pre-erythrocytic, erythrocytic, sexual and mosquito stages may have to be combined into a single target multi-component vaccine[37]. If eradication is to be achieved, malaria vaccine development effort will need to target other malaria parasite species, especially *P.vivax*, where novel vaccines could have enormous impact[49]. The availability of a good vaccine, if administered in combination with other complementary strategies, could play a critical role in the eradication of the disease.

3.4. Treatment of malaria

Accurate diagnosis of malaria is part of an effective disease management[50], and it is usually based on clinical suspicion and on the detection of parasites in the blood (parasitological or confirmatory diagnosis). Because the symptoms of malaria are nonspecific, diagnosis based on clinical features alone might not be accurate and could result in over-treatment. Clinical suspicion of malaria should be confirmed with a parasitological diagnosis: microscopical observation and rapid diagnostic tests, the latter detecting parasite-specific antigens or enzymes and in some cases having a certain ability to differentiate species. PCR has been recently adapted and used for the detection of low levels of strain-specific parasites, although its use is very limited in resource-poor settings.

3.4.1. Antimalarial drugs

Effective malaria chemotherapy aims at treatment of the patient combined with blocking the infectivity of the parasite for the vector by exploiting the differences in metabolism between *Plasmodium* and the host. The therapeutic efficacy of the drugs is limited by factors which include parasite resistance and unespecific drug toxicity[51,52]. Current antimalarial drugs can be classified according to their biological activity (Figure 7) or their chemical structure[53]. Antimalarials ranked by the stages of the life cycle which are targeted by the drug include: blood schizontocides, tissue schizontocides, hypnozoitocides, gametocytocides and sporontocides[53].

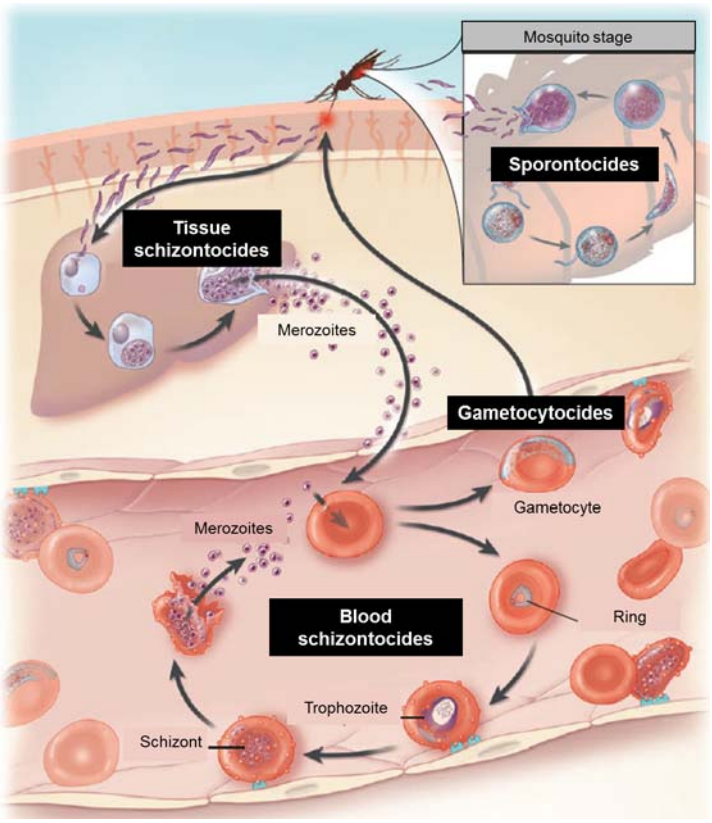

Figure 7. Antimalarial drug activity in the life cycle of *Plasmodium*, showing tissue schizontocides, blood-stage schizontocides, gametocytocides and sporontocides. Modified from[54,55].

1. **Blood schizontocides:** Drugs acting on blood stages of the parasite, inhibiting the growth inside RBCs and terminating clinical attacks of malaria. Drugs belonging to this class can have a quick mode of action: chloroquine, quinine, mefloquine, halofantrine, artemisinin and its derivatives, or a slow mode of action: pyrimethamine, sulfadoxine, sulfones, tetracyclines and atovaquone[50].
2. **Tissue schizontocides for casual prophylaxis:** These drugs act on the primary tissue forms of *Plasmodium* in the liver. By blocking liver stages, further development of the infection can be prevented. However, since no symptoms are presented yet at this stage of the infection, this therapy is not used. Primaquine, pyrimethamine, proguanil and sulfonamides have activity against this stage.

3. **Hypnozoiticides:** Drugs acting on hypnozoites from *P. vivax* and *P. ovale,* which remain latent in the liver. Primaquine is the only available drug for this stage.
4. **Gametocytocides:** These drugs kill the sexual forms of the parasite in the blood, preventing transmission of the infection to the mosquito. Chloroquine and quinine have gametocytocidal activity against *P. vivax* and *P. malariae*, but not against *P. falciparum*. Primaquine and artemisinins have gametocytocidal activity against all human malarial parasite species.
5. **Sporontocides:** Drugs that prevent the development of oocysts in the mosquito, blocking malaria transmission. Primaquine and chloroguanidine have activity against this stage.

Antimalarials can be also classified according to their chemical structure and mechanism of action in different groups: quinine-related drugs, artemisinin and its derivatives, antifolates and other antimalarials[32,50,56].

A. QUININE-RELATED DRUGS

Quinine (QN), an alkaloid derived from the bark of the cinchona tree*,* was the first successful antimalarial used, originally discovered by South American natives and appearing in European therapeutics in the 17th century. It remained the drug of choice until the 1940s, when other drugs with less adverse side effects replaced it. Quinine is still used to treat the disease in certain critical circumstances, such as severe malaria, and in impoverished regions due to its low cost. QN acts as a blood schizontocide against all human malarial parasite species and is gametocytocidal for *P. vivax* and *P. malariae*. It has been proposed that QN prevents the fusion of haemoglobin shuttling vesicles to the food vacuole[57]. Resistance to QN is rare, but some cases have been reported[50].

Chloroquine (CQ) has been the gold standard for the treatment of malaria in the last half century due to its efficacy, low toxicity, and affordability (less than US $0.2 for a three-day adult treatment course). This 4-aminoquinoline acts as a rapid

schizontocide, however, studies indicate adverse effects on kidney[58], cardiovascular system[59,60] and the retina[61]. The mechanism of action of CQ is based on the inhibition of detoxification of toxic heme products by the parasite[62,63]. CQ enters and accumulates in the food vacuole, where it forms a complex with heme (product of hemoglobin digestion), disrupts membrane function, and inhibits the formation of hemozoin, causing the parasite to be poisoned by its own metabolic products[64]. First reports of *P. falciparum* CQ resistance appeared in the 1950s[65,66] and nowadays widespread resistance has rendered it useless against *P. falciparum* infections in most parts of the world, although it still maintains considerable efficacy for the treatment of *P. vivax*, *P. ovale* and *P. malariae* infections. As a prophylactic agent, chloroquine can only be administered as monotherapy in areas where no resistance has been reported.

Primaquine (PQ) is an 8-aminoquinoline that is effective against intrahepatic forms of all malaria parasite species[67], although its mechanism of action is unknown. It is used to provide radical cure of *P. vivax* and *P. ovale* malaria, in combination with a blood schizontocide for the erythrocytic parasites[68]. PQ is also gametocytocidal against *P. falciparum* and has significant activity against *P. vivax* blood stages (and some against asexual stages of *P. falciparum*). In patients with glucose-6-phosphate dehydrogenase (G6PD) deficiency PQ generally produces a hemolysis which may be severe[69,70]. Such toxicological concerns have led to restrictions in the use of primaquine since the incidence of G6PD genetic anomaly is particularly high in areas where malaria is endemic[71].

Mefloquine is a blood schizontocide for *P. falciparum* and *P. vivax* but has no effect on the hepatic forms of the parasite. Mefloquine is used in combination with sulphadoxine/pyrimethamine or artemisinin derivatives as the reference drug for treating chloroquine-resistant malaria[72]. It has a long half-life, which makes it not recommended in areas with high malaria transmission in order to avoid the appearance of parasite resistance. Unfortunately, it suffers from a plethora of side effects[73,74] (headache, palpitations, vertigo, anxiety, hallucinations, insomnia) and cannot be administered in the first trimester of pregnancy[75].

B. ARTEMISININ AND ITS DERIVATIVES

Artemisinin is a sesquiterpene lactone extracted from the leaves of *Artemisia annua* that has been used in China for the treatment of fever for over a thousand years. It is a potent and rapidly acting blood schizontocide and is active against all *Plasmodium* species. It has an unusually broad activity against asexual parasites, killing all stages from young rings to schizonts[53]. In *P. falciparum* malaria, artemisinin also kills the gametocytes, which are otherwise sensitive only to primaquine. Artemisinin and its derivatives are safe and remarkably well tolerated[76], having largely given way to the more potent **dihydroartemisinin** (the active metabolite) and its derivatives, **artemether** (AM), **arteether**, **artemotil** and **artesunate**, which have a better bioavailability[77].

There is no consensus regarding the mechanism through which artemisinin derivatives kill the parasites[78]. Several lines of evidence indicate that they inhibit an essential calcium adenosine triphosphatase, PfATPase 6, exerting their antimalarial action by perturbing redox homeostasis[79]. Other works indicate that their activity depends on the cleavage of a crucial peroxide bond after contact with Fe^{2+}-heme inside the food vacuole, generating free radicals that can alkylate the heme molecule and thus the detoxification of free heme may be inhibited[80]. A more recently described alternative is that artemisinins can disrupt cellular redox circulation[81].

Currently, the most effective treatment for malaria are artemisinin-based combination terapies (ACTs)[82], which decrease the risk of inducing resistance. Because of their short plasma half-life, the artemisinins are combined with other antimalarial drugs with longer plasma half-lives, such as mefloquine. Other ACT's are artesunate with amodiaquine, artemether with lumefantrine and dihydroartemisinin in combination with piperaquine[83]. Unfortunately, recent alarming reports observed the emergence of artemisinin resistant parasites in Southeast Asia, which could derail the current elimination efforts[84].

C. ANTIFOLATES

Antifolates interfere with folate metabolism, which is essential for parasite survival, via inhibition of the enzymes dihydrofolate reductase[85] and dihydropteroate synthase[86]. Both humans and parasites can convert folic acid to tretrahydrofolic acid, which has a key role in the biosynthesis of thymine, purine nucleotides and several amino acids (methionine, glycine, serine, glutamic acid and histidine). The basis of antifolates selective toxicity resides in the fact that humans obtain folic acid from the diet, but parasites can not use exogeneously supplied folic acid and have to synthesize it. Antifolates attack all growth stages of the malaria parasite, and are found to inhibit the early stages in the liver and infective stages in the mosquito, since the folate pathway is essential for the biosynthesis of DNA[87,88].

There are two types of antifolates, type I and II:

Type I antifolates, such as **sulfones** and **sulfonamides** inhibit dihydropteroate synthase since they are structural analogues and competitive antagonists of p-aminobenzoic acid[89]. Treatment with sulfadoxine should be discontinued in any patient developing a rash because of the risk of severe allergic reactions, and other undesiderable effects have been described[90].

Type II antifolates, such as **pyrimethamine** and **proguanil** inhibit dihydrofolate reductase, indirectly blocking the synthesis of purines and some aminoacids.

Because antifolates have on *Plasmodium* a slower-acting effect and a longer half-life than quinolines, they are used in combination: pyrimethamine-sulfadoxine (FANSIDAR®), chloroguanil-dapsone (LAPDAP®) and clhoroguanil-atovaquone (MALARONE®). Antifolates are cheap, have the advantage of single dose therapy and have been widely used, although their activity has been lost in most parts of the world due to the development of resistance[56,87].

D. OTHER ANTIMALARIALS

Atovaquone is a hydroxynaphthoquinone antiparasitic drug active against all *Plasmodium* species. It also inhibits pre-erythrocytic development in the liver, and oocyst development in the mosquito[91]. Atovaquone is a structural analogous of

coenzime Q, thus interfering with cytochrome electron transport[92] and affecting the parasite membrane and nucleic acid synthesis. Atovaquone is comercialized as MEPRON® (GlaxoSmithKline), is well tolerated and effective, but because when used as monotherapy resistance emerges quickly it is usually coformulated with chloroguanil (MALARONE®)[87,91].

Some **antibiotics** have also been used as antimalarials. Most of them act on the apicoplast organelle, which shares similarities with procariotic cells[87].

Tetracyclines[93] and their derivatives (doxycycline) are inhibitors of aminoacyl-tRNA binding during protein synthesis. They have a broad range of uses, including treatment of some bacterial infections: *Chlamydia, Rickettsia, Mycoplasma,* Lyme disease, *Brucella*, tularaemia, plague and cholera. All the tetracyclines have similar adverse effects, among which gastrointestinal alterations, such as nausea, vomiting and diarrhoea, are common. Doxycycline has been assayed alone[94,95], and in combination with chloroquine[96].

Clindamycin inhibits the early stages of protein synthesis by a mechanism similar to that of the macrolides. It is used for the treatment of anaerobic and Gram-positive bacterial infections, babesiosis, toxoplasmosis and *Pneumocystis carinii* pneumonia[97]. Diarrhoea occurs in 2–20% of patients, and in some cases pseudomembranous colitis and other potentially fatal gastrointestinal effects may be developed.

Fosmidomycin is a structural analogue of 2-C-methyl-D-erythrose 4-phosphate, which specifically inhibits 1-deoxy-D-xylulose-5-phosphate reductoisomerase, a key enzyme in the non-mevalonate pathway of isoprenoid biosynthesis, which is not present in humans, and takes place in the apicoplast of the parasite. The discovery of the non-mevalonate pathway in malaria parasites has opened the use of fosmidomycin and other inhibitors of this metabolic route as antimalarial drugs[98]. Since this pathway of isoprenoid biosynthesis has not been extensively used yet as target to treat malaria, it is expected that the parasites do not show

significant resistance to inhibitors of its enzymes. Fosmidomycin is well tolerated and effective, but late recrudescence preclude its use as monotherapy. Fosmidomycin has been tested with favorable results in combination with clindamycin for treatment of uncomplicated malaria[99].

3.4.2. Drug resistance

Resistance in malaria parasites is caused by random genetic mutations that confer reduced susceptibility to antimalarial drugs. Drugs that target a single enzyme can lose their activity by a single mutation in a gene, the so-called monogenic resistance. Mutations are spontaneous and rare, but once present are subjected to the process of selection, which occurs when a parasite population containing a resistant mutant is exposed to a concentration of drug sufficient to kill the susceptible but not the resistant parasites, so that mutants will be selected and transmitted[100].

The ideal pharmacokinetic profile of an antimalarial drug would comprise a rapid achievement of drug levels above the minimal inhibitory concentration, maintenance of such drug levels until all parasites from the initial infection have been killed and then the rapid fall of drug levels to sub-selective concentrations.

The emergence of parasite resistance depends on multiple factors[101], including:

- Mutation rate of the parasite. Higher mutation rates are advantageous for the adaptation to changing environments and enable a faster appearance of resistance. However, they can also lead to deleterious mutations.
- Fitness costs associated with the resistance mutations, since the advantage acquired is balanced by the biological cost from the altered function of the mutated protein.
- Overall parasite load. High parasitemias lead to a faster elimination of deleterious mutations and enhance the selection of compensatory mutations[102].

- Strength of drug selection, which decreases the prevalence of competing sensitive parasites.
- Treatment compliance. Sub-optimal drug concentrations, due to improper dosing, poor pharmacokinetics properties or infections acquired during the elimination phase increase the possibility for drug-tolerant parasites to arise, which is an intermediate stage to full resistance[103].
- Endemicity, since the efficacy of chemotherapy will increase in places where the population demonstrates a potent immune response for malaria and, as a result, the opportunity for manifestation and spread of resistant strains will decrease.

Widespread and indiscriminate use of antimalarials exerts a strong selective pressure on malaria parasites to develop high levels of resistance. Resistance can be prevented, or its onset slowed considerably, by combining antimalarials with different mechanisms of action and ensuring very high cure rates through full adherence to a correct dose regimen. Massive worldwide use of chloroquine, beginning in the late 1940s, was followed fifteen years later by the first reports of CQ-resistant strains of *P. falciparum*. At that time, the alternative to CQ was sulfadoxine-pyrimethamine, which encountered resistant parasites one year after implementation[101]. Today, CQ resistance has spread to the vast majority of malaria-endemic areas, limiting its usefulness.

Resistance to antimalarials has been documented for *P. falciparum, P. malariae* and *P. vivax*. In *P. falciparum*, resistance has been observed in all currently used antimalarials and it is a major threat to malaria control[104,105,106,107]. To decrease the emergency of resistance, almost all antimalarials are administered in combination therapy, with each drug targeting different mechanisms within the parasite. The appearance and spread of drug resistance does not only lead to an increase in treatment failures and mortalities, it also increases the costs associated with treatment and control of malaria[108].

3.4.3. WHO guidelines for the treatment of malaria

The main determinant in antimalarial treatment policy is the therapeutic efficacy of the antimalarial medicines in use. WHO recommends[50] ACTs for the treatment of uncomplicated *P. falciparum* malaria, where no signs of vital organ dysfunction are present. Artemether plus lumefantrine, artesunate plus amodiaquine, artesunate plus mefloquine, artesunate plus sulfadoxine-pyrimethamine and dihydroartemisinin plus piperaquine are ACT options for first-line treatment of uncomplicated *P. falciparum* malaria worldwide during at least 3 days of treatment. Anti-relapse treatment with PQ should only be given to cases with confirmed diagnosis of *P. vivax* or *P. ovale* malaria, and in the absence of contraindications such as G6PD deficiency. For severe malaria it is essential that effective, parenteral (or rectal) antimalarial treatment in full doses is given promptly. For the parenteral treatment of severe malaria, artemisinin derivatives (preferentially artesunate, but also artemether and artemotil) and quinine are given. Parenteral chloroquine is no longer recommended for the treatment of severe malaria, because of widespread resistance.

The current recommended duration of follow-up is a minimum of 28 days for all antimalarial medicines, while it is extended for longer periods of time depending on elimination half-life (42 days for combinations with mefloquine and piperaquine)[50]. Slowly eliminated antimalarials provide the additional benefit of suppressing malaria infections that are newly acquired during the period in which residual antimalarial drug levels persist in the body. On the other hand, these residual drug levels do provide a selection pressure for resistance. In these treatment recommendations, the curative efficacy of the antimalarials has taken precedence over the provision of a period of prophylaxis.

3.4.4. Need for better drug delivery strategies

At present, administration methods of antimalarial drugs release the free compound in the blood stream, from where it can be significantly removed by many tissues and organs before entering pRBCs. Due to this lack of specificity regarding target cells, current oral or intravenous delivery approaches for most antimalarial drugs require multiple doses. However, reduced specificity of toxic drugs demands low concentrations to minimize undesirable side-effects, thus incurring the risk of sublethal doses favouring the appearance of resistant parasite strains. Targeted delivery systems can fulfill the objective of achieving the intake of total doses sufficiently low to be innocuous for the patient but that locally are high enough to be lethal for the malaria parasite due to an increased bioavailability and selectivity of the drugs.

There is a pressing need for new therapeutic strategies against malaria because the disease has to be fought from different fronts and the currently available treatments will not guarantee its eradication. Thus, the future of malaria control also requires efficacious drugs[32] acting on adequate therapeutic targets[109] and the development of effective targeted drug delivery strategies for new malaria therapeutics[78].

4. NANOTECHNOLOGY AND NANOMEDICINE

4.1. Nanotechnology

Nanotechnology encompasses a wide range of techniques and methods for manipulating and using structures on the nanometre scale. One of the aims of nanotechnology is the development of new materials and functional devices by controlling their size and shape[110].

The different methods used in nanotechnology for the production of nanomaterials can be classified in two broad classes: bottom-up and top-down.

- In the bottom-up approach, atoms or molecules are used as building blocks for the realization of bigger structures. This category includes, among others, chemical self-assembly, sol-gel processing, chemical vapour deposition, plasma or flame spraying synthesis, laser pyrolysis and atomic or molecular condensation[111].
- The top-down approach consists in starting from larger pieces of material, i.e. bulk materials or bigger molecules, and producing the intended structure by mechanical or chemical methods. Top-down methods for example include photo-lithography, e-beam lithography, machining, etching and milling[111].

Nowadays nanotechnology allows producing a wide range of different materials, such as nanotubes, nanowires, nanoparticles and nanostructured surfaces, which have applications in many fields because of their unique properties. Nanomaterials may have higher strength, lighter weight, increased control of light spectrum, high surface area to volume ratio and greater chemical reactivity than their larger-scale counterparts, and they are similar in scale to biologic molecules and systems[112]. Such properties arise from two effects. First, the smaller a nanoparticle, the larger proportion of its atoms are on the

surface, which therefore dominates the particle's chemistry and physics. Second, electrons in smaller spaces can change properties such as the color of the light they emit and their chemical reactivity[113]. Gold, for example, is inert in bulk but becomes reactive at the nanoscale.

Nanotechnology is one of the most rapidly evolving areas of science, and in the last decade it has catapulted from being a relatively small field to a world scientific and industrial enterprise. Since biological function depends heavily on units that have nanoscale dimensions, nanodevices at the nanoscale are small enough to interact directly with these units, leading to the development of new biological technologies (e.g., drug delivery systems, imaging probes).

On the other hand, nanotechnology raises many of the same issues as any new technology, including concerns about the toxicity and environmental impact of novel nanomaterials. Toxicity may vary with nanoparticle size, and it could increase on an expanded timescale when eventual protecting biocoatings are removed once inside the cell. Nanotoxicology is an embryonic field and the dynamics and *in vivo* toxicity of nanomaterials are not well known at this time[114]. An improved understanding of the toxicological implications of nanomaterials is needed due to the enormous prospects for the application of nanotechnology in medicine. Regulatory authority guidelines must be developed quickly to ensure safe and reliable transfer of new advances in nanotechnology from laboratory to bedside[115].

4.2. Nanomedicine

Nanomedicine is the application of nanotechnology to medicine, which is defined by The European Science Foundation[115] in the following way:
"*Nanomedicine uses nano-sized tools for the diagnosis, prevention and treatment of disease and to gain increased understanding of the complex underlying patho-physiology of disease. The ultimate goal is improved quality-of-life"*.

Three main areas can be distinguished in the field of nanomedicine:

- **Diagnostics, sensors and imaging tools** used outside the patient. For these applications nanotechnology is used to create new analytic devices with higher sensitivity, lower cost, smaller dimensions or higher throughput.
- **Innovative technologies and biomaterials** that are used for tissue engineering, and to promote tissue repair. These applications frequently require only *ex-vivo* manipulations, and are aimed at the development of biological substitutes that restore, maintain, or improve tissue function or a whole organ[116].
- **Drug delivery systems**. The objective of this research field is to apply nanotechnology (sometimes combined with cell therapy) to the improvement of methods for the administration of pharmaceutical compounds in order to achieve more powerful therapeutic effects.

In the short term, nanomedicine will provide advances in drug discovery, drug delivery and analytical and diagnostic procedures. There are a growing number of marketed nanosized drug delivery systems and imaging agents, and the proliferation of bioanalytical methods for single-molecule analysis and biosensor technology based on nanotechnology represents a huge opportunity to revolutionise diagnostics in the healthcare environment. In the long term, the challenges of nanomedicine are ambitious, and include biosensors coupled to

delivery systems that could combine the *in vivo* diagnostics with a targeted, focused therapy, and nanoimaging technologies designed with non-invasive analytical nanotools with high reproducibility, sensitivity and reliability for the simultaneous detection of several molecules for use in pre-symptom disease.

5. TARGETED DRUG DELIVERY SYSTEMS

The challenge of drug delivery is the liberation of drug agents at the right time in a safe and reproducible manner, usually to a specific target site[117], with minimal exposure for sensitive collateral (non-targeted) tissues and better therapeutic effect.

When designing a nanovector for a specific application, several characteristics will be conferred not only by the nature of the molecules that compose the vector, but also by its size and morphology. In addition, for each administration method, different biological barriers have to be crossed, each one with its own peculiarities that should be considered[118].

An ideal targeted drug nanocarrier will have a broad variety of useful properties, such as:

- Capacity to carry high loads of multiple and diverse molecular cargos.
- Protection of the drug, since the carrier will mask unwanted interactions with the environment until the cargo is released at the target site.
- Prolonged circulation time in the blood, without elimination by the immune system.
- Specific targeting to certain diseases sites, due to targeting ligands attached to the surface of the nanocarrier, and limited accumulation in healthy cells, tissues, or organs.
- Enhanced intracellular penetration with the help of surface-attached cell-penetrating molecules.

- Ease of tracking by labelling the carrier with available contrast agents that can even permit *in vivo* visualization.

The materials that compose the nanovector should be biocompatible and biodegradable. When encapsulating a drug, its biodistribution will be determined by that of the nanocarrier, improving the therapeutic effect. The delivery system itself should be metabolized and cleared from the circulation once its carrier function has been completed. However, an altered distribution of the drug in the organism can lead to changes in side-effect profiles, such as the mild skin toxicity observed in patients treated with liposomal doxorubicin that is not found in patients treated with free doxorubicin.

Particle size is also a key factor in the biological outcomes and internalization processes of nanoparticles (NPs). Whereas structures below 10 nm are rapidly cleared from the blood by renal filtration, those between 10 and 70 nm can penetrate even very small capillaries, and particles with diameters ranging from 70 to 200 nm show the most prolonged circulation times. Larger particles are usually sequestered by the spleen and eventually removed by phagocytes. NPs of size ranges up to 1000 nm can penetrate the intestinal mucosa in less than one hour through intercellular spaces between the enterocytes and M cells lining the Peyer's patches, and have been successfully assayed for the oral delivery of insulin[119,120]. NP size determines the mechanism of internalization (phagocytosis vs endocytosis vs pinocytosis), and therefore subcellular localization. One of the major advances in recent years has been further reduction in the size of these delivery systems: existing polymeric molecular assemblies that are nanometer in scale can be easily injected or inhaled and are capable of being internalized by many types of human cells.

Passive targeting refers to the accumulation of the drug-loaded carrier at a particular body site due to pathophysiological and anatomic features; for instance nanocarriers can penetrate the tumour vasculature through its leaky endothelium and in this way accumulate in solid tumours due to the enhanced

permeation and retention effect, although some nanoparticles might also be taken up nonspecifically. In contrast, **targeted delivery** is achieved through the functionalization of the nanovector surface with appropriate ligands (such as peptides, antibodies, polysaccarides or oligonucleotides) to dock them to specific target sites, avoiding non-specific binding to other cells. Active nanoparticle targeting is particularly essential for the delivery of biomacromolecules (e.g. DNA and siRNA) that require intracellular delivery for bioactivity. The disadvantage of this approach is that ligand-attached nanocarriers may induce an undesirable immunological response due to the proteic nature of some ligands. Camouflage elements (such as polyethylene glycol, PEG) have been designed to evade immune surveillance and to extend blood residence time and half-life of nanovectors. The number of ligands per nanocarrier and the suitable PEG chain length at their surface must be adjusted to properly expose the ligand for cell recognition[121]. Nanoparticles can also be modified to achieve efficient intracellular targeting to specific organelles: anionic particles usually remain in lysosomes whereas those positively charged become predominantly localized in the cytoplasm and within mitochondria[122].

Although there is a large variety of drug delivery systems (Figure 8), here we will focus on encapsulation nanodevices of controlled dimensions and having the capability of being targeted to specific cell types or subcellular compartments:

Liposomes are self-assembling lipid bilayers generally formed by amphiphilic phospholipids and cholesterol surrounding an aqueous core. Encapsulation of hydrophobic and hydrophilic compounds into the bilayer or the inner cavity, respectively, can be achieved using a variety of loading techniques. Liposomal carriers prevent the enzymatic degradation of incorporated drugs and can be functionalized with specific ligands for the improvement of target selectivity. Several liposomal drugs are approved for the treatment of different types of cancer. Liposomes can be combined with a large variety of nanomaterials, such as mesoporous silica nanoparticles or superparamagnetic iron oxide nanocores. Because the unique features of both the magnetizable colloid and the versatile

lipid bilayer can be joined, the resulting so-called magnetoliposomes can be exploited in a great array of biotechnological and biomedical applications, including magnetic resonance imaging, hyperthermia cancer treatment and drug delivery.

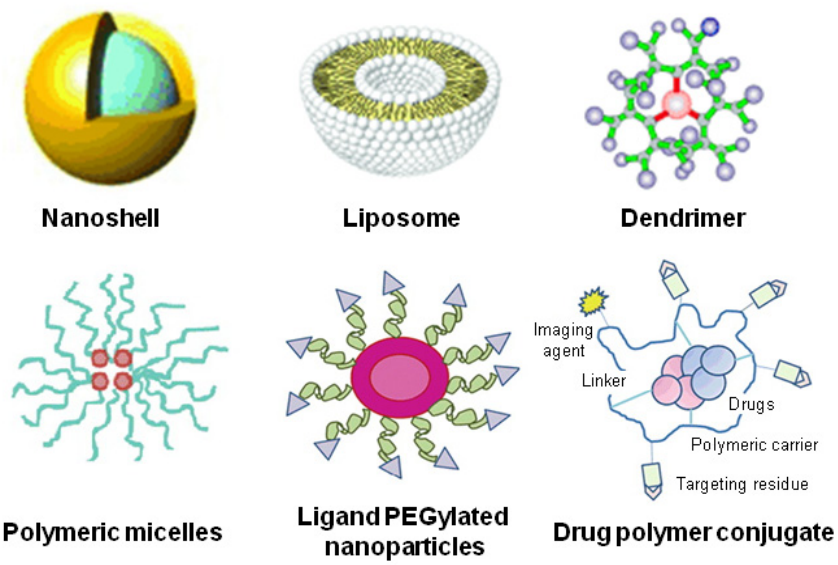

Figure 8. Some nanosystems for drug delivery, modified from[123,124].

Layer-by-layer systems are based on the sequential adsorption of positively and negatively charged materials around templates of different sizes and shapes, where the desired molecules can be solubilized in one of the layers during film formation. When coating particles, assembly is repeated until the required number of bilayers is formed around the core NP for the controlled delivery kinetics of the compound. Numerous substrates can be encapsulated with this technique including dyes, enzymes, drugs and cells, and the outer surface of the system presents and ideal platform for the functionalization with targeting molecules.

Solid lipid nanoparticles (SLNs) are particulated solid lipid core matrix NPs that can solubilize lipophilic molecules. SLNs combine the advantages of polymeric NPs, emulsions and liposomes, since they present no toxicity, great stability, controlled drug release and can be functionalized for targeting purposes. However, SLNs present limited drug loading capacity.

Nanoemulsions are a dispersion of immiscible droplets, ideal for the solubilization of hydrophobic drugs. Nanoemulsions have recently become increasingly important as potential vehicles for the controlled delivery of cosmetics and for the optimized dispersion of active ingredients in particular skin layers. Similar to liposomes, they support the skin penetration of active ingredients and thus increase their concentration in the skin and can be prepared in a variety of formulations such as foams, creams, liquids, and sprays.

Protocells[125] are lipid bilayer-wrapped nanoporous silica NPs that can be loaded with a combination of diverse cargos into their nanoporous silica core, and whose lipid membranes can be functionalized with targeting agents and PEG. Protocells have been shown to increase specific target-cell binding compared to liposomes due to their high resistance against destabilization in the blood and reduced leakage of drug cargo.

Polymer-drug conjugates consist of linear polymers that are used as drug carriers. Drugs can be conjugated via electrostatic interactions or covalent bonds, the latter requiring a drug linker that is stable during conjugate transport and able to release drug at an optimum rate on arrival at the target site. Polymer-drug conjugates increase aqueous solubility of drugs and present a reduced toxicity and prolonged circulation time when compared to free drugs.

Polymeric nanoparticles: nanospheres and nanocapsules. These delivery systems consist of a polymeric matrix with a therapeutic agent encapsulated inside or attached onto its surface. Nanospheres are dense polymeric matrices in which the drug may be dispersed within the particle or absorbed on the sphere surface, whereas nanocapsules present a polymeric shell surrounding a liquid core.

Polymer micelles are self-assembling colloidal aggregates of amphipathic molecules, which form micelles when their concentration reaches the critical micellar concentration. Micelles present a hydrophobic core for drug loading and a

hydrophilic shell, which can be functionalized with targeting agents. Micelles have a controlled size, are easy to prepare and present low toxicity and prolonged circulation time.

Polymersomes are capsules composed of block copolymers with a bilayered membrane enclosing an aqueous compartment, with the potential of encapsulating hydrophilic and hydrophobic drugs. Polymersomes present a less fluid membrane than liposomes, but are very stable and their architecture can be easily tuneable.

Branched polymers/dendrimers are polymeric NPs formed by repeated hyperbranched monomeric units covalently linked around a central core, via convergent or divergent synthesis, where the generation of dendrimers is defined by the level of repetition units. They possess a highly functionalizable surface that can be modified for the attachment of drugs or targeting ligands, and present many cavities that may contain drugs which are protected from fast degradation in the physiological environment. However, synthesis is time-consuming and some of them are toxic due to terminal amino groups and their cationic character.

Inorganic nanoparticles with a core composed of metals such as gold, silver, iron, cobalt or platinum. These NPs can combine different properties in the same structure, based on different compositions of the core and the shell. The metallic core can be built to have physical properties making the NP responsive to mild external signals so that its movement can be directed from outside the body. The NP shell can be functionalized with targeting molecules in order to direct it to the desired location. Gold colloids have been postulated as promising candidates in nanomedicine due to their bioinertness, cellular imaging ability, and presumed nontoxicity[126], and they have been proposed for the delivery of drugs. However, recent data have shown that gold nanoparticles induced changes in cellular morphology, mitochondrial function, mitochondrial membrane potential, intracellular calcium levels, DNA damage-related gene expression, and of p53 and caspase-3 expression levels in vitro[127]. Although metallic nanoparticles provide

stability and enhanced detection capabilities of the nanobiosystem, some metals are toxic in elemental form and other biodegradable nanobiosystems threaten their development.

Because of their combination of properties (subcellular size, controlled release capability, and susceptibility to external activation) devices provided by nanotechnology will enable imminent new applications in biological and medical science. Furthermore, the engineering of multifunctional pharmaceutical nanocarriers combining several useful properties in one particle that target, image and destroy (for instance, tumours) can significantly enhance the efficacy of many therapeutic and diagnostic protocols[128].

Over two dozen nanotechnology products have been approved by the US Food and Drug Administration for clinical use, and many are under clinic and preclinic development. Interestingly, the majority of these clinically approved nanotechnology products consist of liposomal drugs and polymer–drug conjugates, generally lacking active targeting or controlled drug release components. Despite their enormous potential for drug delivery, the transfer of targeted delivery systems has faced considerable challenges, and only a handful of candidates have made it to clinical trials (Table 1). Among others, an essential aspect for the successful development of targeted nanoparticles resides on the choice of targeting elements, where biocompatibility, cell specificity, binding affinity, and purity of the ligand should be considered[129]. Other important factors that have to be taken into account are the size and charge of the targeting molecules and their ease of modification and conjugation to the nanoparticles. The choice of ligand, from a practical perspective, is also dependent on production cost, scalability, and stability in mass production. With continuous advances in identifying new biomarkers and associated targeting ligands, and in engineering nanoparticle delivery systems with optimal physicochemical properties, it will be increasingly feasible to develop targeted and controlled release nanoparticle products as promising candidates for clinical transfer.

PLATFORM	TRADE NAME	TARGETING LIGAND	DRUG	CLINICAL STAGE
PEGylated liposome	MCC-465	$F(ab')_2$ fragment of human antibody GAH	Doxorubicin	Phase I
NGPE liposome	MBP-426	Transferrin	Oxaliplatin	Phase I/II
Liposome	SGT-53	Single-chain antibody fragment	p53 gene	Phase I
Cyclodextrin-based polymeric NP	CALAA-01	Transferrin	si RNA	Phase I
PEGylated poly(lactic-co-glycolic acid) NP	BIND-014	Peptide	Docetaxel	Phase I

Table 1. Targeted delivery systems in different stages of clinical trials, reproduced from[129].

5.1. Liposomes for drug delivery

Liposomes are able to carry a broad spectrum of drugs, including chemotherapeutic compounds, immunomodulators, imaging agents, chelating compounds, hemoglobin, cofactors and genetic material. Liposomes are classified by their size and number of bilayers into three classes: multilamellar vesicles (with five or more lamellae and ranging from 100 nm to 1 μm), small unilamellar vesicles (size under 100 nm) and large unilamellar vesicles (larger than 100 nm). Formulation parameters such as lipid composition, lipid membrane fluidity, surface charge, steric stabilization and vesicle size have been optimized to extend the therapeutic index of liposomal drugs over conventional formulations.

The strong hydrophobic interactions within the liposome bilayer minimize dissociation in serum and blood, and the leakage of encapsulated compounds. Liposomes improve the delivery of bioactive molecules by functioning as circulating microreservoirs for sustained release[130] after intravenous,

intraperitoneal, intramuscular or subcutaneous injections. Liposomes stabilize drugs and can overcome barriers for cellular and tissue uptake to direct their contents to specific sites *in vivo*.

Main reasons for using liposomes as drug carriers[131]:

Directionality	Liposomes can target a drug to the intended site of action (site-specific delivery) or can also direct it away from a site that is particulary sensitive to the toxic action of the drug (site-avoidance delivery).
Durability	The entrapped drug is released slowly, allowing therapeutic drug levels to be maintained either in the bloodstream or at the local administration site for a prolonged time. Thus, frequency of administration decreases.
Protection	Drugs incorporated in liposomes, in particular hydrophilic compounds encapsulated inside liposomes, are protected from degradation.
Internalization	Liposomes promote the intracellular delivery of drugs that otherwise not be able to enter the cell in their free form due to unfavorable physicochemical properties.
Amplification	If the drug is an antigen, liposomes can act as immunological adjuvants in vaccine formulations.

Delivery modes of liposomal contents to cells, include extracellular release, membrane fusion, endocytosis and fagocytosis[132] (Figure 9). Following surface adsorption, liposomes may remain bound to the outer cell membrane where they may breakdown, releasing their entrapped contents outside the cell or alternatively, they may fuse with cells, delivering their contents to the cytoplasm. Receptor-mediated endocytosis occurs when particles have a size smaller than 150 nm, and phagocytosis only in specific cells such as macrophages. Liposome contents are natural constituents of cell membranes, and as such are eliminated by normal metabolic routes, have low toxicity and are well tolerated.

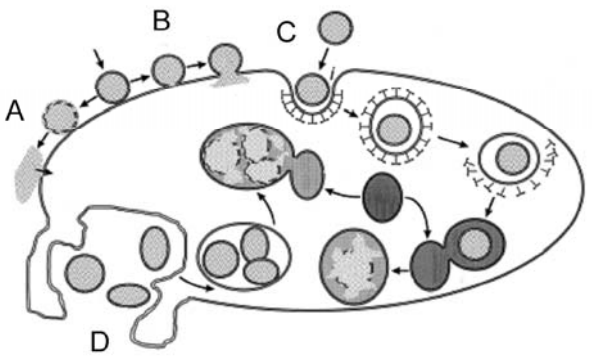

Figure 9. Delivery of liposome contents to cells. (A) Extracellular release of liposomal contents, (B) fusion of liposomes with the cell membrane, (C) receptor-mediated endocytosis and (D) phagocytosis. Reproduced from[132].

To increase blood residence time *in vivo*, liposomes can be coated with PEG, to reduce mononuclear phagocyte system uptake[133,134]. This prolonged residence in blood is based on steric stabilization of liposomes that can lead to reductions in liposome aggregation and plasma protein adsorption. Decreasing size, negative charge density and fluidity in the bilayer also increase circulation times. Liver and spleen are the major organs for non-specific liposome uptake due to their enrichment in mononuclear phagocyte system macrophages and their rich blood supply. Non PEGylated liposomes are attractive candidates for drug delivery to infected macrophages and for antigen delivery in liposome-based vaccines.

Targeting ligands can be conjugated to the surface of liposomes in order to enhance their selectivity (Figure 10). Given a suitable antibody with high specificity and affinity for the target antigen, the critical factor is the accessibility of target cells to the immunoliposomes, mainly cells in the intravascular compartment or accessible through leaky vascular structures. Once the liposomes bind to the target cells, the entrapped drugs must be released to the appropiate subcellular compartment. Using liposomes, enhanced safety and efficacy have been achieved for a wide range of drugs, including anticancer, antivirals, antifungals, antimicrobials, antiparasitics, vaccines and gene therapeutics[135].

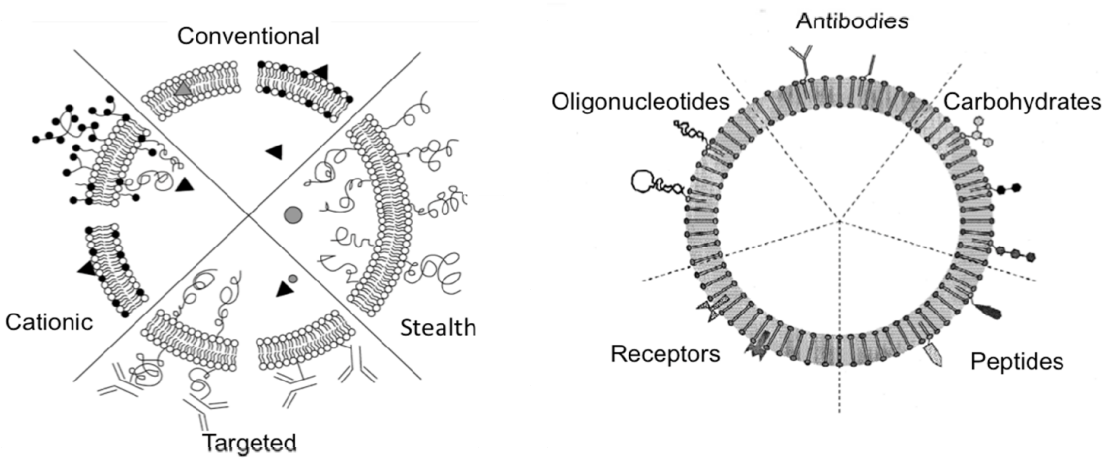

Figure 10. Schematic representation of four main liposome types (left) and ligands used for targeted liposomes (right), reproduced from[131,132].

Quality control assays of liposomal formulations[136] include basic characterization assays (pH, osmolarity, phospholipid concentration), chemical stability studies (phospholipid hydrolysis, drug entrapment, drug degradation), and physical characterization (size distribution, zeta potential, appearance, electrical surface potential). Liposomes shelf-life is limited by two factors: physical instability, which includes liposome aggregation or fusion and drug leakage from or through the bilayer; and chemical instability, due to hydrolysis and oxidation of phospholipids. Lyophilization is useful for the long-term storage of liposome-based drugs, and sugars like lactose or sucrose are used as cyroprotectants to maintain particle size after the freeze-drying-rehydration cycle.

Several liposome-based products have been commercialized while others are into clinical development, with a proven reduced toxicity and better biodistribution that non-liposomal formulations[137]. New generation liposomes include cationic liposomes, temperature sensitive liposomes, and virosomes. Some liposomal products that have reached the market[138] are listed in Table 2.

PRODUCT NAME	ROUTE OF INJECTION	DRUG	LIPOSOME TYPE	INDICATION
Ambisome®	i.v.	Amphotericin B	Non PEG	Fungal infections
DaunoXome®	i.v.	Daunorubicin	Non PEG	Kaposi's sarcoma
DepoCyt®	Spinal	Cytarabine	Non PEG	Neoplastic and lymphomatous meningitis
DepoDur®	Epidural	Morphine sulfate	Non PEG	Pain management
Doxil®	i.v.	Doxorubicin	PEG	Ovarian/breast cancer Kaposi's sarcoma
Enpaxal®	Intramuscular	Inactivated hepatitis A virus	Non PEG	Hepatitis A vaccine
Inflexal V®	Intramuscular	Inactivated hemagglutinine of Influenza virus	Non PEG	Influenza vaccine
Lipo-dox®	i.v.	Doxorubicin	PEG	Ovarian/breast cancer Kaposi's sarcoma
Mepact®	i.v.	Mifamurtide	Non PEG	Osteosarcoma
Myocet®	i.v.	Doxorubicin	Non PEG	Breast cancer
Visudyne®	i.v.	Verteporfin	Non PEG	Age-related macular degeneration, pathologic myopia and ocular histoplasmosis

Table 2. Commercialized liposomal formulations, reproduced from[138]. PEG: PEGylated.

5.2. Polymers for drug delivery

Polymers are a promising approach to the targeted delivery of pharmaceuticals: they are small and can diffuse well in the tissues and inside cells and cellular organelles, can be functionalized with tracking and targeting molecules, and there is a wide choice of materials and molecular structures for their assembly. Polymers are extensively applied in medicine and biotechnology, as well as in food and cosmetics industries. Their physical, chemical and biological characteristics can be tuned to meet specific applications. Various polymer-based controlled release systems for proteins have been recently approved by regulatory

authorities, and are showing how biomaterials can be used to improve the safety, farmacokinetics and half-life of drugs. Biodegradable polymeric nanoparticles, which degrade into products that can be completely eliminated, range in size between 10 and 1000 nm[139,140]. The most promising biodegradable synthetic polymers used for biomedical applications are: poly(hydroxyacid)s, poly(caprolactone)s, poly(ester-ester)s, poly(orthoester)s, poly(anhydride)s, poly(phosphazene)s and poly(aminoacid)s.

Polymers can encapsulate drugs, protect them from fast degradation in the physiological environment and release them at sustained rates in the optimal range of drug concentration, thus enhancing the *in vivo* therapeutic efficacy, maximizing patient compliance, and facilitating the use of highly toxic, poorly soluble, or relatively unstable drugs. Compared with other colloidal carriers, polymeric nanoparticles present a higher stability when in contact with the biological fluids. Methods for the preparation of surface-modified sterically stabilized particles are reviewed in the literature[140,141].

Polymeric nanoparticles can carry drugs in adsorbed, dissolved, entrapped, encapsulated, or covalently bound form. Drug loading into nanoparticles is usually done by one of these three methods: incorporation of the drug at the time of nanoparticle synthesis, adsorption after NPs formation by incubating these in a solution of the drug, or chemical conjugation of drugs into preformed NPs. Properties of the NPs are largely dependent on the polymer employed, and biocompatibility issues are a main concern.

5.2.1. Polyamidoamines family

Poly(amidoamines)s (PAAs) represent a family of biodegradable and biocompatible polymers with a recognized potential in the pharmaceutical field. PAAs are obtained by Michael type polyaddition of primary or bis-secondary amines to bisacrylamides. The synthetic polymer obtained presents tert-amino and amido groups regularly arranged along the main chain.

The preparation process of PAAs is simple, environmentally friendly and easily scaleable, thus being suitable to be commercialized in regions characterized by low per-capita income. Polymerization takes place in solvents carrying mobile protons, such as water or alcohols, without added catalysts at room temperature[142]. High temperatures accelerate the polyaddition reaction rate but the resulting polymers show a lower molecular mass because of the increase of hydrolysis. It has been demonstrated that the degradation rate of PAAs in aqueous media is strongly influenced by both the structure of the amide and the amine moieties and increases at basic pH and higher temperatures. Furthermore, degradation seems not to be affected by the presence of isolated lysosomal enzymes at pH 5.5[143]. PAAs and their low molecular mass degradation products are often non-cytototoxic (dependending on backbone chemistry). The average molecular mass of the PAAs usually ranges from 10,000 to 80,000 Da with a polydispersity index of 1.2-1.8 depending on the purification method. Narrow polydispersity fractions can be obtained by fractionation techniques, such as ultrafiltration. Most PAAs are soluble in water as well as in chloroform, lower alcohols, dimethyl sulfoxide and other polar solvents. However, amphoteric PAAs dissolve only in water and show a tendency to assume extended chain conformation in solution.

PAAs are inherently highly functional polymers. The introduction of additional groups in PAAs as side substituents can be easily achieved by starting from the corresponding functional monomers. As a rule, chemical groups capable of reacting with activated double bonds under the conditions of PAA synthesis (SH, NH_2, NR and PH_2) can not be introduced directly. All PAAs contain tert-amine groups in their main chain[144], therefore in the absence of additional acid or basic substituents, they are low to medium strength polymeric bases that can be classified as polyelectrolytes[145]. Amphoteric PAAs deriving from aminoacids carry both carboxyl and amino groups attached to the same monomer, and therefore in solution they change their net average charge as a function of pH. Movement from a neutral to an acidic pH results in a conformational change from a relatively coiled hydrophobic structure to a relaxed hydrophilic

conformation at acidic pH[146]. Peptide or proteins can be easily inserted for targeting purposes either as pendants or as integral portions of the polymer chain. Other targeting elements, such as sugar moieties, can be inserted by simply adding amino-sugars to the polymerization recipe[147].

We have focused our research in three polyamidoamines: ISA23, ISA1 and AGMA1 (Figure 11). ISA23, a prevailingly anionic amphoteric PAA, is obtained by polyaddition of 2-methylpiperazine to 2,2-bis(acrylammido)acetic acid. The polycationic polymer ISA1 is formed by Michael type polyaddition of bis(acryloyl)piperazine, 2-methylpiperazine and bis(hydroxyethyl-ethylenediamine. Cationic PAAs are usually two or more orders of magnitude less cytotoxic (IC_{50} in the range 0.5-3 mg/ml) than other commonly used polycations such as poly-L-lysine and poly(ethyleneimine), and amphoteric PAAs are even more biocompatible. The peptidomimetic PAA, named AGMA1, has been obtained by polyaddition reaction of bis(acrylamido)acetic acid and agmatine (4-aminobutylguanidine)[148]. AGMA1 carries guanidine and carboxyl groups and shows a strong structural resemblance to the tripetide arginine-glycine-aspartic acid (RGD sequence), which is known to play a role in the integrin-mediated adhesion to the extracellular matrix. The repeating unit of AGMA1 contains three ionisable groups, a strong acid (pK_a= 2.3), a medium-strength base (pK_a= 7.4), and a strong base ($pK_a \geq$ 12.1). At pH 7.4 the average excess positive charge is 0.55 per unit, but this amphoteric polymer showed a very low toxicity (IC_{50}> 5 mg/ml).

Cells internalize PAAs via the endocytic pathway. In intracellular compartments, where the pH is first lowered to 6.5 (endosomes) and then to 5.0 (lysosomes), they become prevailingly cationic and display endosomolytic properties[149]. Fluorescence microscopy revealed co-localization of ISA1 and ISA23 with Lysotracker (marker for lysosome and late endocytic structures). ISA1 also co-localized with the Early Endosomal Antigen 1 that accumulates in early endocytic structures[150]. The body distribution of radioactive labeled ISA23 and ISA1 revealed differences between them. While ISA1 was captured rapidly by

the liver rapidly, ISA23 circulated for prolonged time in the bloodstream[146] showing a tendency to localize in tumours. This high permanence time in the blood by ISA23 is an important feature to take into account when selecting a candidate for the design of the nanovector, since this increased circulation will potentially facilitate the interaction of the polymer with the infected pRBC membranes.

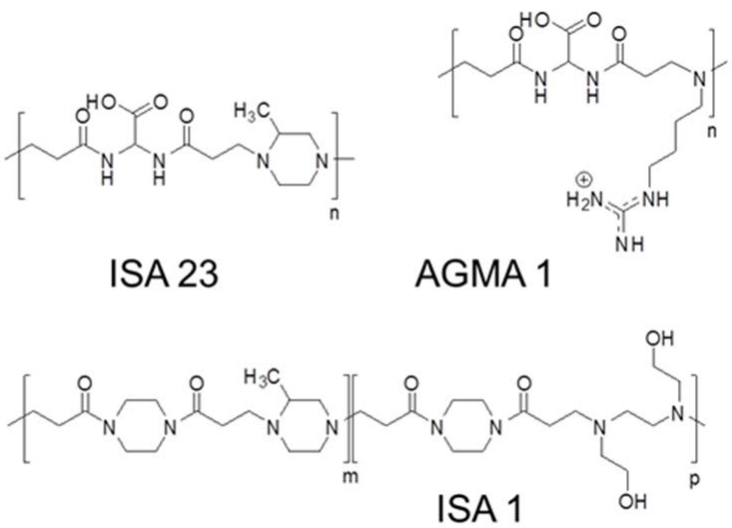

Figure 11. Structure of ISA23, AGMA1 and ISA23.

PAAs were first tested for their ability to form polyelectrolyte stable complexes with heparin, in order to neutralise the anticoagulant activity of heparin[147,151] and results were confirmed with PAA-crosslinked resins, which have also been assayed for metal ion complexation[152]. Early in the 1970's several PAAs were shown to display inherent antitumour activity, reducing the number and average weight of Lewis lung tumour metastases after i.v. administration in mice, with different grades of toxicity and activity[153]. More recently PAAs have been adopted as carriers for anticancer drugs such as mytomycin C, platinates[154] and doxorubicin. Conjugation of doxorubicin to polymers[155] improves drug solubility, increases residence time in the blood, decreases toxicity and, due to the enhanced permeability retention effect, is able to mediate improved tumour targeting. As doxorubicin is inactive in the conjugated form and can be released selectively at

the tumour site, the drug can act primarily against tumour cells with minimal normal tissue damage. Doxorubicin has also been coupled to polymers via an acid-sensitive linker, facilitating the release of the drug in a biologically active form in the endosomal compartment[156]. Agmatine-containing amphoteric polymers have been tested as carriers for drug delivery and as transfection promoters[150,149]. *In vitro* assays demonstrated the ability of the polymer to interact with cell membranes in a non-disruptive way and to effectively protect DNA by enzymatic degradation in biological environment and to promote stable gene transfection in living cells[157], being currently studied as a synthetic alternative to fusogenic peptides.

PAAs have been designed with potential for use as polymeric drugs, polymer-drug conjugates, polymer-protein conjugates, polymeric micelles to which drug is covalently bound and multi-component polyplexes being developed as non-viral vectors[158]. Unlike low molecular mass soluble polymer conjugates, there are some tfexamples of the routine use of high molecular mass polymers conjugated to drugs (e.g. Oncospar®).

5.2.2. Dendrimers

Dendrimers are highly branched, star-shaped macromolecules of polymeric nature with nanometer-scale dimensions. Dendrimers belong to the dendritic polymers family and have unique properties associated such as uniform size, high degree of branching, monodispersity, water solubility, multivalency, well-defined molecular weight and available internal cavities, which make them attractive for drug delivery applications[159].

Dendrimers are defined by three components: a central core, an interior dendritic structure (the branches), and the shell. The core controls the shape, directionality and multiplicity of the dendrimer. The interior affects the solubility and host-guest properties and the surface of the dendrimer can be further polymerized or modified with functional peripheral groups. Both the core and the number/type of

interior branching units affect the overall dendrimer morphology. Dendritic macromolecules present a generational growth (G); the first generation is generally called G1, the second one G2. Because dendrimer size increases linearly while the number of surface groups increases exponentially for each generation, steric crowding at the surface occurs. Hence, dendrimers at low generations are usually flexible and open, while dendrimers at higher generations form more dense structures.

A large number of dendrimers with a broad variety of architectures have been developed. Some of the commonly referenced dendrimer structures are polyamidoamine (PAMAM), poly(L-lysine), polyamide, polyester (PGLSA-OH), polypropylenimine (PPI) and poly(2,2- bis(hydroxymethyl)propionic acid (*bis*-MPA) structures (Figure 12).

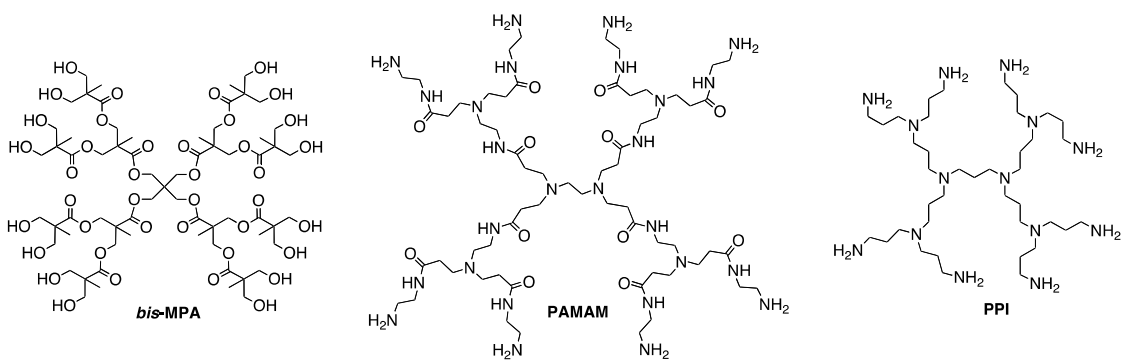

Figure 12. Chemical structures of some commonly used dendrimers.

Most dendrimers are synthesized following either a convergent or divergent route. In the convergent approach, the synthesis proceeds from the surface of the dendrimer inward to form a dendron that reacts with a suitable core to complete the synthesis. The convergent approach is advantageous because only a limited number of active sites are present per reaction, reducing structural defects in the product. In the divergent synthesis, dendrimer growth starts from a polyfunctional core and proceeds radially outward with the stepwise addition of successive layers of building blocks.

Dendrimers can encapsulate and solubilize drugs and increase their circulation time. If a drug is carried by a dendrimer larger than 5 nm, the size of the carrier exceeds the renal threshold and is less able to be filtered out of the bloodstream by the kidneys. Targeting agents can be used in order to improve dendrimer delivery to a specific location and thus reduce the side effects of treatment. Dendrimers have been tested for drug delivery though different administration routes, such as oral, transdermal, ocular and intravenous[160].

However, in spite of their broad applicability, associated toxicity due to the terminal amino groups and cationic charge of PAMAM and PPI dendrimers hampers their clinical applications. One approach to improve dendrimer biocompatibility contemplates surface modifications, including capping of the terminal $-NH_2$ groups with neutral or anionic moieties such as PEG. Current work is being focused on improving the unspecific toxicity of dendrimers, finding out cost-effective synthesis strategies, and the optimization of drug conjugation to dendrimers for successful commercialization of this technology.

6. NANOTECHNOLOGY APPLIED TO MALARIA

6.1. Microfluidics and biosensors for diagnostics

An important area of focus of current biomedical research is the development of nanotechnology-based molecular diagnostic platforms and the adaptation of existing ones for infectious disease diagnostics. In the last decades there have been many advances in diagnostic technologies, but infectious disease diagnostics are still based on half a century-old technologies that have several limitations, such as low speed of analysis, need for skilled operators, poor detection threshold and inability to detect simultaneously multiple strains of infectious agents[123]. Gold standard techniques for malaria diagnostics include microscopy, rapid diagnostics tests (RDTs) and more recently PCR-based point-of-care tests.

One of the examples of nanotechnology-based diagnostics systems are nanoparticle labels used in flow immunochromatographic tests, which rely on the same principles as ELISA and can detect antibodies in blood or in other body fluids[161]. These RDTs are able to detect parasitemia levels of ≤ 500 parasites/μL for *P. falciparum*, but for other species the detection limit is higher because available target antigens are not as well characterized. A cheap and user-friendly test based on the agglutination of polystyrene particles functionalized with antigen (or antibody) in the presence of *P. falciparum* specific antibody (or antigen) has been developed and successfully evaluated for field use[162]. An important concern regarding nanotechnology-based diagnostic platforms is that the improvement of their specificity and efficacy requires adequate antigens.

A magneto-optic technology based on hemozoin detection was developed for rapid and quantitative diagnostic of malaria in an *in vivo* and non-invasive format[163]. Under an external magnetic field hemozoin gives rise to an induced optical dichroism, which is proportional to its concentration, allowing malaria parasite detection in blood and tissues with low interference of biological compounds.

Microfluidics-based technology has potential for the design of point-of-care malaria diagnostics devices[164]. A RDT strip chip has been designed for diagnostics of malaria infection[165], where different lines clearly visible to the naked eye indicate the presence of specific antigens in blood. Many groups are focusing their research on these devices as diagnostic systems, but progress is still needed to reduce costs; one example is the European Union funded NANOMAL project[166], which is developing a simple, rapid and affordable point-of-care handheld diagnostic device for malaria diagnostics and detection of drug resistant parasites within minutes.

Accurate tools for the identification of parasites in order to assess the severity of the illness and advise proper treatment to the patient could help to control the spread of malaria, because many patients in developing countries are treated of malaria due to a symptoms-based diagnostic. Although the advantages of nanotechnology have not been fully applied to infectious disease detection in the developing world, it can potentially address many of the challenges outlined by the WHO for the delivery of rapid and effective point-of-care diagnostics.

6.2. Nanobiosensors for the discovery of new potential drugs

Nanotechnology can also be applied to the discovery of potential new therapeutic agents by individual molecule handling techniques like single-molecule force spectroscopy (SMFS), a potent tool for the study of biomolecular interactions that uses atomic force microscopy or optical tweezers for the measurement of dissociation forces of single-lingand-receptor complexes (e.g. enzyme-substrate, enzyme-inhibitor, receptor-ligand, antibody-antigen, protein-DNA) in the piconewton range.

Previous research in our group[167] has explored the capability of atomic force microscopy SMFS to identify inhibitors of the non-mevalonate pathway of isoprenoid biosynthesis present in the apicoplast of *Plasmodium* as a proof-of-concept model system that could be developed into an efficient screening device for the discovery of new antibiotics and antimalarials. As mentioned previously, since the non-mevalonate pathway is absent in animals, inhibitors of this metabolic route could be used for the treatment of certain bacterial and protozoan infections without undesired side-effects, with a higher efficacy and a reduced appearance of resistance. However, this area of study has had only a very limited presence in the research related to diseases in developing countries.

6.3. Drug delivery strategies for antimalarials

Nanocarriers are useful tools to improve the pharmacokinetic profile of drugs that due to poor water solubility, low bioavailability and high toxicity have been limitedly implemented in the pharmacotherapy.

Due to their several benefits drug delivery strategies could play an important role for the treatment of malaria:

- Delivery of sufficiently high local amounts of drugs to avoid the development of resistant parasite strains[168], a common risk when using sustained low doses to limit the toxicity of the drug for the patient.
- Improvement of the efficacy of currently used antimalarials.
- Use of orphan drugs never assayed as malaria therapy, e.g. because of their high and unespecific toxicity.
- Increased efficacy of the immune response in vaccine formulations.

However, mainly because of the lack of economic incentives, the application of targeted drug delivery strategies to malaria therapy has been underresearched for many years by drug discovery companies, which have focused their attention on the application of these tools to more profitable pathologies, in particular, cancer. Antimalarial drugs, such as CQ and PQ, have been encapsulated in liposomes in order to protect them from degradation and to obtain a sustained release with minimal side effects. Artemether has a low oral bioavailability due to its low hydrosolubility and degradation in the acidic environment of the stomach. Moreover, because artemether is not suitable for i.v. injection, the drug can not be used for the treatment of severe malaria cases and many efforts in the development of new delivery strategies are being currently explored. Like artemether, other new drug candidates are excluded in initial *in vitro* tests because of their low aqueous solubility, and drug delivery systems could be used as delivery agents for these compounds. In the case of hydrosoluble compounds, drug delivery strategies increase their capacity to cross biological membranes.

The main strategies for targeting antimalarial drugs to pRBCs and occasionally to hepatocytes are passive and active targeting. **Passive targeting** is adequate for targeting cells with phagocytic properties such as macrophages, but not RBCs, because these are phagocytically and endocytically inactive. However, passive targeting with conventional nanocarriers could be used for the treatment of *P. vivax* infections in which hypnozoites (the dormant forms of the parasite in hepatocytes) are located side by side with Kupffer cells, which are phagocytically active, leading to a nanocarrier accumulation at this site (Figure 13B). Passive pRBC targeting can be achieved by surface modification with hydrophilic polymers such as PEG, which delays phagocytosis and results in **long circulating nanocarriers** with increased drug half-life in the blood. These prolonged circulation time allows an increased contact of nanovectors with pRBCs (Figure 13A) and potentially less toxic effects to other tissues due to the reduced volume of distribution of the drug. **Active targeting** is achieved by the functionalization of nanocarriers with cell-specific ligands, allowing a preferential accumulation of the drug in the target cells, pRBCs and hepatocytes (Figure 13C). The identification of new *Plasmodium*-infected cell targets can also be used to modify existing drug delivery systems employing nanotechnology to deliver antimalarial drug molecules to the newly-targeted sites of action more effectively.

An ideal targeted drug delivery system of antimalarials would be modulable, adaptable, and versatile:

- **Modulability:** Optimization of liposome formulation and polymer composition can lead to a sufficiently cheap (≤ 1€/dose) and stable nanovector (≥ 50% activity after ≥ 1 month at 37°C) that can be used for the treatment of severe or uncomplicated malaria.
- **Adaptability:** With minor modifications of their parts, the nanovectors can be adapted to carry new targeting molecules and different drugs.

- **Versatility:** The technology developed can be applied to the targeted drug delivery of compounds for the treatment of a wide array of diseases triggered by intracellular parasites.

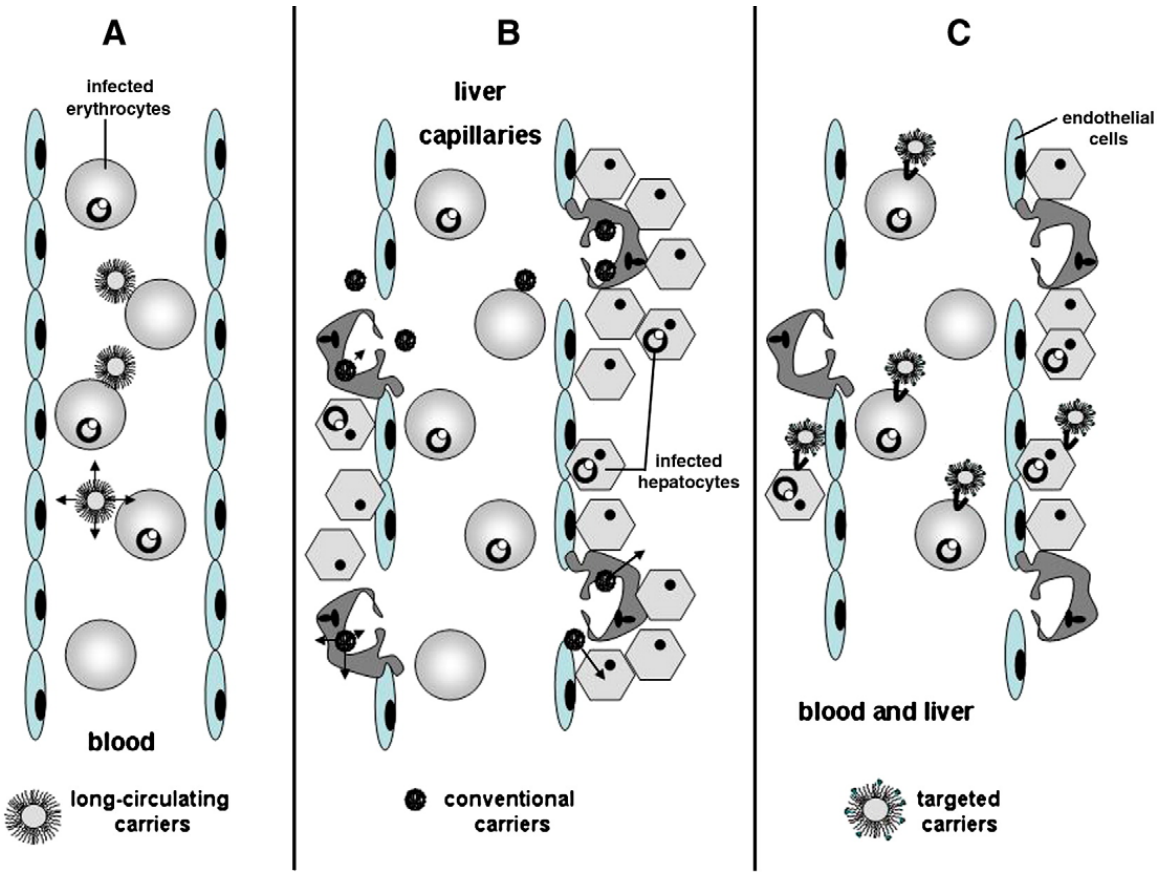

Figure 13. Representation of three targeting strategies for the use of antimalarial nanocarriers in *P. yoelii*-infected mice. (A) Surface-modified long circulating carriers; (B) Conventional, unmodified carriers; (C) Ligand-modified nanocarriers for the targeting to pRBCs and liver. Reproduced from[169].

6.3.1. Lipid-based carriers in malaria

RBCs do not have a endocytic machinery, and for this reason liposomes can be an efficacious system to deliver cargo into the cell by a simple membrane fusion process, which occurs on a length scale of nanometres and a timescale of milliseconds[170]. Covalent attachment of specific antibodies to liposomes has been proven to modify tissue distribution *in vivo*: targeted liposomes presented a decrease in non-specific uptake by the liver and an enhanced ability to interact with RBCs, showing a very fast binding kinetics[171]. Transferrin-conjugated SLNs were tested for their ability to target QN to the brain for the treatment of cerebral malaria and fluorescence studies revealed an enhanced uptake of QN-conjugated SLNs in the brain compared to non-targeted SLNs[172].

Reports indicate the sustained prolonged release of CQ[173] and PQ[174] when using lipid-based delivery systems. Earlier studies have shown that encapsulation of CQ in liposomes bearing anti-RBC antibody on their surfaces enabled the specific recognition of *P. berghei*-infected erythrocytes[173]. These liposomes presented a marked increased efficacy against *P. berghei* infections in mice, even in CQ resistant infections[175,176]. When administered inside liposomes, chloroquine has been described to increase its maximal tolerable dose and its efficacy against malarial infections, due to the simultaneous delivery of several drug molecules. These previous results indicate that the selective targeting of drugs to pRBCs can help to cure malaria infections (even those resistant to common drugs) using a lower dose of antimalarial.

As described above, PQ can have adverse effects especially in patients with G6PD deficiency. Some studies have reported PQ encapsulation in different carriers in order to modify its toxic profile[177,178,179]. Encapsulation of PQ into liposomes has been shown to reduce its toxicity due to a decrease of the drug levels in organs such as lungs, heart or brain[177].

PEGylated liposomes incorporating a *P. berghei* amino acid sequence have been shown to greatly increase their targeting to liver[180,181] in comparison to other organs, such as heart, lungs and kidneys, without evidence of inflammation in liver tissue. These findings open the possibility of targeting sporozoites to block infection, and dormant parasites in the liver for the treatment of malaria recrudescence.

Because artemisinin derivatives have the limitation of their short half-life *in vivo*, liposomal formulation of these drugs has been developed to overcome this problem. Artesunate liposomes, with a 100% entrapment efficacy, increased drug bioavailability[182], thus opening the perspective of a reduction in dosing frequency. AM liposomes prevented malaria recrudescence in malaria-infected mice[183] and oral administration of arteether in liposomes[184] showed higher bioavailability than the free drug, with a faster and better absorption in rabbits. In addition, these liposomes were succesfully administered intravenously and the results obtained indicated a longer half-life in comparison to other artemisinin derivatives, thus opening the possibility of an i.v. arteether treatment with prolonged effect in high-risk malaria patients.

Liposomal nanovectors are adequate for parenteral delivery, indicated in cases of severe or complicated malaria, or if the patient is vomiting and unable to take oral drugs[50]. Parenteral treatment in the form of a vaccine or of targeted liposomal delivery can be a useful weapon for the *last mile* in a malaria eradication strategy[185], but formulations adequate for oral administration would be a valuable contribution for the treatment of malaria in endemic rural areas with poor health care systems. However, liposomes and whole antibodies are difficult to formulate for oral intake, which will likely require smaller (but equally 100% specific) targeting agents and drug-containing nanocarriers.

Self-emulsifying systems (oil-in-water) have been designed for the solubilization and increase of the bioavailability of orally taken hydrophobic drugs, for instance β-arteether[186], by protecting them from enzymatic and/or chemical hydrolysis

while maintaining them in solution during their passage through the gastrointestinal tract until their intestinal absorption. A solid microemulsion, NanOsorb®, has been reported as safe for the oral delivery of AM, showing an increased efficacy in mice compared to the free AM marketed formulation. PQ has also been assayed in nanoemulsions for oral administration, showing higher accumulation in the liver than free PQ and an improved activity in *P. berghei*-infected mice[187].

Transdermal delivery provides an alternative route for the administration of antimalarials, where first-pass hepatic metabolism is avoided and administration is easy. The limitation in a transdermal route can be low skin permeability, although cationic liposomes could be used to enhance permeabilization. Clindamycin has been encapsulated in different liposome formulations, and cationic liposomes appeared to provide higher liposome stability and increased skin permeation of the drug in mice[188].

Despite all these promising pioneering assays, liposomal-based targeted drug delivery has not progressed towards a working strategy for malaria therapeutics, probably because of the absence, at the times of the studies, of specific markers for *Plasmodium*-infected cells that could be used for targeted drug delivery. Moreover, the vast majority of approaches focus on *in vivo* studies of liposomal drug efficacy and lack *in vitro* studies for the characterization of the interaction of pRBCs with liposomes and the delivery of liposomal content inside target cells or in the presence of other cell types.

6.3.2. Polymer-based nanocarriers

Polymer-based nanocarriers for the drug delivery of antimalarials have the advantage over liposomes of being capable to be more easily formulated for oral delivery. This characteristic is relevant for malaria chemotherapy given the current need for the massive administration of antimalarial drugs in isolated rural areas where individualized i.v. injection of liposomal formulations is not possible.

Several polymeric nanoparticle devices have been used to deliver anti-malarial drugs in mice[56], including halofantrine[189], artemisin derivatives[190], chloroquine[191] and PQ[178]. Pharmacokinetic evaluation of albumin-encapsulated PQ targeted to the mouse liver showed significant higher concentration of PQ in liver tissues relative to the free drug, demonstrating a sustained release of PQ for at least 48 post-i.p. administration[178]. These micron-sized NPs are a useful and inexpensive technique for the encapsulation of PQ. Gelatin, glutaraldehyde and polyacrylamide nanoparticles have also been studied for controlled PQ delivery.

Biodegradable chitosan nanoparticles conjugated with antisense oligodeoxynucleotides for the silencing of *Plasmodium* topoisomerase II inhibited the growth of *P. falciparum in vitro*[192], showing a higher sequence-specific inhibition than free oligodeoxynucleotides. NPs demonstrated effective protection of oligonucleotides against nuclease degradation, which is a major requirement for the *in vivo* use of antisense technology. Despite the absence of endocytic processes in pRBCs, it has been demonstrated that particles up to 50–80 nm in diameter access intracellular parasites[193], and once inside the cell, chitosan has been shown to be degraded *in vitro* and *in vivo*, ensuring both biocompatibility and adequate drug release.

PEG-coated and non-coated polylactic acid nanoparticles loaded with halofantrine have been assayed for the treatment of murine malaria after i.v. administration[189]. Nanocapsules could administer a dose of halofantrine that was toxic in the solubilized form of the drug, increased the bioavailability of the drug in plasma and affected parasite development. Interestingly, coated and non-coated NPs had complementary properties. Non-coated NPs provided a fast effect in parasitemia control due to a relatively rapid release of drug, whereas PEG-coated formulations showed a more sustained effect because of their continued presence in the circulation. A mixture of the two types of NPs could be used as a delivery system for i.v. administration of halofantrine.

NPs have also been assayed for the oral delivery of curcumin in *P. yoelii*-infected mice[194]. Curcuminoids have been reported to exhibit many promising pharmaceutical activities but their poor oral absorption, due to low hydrosolubility and rapid metabolism, is a limitation for their clinical use. Chitosan NPs prevented curcumin degradation, were able to interact with a significant proportion of the RBC population, inhibited parasite heme polymerization *in vitro* and cured mice from malaria infection when starting parasitemias were low.

Dendrimers consisting of different molecules, such as amino acids, can greatly reduce the toxicity associated with amine-terminated dendrimers, such as polyamidoamine and polypropylene imine dendrimers. Galactose-coated dendrimers have been assayed for CQ delivery[191], showing reduced phagocytosis, immunogenicity and hemolytic toxicity, being a safer alternative compared to their uncoated formulations both *in vitro* and *in vivo*. A long-circulating dendrimer was prepared for the solubilization of AM[190] for i.v. admininistration, using micelles formed by assembly of block copolymers. This formulation solubilized AM, increased its stability and prolonged its release.

A PEG-lysine type dendrimer conjugated to chondroitin sulfate A (CSA) presented a prolonged release of AM after i.v. administration[195]. CSA coating increased the amount of drug loading and its sustained release, decreased the unespecific cytotoxicity of the dendrimer and showed higher activity in *in vitro* studies. These good properties were also observed for CSA-coated poly-L-lysine-based dendrimers having a PEG amino core for the controlled release of CQ. Despite these promising *in vitro* results, to the best of our knowledge there are no published studies on the *in vivo* efficacy of dendrimer-antimalarial drug conjugates.

Polymers (polylactic acid, gelatin or chitosan) are matrices for ceramic particles that can introduce a tailored biodegradable drug. Gelatin and cross-linked gelatin ceramic implants have been reported to sustain blood concentrations of CQ *in vivo*[196].

Novel targeted delivery formulations can improve the efficacy, specificity, tolerability and therapeutic index of existing antimalarias and are likely to modify the traditional oral dosing schedule of drugs. Formulation and evaluation of novel drug delivery systems is not only less expensive than developing new drugs but may also improve delivery of compounds at the desired rates for a progress in malaria chemotherapy. In fact, therapeutic failure has also been attributed in part to adverse effects of antimalarial drugs and patients' non-compliance due to inconvenient dosing schedules[56]. A realistic nanovector against malaria should ideally be small, specific, and low cost. It should also contain exchangeable, continuously improved targeting and antimalarial moieties against changing antigens and metabolic targets of the parasite. Some of the nanovectors presented in this work can fulfill these conditions, and can be the spearhead of a new generation of nanovessels, whose objective in the mid-term must be to enter the preclinical pipeline as economically affordable new antimalarial therapy.

OBJECTIVES

The objective of this PhD thesis is the development of a prototype nanovector for the targeted delivery of antimalarial drugs exclusively to Plasmodium-infected red blood cells and the understanding of the importance of the main parameters in the design of the nanocarrier that determine its performance.

This general objective will be approached through the following defined experimental steps:

1. Design and engineering of an immunoliposomal nanocarrier able to (i) encapsulate antimalarial drugs, (ii) dock specifically to pRBCs, and (iii) release its contents inside these cells, but not into non-infected RBCs.
2. Synthesis and evaluation of polymers as targeted nanocarriers of antimalarial drugs towards pRBCs.
3. Characterization of the *in vitro* efficacy of antimalarial drugs when delivered inside targeted immunoliposomes and polymers.
4. *In vivo* study of the performance of liposomal and polymeric nanovectors.
5. Exploration of new targeting molecules for future antimalarial-containing nanovectors.

RESULTS

ARTICLE 1

A nanovector with complete discrimination for targeted delivery to Plasmodium falciparum-infected versus non-infected red blood cells in vitro.

Patricia Urbán, Joan Estelrich, Alfred Cortés, and Xavier Fernàndez-Busquets.

Journal of Controlled Release, 2011 Apr 30; 151(2):202-11.

ARTICLE 2

Study of the efficacy of antimalarial drugs delivered inside targeted immunoliposomal nanovectors.

Patricia Urbán, Joan Estelrich, Alberto Adeva, Alfred Cortés, and Xavier Fernàndez-Busquets.

Nanoscale Research Letters, 2011; 6:620.

ARTICLE 3

Demonstration of specific binding of heparin to Plasmodium falciparum-infected vs non-infected red blood cells by single-molecule force spectroscopy.

Juan José Valle-Delgado, Patricia Urbán, and Xavier Fernàndez-Busquets.

Nanoscale, 2013. In press.

ARTICLE 4

Nanomedicine against malaria: use of poly(amidoamine)s for the targeted drug delivery to Plasmodium.

Patricia Urbán, Fabio Fenili, Juan José Valle-Delgado, Nicolò Mauro, Amedea Manfredi, Elisabetta Ranucci, Paolo Ferruti, and Xavier Fernàndez-Busquets.

Preparing for submission.

ARTICLE 1

A nanovector with complete discrimination for targeted delivery to *Plasmodium falciparum*-infected versus non-infected red blood cells *in vitro*

Drug delivery strategies represent a promising approach for increasing bioavailability and selectivity of drugs and therefore minimizing the side effects of malaria treatment and the appearance of resistant parasite strains, which hinder the control of malaria. In this article, we propose the development of liposomal nanocarriers for the targeted delivery of their contents to pRBCs. Antimalarials encapsulated inside liposomes have been widely used against murine malaria, but there is little data on liposome targeting to RBCs infected with human-specific strains of *Plasmodium* and a lack of studies of specific cell recognition, efficacy of cargo delivery and subcellular targeting of liposomes in pRBCs.

Liposomes encapsulating *quantum dots* were covalently functionalized with oriented, specific half-antibodies against pRBCs infected with *P. falciparum* late forms trophozoites and schizonts and confocal fluorescence microscopy was used in order to assess nanovector specificity and subcellular targeting. Results obtained show that in less than 90 minutes, liposomes dock to pRBC plasma membranes and release their cargo to the cell. 100.0% of late form-containing pRBCs and 0.0% of non-infected RBCs in *P. falciparum* cultures are recognized and permeated by the content of targeted immunoliposomes (Figure 14). Liposomes not functionalized with antibodies are also directed to pRBCs, although with less affinity than immunoliposomes. In preliminary assays, the antimalarial drug chloroquine at a concentration of 2 nM, ≥ 10 times below its IC_{50} in solution, cleared 26.7 ± 1.8% of pRBCs when delivered inside targeted immunoliposomes.

Other cell types beside RBCs will be exposed to immunoliposomes in the blood stream, mainly leukocytes and blood vessel endothelium. Endothelial cells are sufficiently abbundant to compete with RBCs for liposome uptake. In supplementary data we show that endothelial cells incorporate liposomes and immunoliposomes but when living pRBCs were added to HMEC-1 cultures, the uptake by endothelial cells does not significantly affect the delivery of immunoliposome contents to pRBCs.

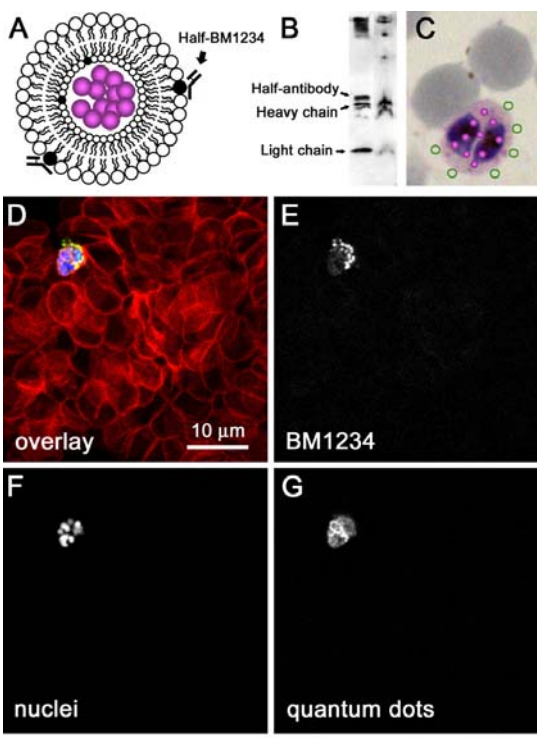

Figure 14. Confocal fluorescence microscopy analysis of the delivery of immunoliposome cargo to pRBCs, corresponding to figure 6 in the article. (A) Cartoon showing a quantum dot-containing liposome functionalized with half-antibodies. (B) Western blot analysis of BM1234half-antibodies (left lane), and (right lane) immunoliposomes. (C) Graphical scheme of the expected performance of nanovectors when added to a *P. falciparum* culture. (D) Confocal fluorescence microscopy section of a suspension of living RBCs that had been treated with immunoliposomes. The selected field contains a single pRBC among tens of non-infected cells, showing the fluorescence of RBC plasma membranes (red), antibody detection (green), quantum dots (white), and nuclei (blue). For an easier visualization of quantum dots and antibodies only in pRBCs, the fluorescence signals for (E) antibody, (F) nuclei, and (G) quantum dots are shown separately in white color.

Journal of Controlled Release 151 (2011) 202–211

Contents lists available at ScienceDirect

Journal of Controlled Release

journal homepage: www.elsevier.com/locate/jconrel

A nanovector with complete discrimination for targeted delivery to *Plasmodium falciparum*-infected versus non-infected red blood cells *in vitro*

Patricia Urbán [a,b,c], Joan Estelrich [d], Alfred Cortés [e,f], Xavier Fernàndez-Busquets [a,b,c,*]

[a] *Nanobioengineering Group, Institute for Bioengineering of Catalonia, Baldiri Reixac 10-12, Barcelona E08028, Spain*
[b] *Biomolecular Interactions Team, Nanoscience and Nanotechnology Institute (IN²UB), University of Barcelona, Martí i Franquès 1, Barcelona E08028, Spain*
[c] *Barcelona Centre for International Health Research (CRESIB, Hospital Clínic-Universitat de Barcelona), Rosselló 132, Barcelona E08036, Spain*
[d] *Departament de Fisicoquímica, Facultat de Farmàcia, IN²UB, University of Barcelona, Av. Joan XXIII, s/n, Barcelona E08028, Spain*
[e] *Institute for Research in Biomedicine, Barcelona Science Park, Baldiri Reixac 10-12, Barcelona E08028, Spain*
[f] *Institució Catalana de Recerca i Estudis Avançats (ICREA), Passeig Lluís Companys 23, Barcelona E08018, Spain*

ARTICLE INFO

Article history:
Received 7 October 2010
Accepted 4 January 2011
Available online 9 January 2011

Keywords:
Antimalarial chemotherapy
Chloroquine
Half-antibodies
Immunoliposomes
Malaria
Nanomedicine

ABSTRACT

Current administration methods of antimalarial drugs deliver the free compound in the blood stream, where it can be unspecifically taken up by all cells, and not only by *Plasmodium*-infected red blood cells (pRBCs). Nanosized carriers have been receiving special attention with the aim of minimizing the side effects of malaria therapy by increasing drug bioavailability and selectivity. Liposome encapsulation has been assayed for the delivery of compounds against murine malaria, but there is a lack of cellular studies on the performance of targeted liposomes in specific cell recognition and on the efficacy of cargo delivery, and very little data on liposome-driven antimalarial drug targeting to human-infecting parasites. We have used fluorescence microscopy to assess *in vitro* the efficiency of liposomal nanocarriers for the targeted delivery of their contents to pRBCs. 200-nm liposomes loaded with quantum dots were covalently functionalized with oriented, specific half-antibodies against *P. falciparum* late form-infected pRBCs. In less than 90 min, liposomes dock to pRBC plasma membranes and release their cargo to the cell. 100.0% of late form-containing pRBCs and 0.0% of non-infected RBCs in *P. falciparum* cultures are recognized and permeated by the content of targeted immunoliposomes. Liposomes not functionalized with antibodies are also specifically directed to pRBCs, although with less affinity than immunoliposomes. In preliminary assays, the antimalarial drug chloroquine at a concentration of 2 nM, ≥10 times below its IC_{50} in solution, cleared 26.7 ± 1.8% of pRBCs when delivered inside targeted immunoliposomes.

1. Introduction

Malaria is an acute and/or chronic infection caused by protozoans of the genus *Plasmodium*. Clinical manifestations can include fever, chills, prostration and anaemia. Severe disease can include severe anaemia, metabolic acidosis, cerebral malaria and multi-organ system failure, and coma and death may ensue. Malaria is one of the leading causes of morbidity and mortality in the tropics, with 300 million to 500 million estimated clinical cases and 1.5 million to 2.7 million deaths worldwide per year, of which the large majority are children below 5 years [1,2]. The recent call for the elimination and eradication of the disease requires research from multiple fronts, including developing strategies for the efficient delivery of new medicines [3]. Four species cause disease in humans: *P. vivax*, *P. ovale*, *P. malariae*, and *P. falciparum*, with the latter causing the most deadly and severe cases. In the life cycle of *Plasmodium* parasites (for a review see [4]) the female *Anopheles* mosquito inoculates during a bite *Plasmodium* sporozoites that in the liver bind to and infect hepatocytes and proliferate into thousands of merozoites. Merozoites rupture from the hepatocytes and invade red blood cells (RBCs), where they develop first into rings, and then into the late forms trophozoites and schizonts. Schizont-infected RBCs burst and release more merozoites, which start the blood cycle again. Because the blood-stage infection is responsible for all symptoms and pathologies of malaria, *Plasmodium*-infected RBCs (pRBCs) are a main chemotherapeutic target [5].

The need to develop new strategies to treat malaria is urgent if one considers that the cases of resistance to current antimalarial agents are increasing, especially in zones in which *P. falciparum* is endemic, and calls for combined therapy approaches [3,6]. Several drugs show different degrees of toxicity, which limits their use because current administration forms release the free compound in the blood and offer little specificity regarding the targeted cells [7]. Consequently, to achieve therapeutic levels that extend over time, the initial concentration of the drug in the body should be high. But on the other hand, if the administered chemical has unspecific toxicity, the low doses that are

* Corresponding author. Nanobioengineering Group, Institute for Bioengineering of Catalonia, Baldiri Reixac 10-12, Barcelona E08028, Spain. Tel./fax: + 34 93 403 7180/7181.
E-mail address: xfernandez_busquets@ub.edu (X. Fernàndez-Busquets).

0168-3659/$ – see front matter © 2011 Elsevier B.V. All rights reserved.
doi:10.1016/j.jconrel.2011.01.001

required contribute to the development of resistant parasite strains [8]. The challenge of drug delivery is the liberation of adequate doses of therapeutic agents to a specific target site at the right time in a safe and reproducible manner [9]. A number of mechanisms can provide controlled release, including transdermal patches, implants, inhalation systems, bioadhesive systems, and nanoencapsulation [10–12]. Taking into acount the peculiarities of RBCs and malaria parasites, lipid-based nanocarriers have been one of the most promising approaches [13].

Liposomes are synthetic lipid bilayer-enclosed structures up to several hundred nm in diameter that can improve the delivery of bioactive molecules by functioning as circulating microreservoirs for sustained release [14,15]. Liposomes bearing cell-specific recognition ligands on their surfaces have been widely considered as drug carriers in therapy [16,17], and liposome encapsulation has been assayed for the targeted delivery of compounds against murine malaria [18–20]. Liposomal nanovessels incorporating a *P. berghei* amino acid sequence have been shown to greatly increase their targeting to liver [21,22], suggesting that they can be an adequate vector to channel antimalarials towards the hepatocyte stages of the parasite. Despite these promising early results, liposomal-based targeted delivery has not progressed yet towards a working strategy to fight malaria, probably because of the lack of sufficiently specific markers for *Plasmodium*-infected cells. Throughout the intraerythrocytic phase of its lifecycle the malaria parasite modifies the plasma membrane of the host RBC [23–25], and the identification of pRBC-specific labels is of interest in the search for potential targets in drug delivery strategies [26,27]. *Plasmodium* proteins are also found in the plasma membrane of pRBCs [25], but those currently known are highly variable and do not represent good choices for targeted drug delivery strategies [28].

Different methods have been used to minimize the uptake of circulating liposomes by blood nucleated cells, such as the coating of liposomes with polyethyleneglycol [29,30]. However, it is surprising that to date there is not a single protocol available for the specific targeting of liposomal contents to pRBCs versus non-infected RBCs, which are by far the main particles to avoid in a targeted drug delivery strategy given their similarity and abundance compared to pRBCs. Discriminating parasitized from non-parasitized RBCs would allow the use of drugs targeting vital cell components present also in *Plasmodium*-free RBCs, such as cytoskeletal or plasma membrane elements, hemoglobin structure, or glycolytic enzymes. In addition to a complete lack of cellular studies on the performance of targeted liposomes in specific pRBC recognition and on the efficacy of cargo delivery, most assays up to date have been performed with mouse-specific *Plasmodium* species, and very little data on liposome-driven antimalarial drug delivery is available for human-infecting parasites. We have undergone the development of a nanovector for the targeted delivery of antimalarial drugs into human pRBCs. The first phase of the vector development contemplates the design of a nanocarrier able to (i) encapsulate drugs, (ii) dock specifically to pRBCs, and (iii) release its contents inside these cells, but not in non-infected RBCs. Here we present the experimental approach followed to achieve these objectives.

2. Materials and methods

2.1. Materials

Except where otherwise indicated, all reagents were purchased from Sigma-Aldrich (St. Louis, MO, USA). Commercial monoclonal antibodies against *P. falciparum* pRBCs BM1232 and BM1234 were obtained from Acris (Herford, Germany).

2.2. Binding of antibodies to gold nanoparticles

Biotinylated Protein G (1 mg/ml, Pierce Biotechnology), streptavidin-labeled gold nanoparticles (Nanocs Inc., NY, USA), and anti-glycophorin A antibodies (1 mg/ml, Acris) were mixed in equimolar amounts in a phosphate-buffered solution, pH 7.4 (PBS) and incubated for 3 h at 4 °C. Blocking of Protein G free reactive sites was achieved by incubation with Fc fragments (Chemicon International, Inc., CA, USA) for an hour at 4 °C. The sample was finally spun down for 5 min at 16,000 *g* and washed with PBS twice. Functionalized gold nanoparticles were incubated overnight with washed RBCs (see below) at 4 °C before sample processing for confocal or transmission electron microscopy.

2.3. Liposome preparation

Liposomes were prepared by the lipid film hydration method [31]. Different lipid combinations were tested in order to establish a liposomal formulation with low hemolytic activity and low general cytotoxicity. Lipids (phosphatidylcholine, PC; phosphatidylethanolamine, PE; cholesterol; 1,2-dioleoyl-*sn*-glycero-3-phosphatidylcholine, DOPC, Avanti Polar Lipids Inc., Alabaster, AL, USA; all ≥99% purity according to thin layer chromatography analysis) were dissolved in chloroform:methanol (2:1 v/v) in a round-bottomed flask. Organic solvents were removed by rotary evaporation under reduced pressure at 37 °C to yield a thin lipid film on the walls of the flask, and remaining solvent traces were eliminated by drying under N_2 flow for 30 min. Films were left overnight in a desiccator to ensure the complete removal of chloroform. The dry lipids were hydrated in PBS at 37 °C to obtain a concentration of 10 mM and multilamellar liposomes were formed by 3 cycles of constant vortexing followed by bath sonication for 4 min each. Multilamellar liposomes were downsized to form uni- or oligolamellar vesicles by extrusion through 200-nm polycarbonate membranes (Poretics, Livermore, CA, USA) in an extruder device (LiposoFast, Avestin, Ottawa, Canada). Liposome size was determined by dynamic light scattering using a Zetasizer NanoZS90 (Malvern Ltd, Malvern, UK). Liposomes encapsulating the fluorescent probe pyranine (10 mM), 120 nM 655 ITK™ carboxyl quantum dots (Molecular Probes), or the antimalarial drug chloroquine were prepared by dissolving them in the hydration buffer. Finally, liposomes were purified by molecular exclusion chromatography (Zeba desalt spin columns, Pierce Biotechnology), and immunoliposomes were functionalized with half-antibodies as described below.

2.4. Generation of half-antibodies and immunoliposomes

The mild reducing agent 2-mercaptoethylamine-HCl (MEA, Pierce Biotechnology) was used to generate half-antibodies [32,33]. 90 μl of a 0.1 mg/ml antibody solution in PBS was added to 10 μl of 10× reaction buffer (PBS containing 5 mM EDTA and 50 mM MEA), and incubated for 90 min at 37 °C in a water bath. Unreacted MEA was separated from reduced half-antibodies by molecular exclusion chromatography. For the coupling of targeting antibodies to liposomes we followed established protocols [34] that use 1,2-dipalmitoyl-sn-glycero-3-phosphoethanolamine-N-[4-(p-maleimidophenyl)butyramide] (MPB-PE, Avanti Polar Lipids Inc.) to incorporate proteins into liposomes through the reaction of the maleimide group in the lipid with a thiol group from the ligand. In the case of antibodies the free thiol was obtained by generating half-antibodies as described above. MPB-PE-containing liposomes (10 mM lipid) were incubated with half-antibodies (0.01 μg/μl, 133 nM half-antibody assuming complete reduction by MEA) overnight at 4 °C. Immunoliposomes were pelleted by ultracentrifugation (100,000 *g*, 2×, 45 min, 4 °C), and finally resuspended in 10 volumes of PBS and kept at 4 °C for up to 2 weeks before adding them to RBC-containing samples. Because MPB-PE is always in a large molar excess relative to antibodies (ca. 1000-fold), all half-antibodies should be bound to liposomes. Assuming complete efficiency of MEA treatment and incorporation of all lipids into unilamellar 200-nm liposomes, about 5 half-antibody

molecules will be bound to each liposome (M_r DOPC = 786; area occupied by DOPC in a lipid bilayer = 0.7 nm^2/molecule [35]; M_r of a 100-nm radius unilamellar liposome = 2.8×10^8).

2.5. Western blots

Electrophoresis was performed in 10% SDS-polyacrylamide gels using the Mini Protean II System (Bio-Rad Laboratories Inc.). Samples were boiled in the presence of sample buffer for 5 min, electrophoresed at room temperature, and transferred to a polyvinylidene difluoride membrane (Hybond-P, Amersham Biosciences) at 300 mA for 3 h at 4 °C. The membrane carrying the blotted proteins was blocked with 100 mM Tris–HCl, pH 7.4, 100 mM $MgCl_2$, 1% Triton X-100, 0.5% Tween-20, 5% FCS, and 1% BSA, and incubated for 1 h with goat anti-mouse antibody conjugated to horseradish peroxidase (Upstate) diluted 1:2000 in blocking buffer. Immunoreactivity was detected using enhanced chemiluminescence (ECL, Amersham Biosciences) and imaged on medical X-ray film (Fujifilm, FUJI). Molecular masses were estimated using commercial protein markers (Bio-Rad Laboratories Inc.).

2.6. Treatment of blood

Human blood group B, collected in citrate–phosphate–dextrose (CPD) buffer, was provided by the *Banc de Sang i Teixits* at the *Hospital Vall d'Hebron* in Barcelona (www.bancsang.net/ca). 10 ml of full blood was collected in 50-ml centrifuge tubes, spun for 5 min at 1200 *g*, and plasma and buffy coat were removed. The resulting RBC pellet was resuspended in 40 ml of washing medium containing 10.4 g/l RPMI-1640 (Invitrogen), 25 mM HEPES, 100 μM hypoxanthine, 12.5 μg/ml gentamicin, and 23.8 mM sodium bicarbonate, pH 7.2. After centrifugation at 1200 *g* for 10 min the supernatant was discarded, and after another washing step in 15-ml tubes, the RBC pellet was taken up in one volume of Roswell Park Memorial Institute (RPMI) complete medium (washing medium supplemented with 0.5% Albumax, 0.2% glucose, 25 μg/ml gentamicin, 50 μg/ml hypoxanthine, and 2 mM glutamine), stored at 4 °C and used within 10 days (washed RBCs).

2.7. Cytotoxicity and hemolysis assays

Human Microvascular Endothelial Cells (HMEC-1, CDC) and 3T3 fibroblasts were cultured in MCDB (Invitrogen) or Dulbecco's modified Eagle's medium (DMEM, Biological Industries, Israel), respectively, supplemented with 10% heat-inactivated foetal bovine serum (FBS, PAA Laboratories, Germany), 1% each penicillin/streptomycin (Biological Industries), and 10 mM glutamine (HMEC-1) or 1% glutamine plus 1% sodium pyruvate (3T3). For cytotoxicity assays 5000 cells/well were plated in 96-well plates (Thermo Fisher Scientific Inc.) and after 24 h at 37 °C in 5% CO_2 atm the medium was substituted by 100 μl of liposome-containing (100 μM lipid final concentration) culture medium without FBS, and incubation was resumed for 48 h. 10 μl of 4-[3-(4-iodophenyl)-2-(4-nitrophenyl)-2H-5-tetrazolio]-1,3-benzene disulfonate labeling reagent (WST-1, Roche Diagnostics GmbH) was added to each well, and the plate was incubated in the same conditions for 3 h. After thoroughly mixing for 1 min on a shaker, the absorbance of the samples was measured at 440 nm using a Benchmark Plus microplate reader (Bio-Rad Laboratories Inc.). WST-1 in the absence of cells was used as blank and samples were prepared in triplicate for each experiment.

For hemolysis assays, human blood collected in CPD buffer was washed as described previously. After the last washing step RBCs were diluted in PBS to yield a solution with 3% hematrocrit. 200 μl of RBCs from this suspension and 2 μl of each liposome sample (100 μM lipid final concentration) were added to a 96-well plate. Each assay was performed in triplicate, including positive (1% Triton X-100) and negative (PBS) controls. After incubating for 3 h at 37 °C, samples were collected in eppendorf tubes, spun at 16,000 *g* for 5 min, and the supernatant absorbance was measured at 541 nm.

2.8. Plasmodium falciparum cell culture and growth inhibition assays

Cultures of *P. falciparum* strains 3D7 and D10 were grown *in vitro* in group B human RBCs using previously described conditions [36]. Briefly, parasites (thawed from glycerol stocks) were cultured at 37 °C in Petri dishes containing RBCs in RPMI complete medium under a gas mixture of 92% N_2, 5% CO_2, and 3% O_2. Synchronized cultures were obtained by 5% sorbitol lysis [37], and the medium was changed every 2 days maintaining 3% hematocrit. If necessary to study stage-specific differential protein expression like band 3 (increasingly expressed in pRBCs infected by late ring forms), parasites were selected by gelatin flotation to enrich in trophozoites and schizonts. For culture maintenance, parasitemias were kept below 5% late forms by dilution with washed RBCs. Liposomes and immunoliposomes (at a final concentration of 100 μM lipid) were incubated with washed living RBCs or pRBC cultures for 90 min at 37 °C. After incubation cells were spun down 2× at 2 min each at 1000 *g* and washed with PBS before processing for fluorescence microscopy or transmission electron microscopy.

For growth inhibition assays, parasitemia was adjusted to 1.5% with more than 90% of parasites at ring stage after sorbitol synchronization. 200 μl of this *Plasmodium* culture was plated in 96-well plates and incubated in the presence of liposomes for 48 h in the conditions described above. For chloroquine assays, synchronized cultures were incubated for 24 h before addition of drug to allow for the appearance of late forms presenting the epitope recognized by BM1234 bound to immunoliposomes. Parasitemia was determined by microscopic counting of blood smears, or by fluorescence-assisted cell sorting (FACS). Smears were fixed in methanol for a few seconds and then stained for ten minutes with Giemsa (Merck Chemicals, Germany) diluted 1:10 in Sorenson's Buffer, pH 7.2. After washing with distilled water and drying, the ratio of infected versus non-infected RBCs was determined by microscopic analysis.

For FACS analysis, several nucleic acid dyes had been assayed and Syto 11 was found to be the best stain for the discrimination of parasitized from non-parasitized RBCs. Each sample was diluted at 1:200 in PBS and Syto 11 (0.5 mM in DMSO) was added to a final concentration of 0.5 μM. Samples were analyzed using an Epics XL flow cytometer (Coulter Corporation, Miami, Florida), set up with the standard configuration. Excitation of the sample was done using a standard 488 nm air-cooled argon-ion laser at 15 mW power. Forward scatter and side scatter were used to gate the RBC population. Syto 11 green fluorescence was collected in a logarithmic scale with a 550 dichroic long filter and a 525 band pass filter. The single-cell population was selected on a forward-side scatter scattergram, and the fluorescence from this population was analyzed. Parasitemia was expressed as the number of parasitized cells per 100 erythrocytes.

2.9. Transmission electron microscopy (TEM)

Erythrocytes incubated with immunoliposomes were fixed at 4 °C for 2 h in 2% paraformaldehyde and 2.5% glutaraldehyde in PBS, followed by 4× 10 min PBS washes. Fixed samples were treated for 2 h with OsO_4, washed 4× at 10 min each with H_2O, and dehydrated in an ascending series of acetone, from 50% to 100%. The samples were infiltrated with gentle stirring at room temperature by gradually substituting the solvent by acrylic Epon resin (Electron Microscopy Sciences, Hatfield, PA) (acetone:resin 3:1, 2:2, and 1:3, v/v), with three final immersions in pure resin. The sample was finally poured in the adequate blocks and let to polymerize under UV light. Sections were obtained with a Leica Ultracut UCT ultramicrotome (Leica Microsystems GmbH, Wetzlar, Germany), mounted on formvar-coated 200-mesh copper grids, and finally stained with 2% uranyl

acetate and 0.8% lead citrate in water. Samples were observed in a JEM-1010 electron microscope (Jeol, Japan) operated at 80 kV.

For cryo-TEM analysis of the preparations of liposomes loaded with quantum dots, a thin aqueous film was formed by dipping a glow-discharged holey carbon grid in the liposome suspension and then blotting the grid against filter paper. The resulting thin sample films spanning the grid holes were vitrified by plunging the grid (kept at 100% humidity and room temperature) into ethane, which was maintained at its melting point with liquid nitrogen, using a Vitrobot (FEI Company, Eindhoven, The Netherlands). The vitreous films were transferred to a Tecnai F20 TEM (FEI Company) using a Gatan cryotransfer, and the samples were observed in a low dose mode. Images were acquired at 200 kV at a temperature between −170 °C and −175 °C, using low-dose imaging conditions not exceeding 20 $e^{-}/Å^2$, with a 4096×4096 pixel CCD Eagle camera (FEI Company), and digitized with the TIA (Tecnai Image Adquisition) programme.

2.10. Fluorescence microscopy

Immunofluorescence assays for free BM1232 and BM1234 monoclonal antibodies were done at a final concentration of 2 μg antibody/ml *P. falciparum* cell cultures. Free antibodies, anti-glycophorin A-conjugated gold nanoparticles, and (immuno)liposomes containing 10 mM pyranine or 120 nM 655 ITK™ carboxyl quantum dots were incubated with non-infected RBCs or with 3D7 or D10 *P. falciparum* cell cultures for 90 min at 37 °C with gentle stirring. Free antibodies were assayed with both fixed and nonfixed cells, whereas nanoparticles and (immuno)liposomes were always added to living cells. Primary antibodies were detected with a secondary fluorescent antibody AlexaFluor 488 goat anti-mouse $F(ab')_2$ (Molecular Probes, Eugene, OR, USA). Parasite nuclei were stained with 4′ 6-diamino-2-phenylindole (DAPI, Invitrogen) during secondary antibody incubation. When required, the RBC membrane was labeled with wheat germ agglutinin(WGA)-tetramethylrhodamine conjugate (Molecular Probes). After the corresponding incubations and PBS washing steps, the samples were fixed for 20 min with 3% (v/v) paraformaldehyde in 0.1 M sodium phosphate buffer, pH 7.4, and finally mounted with Mowiol (Calbiochem, Merck Chemicals) following standard protocols [38]. Slides were analyzed with a Nikon E1000 fluorescence microscope using a Plan Apochromatic 100×1.4 oil objective or with a Leica SP2 confocal microscope, using an HCX Plan Apochromatic 63×NA 1.3 oil objective at several zoom factors.

For high-resolution fluorescence confocal microscopy, samples were imaged with a Leica TCS SP5 laser scanning confocal microscope equipped with an acoustic optical beam splitter, a DMI6000 inverted microscope, blue diode (405 nm), Ar (458/476/488/496/514 nm), diode pumped solid state (561 nm), and HeNe (594/633 nm) lasers, and APO 63× oil (NA 1.4) or glycerol (NA 1.3) immersion objective lenses. DAPI, quantum dot, AlexaFluor 488, reflection (for hemozoin detection), and WGA-rhodamine images were acquired sequentially using 405, 458, 488, 488 and 561 laser lines, and emission detection ranges 415–480 nm, 630–735 nm, 500–550 nm, 480–500 nm, and 571–625 nm, respectively, with the confocal pinhole set at 1 Airy units. Bright field transmitted light images were acquired simultaneously. Images were acquired at 400 Hz in a 512×512 pixels format, 8× zoom, and pixel size of 60×60 nm.

3. Results

3.1. Preparation of immunoliposomes

In order to select a liposome preparation not affecting RBC integrity we first performed hemolysis assays with different basic lipid formulations (Table 1). Liposomes containing DOPC:cholesterol 80:20 induced virtually no hemolysis and were thus selected for the next steps. Unilamellar liposomes with a mean diameter of 200 nm (Fig. 1A) were prepared following established protocols [39], yielding suspensions with a polydispersity index <0.1.

Table 1
Hemolysis induced by different liposome formulations.

Lipid formulation	Hemolysis (relative to PBS)
1% Triton (positive control)	100.0 ± 1.3%
PC	0.8 ± 0.7%
DOPC	0.4 ± 0.4%
DOPC:cholesterol 80:20	−0.1 ± 0.0%
DOPC:cholesterol:PE 77.5:20:2.5	0.3 ± 0.6%
DOPC:cholesterol:PE 65:20:15	−0.1 ± 0.0%
DOPC:cholesterol:MPB-PE 77.5:20:2.5	0.1 ± 0.2%
DOPC:cholesterol:MPB-PE 65:20:15	0.0 ± 0.3%

For the covalent oriented binding of antibodies to liposomes (Fig. 1B) a fast and non-aggressive method was chosen which consisted of treatment with the mild reducing agent 2-mercaptoethylamine (MEA) to generate half-antibodies containing a free thiol group adequate for their covalent linkage to thiol-reacting lipids [34] (Fig. 1C). Western blot analysis of the resulting fragmentation of anti-glycophorin A antibodies indicated that MEA treatment of IgG isotype consistently generated an acceptable amount of half-antibody over a wide range of MEA concentrations (Fig. 1D), although heavy and light chains were also released. Half-antibodies were freed from MEA by size exclusion chromatography and immediately added to liposomes containing the lipid derivative MPB-PE (Fig. 1E) in a proportion of DOPC:cholesterol:MPB-PE 77.5:20:2.5. Reaction of the MPB-PE maleimide group with the free thiol in half-antibody molecules resulted in the formation of immunoliposomes (Fig. 1F). MPB-PE did not

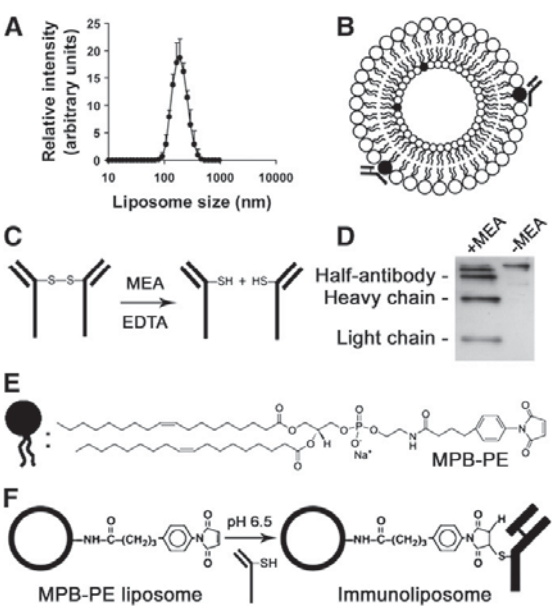

Fig. 1. Preparation of immunoliposomes. (A) Dynamic light scattering analysis of liposome size distribution. (B) Cartoon showing a liposome functionalized with half-antibodies bound to MPB-PE, represented as black lipid molecules. (C) Scheme of the generation of half-antibodies through reduction with MEA (modified from Pierce Biotechnology catalog). (D) Western blot analysis of anti-glycophorin A IgGs (right lane) before and (left lane) after MEA treatment. (E) Structure of MPB-PE (extracted from Avanti Lipids catalog), represented as black lipid molecules in panel (B). (F) Scheme of the reaction of free thiols in half-antibodies with the maleimide group of MPB-PE to generate immunoliposomes (modified from [34,40]).

Table 2
Cell viability of HMEC-1 and 3T3 cells treated with DOPC:cholesterol:MPB-PE (77.5:20:2.5) liposomes and BM1234-conjugated immunoliposomes (see below) at 100 μM and 1 mM final lipid concentration.

(Immuno)liposome concentration	Cell viability (relative to PBS) HMEC-1/3T3
Liposomes (1 mM lipid)	98.6 ± 3.8%/96.7 ± 3.5%
Liposomes (100 μM lipid)	100.3 ± 0.7%/99.6 ± 5.1%
Immunoliposomes (1 mM lipid)	100.4 ± 6.0%/100.9 ± 0.8%
Immunoliposomes (100 μM lipid)	101.6 ± 4.8%/99.3 ± 4.8%

induce hemolysis up to a content of 15% in the liposome formulation (Table 1).

At the lipid concentration and liposome formulation used below in pRBC cultures, immunoliposomes did not induce significant unspecific cytotoxicity on fibroblasts and endothelial cells (Table 2). In growth inhibition assays, *Plasmodium* viability was not affected by the presence of DOPC:cholesterol:MPB-PE (77.5:20:2.5) liposomes (1 mM lipid; 0.3 ± 0.9% inhibition of growth relative to liposome-free medium according to FACS analysis).

3.2. Half-antibody targeting of liposomes towards red blood cells

To assess whether half-antibodies were able to efficiently direct liposomes to target cells we performed confocal immunofluorescence microscopy assays using antibodies against the RBC cell surface protein glycophorin A. Streptavidin-functionalized gold nanoparticles conjugated to whole human anti-glycophorin A IgG antibodies through intervening biotin-labeled protein G bound to RBCs with the expected homogeneous pattern (Fig. 2A, and B). 200-nm immunoliposomes functionalized with anti-glycophorin A half-antibodies also targeted RBCs with high efficiency (Fig. 2C, and D). The resulting few fluorescent patches per cell were consistent with the arrival of antibodies concentrated on the surface of a smaller number of particles (liposomes). The size of many fluorescent areas reached more than 1 μm across, suggesting fusion and subsequent spreading of the liposome lipid bilayer within the erythrocyte plasma membrane. TEM analysis of RBCs treated with anti-glycophorin A half-antibody-functionalized liposomes showed abundant events of liposome-RBC docking (Fig. 2E), and of apparent fusion processes (Fig. 2F,G). Fusion events visualized by TEM showed intimate apposition of RBC and liposome membranes, with an area of low electron density in the zones inside RBCs opposite liposome contact points (Fig. 2G), suggestive of infiltration of liposomal contents into erythrocytes.

In addition to specific docking, an efficient antimalarial targeted drug delivery system requires release of the liposome cargo to target cells. In a proof of concept assay we added to RBC suspensions with ca. 10% hematocrit 200-nm liposomes loaded with the green fluorescent dye pyranine and targeted with anti-glycophorin A half-antibodies. Liposomes were observed to bind RBCs but pyranine fluorescence could not be detected inside the cells (Fig. 2H), indicating that whole liposomes did not enter the erythrocyte. Analysis of the pile up of confocal fluorescence microscopy sections spanning whole RBCs (Fig. 2H) revealed fluorescent spots of different sizes on RBC plasma membranes, suggestive of pyranine-containing liposomes in different stages from membrane docking through membrane fusion and release of their content. If pyranine entered RBCs due to a membrane fusion process followed by liposome content delivery, its ca. 14,000-fold dilution probably resulted in a fluorochrome concentration far below the microscope detection limit.

3.3. Delivery of immunoliposome cargo inside RBCs

To circumvent the obstacle of low pyranine fluorescence at its large dilution inside RBCs we made use of luminescent semiconductor

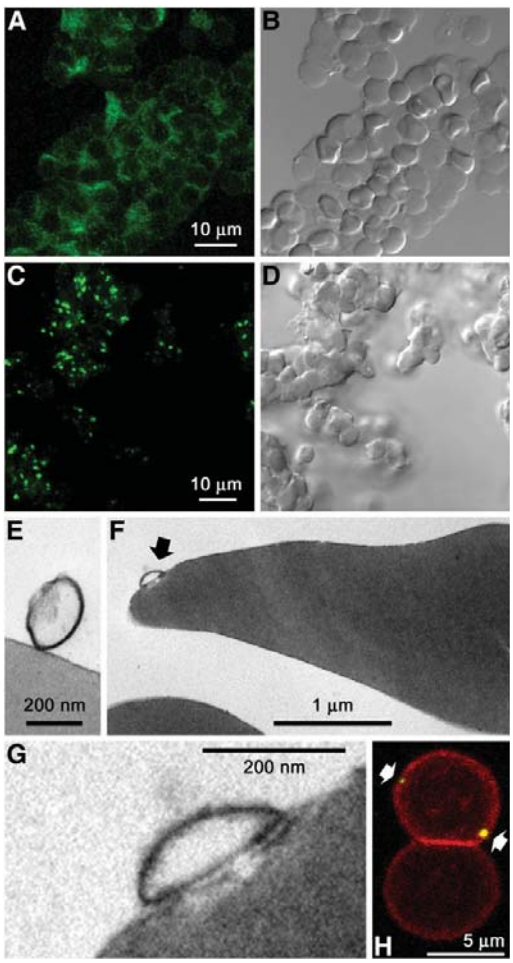

Fig. 2. Half-antibody targeting of liposomes towards RBCs. (A,B) Whole human anti-glycophorin A antibodies were conjugated to 5-nm gold beads, added to a suspension of human RBCs, and (A) detected by confocal fluorescence microscopy. (C–G) Half-antibodies against glycophorin A were conjugated to liposomes, and added to a suspension of human RBCs. The resulting samples were analyzed by (C) confocal fluorescence microscopy and (E–G) TEM. Panels (A) and (C) show the fluorescence of secondary antibodies against anti-glycophorin A IgGs. Panels (B) and (D) show the phase contrast images of the fields in panels (A) and (C), respectively. The arrow in panel (F) indicates a liposome-RBC fusing event shown at higher magnification in panel (G). (H) Immunoliposomes conjugated to anti-glycophorin A half-antibodies were loaded with the fluorescent green dye pyranine and added to RBC suspensions. The confocal fluorescence microscopy image shown corresponds to the detection of RBC membranes (red) and pyranine (green) in a stack of 18 individual sections. The arrows indicate sites of liposome-RBC binding.

nanocrystals termed quantum dots [41]. Quantum dots provide unique intrinsic photophysical properties for potential medical, diagnostic and basic research applications, among them high quantum yields and high molar extinction coefficients along with exceptional resistance to both chemical and photodegradation. Quantum dot encapsulation into liposomes can be studied by electron microscopy and their release to RBCs can be conveniently followed by fluorescence microscopy over a wide concentration range, a versatility that cannot be matched by small fluorochromes. According to cryo-TEM analysis, 655 ITK™ carboxyl quantum dot-loaded liposomes that had been purified by size exclusion chromatography contained

variable numbers of quantum dots that were either associated to the membrane or free in the liposomal lumen (Fig. 3A–D). Under the preparation conditions used in this work, approximately half of the liposomes were observed to contain at least one quantum dot. When such liposomes targeted with anti-glycophorin A half-antibodies were added to RBCs cultured at ca. 7% hematocrit, antibody detection indicated an efficient targeting (Fig. 3E). Quantum dot fluorescence was observed in RBCs, apparently associated with preference to the plasma membrane (Fig. 3F), but also in the cytosol, suggesting that targeted liposomes can be efficient carriers of both cytosolic and membrane-bound drugs.

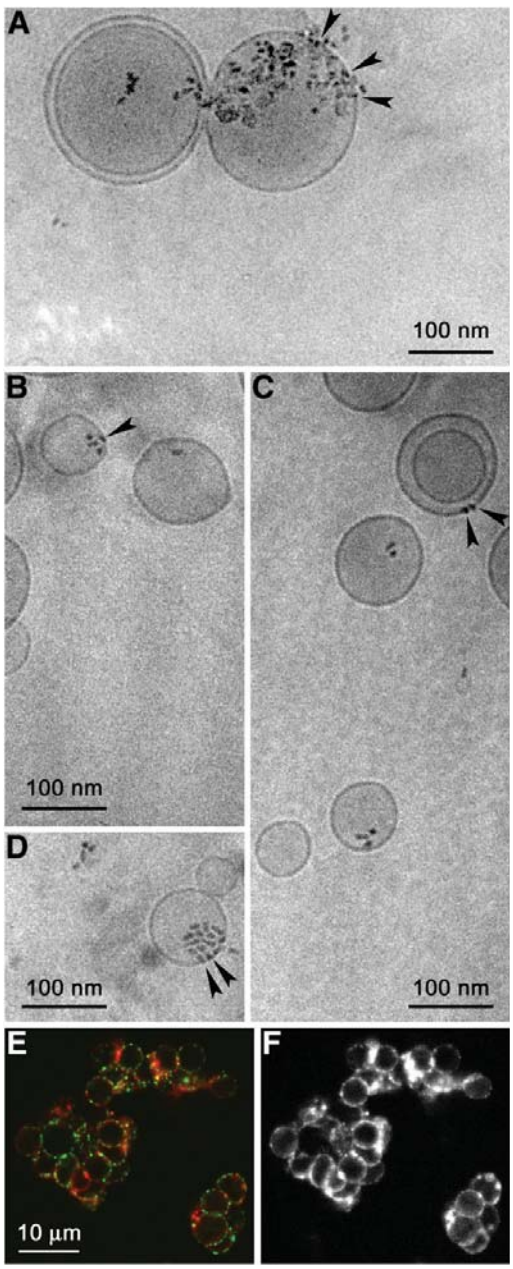

Fig. 3. Delivery of immunoliposome cargo inside RBCs. (A–D) Cryo-TEM images of liposomes loaded with 655 ITK™ carboxyl quantum dots and purified by molecular exclusion chromatography. Arrowheads indicate quantum dots associated to liposome membranes. (E) Confocal fluorescence microscopy image of RBCs treated with 655 ITK™ carboxyl quantum dot-containing immunoliposomes conjugated to anti-glycophorin A half-antibodies, showing the localization of targeting antibody in green and of quantum dots in red. (F) Image showing in white only the fluorescence of quantum dots in panel E to illustrate their delivery to RBCs.

3.4. Analysis of the binding to pRBCs of specific antibodies

In the search for antibodies having a high specificity for pRBCs we explored commercially available monoclonal antibodies prepared using as immunogen *P. falciparum* fractions, and two antibodies, BM1232 and BM1234, were finally selected. Both monoclonal antibodies, of the IgM isotype, were raised in mice against a trypsinized fraction of *P. falciparum* conjugated with mouse albumin, and when tested on fixed cultures of the 3D7 strain they bound pRBCs with high specificity (Fig. 4). BM1234 had complete discrimination for late forms (Fig. 4A,B, and E), with 100.0% ($n = 290$) recognition of mature trophozoite- and schizont-infected RBCs and 0.0% ($n > 1000$) binding to non-infected RBCs. BM1232 reacted specifically with pRBCs infected by all forms of the parasite (99.0% pRBC recognition, $n = 303$), likely binding *Plasmodium* itself (Fig. 4C,D, and F). BM1234 and BM1232 also recognized with complete specificity pRBCs infected with late forms and with all forms, respectively, of the *P. falciparum* D10 strain, exhibiting the same distinct fluorescence patterns as in 3D7 (data not shown). The efficacy of BM1234 and BM1232 in discriminating pRBCs from RBCs is illustrated by comparing it with the low specificity obtained with antibodies raised by us against certain regions of the anion transporter band 3 protein (Supplementary data, Fig. S1), which had been described as good pRBC markers [42]. Band 3 is an endogenous erythrocyte protein which undergoes a conformational change upon *Plasmodium* infection, exposing previously hidden epitopes. Because these regions are also made accessible in non-infected RBCs by band 3 clustering [23], the significant reactivity of our antibodies with non-infected RBCs might be due to clustering induction by our *in vitro* culture conditions. On the contrary, BM1232 and BM1234 always showed complete discrimination.

Both BM1232 and BM1234 were highly specific in binding RBCs infected by all stages and by late forms, respectively, of *P. falciparum* parasites. However, fluorescence microscopy images (Fig. 4) indicated that whereas BM1232 was detecting internal pRBC structures, BM1234 seemed to bind pRBCs externally. Detailed subcellular localization by confocal fluorescence microscopy of BM1234 binding sites on pRBCs (Fig. 5) confirmed a peripheral spotted pattern. Because the recognition of extracellular epitopes is an essential requirement for a targeted delivery strategy, BM1234 was selected for the subsequent assembly of a prototype nanovector.

3.5. Delivery of immunoliposome cargo inside pRBCs

Based on the results presented above we assembled a prototype nanovector (Fig. 6A) consisting of 655 ITK™ carboxyl quantum dots encapsulated in immunoliposomes with the formulation DOPC: cholesterol:MPB-PE 77.5:20:2.5. Treatment of the IgM isotype monoclonal antibody BM1234 with MEA provided a sample highly enriched in the half-antibody species (Fig. 6B, left lane). When the MEA-treated sample was added to MPB-PE-containing liposomes, half-antibodies were the main immunoliposome-bound species, followed by heavy chains and a small proportion of light chains (Fig. 6B, right lane). Quantum dot-loaded immunoliposomes were added to 3% hematocrit living cultures of the *P. falciparum* 3D7 strain at a concentration in the dish of 100 μM lipid to analyze whether they exhibited the expected targeting towards pRBCs (Fig. 6C). After incubating for 90 min with gentle stirring the samples were processed

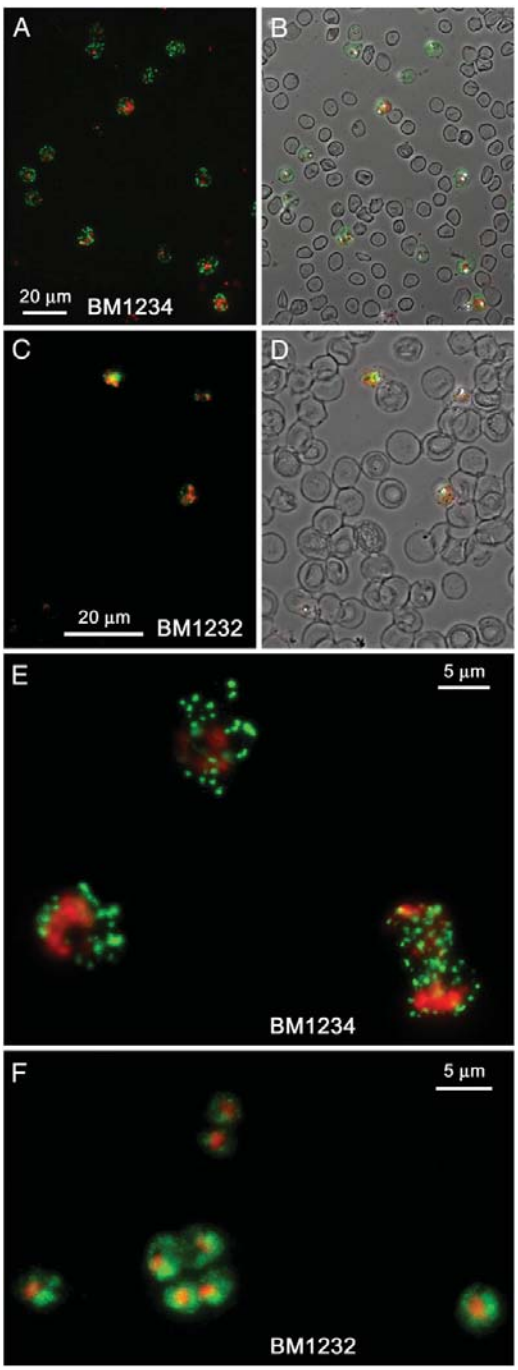

Fig. 4. Fluorescence microscopy study of the binding to pRBCs of antibodies raised against *P. falciparum* antigens. Monoclonal antibodies (A,B, and E) BM1234 and (C,D, and F) BM1232 were added to fixed *P. falciparum* cultures of the 3D7 strain and their binding was detected by fluorescence microscopy using a secondary antibody (green signal). DAPI fluorescence (red signal) is used to indicate pRBCs. Panels (B) and (D) are phase contrast images showing the overlap with RBCs of fluorescence signals in panels (A) and (C), respectively.

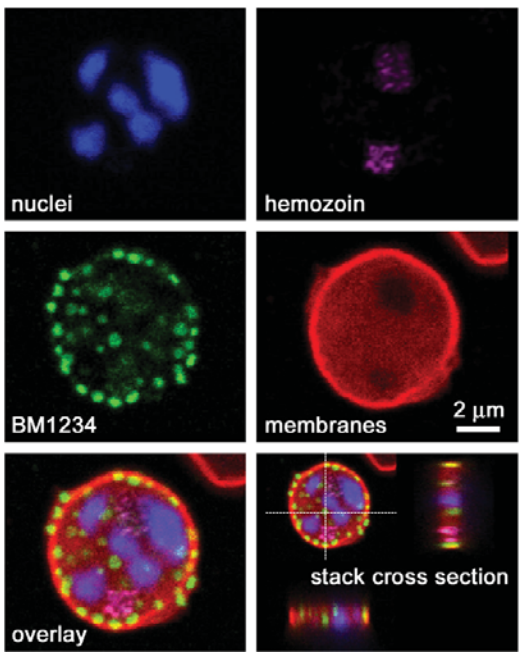

Fig. 5. Confocal fluorescence microscopy study of the subcellular localization of BM1234. Monoclonal antibody BM1234 was added to *P. falciparum* cultures of the 3D7 strain and its binding was detected by confocal fluorescence microscopy using a secondary antibody (green). DAPI (nuclei) and hemozoin fluorescence are used to indicate pRBCs. The RBC plasma membrane is shown in red. The four upper panels correspond to a single confocal section, and are overlaid in the lower left panel. The lower right panel shows two perpendicular cross sections throughout the stack of images.

for detection of quantum dots, antibody, and parasite nuclei by confocal fluorescence microscopy (Fig. 6D–G). The results obtained showed an invariable colocalization of the three signals only in late form-containing pRBCs. Quantitative targeting analysis (Fig. 6H) revealed that quantum dots were present in 100.0% ($n = 247$) of mature trophozoite- and schizont-containing pRBCs and in 0.0% ($n > 1000$) of non-infected RBCs. In controls performed with quantum dots encapsulated in liposomes lacking antibody functionalization (Fig. 6I), we detected quantum dots in a significant number (41.7%; $n = 252$) of late form-containing pRBCs. Although the fluorescence signal was relatively weak, the complete absence of quantum dots in non-infected RBCs (0.0%; $n > 1000$) suggested an intrinsic affinity of liposomes for pRBCs, even without specific targeting.

Again, BM1234-specific fluorescence exhibited a dotted pattern only on pRBCs (Fig. 7), whereas the fluorescence of quantum dots was clearly observed only inside pRBCs. The almost exclusively peripheral BM1234 localization and the homogeneous intracellular quantum dot fluorescence are in agreement with a process of liposome fusion and delivery of its contents inside the cell.

Other cell types besides RBCs will be exposed to targeted liposomes used as drug carriers in the blood stream, mainly leukocytes and blood vessel endothelium. Of these, leukocytes are in numbers several orders of magnitude below those of RBCs, but endothelial cells are sufficiently abundant to compete with RBCs for liposome intake. We have shown above that at the liposome concentrations used in this work HMEC-1 cells do not experience significant cytotoxic effects. However, they might contribute to the clearance from the blood of a significant amount of liposomes, thus reducing the efficacy of nanovector preparations. To explore this issue, we added living pRBCs to HMEC-1 cultures and after allowing a

time for cell deposition, delivery of immunoliposome cargo was explored as above. The results obtained (Supplementary data, Fig. S2) show that although endothelial cells incorporate liposome- (Fig. S2A) and immunoliposome-contained quantum dots (Fig. S2B), they do so in small amounts that do not affect the delivery of immunoliposome contents to pRBCs (Fig. S2C).

3.6. Targeted delivery of chloroquine

To make a preliminary assessment of the therapeutic capability of our immunoliposomal nanovector we used the antimalarial drug chloroquine at a concentration of 2 nM, ≥10 times below its reported IC_{50} in solution [43]. According to FACS analysis, soluble 2 nM chloroquine had virtually no effect on *P. falciparum* ($3.4 \pm 1.0\%$ inhibition of growth), whereas the same overall concentration administered inside targeted immunoliposomes induced $26.7 \pm 1.8\%$ *P. falciparum* growth inhibition. Because chloroquine targets a metabolic pathway inside the food vacuole [44], these results provide additional confirmation of the delivery of immunoliposomal contents inside pRBCs.

4. Discussion

Nanosized carriers have been receiving special attention with the aim of minimizing the side effects of malaria therapy by increasing bioavailability and selectivity of drugs [11]. RBCs have very poor endocytic processes, and for this reason liposomes docked by specific antibodies to RBCs can be an efficient system to deliver cargo into the cell by a simple membrane fusion process [45–47]. Liposomization of chloroquine has been described to increase its maximal tolerable dose and its efficacy against malarial infections [48]. Earlier studies have shown that encapsulation of chloroquine in liposomes bearing anti-pRBC antibody on their surfaces markedly increased its efficacy against *P. berghei* infections in mice [18,49]. This improvement was attributed to the specific interaction of the targeting monoclonal antibody $F(ab')_2$ fragments with pRBCs and to the efficient internalization of liposomes by infected cells [18]. Our data obtained with the human-infecting species *P. falciparum* show that provided the availability of sufficiently specific targeting molecules, drugs carried by liposomes can be delivered to pRBCs with complete specificity relative to non-infected RBCs, but liposomes docked to pRBCs are not internalized as a whole. Because according to cryo-TEM images we are delivering quantum dots inside liposomes, and because liposome-bound targeting antibody and quantum dots always colocalize in pRBCs, we deduce that liposomes fuse and deliver their contents inside pRBCs.

In view of future *in vivo* assays, reducing the amount of targeting antibodies will contribute to minimize the risk of triggering immune responses leading to liposome elimination. With this objective, we have used a previously described fast and non-aggressive strategy for the highly efficient covalent binding of half-antibodies to liposomes through the thiol groups in the hinge regions of immunoglobulin heavy chains [34]. This represents an improvement over the most generally used method for the covalent immobilization of antibody molecules through free amino groups [18], which has the risk of chemically modifying functionally important amino groups in the antigen-binding region of an antibody, causing impairment or loss of function. The resulting significant amount of defective antibody conjugates demands using higher antibody concentrations that will increase the risk of detection by the immune system of the host. An alternative strategy for the oriented immobilization of antibodies is

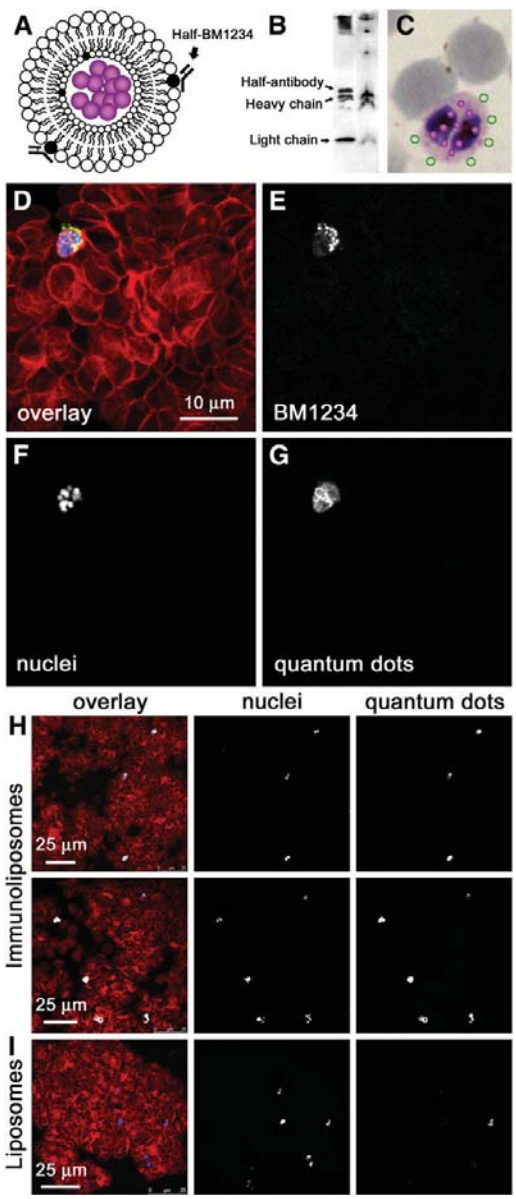

Fig. 6. Confocal fluorescence microscopy analysis of the delivery of immunoliposome cargo to pRBCs. (A) Cartoon showing a quantum dot-containing liposome functionalized with half-antibodies. (B) Western blot analysis of the result of treating the monoclonal antibody BM1234 with MEA, (left lane) after MEA treatment, and (right lane) after addition to MPB-PE-containing liposomes. Immunoliposomes were purified by ultracentrifugation prior to electrophoresis. (C) Graphical scheme of the expected performance of nanovectors when added to a *P. falciparum* culture containing both infected and non-infected cells. (D) Confocal fluorescence microscopy section of a suspension of RBCs containing ca. 5% pRBCs that had been treated, for 90 min and prior to fixation, with a preparation of immunoliposomes assembled as depicted in panel (A). The selected field contains a single pRBC among tens of non-infected cells, showing the fluorescence of RBC plasma membranes (red), antibody detection (green), quantum dots (white), and nuclei (blue). For an easier visualization of the colocalization of quantum dots and antibodies only in pRBCs, the fluorescence signals for (E) antibody, (F) nuclei, and (G) quantum dots are shown separately in white color. (H,I) Examples of images used for the quantitative confocal fluorescence microscopy analysis of suspensions of RBCs containing ca. 5% pRBCs, treated (H) with quantum dot-containing immunoliposomes or (I) with quantum dot-loaded liposomes not functionalized with antibodies. The fluorescence signals for nuclei and quantum dots are shown separately in white color, where only the originally weak quantum dot signal in panel (I) (see overlay) has been deliberately increased with the imaging software.

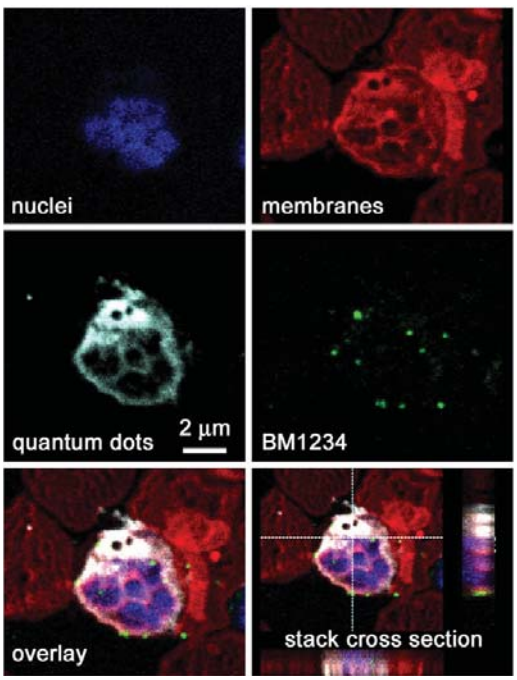

Fig. 7. Confocal fluorescence microscopy study of the subcellular localization of liposome-delivered quantum dots. Immunoliposomes targeted with BM1234 half-antibodies and loaded with 655 ITK™ carboxyl quantum dots were added to living *P. falciparum* cultures of the 3D7 strain. After 90 min of incubation the sample was processed for confocal fluorescence microscopy detection of cell membranes (red), nuclei (blue), quantum dots (white), and secondary antibodies against BM1234 (green). The four upper panels correspond to a single confocal section of a pRBC among several non-parasitized RBCs, and are overlaid in the lower left panel. The lower right panel shows two perpendicular cross sections throughout the stack of images.

the preparation of immunoconjugates using the oligosaccharide moieties in the antibody Fc region [50]. However, this protocol involves oxidation steps and use of heterobifunctional crosslinkers that make it a longer process than the straightforward mercaptoethylamine reduction yielding half-antibodies. A second factor which contributes to the reduction of targeting antibody amounts is an elevated specificity; in our hands, a *Plasmodium*-encoded target such as the epitope recognized by BM1234 has been more adequate than an RBC-endogenous protein like band 3.

Immunocytochemistry data obtained with two different *P. falciparum* strains, 3D7 and D10, provided identical fluorescence patterns for BM1234 binding. This suggests that the epitope being recognized might be relatively conserved, an important factor for a widespread use of the nanovector and for a lasting efficacy before resistances appear within the parasite's distribution range. The finding that liposomes not functionalized with targeting antibodies are also specifically directed to pRBCs, albeit with a much lower yield in terms of the amount of delivered cargo, can be of importance in relation to bypassing the parasite's evolution of resistance through target molecule modification. This phenomenon could be useful for the development of a drug delivery vessel whose targeting might be based on membrane lipid particularities of the pRBC plasma membrane that are likely to be less prone to quick evolutionary change than individual proteins. Peeters et al. [48] had already shown that encapsulation of chloroquine in nontargeted liposomes increased the effectiveness of the drug against *P. berghei*. The intrinsic affinity of liposomes for pRBCs could be related to modifications of the erythrocyte surface upon *Plasmodium* infection [25,51]. Previous work has suggested that pRBCs become leaky prior to rupture [52], and that the site of parasite invasion on the membrane never completely closes, leaving a pore and a small duct extending into the parasitophorous vacuole [53]. Such an anomalous membrane has been proposed as an explanation for the observed permeability of pRBCs to certain antibodies [54]. Most likely, the reported altered plasma membrane structure of pRBCs facilitates in some way the docking of randomly interacting liposomes, a phenomenon not occurring upon random interactions of liposomes with non-infected RBCs. In the presence of specific antibodies on the liposome surface, docking to pRBC membranes would reach 100% efficiency through antibody-antigen binding.

The work presented here constitutes the first qualitative and quantitative study at the cellular and subcellular level of the performance of liposomes specifically targeted to pRBCs, and demonstrates the feasibility of constructing a carrier able to completely discriminate RBCs from pRBCs, and of delivering its contents to the latter. Docking to pRBC surfaces through specific molecular components such as antibodies likely facilitates membrane fusion in the absence of fusogenic lipids. The short time of less than 90 min required to achieve 100% targeting specificity is an encouraging result that opens good perspectives regarding the development of a rapid delivery nanovector capable of competing with liposome clearance from blood by macrophages [29,30] and the liver [21,22]. Although liposomes are difficult to formulate for oral intake, they can be used in parenteral administration, indicated in all patients with severe or complicated malaria, those at high risk of developing severe disease, or if the patient is vomiting and unable to take oral antimalarials [55]. Parenteral treatment in the form of a vaccine or of targeted liposomal delivery can be a useful weapon for the *last mile* in a malaria eradication strategy [56]. This scenario would be compatible with an individualized administration of highly toxic compounds specifically targeted to pRBCs with good accuracy.

Previous results showed that immunoliposomal chloroquine when administered at a concentration in blood of 0.2 mM was capable of controlling *P. berghei* infections in mice [18]. The preliminary *in vitro* results presented here with the human-infecting species *P. falciparum* show that immunoliposomal delivery of chloroquine can improve drug efficiency several fold, clearing $26.7 \pm 1.8\%$ of parasites when administered at 2 nM, well below the IC_{50} of 20 to 30 nM reported for the most sensitive *P. falciparum* strains [43]. This good performance of our immunoliposomal nanovector is highlighted by the fact that chloroquine already has a natural carrier across the RBC membrane [57], which contributes to concentrate the drug inside these cells. The fast, specific targeting of immunoliposomes towards pRBCs can facilitate adjusting the amount of encapsulated drugs to a low overall concentration that however guarantees a localized delivery of highly toxic doses only to *Plasmodium*-parasitized cells. This, in turn, opens perspectives for the use in antimalarial therapy of already existing drugs that are not being tested because of their high toxicity and/or elevated unspecificity. The different parts of such a nanocarrier (targeting molecules, lipid formulation, intraliposomal contents, and the nanocapsule itself) can be substituted by new elements, to assemble vessels for the delivery of drugs to different *Plasmodium* species or intracellular targets, tailored to fit the specificity of the encapsulated antimalarial agent or different administration forms. However, a balance between complexity, efficacy, and cost will be necessary to obtain the simplest and cheapest system capable of significantly reducing or eliminating detectable parasitemia in people living in malaria-endemic areas.

Acknowledgements

This work was supported by grants BIO2008-01184 and CSD2006-00012 from the Ministerio de Ciencia e Innovación, Spain, which included FEDER funds, and by grant 2009SGR-760 from the Generalitat

de Catalunya, Spain. A fellowship of the Instituto de Salud Carlos III (Spain) is acknowledged by Patricia Urbán. We acknowledge the support of the Scientific and Technical Services of the University of Barcelona (confocal microscopy, cytometry, and cryo-electron microscopy units), and of Lídia Bardia from the Advanced Digital Microscopy Core Facility at the Barcelona Science Park. We are also grateful to Olga Esteban for her help with endothelial cell culture and to Noelia Camacho, Núria Rovira and Valerie Crowley for *Plasmodium* cultures. We acknowledge Dr. Edwin Ades and Mr. Francisco J. Candal of the Centers for Disease Control and Prevention (CDC) and Dr. Thomas Lawley of Emory University as the developers of HMEC-1.

Appendix A. Supplementary data

Supplementary data to this article can be found online at doi:10.1016/j.jconrel.2011.01.001.

References

[1] S. Vangapandu, M. Jain, K. Kaur, P. Patil, S.R. Patel, R. Jain, Recent advances in antimalarial drug development, Med. Res. Rev. 27 (2007) 65–107.
[2] E.A. Okiro, A. Al Taiar, H. Reyburn, R. Idro, J.A. Berkley, R.W. Snow, Age patterns of severe paediatric malaria and their relationship to *Plasmodium falciparum* transmission intensity, Malar. J. 8 (2009) 4.
[3] T.N. Wells, P.L. Alonso, W.E. Gutteridge, New medicines to improve control and contribute to the eradication of malaria, Nat. Rev. Drug Discov. 8 (2009) 879–891.
[4] R. Tuteja, Malaria — an overview, FEBS J. 274 (2007) 4670–4679.
[5] K.S. Griffith, L.S. Lewis, S. Mali, M.E. Parise, Treatment of malaria in the United States: a systematic review, JAMA 297 (2007) 2264–2277.
[6] M. Enserink, Malaria's drug miracle in danger, Science 328 (2010) 844–846.
[7] K. Na-Bangchang, J. Karbwang, Current status of malaria chemotherapy and the role of pharmacology in antimalarial drug research and development, Fundam. Clin. Pharmacol. 23 (2009) 387–409.
[8] N.J. White, Assessment of the pharmacodynamic properties of antimalarial drugs in vivo, Antimicrob. Agents Chemother. 41 (1997) 1413–1422.
[9] G. Orive, R.M. Hernández, A. Rodríguez Gascón, A. Domínguez-Gil, J.L. Pedraz, Drug delivery in biotechnology: present and future, Curr. Opin. Biotechnol. 14 (2003) 659–664.
[10] Z. Zhang, W. Cao, H. Jin, J.F. Lovell, M. Yang, L. Ding, J. Chen, I. Corbin, Q. Luo, G. Zheng, Biomimetic nanocarrier for direct cytosolic drug delivery, Angew. Chem. Int. Ed Engl. 48 (2009) 9171–9175.
[11] N.S. Santos-Magalhaes, V.C. Mosqueira, Nanotechnology applied to the treatment of malaria, Adv. Drug Deliv. Rev. 62 (2010) 560–575.
[12] O.C. Farokhzad, R. Langer, Impact of nanotechnology on drug delivery, ACS Nano 3 (2009) 16–20.
[13] A.A. Date, M.D. Joshi, V.B. Patravale, Parasitic diseases: liposomes and polymeric nanoparticles versus lipid nanoparticles, Adv. Drug Deliv. Rev. 59 (2007) 505–521.
[14] G. Storm, H.P. Wilms, D.J. Crommelin, Liposomes and biotherapeutics, Biotherapy 3 (1991) 25–42.
[15] N. Maurer, D.B. Fenske, P.R. Cullis, Developments in liposomal drug delivery systems, Expert Opin. Biol. Ther. 1 (2001) 923–947.
[16] Y. Barenholz, Liposome application: problems and prospects, Curr. Opin. Colloid Interface Sci. 6 (2001) 66–77.
[17] A.M. Robinson, J.E. Creeth, M.N. Jones, The specificity and affinity of immunoliposome targeting to oral bacteria, Biochim. Biophys. Acta 1369 (1998) 278–286.
[18] M. Owais, G.C. Varshney, A. Choudhury, S. Chandra, C.M. Gupta, Chloroquine encapsulated in malaria-infected erythrocyte-specific antibody-bearing liposomes effectively controls chloroquine-resistant *Plasmodium berghei* infections in mice, Antimicrob. Agents Chemother. 39 (1995) 180–184.
[19] N.S. Postma, C.C. Hermsen, J. Zuidema, W.M. Eling, *Plasmodium vinckei*: optimization of desferrioxamine B delivery in the treatment of murine malaria, Exp. Parasitol. 89 (1998) 323–330.
[20] N.S. Postma, D.J. Crommelin, W.M. Eling, J. Zuidema, Treatment with liposome-bound recombinant human tumor necrosis factor-α suppresses parasitemia and protects against *Plasmodium berghei* k173-induced experimental cerebral malaria in mice, J. Pharmacol. Exp. Ther. 288 (1999) 114–120.
[21] R.T. Robertson, J.L. Baratta, S.M. Haynes, K.J. Longmuir, Liposomes incorporating a *Plasmodium* amino acid sequence target heparan sulfate binding sites in liver, J. Pharm. Sci. 97 (2008) 3257–3273.
[22] K.J. Longmuir, R.T. Robertson, S.M. Haynes, J.L. Baratta, A.J. Waring, Effective targeting of liposomes to liver and hepatocytes in vivo by incorporation of a *Plasmodium* amino acid sequence, Pharm. Res. 23 (2006) 759–769.
[23] E. Winograd, J.G. Prudhomme, I.W. Sherman, Band 3 clustering promotes the exposure of neoantigens in *Plasmodium falciparum*-infected erythrocytes, Mol. Biochem. Parasitol. 142 (2005) 98–105.
[24] A. Craig, A. Scherf, Molecules on the surface of the *Plasmodium falciparum* infected erythrocyte and their role in malaria pathogenesis and immune evasion, Mol. Biochem. Parasitol. 115 (2001) 129–143.
[25] S. Kyes, P. Horrocks, C. Newbold, Antigenic variation at the infected red cell surface in malaria, Annu. Rev. Microbiol. 55 (2001) 673–707.
[26] P.D. Parker, L. Tilley, N. Klonis, *Plasmodium falciparum* induces reorganization of host membrane proteins during intraerythrocytic growth, Blood 103 (2004) 2404–2406.
[27] K. Kirk, Channels and transporters as drug targets in the *Plasmodium*-infected erythrocyte, Acta Trop. 89 (2004) 285–298.
[28] B.M. Cooke, K. Lingelbach, L.H. Bannister, L. Tilley, Protein trafficking in *Plasmodium falciparum*-infected red blood cells, Trends Parasitol. 20 (2004) 581–589.
[29] D.D. Lasic, F. Martin, Stealth Liposomes, CRC Press, Boca Raton, FL, USA, 1995.
[30] E. Kajiwara, K. Kawano, Y. Hattori, M. Fukushima, K. Hayashi, Y. Maitani, Long-circulating liposome-encapsulated ganciclovir enhances the efficacy of HSV-TK suicide gene therapy, J. Control. Release 120 (2007) 104–110.
[31] R.C. MacDonald, R.I. MacDonald, B.P. Menco, K. Takeshita, N.K. Subbarao, L.R. Hu, Small-volume extrusion apparatus for preparation of large, unilamellar vesicles, Biochim. Biophys. Acta 1061 (1991) 297–303.
[32] A. Raab, W. Han, D. Badt, S.J. Smith-Gill, S.M. Lindsay, H. Schindler, P. Hinterdorfer, Antibody recognition imaging by force microscopy, Nat. Biotechnol. 17 (1999) 901–905.
[33] A.A. Karyakin, G.V. Presnova, M.Y. Rubtsova, A.M. Egorov, Oriented immobilization of antibodies onto the gold surfaces via their native thiol groups, Anal. Chem. 72 (2000) 3805–3811.
[34] F.J. Martin, D. Papahadjopoulos, Irreversible coupling of immunoglobulin fragments to preformed vesicles. An improved method for liposome targeting, J. Biol. Chem. 257 (1982) 286–288.
[35] D.J. Crommelin, Influence of lipid composition and ionic strength on the physical stability of liposomes, J. Pharm. Sci. 73 (1984) 1559–1563.
[36] S.L. Cranmer, C. Magowan, J. Liang, R.L. Coppel, B.M. Cooke, An alternative to serum for cultivation of *Plasmodium falciparum* in vitro, Trans. R. Soc. Trop. Med. Hyg. 91 (1997) 363–365.
[37] C. Lambros, J.P. Vanderberg, Synchronization of *Plasmodium falciparum* erythrocytic stages in culture, J. Parasitol. 65 (1979) 418–420.
[38] P. Leivar, V.M. González, S. Castel, R.N. Trelease, C. López-Iglesias, M. Arró, A. Boronat, N. Campos, A. Ferrer, X. Fernàndez-Busquets, Subcellular localization of Arabidopsis 3-hydroxy-3-methylglutaryl-coenzyme A reductase, Plant Physiol. 137 (2005) 57–69.
[39] L.D. Mayer, M.J. Hope, P.R. Cullis, Vesicles of variable sizes produced by a rapid extrusion procedure, Biochim. Biophys. Acta 858 (1986) 161–168.
[40] I. Dufresne, A. Desormeaux, J. Bestman-Smith, P. Gourde, M.J. Tremblay, M.G. Bergeron, Targeting lymph nodes with liposomes bearing anti-HLA-DR Fab' fragments, Biochim. Biophys. Acta 1421 (1999) 284–294.
[41] J.B. Delehanty, H. Mattoussi, I.L. Medintz, Delivering quantum dots into cells: strategies, progress and remaining issues, Anal. Bioanal. Chem. 393 (2009) 1091–1105.
[42] I. Crandall, I.W. Sherman, Antibodies to synthetic peptides based on band 3 motifs react specifically with *Plasmodium falciparum* (human malaria)-infected erythrocytes and block cytoadherence, Parasitology 108 (1994) 389–396.
[43] A.B. Sidhu, D. Verdier-Pinard, D.A. Fidock, Chloroquine resistance in *Plasmodium falciparum* malaria parasites conferred by *pfcrt* mutations, Science 298 (2002) 210–213.
[44] D.J. Sullivan Jr., H. Matile, R.G. Ridley, D.E. Goldberg, A common mechanism for blockade of heme polymerization by antimalarial quinolines, J. Biol. Chem. 273 (1998) 31103–31107.
[45] A. Singhal, C.M. Gupta, Antibody-mediated targeting of liposomes to red cells in vivo, FEBS Lett. 201 (1986) 321–326.
[46] J.C. Shillcock, R. Lipowsky, Tension-induced fusion of bilayer membranes and vesicles, Nat. Mater. 4 (2005) 225–228.
[47] J.J. Wheeler, L. Palmer, M. Ossanlou, I. MacLachlan, R.W. Graham, Y.P. Zhang, M.J. Hope, P. Scherrer, P.R. Cullis, Stabilized plasmid-lipid particles: construction and characterization, Gene Ther. 6 (1999) 271–281.
[48] P.A. Peeters, C.W. Huiskamp, W.M. Eling, D.J. Crommelin, Chloroquine containing liposomes in the chemotherapy of murine malaria, Parasitology 98 (1989) 381–386.
[49] A.K. Agrawal, A. Singhal, C.M. Gupta, Functional drug targeting to erythrocytes in vivo using antibody bearing liposomes as drug vehicles, Biochem. Biophys. Res. Commun. 148 (1987) 357–361.
[50] C.-W. Vogel, Preparation of immunoconjugates using antibody oligosaccharide moieties, in: C.M. Niemeyer (Ed.), Methods in Molecular Biology, Humana Press Inc., Totowa, NJ, 2004, pp. 87–108.
[51] I.W. Sherman, Membrane structure and function of malaria parasites and the infected erythrocyte, Parasitology 91 (1985) 609–645.
[52] J.A. Lyon, J.M. Carter, A.W. Thomas, J.D. Chulay, Merozoite surface protein-1 epitopes recognized by antibodies that inhibit *Plasmodium falciparum* merozoite dispersal, Mol. Biochem. Parasitol. 90 (1997) 223–234.
[53] I.D. Goodyer, B. Pouvelle, T.G. Schneider, D.P. Trelka, T.F. Taraschi, Characterization of macromolecular transport pathways in malaria-infected erythrocytes, Mol. Biochem. Parasitol. 87 (1997) 13–28.
[54] E.S. Bergmann-Leitner, E.H. Duncan, E. Angov, MSP-1p42-specific antibodies affect growth and development of intra-erythrocytic parasites of *Plasmodium falciparum*, Malar. J. 8 (2009) 183–194.
[55] D.G. Lalloo, D. Shingadia, G. Pasvol, P.L. Chiodini, C.J. Whitty, N.J. Beeching, D.R. Hill, D.A. Warrell, B.A. Bannister, UK malaria treatment guidelines, J. Infect. 54 (2007) 111–121.
[56] G. Vogel, The 'do unto others' malaria vaccine, Science 328 (2010) 847–848.
[57] A. Yayon, H. Ginsburg, The transport of chloroquine across human erythrocyte membranes is mediated by a simple symmetric carrier, Biochim. Biophys. Acta 686 (1982) 197–203.

SUPPLEMENTARY DATA

Among the modifications experienced by the RBC surface upon *Plasmodium* infection, conformational changes in the anion transporter band 3 protein have attracted attention as a possible candidate for targeted drug delivery strategies, and antibodies against band 3 regions that are more exposed in infected cells were described to be efficient in discriminating RBCs from pRBCs [1;2]. We raised rabbit polyclonal antibodies against three synthetic peptides corresponding to the exposed extracellular loops of human band 3 XL3, XL4, and XL7. The three antibodies were tested against cell cultures of the 3D7 *P. falciparum* strain (Figure S1A), gelatin-enriched to obtain a higher parasitemia (Figure S1B). Only anti-XL3 showed certain specificity for pRBCs (Figure S1C-E), although a strong unspecific fluorescence could also be observed in non-infected RBCs. We judged that this result rendered our anti-band 3 antibodies unadequate for their use in the further development of targeted nanovectors, which required specificity approaching 100%.

Generation of polyclonal antibodies against band 3 protein peptides

Synthetic peptides based on human RBC band 3 motifs in exofacial loops XL3, XL4, and XL7, containing amino acid sequences 546-555 (DHPLQKTYNY), 628-642 (YTQKLSVPDGFKVSN), and 821-834 (DVPYVKRVKTWRMH), were used to produce polyclonal antibodies. Peptides were synthesized with an additional cysteine at the carboxy terminal end for their use in the affinity purification of specific antibodies. Synthesis was done by the Peptide Synthesis Service at the Scientific and Technical Services of the University of Barcelona. Immunization of rabbits was done following standard protocols at the facilities of the Animal Experimentation Services at the University of Barcelona. Serum antibodies were purified by affinity chromatography using the corresponding peptides immobilized on agarose beads (SulfoLink Kit, Pierce Biotechnology,

Rockford, IL, USA), assayed by Enzyme-Linked ImmunoSorbent Assay (ELISA), and finally stored at -20 °C.

Immunofluorescence assays for anti-XL3, -XL4, and -XL7 rabbit polyclonal antibodies were performed in gelatin-enriched 3D7 *P. falciparum* cell cultures. Anti-band 3 antibodies were incubated with the cells for 1 h at 37 °C at a final concentration of 2 µg antibody/ml and detected with a secondary AlexaFluor 488 goat anti-rabbit (Molecular Probes, Eugene, OR, USA).

Cocultures of pRBCs with HMEC-1

Knob-bearing erythrocytes infected with mature blood-stage parasites were enriched from *in vitro* cultures by gelatin sedimentation and were added to a 75% confluent monolayer of HMEC-1 cells (ratio of pRBCs to HMEC-1 50:1) in MatTek Petri dishes (Ashland, MA, USA). After 90 min at 37 °C, unbound erythrocytes were removed by repeated washing with PBS and cells were incubated with liposomes or immunoliposomes containing 120 nM quantum dots for 90 minutes at 37 °C. Nuclei, cell membranes, quantum dots, and targeting antibodies were detected as described in the fluorescence microscopy methods.

References

[1] E. Winograd, J.G. Prudhomme, I.W. Sherman, Band 3 clustering promotes the exposure of neoantigens in *Plasmodium falciparum*-infected erythrocytes, Mol. Biochem. Parasitol. 142 (2005) 98-105.

[2] I. Crandall, I.W. Sherman, Antibodies to synthetic peptides based on band 3 motifs react specifically with *Plasmodium falciparum* (human malaria)-infected erythrocytes and block cytoadherence, Parasitology 108 (1994) 389-396.

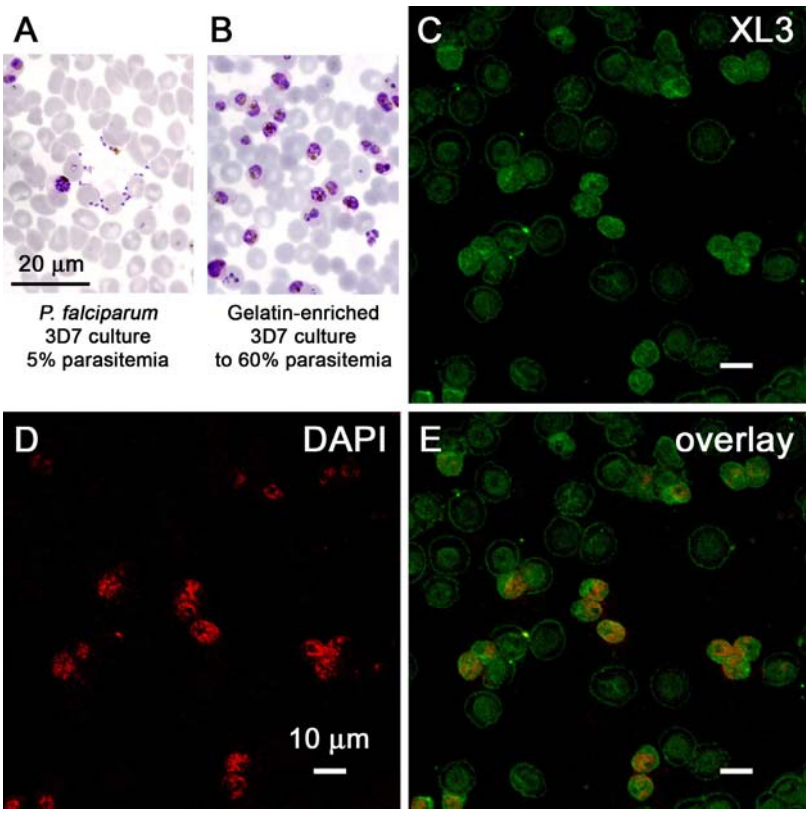

Fig. S1. Binding to pRBCs of anti-band 3 antibodies. *P. falciparum* cultures containing (A) 5% pRBCs were gelatin-enriched to achieve (B) ca. 60% parasitemia. Enriched suspensions were treated with rabbit polyclonal antibodies XL3 raised against the extracellular loop 3 of human band 3 protein. Confocal fluorescence microscopy was used to detect (C) XL3 with a second fluorescent antibody and (D) *Plasmodium* nuclei using DAPI staining. Panel (E) shows the overlay of both images.

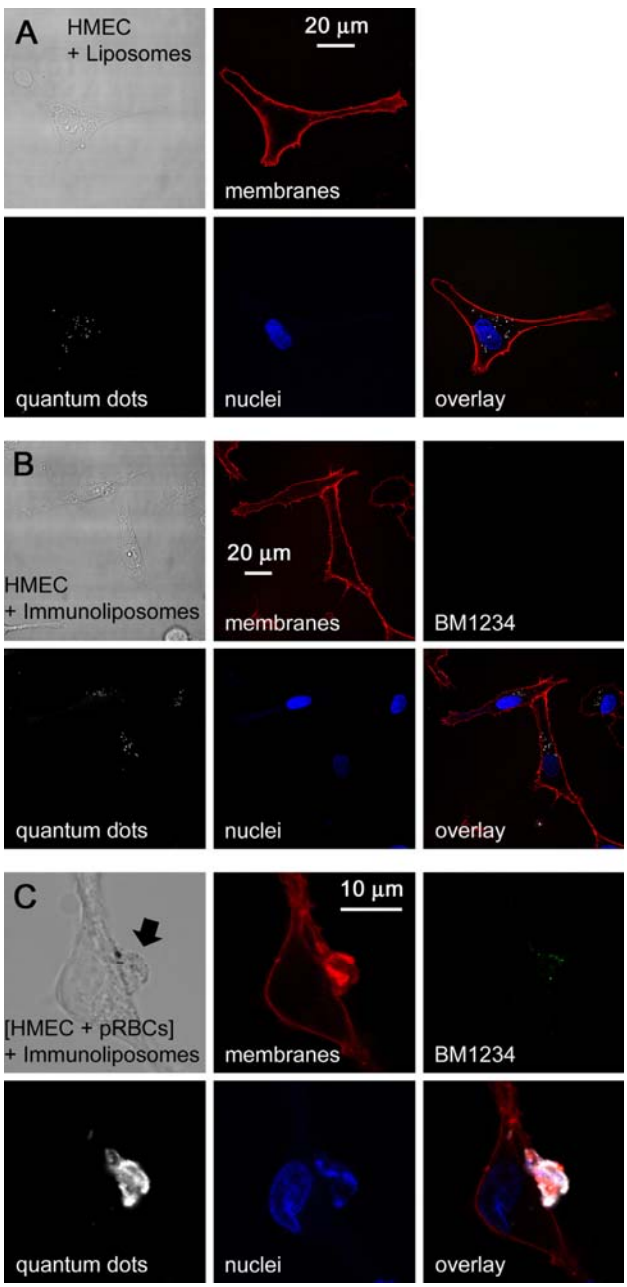

Fig. S2. Confocal fluorescence microscopy study of the fate of quantum dot-containing immunoliposomes added to a mixture of living HMEC-1 and pRBCs. Quantum dot-loaded (A) liposomes or (B,C) BM1234-functionalized immunoliposomes were added to (A,B) HMEC-1 or (C) to a mixture of HMEC-1 and pRBCs, and incubated for 90 min before proceeding to fixation and microscopic analysis. For each experiment are shown a phase contrast image and the fluorescence detection of membranes, quantum dots, nuclei, and (only for immunoliposome-containing samples) BM1234. The bottom right image in each panel shows the overlay of fluorescence signals. The arrow in panel C indicates a pRBC.

ARTICLE 2

Study of the efficacy of antimalarial drugs when delivered inside targeted immunoliposomal nanovectors

In this article, we present a quantitative study of the efficacy of the previously designed nanovector in improving the activity of the antimalarial drugs chloroquine and fosmidomycin, and discuss its characteristics and room for improvement regarding future animal assays that might place this prototype on the threshold of clinical trials.

For an accurate estimation of the nanovector performance, the determination of the exact concentration of the drug even in low amounts is crucial, so we have developed an HPLC-based method for the precise determination of the concentrations in the liposomal preparations of chloroquine and of a second antimalarial drug, fosmidomycin.

In a classical *Plasmodium* growth inhibition assay, the drug is added at the ring stage, and after 48 hours of incubation throughout a complete erythrocytic cycle, parasitemia is determined. The targeting antibody used in BM1234 immunoliposomes binds preferentially to pRBCs containing late maturation stages of the parasite, so we speculated that a BM1234-mediated targeted delivery of immunoliposome-encapsulated drugs would be more efficient if administered to trophozoites rather than to rings. Therefore, we have also assayed the addition of targeted nanovectors at the trophozoite stage (24 h later than in the standard protocol), determining parasitemia by FACS analysis and Giemsa-stained blood smears after a further 48 h of incubation. Encapsulation in immunoliposomes as described here improves drug efficacy by an order of magnitude: similar drug amounts kill 10 times more parasites if encapsulated and the best performing immunoliposomes are those added to *Plasmodium* cultures having a larger number of late form-containing pRBCs.

An average of five antibody molecules per liposome significantly improves in cell cultures the performance of immunoliposomes over non-functionalized liposomes as drug delivery vessels. Increasing the number of antibodies on the liposome surface correspondingly increases performance, with a reduction of 50% parasitemia achieved with immunoliposomes encapsulating 4 nM chloroquine and bearing an estimated 250 BM1234 units (Figure 15). The remarkable capacity of liposomes to inject their contents into pRBCs presumably has its basis on alterations of the pRBC plasma membrane rendering it less elastic and thus limiting the rebounding of colliding liposomes. The resulting slightly longer interactions, a phenomenon exacerbated if targeting antibodies are present, likely allow enough time for the physical phenomenon of lipid bilayer fusion to occur. This hypothesis could also explain why liposomes devoid of the antibody do perform better when added at the trophozoite stage since the membrane of ring-containing pRBCs is more similar to uninfected erythrocytes than that of pRBCs infected by later forms.

BM1234 immunoliposomes can also be an efficient drug delivery vessel for the administration of liposoluble drugs against *P. falciparum*; unlike chloroquine and fosmidomycin, the solubility of hydrophobic compounds will be low when free in plasma, but can be significantly increased when incorporated in the lipid bilayers of liposomes.

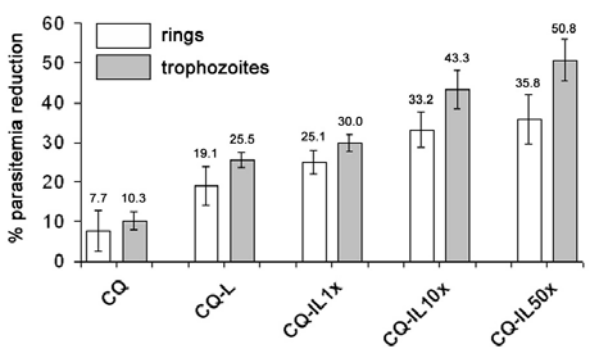

Figure 15. Effect on *P. falciparum* viability of increasing amounts of BM1234 antibody on chloroquine-containing immunoliposomes, corresponding to figure 4C in the article. The amount of chloroquine added to the culture was 4 nM in all samples. 1X, 10X, and 50X correspond respectively to 5, 50, and 250 estimated antibody molecules per liposome.

Urbán et al. Nanoscale Research Letters 2011, 6:620
http://www.nanoscalereslett.com/content/6/1/620

Nanoscale Research Letters
a SpringerOpen Journal

ORIGINAL PAPER Open Access

Study of the efficacy of antimalarial drugs delivered inside targeted immunoliposomal nanovectors

Patricia Urbán[1,2,3], Joan Estelrich[2,4], Alberto Adeva[5], Alfred Cortés[3,6,7] and Xavier Fernàndez-Busquets[1,2,3*]

Abstract

Paul Ehrlich's dream of a 'magic bullet' that would specifically destroy invading microbes is now a major aspect of clinical medicine. However, a century later, the implementation of this medical holy grail continues being a challenge in three main fronts: identifying the right molecular or cellular targets for a particular disease, having a drug that is effective against it, and finding a strategy for the efficient delivery of sufficient amounts of the drug in an active state exclusively to the selected targets. In a previous work, we engineered an immunoliposomal nanovector for the targeted delivery of its contents exclusively to *Plasmodium falciparum*-infected red blood cells [pRBCs]. In preliminary assays, the antimalarial drug chloroquine showed improved efficacy when delivered inside immunoliposomes targeted with the pRBC-specific monoclonal antibody BM1234. Because difficulties in determining the exact concentration of the drug due to its low amounts prevented an accurate estimation of the nanovector performance, here, we have developed an HPLC-based method for the precise determination of the concentrations in the liposomal preparations of chloroquine and of a second antimalarial drug, fosmidomycin. The results obtained indicate that immunoliposome encapsulation of chloroquine and fosmidomycin improves by tenfold the efficacy of antimalarial drugs. The targeting antibody used binds preferentially to pRBCs containing late maturation stages of the parasite. In accordance with this observation, the best performing immunoliposomes are those added to *Plasmodium* cultures having a larger number of late form-containing pRBCs. An average of five antibody molecules per liposome significantly improves in cell cultures the performance of immunoliposomes over non-functionalized liposomes as drug delivery vessels. Increasing the number of antibodies on the liposome surface correspondingly increases performance, with a reduction of 50% parasitemia achieved with immunoliposomes encapsulating 4 nM chloroquine and bearing an estimated 250 BM1234 units. The nanovector prototype described here can be a valuable platform amenable to modification and improvement with the objective of designing a nanostructure adequate to enter the preclinical pipeline as a new antimalarial therapy.

Keywords: antimalarial chemotherapy, chloroquine, fosmidomycin, half-antibodies, immunoliposomes, malaria, nanomedicine, targeted drug delivery

Introduction

Malaria is an acute and/or chronic infection caused by protozoans of the genus *Plasmodium*. Clinical manifestations are fever, chills, prostration, and anemia, whereas severe disease can include metabolic acidosis, cerebral malaria, and multiorgan system failure, and coma and death may ensue. More than 40% of the world's population lives with some risk of contracting malaria, with most recent estimates suggesting several hundred million clinical cases and 800,000 deaths each year [1,2], of which the large majority are children below 5 years [3,4]. The recent call for the elimination and eradication of the disease requires research from multiple fronts, including developing strategies for the efficient delivery of new medicines [5]. Four species cause diseases in humans: *P. vivax*, *P. ovale*, *P. malariae*, and *P. falciparum*, with the latter causing the most deadly and severe cases. In the life cycle of *Plasmodium* parasites

* Correspondence: xfernandez_busquets@ub.edu
[1]Nanobioengineering Group, Institute for Bioengineering of Catalonia, Baldiri Reixac 10-12, Barcelona, E08028, Spain
Full list of author information is available at the end of the article

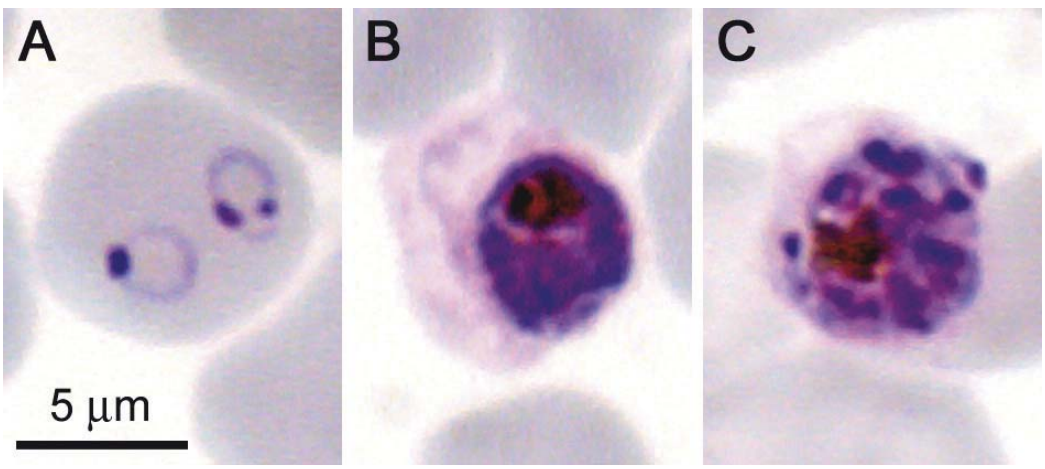

Figure 1 Giemsa staining of *Plasmodium*-infected RBCs. At the ring (**A**), trophozoite (**B**), and schizont (**C**) stages of *P. falciparum*.

(for a review, see Tuteja [6]), the female *Anopheles* mosquito inoculates, during a bite, *Plasmodium* sporozoites that bind to and infect hepatocytes and proliferate into thousands of merozoites in the liver. Merozoites rupture from the hepatocytes and invade red blood cells [RBCs], where they develop first into rings and then into the late forms, trophozoites and schizonts (Figure 1). Schizont-infected RBCs burst and release more merozoites, which start the blood cycle again. Because the blood-stage infection is responsible for all symptoms and pathologies of malaria, *Plasmodium*-infected RBCs [pRBCs] are a main chemotherapeutic target [7].

The need to develop new strategies to treat malaria is urgent if one considers that the cases of resistance to current antimalarial agents increase, especially in zones in which *P. falciparum* is endemic, and calls for combined therapy approaches [5,8]. Several drugs show different degrees of toxicity, which limits their use because current administration forms release the free compound in the blood and offer little specificity regarding the targeted cells [9]. Consequently, to achieve therapeutic levels that extend over time, the initial concentration of the drug in the body should be high. On the other hand, if the administered chemical has unspecific toxicity, the low doses required contribute to the development of resistant parasite strains [10]. The challenge of drug delivery is the liberation of adequate doses of therapeutic agents to a specific target site at the right time in a safe and reproducible manner [11]. A number of mechanisms can provide controlled release, including transdermal patches, implants, inhalation systems, bioadhesive systems, and nanoencapsulation [12-14], but few of these have been designed for specificity. Taking into account the peculiarities of pRBCs, lipid-based nanocarriers have been one of the most promising approaches for the targeted delivery of antimalarial drugs [15].

Liposomes are synthetic lipid bilayer-enclosed structures up to several hundred nanometers in diameter that can improve the delivery of bioactive molecules by functioning as circulating microreservoirs for sustained release [16,17]. Liposomes bearing cell-specific recognition ligands on their surfaces have been widely considered as drug carriers in therapy [18,19], and liposome encapsulation has been assayed for the targeted delivery of compounds against murine malaria [20-22]. Liposomal nanovessels incorporating a *P. berghei* amino acid sequence have been shown to greatly increase their targeting to the liver [23,24], suggesting that they can be an adequate vector to channel antimalarials towards the hepatocyte stages of the parasite.

In a previous work [25], we engineered an immunoliposomal nanovector for the targeted delivery of its contents exclusively to pRBCs. Two hundred-nanometer liposomes loaded with quantum dots were covalently functionalized with oriented, specific half-antibodies against *P. falciparum* late form-infected pRBCs. In less than 90 min, 100% of late form-containing pRBCs and 0% of noninfected RBCs in living *P. falciparum* cultures were infiltrated by the content of targeted immunoliposomes. Here, we present a quantitative study of the efficacy of this nanovector in ameliorating the activity of the antimalarial drugs chloroquine and fosmidomycin, and discuss its characteristics and room for improvement regarding future animal assays that might place this prototype on the threshold of clinical trials.

Materials and methods

Materials

Except where otherwise indicated, all reagents were purchased from Sigma-Aldrich Corporation (St. Louis, MO, USA). The commercial monoclonal antibody BM1234 against *P. falciparum* pRBCs was obtained from Acris Antibodies GmbH (Herford, Germany).

Liposome and immunoliposome preparation

Liposomes were prepared by the lipid film hydration method [26], with the lipid formulation 1,2-dioleoyl-*sn*-glycero-3-phosphatidylcholine [DOPC] (Avanti Polar Lipids, Inc., Alabaster, AL, USA)/cholesterol 80:20, as described previously [25]. The dry lipids were hydrated at 37°C in phosphate-buffered saline [PBS] containing the antimalarial drug to obtain a concentration of 10 mM lipid. For the coupling of targeting antibodies to liposomes, we followed established protocols [27] that use 1,2-dipalmitoyl-*sn*-glycero-3-phosphoethanolamine-*N*-[4-(*p*-maleimidophenyl)butyramide] [MPB-PE] (Avanti Polar Lipids, Inc.) to incorporate proteins into liposomes (DOPC/cholesterol/MPB-PE 77.5:20:2.5, 10 mM lipid) through the reaction of the maleimide group in the lipid with a thiol group from the ligand [25].

Quantification of chloroquine and fosmidomycin

The amount of chloroquine and fosmidomycin encapsulated inside liposomes was determined using high-performance liquid chromatography with tandem mass spectrometry [HPLC-MS/MS]. Prior to analysis, lipids were extracted following stardard protocols [28] in order to release the entrapped drug. Briefly, 100 μl of liposome sample was mixed with 225 μl of cold methanol and 125 μl of chloroform. Phase separation was achieved by adding 125 μl of 0.1 M HCl and 125 μl of chloroform. After mixing thoroughly, the samples were spun down at 7,500 × *g* for 5 min. The upper water-methanol layer, containing the drug that had been encapsulated inside liposomes, was collected and stored at -20°C until analysis. HPLC analysis was performed in an Alliance 2695 chromatographic system (Waters Corporation, Milford, MA, USA) using an Atlantis dC18 analytical column (internal diameter [i.d.] 150 × 2.1 mm, 5 μm, Waters Corporation) for chloroquine and a Luna C18 analytical column (i.d. 150 × 2.0 mm, 5 μm, Phenomenex, Torrance, CA, USA) for fosmidomycin, with mobile phase A (0.2% formic acid in water) and B (acetonitrile). The linear gradient for the determination of chloroquine at a flow rate of 0.3 ml/min was (% mobile phase B/min) 0/0, 10/2, 40/17, and 90/22 whereas for the determination of fosmidomycin at a flow rate of 0.4 ml/min, it was 0/0, 0/5, and 95/10. The HPLC system was coupled to a SCIEX API 365 Triple Quadrupole mass spectrometer equipped with a Turbo Ion Spray ion source (PerkinElmer, Waltham, MA, USA). For quantification purposes, data were collected in the multiple reaction monitoring mode with positive-ion detection for chloroquine and negative-ion detection for fosmidomycin, tracking the transition of the parent and product ions specific for each compound: 320.3/141.9 and 320.3/246.7 for chloroquine and 182.0/79.0 and 182.0/136.0 for fosmidomycin.

Cryo-electron microscopy

For cryo-electron microscopy analysis of the preparations of liposomes, a thin aqueous film was formed by dipping a glow-discharged holey carbon grid in the liposome suspension and then blotting the grid against a filter paper. The resulting thin sample films spanning the grid holes were vitrified by plunging the grid (kept at 100% humidity and room temperature) into ethane, which was maintained at its melting point with liquid nitrogen, using a Vitrobot (FEI Company, Eindhoven, The Netherlands). The vitreous films were transferred to a Tecnai F20 transmission electron microscope [TEM] (FEI Company) using a cryotransfer (Gatan, Inc., Pleasanton, CA, USA), and the samples were observed in a low-dose mode. Images were acquired at 200 kV at a temperature between -170°C and -175°C, using low-dose imaging conditions not exceeding 20 $e^-/Å^2$, with a 4,096 × 4,096 pixel CCD Eagle camera (FEI Company), and digitized with the Tecnai Image Acquisition program.

Plasmodium falciparum cell culture and growth inhibition assays

The *P. falciparum* 3D7 strain was grown *in vitro* in group B washed human RBCs prepared as described elsewhere [25] using previously described conditions [29]. Briefly, parasites (thawed from glycerol stocks) were cultured at 37°C in Petri dishes containing RBCs in RPMI complete medium under a gas mixture of 92% N_2, 5% CO_2, and 3% O_2. Synchronized cultures were obtained by 5% sorbitol lysis [30], and the medium was changed every 2 days maintaining 3% hematocrit. For culture maintenance, parasitemias were kept below 5% late forms by dilution with washed RBCs. For standard growth inhibition assays, parasitemia was adjusted to 1.5% with more than 90% of parasites at the ring stage after sorbitol synchronization. For modified growth inhibition assays, synchronized cultures were incubated for 24 h before addition of the drug to allow for the appearance of late forms presenting the epitope recognized by BM1234 bound to immunoliposomes. Two hundred microliters of these living *Plasmodium* cultures were plated in 96-well plates and incubated for 48 h at 37°C

in the presence of free drugs and drugs encapsulated in liposomes and immunoliposomes at a final concentration of 100 μM lipid. Parasitemia was determined by microscopic counting of blood smears or by fluorescence-assisted cell sorting [FACS]. Smears were fixed in methanol for a few seconds and then stained for 10 min with Giemsa (Merck Chemicals, Darmstadt, Germany) diluted 1:10 in Sorenson's buffer, pH 7.2. After washing with distilled water and drying, the ratio of the infected vs. noninfected RBCs was determined by microscopic analysis. For FACS analysis, noninfected RBCs and samples containing pRBCs were diluted to a final concentration of 1 to 10 × 10^6 cells/ml. The cell suspension was stained with SYTO 11 (0.5 mM stock in DMSO, Molecular Probes, Eugene, OR, USA) to a final concentration of 0.5 μM, and samples were incubated for 5 to 10 min prior to analysis in a Cytomics FC 500 MPL (Beckman Coulter, Inc., Fullerton, CA, USA) set up with the standard configuration. Excitation of the sample was done using a 488-nm, air-cooled, argon-ion laser at 15-mW power using forward and side scatter to gate the RBC population, and SYTO 11 green fluorescence (525 nm) was collected in a logarithmic scale. The single-cell population was selected on a forward-side scattergram, and the green fluorescence from this population was analyzed. Parasitemia was expressed as the number of parasitized cells per 100 erythrocytes.

Statistical analysis

Data are presented as the mean ± standard error of at least three independent experiments, and the corresponding standard errors in histograms are represented by error bars. Statistical analyses were performed using the Statgraphics Centurion XVI.I data analysis and statistical software. The parametric Student's t test was used to compare two independent groups when data followed a Gaussian distribution. Otherwise, the nonparametric Mann-Whitney test was used. Differences were considered significant when the p value was ≤ 0.05.

Confocal fluorescence microscopy

For immunofluorescence assays, pRBC smears were fixed in ice for 2 min in acetone/methanol (90:10) and incubated with 2 μg BM1234 monoclonal antibody/ml PBS containing 0.75% w/v BSA for 90 min at 37°C. After PBS washing steps, primary antibodies were detected with a secondary fluorescent antibody Alexa Fluor 488 goat anti-mouse $F(ab')_2$ (Molecular Probes). Parasite nuclei were stained with 4'6-diamino-2-phenylindole [DAPI] (Invitrogen Corporation, Carlsbad, CA, USA) during the secondary antibody incubation, and the RBC membrane was labeled with a wheat germ agglutinin [WGA]-tetramethylrhodamine conjugate (Molecular Probes). After the corresponding incubations and PBS washing steps, the samples were finally mounted with Mowiol (Calbiochem, Merck Chemicals) following standard protocols [31]. The samples were imaged with a TCS SP5 laser scanning confocal microscope equipped with an acoustic optical beam splitter (Leica Microsytstems Inc., Buffalo Grove, IL, USA), a DMI6000 inverted microscope (Leica Microsytstems Inc.), blue diode (405 nm), Ar (458/476/488/496/514 nm), diode-pumped solid-state (561 nm), and HeNe (594/633 nm) lasers, and APO ×63 oil (NA 1.4) or glycerol (NA 1.3) immersion objective lenses. DAPI, Alexa Fluor 488, reflection (for hemozoin detection), and WGA-rhodamine images were acquired sequentially using 405, 488, 488, and 561 laser lines and emission detection ranges 415 to 480 nm, 500 to 550 nm, 480 to 500 nm, and 571 to 625 nm, respectively, with the confocal pinhole set at 1 airy unit. Bright field transmitted light images were acquired simultaneously at 400 Hz in a 512 × 512 pixel format, ×8 zoom, and a pixel size of 60 × 60 nm.

Results and discussion

In preliminary *in vitro* assays, chloroquine showed an improved efficacy as an antimalarial when delivered inside targeted immunoliposomes [25]. However, difficulties in determining the exact concentration of the drug due to the low administered amounts prevented an accurate estimation of the nanovector performance. Here, we have established an HPLC method for the reliable quantification of chloroquine and fosmidomycin with good linearity ranges of 0.1 to 100 ng/ml (Y = 0.0223X - 1.98 × 10^{-13}, r^2 = 0.9942) and 5 to 2,500 ng/ml (Y = 246X, r^2 = 0.9997), respectively (Figure 2). The detection limits obtained have been 0.04 ppb for chloroquine and 1 ppb for fosmidomycin.

For immunoliposome assembly, different lipid combinations had been tested in order to establish a formulation with low hemolytic activity and low general cytotoxicity, which is DOPC/cholesterol/MPB-PE 77.5:20:2.5 [25]. Liposomes formed in this way were stable and generally did not coalesce even after high-speed centrifugation (Figure 3A), but occasionally, fusion events were observed (Figure 3B). Although dynamic light scattering analysis indicated that the liposome population had a mean diameter of 200 nm and a lower limit of 100 nm, TEM images showed a significant number of smaller liposomes down to 50 nm across. Most liposomes were unilamellar but a substantial fraction of them (about 10%) were enclosed by two or more lipid bilayers.

The targeting antibody BM1234 used in this work is specific for pRBCs infected by the trophozoite and schizont forms, but it does not bind significantly to ring-stage pRBCs [25]. For this reason, we speculated that a BM1234-mediated targeted delivery of immunoliposome-encapsulated drugs would be more efficient if

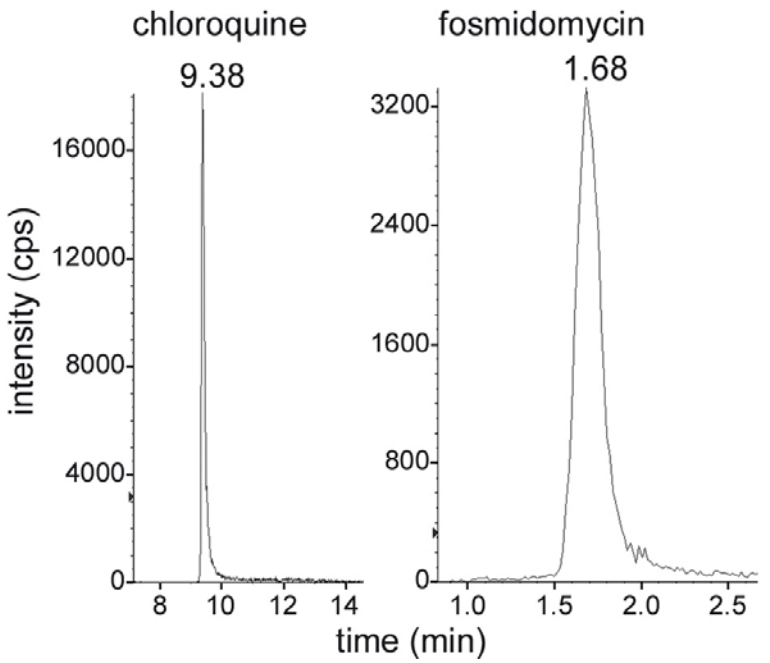

Figure 2 HPLC chromatograms showing the retention times of chloroquine and fosmidomycin extracted from immunoliposomes.

administered to trophozoites rather than to rings. In a classical *Plasmodium* growth inhibition assay, the drug is added at the ring stage, and after 48 h of incubation throughout a complete erythrocytic cycle, parasitemia is determined. Here, we have also assayed the addition of our targeted nanovectors at the trophozoite stage (24 h later than in the standard protocol), determining parasitemia by FACS analysis and Giemsa-stained blood smears after a further 48 h of incubation. The results obtained (Figure 4A) show that in growth inhibition assays performed 48 h after being administerd to pRBC cultures, 2 nM chloroquine or 360 nM fosmidomycin in solution reduces parasitemia by 3% to 6% when added at either the ring or the trophozoite stage. Liposomal chloroquine and fosmidomycin used at respective final concentrations of 1.6 and 325 nM reduce parasitemia by

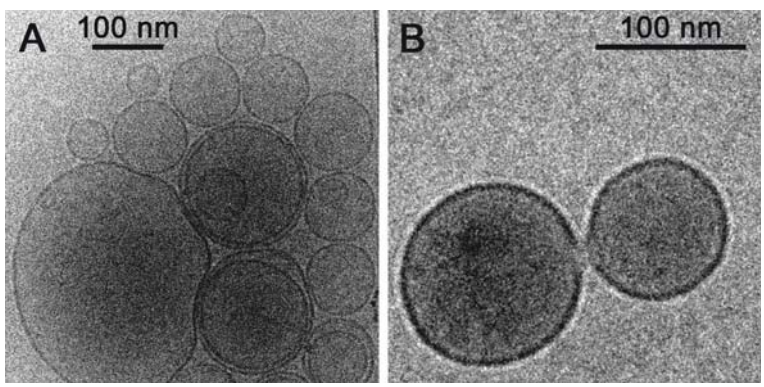

Figure 3 Cryo-TEM images of liposomes.

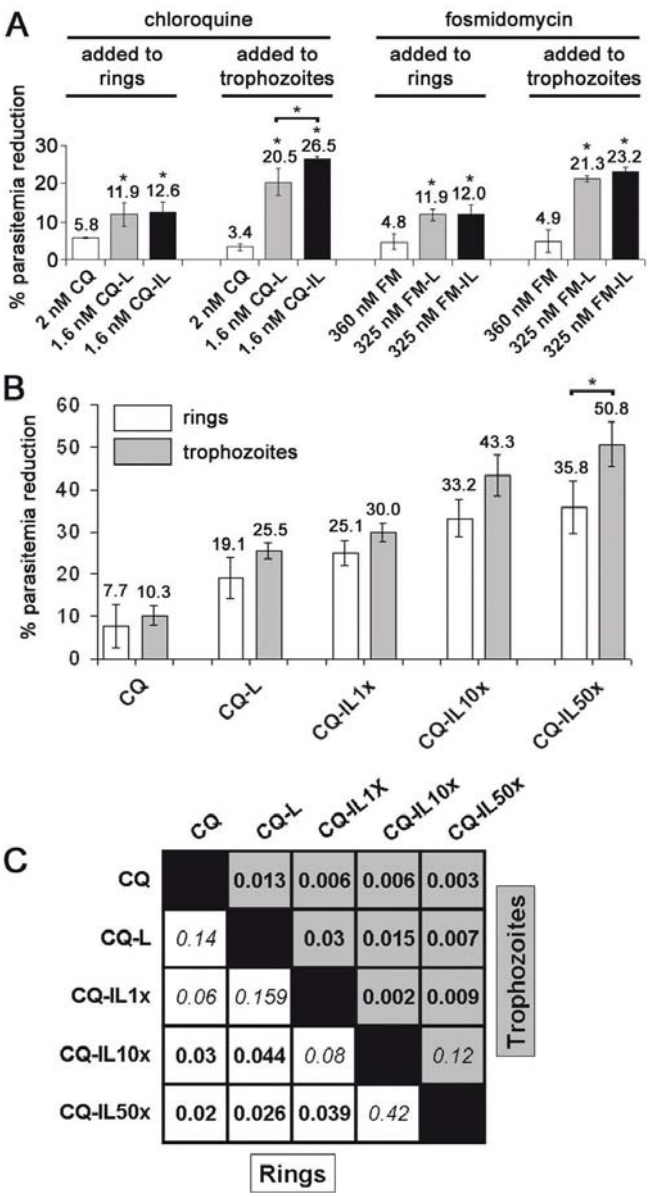

Figure 4 Growth inhibition assays. (**A**) Effect on *P. falciparum* viability of chloroquine (CQ) and fosmidomycin (FM), free or encapsulated in liposomes (L) or immunoliposomes (IL) and added at the ring or the trophozoite stage. The values express percentage of reduction respective to the parasitemia of controls without drug added. Asterisks on top of individual bars indicate significant differences ($p \leq 0.05$) in relation to the corresponding control sample of the non-encapsulated drug. (**B**) Effect on *P. falciparum* viability of increasing amounts of BM1234 antibody on chloroquine-containing immunoliposomes. The amount of chloroquine added to the culture was 4 nM in all samples. 1×, 10×, and 50 × correspond respectively to 5, 50, and 250 estimated antibody molecules per liposome. The asterisk indicates a significant difference ($p \leq 0.05$). (**C**) Grid showing the *p* values within the trophozoite and ring sample groups in the experiment from panel B. Bold numbers indicate a significant difference ($p \leq 0.05$).

> 10% when added at the ring stage and by > 20% when added at the trophozoite stage. The best results have been obtained with chloroquine and fosmidomycin encapsulated in immunoliposomes, which resulted in *ca*. eightfold and fivefold improvement for encapsulated drug concentrations 80% and 90% that of the free compound, respectively. On an average, encapsulation in immunoliposomes as described here improves drug efficacy by an order of magnitude: similar drug amounts kill 10 times more parasites if encapsulated, and 10 times less encapsulated drug eliminates approximately the same number of parasites than the free compound: when added at the trophozoite stage, 20 nM soluble chloroquine kills 28.1 ± 0.6% of parasites vs. 26.5 ± 0.5% for the immunoliposome-encapsulated drug at 1.6 nM final concentration. The efficacy of the nanovector is particularly relevant in the case of chloroquine, which has an endogenous carrier across human erythrocyte membranes that accumulates the drug selectively in these cells [32]. As expected, because the targeting antibody used here does not recognize ring-infected pRBCs, the efficacy of the immunoliposomes is much better when administered at the trophozoite stage. This observation has clinical implications related with the synchrony of falciparum malaria infection in humans, namely the administration of such stage-specific nanovectors should be timed at the moment when the targeted form is at its highest concentration in the blood. Although this can be readily determined by FACS analysis, Giemsa staining and a microscopic observation provide a more affordable way to quickly estimate the intraerythrocytic phase of the infection.

We have calculated that the protocol used for the preparation of the samples from Figure 4A results in an average number of five antibody molecules per liposome [25], and the data presented here indicate that this is the minimal antibody/liposome ratio that significantly improves the activity of immunoliposomal drugs. This ratio was sufficient to provide a complete pRBC targeting specificity according to the delivery of immunoliposome-contained quantum dots [25], but the same amount of targeting antibody in immunoliposomes does not result in a 100% elimination of parasitemia at the low antimalarial drug concentrations assayed. Because the role of targeting antibodies is most likely to anchor liposomes to pRBCs when a random collision occurs, the *in vitro* efficacy of immunoliposomes as drug delivery vessels can likely be increased by incorporating more antibodies on their surfaces. As shown in Figure 4B, C, increasing the antibody concentration in immunoliposomes containing 4 nM chloroquine results in a corresponding significant increase of nanovector performance, reaching a clearance of 50% parasitemia for liposomes studded with an estimated 250 antibody molecules. However, keeping the antibody concentration as low as possible will contribute to reduce the immune response towards plasma-circulating immunoliposomes. Thus, when designing *in vivo* assays, a balance has to be reached between a sufficiently high density of targeting antibody for efficient drug delivery and levels below those triggering fast lymphocyte uptake. Since another factor affecting the number of random encounters between liposomes and pRBCs is the movement of both particles in solution, we expect that the turbulent mixing in the bloodstream will permit the use of low targeting antibody amounts. As mentioned above, BM1234 immunoliposomes deliver their contents to all pRBCs present in a sample, but when loaded with drug, they are not able to eliminate all *Plasmodium* parasites. It is possible that an increased performance can be achieved even with a few targeting antibody molecules per liposome if the amount of the encapsulated drug could be increased. In this regard, Ashley et al. [33] have assembled liposome-enclosed silica nanoparticles termed protocells, able to carry high anticancer drug payloads, with a single protocell having the capacity to kill a cancer cell. It would be worth exploring if such protocells can also be used as antimalarial drug-containing structures.

The preferential binding of BM1234 to trophozoites and schizonts suggested a differential subcellular localization of the corresponding antigen throughout the intraerythrocytic cycle of *P. falciparum*. This antibody had been selected for its binding to external features of pRBCs [25], which was a necessary condition for the targeting of these cells *in vivo*. When pRBCs are fixed with acetone/methanol prior to immunocytochemistry, BM1234 is observed to bind internal pRBC structures also (Figure 5). These are likely corresponding to regions in the endomembrane system built by *Plasmodium* that delineate the trafficking of the BM1234 antigen from its synthesis towards its final location in the pRBC plasma membrane. Alternatively, they could also represent internalization routes of externally exposed antigens. As expected, the subcellular localization of BM1234 antigens is changing during the intraerythrocytic cycle. A dominant spotted pattern in early trophozoites (Figure 5A) is consistent with the binding to pRBC intracellular membranous structures termed Maurer's clefts. In late trophozoites (Figure 5B) and especially in schizonts (Figure 5C), BM1234 binds structures on the periphery of the pRBC.

The remarkable capacity of liposomes to inject their contents into pRBCs presumably has its basis on alterations of the pRBC plasma membrane, rendering it less elastic and thus limiting the rebounding of colliding liposomes. The resulting slightly longer interactions, a phenomenon exacerbated if targeting antibodies are

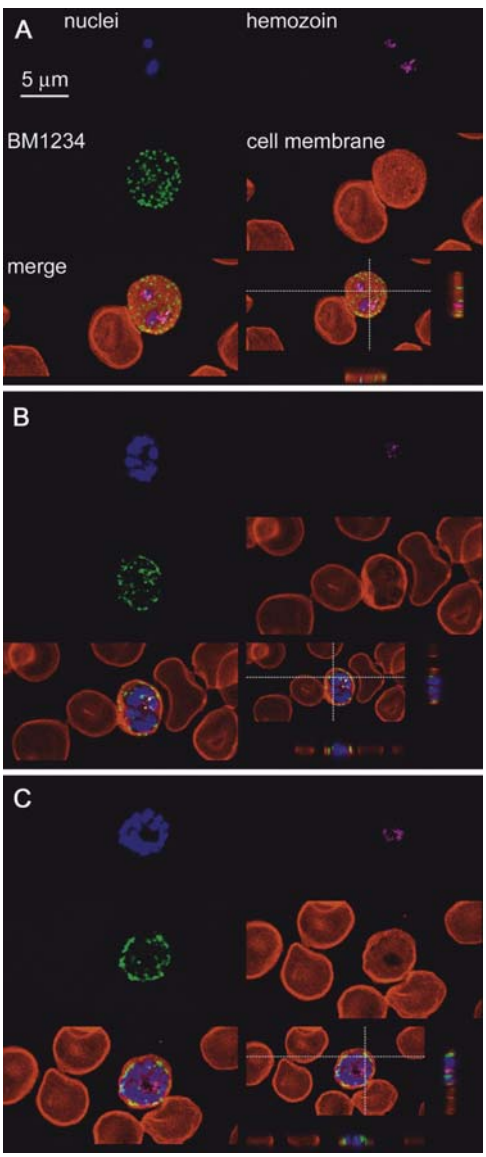

Figure 5 Confocal fluorescence microscopy study of the subcellular localization of BM1234. Early trophozoites (**A**), late trophozoites (**B**), and schizonts (**C**). Monoclonal antibody BM1234 was added to acetone/methanol-fixed *P. falciparum* cultures of the 3D7 strain, and its binding was detected by confocal fluorescence microscopy using a secondary antibody (green). DAPI (nuclei, in blue) and hemozoin fluorescence (pink) are used to indicate pRBCs. The RBC plasma membrane is shown in red. The four upper panels correspond to a single confocal section and are overlaid in the lower left panel. The lower right panel shows two perpendicular cross sections throughout the stack of images.

present, likely allow enough time for the physical phenomenon of lipid bilayer fusion to occur. This hypothesis could also explain why liposomes devoid of the antibody do perform better when added at the trophozoite stage since the membrane of ring-containing pRBCs is more similar to uninfected erythrocytes than that of pRBCs infected by later forms.

Conclusions

Next in our agenda is to advance towards a nanovector-based antimalarial delivery strategy suitable to enter preclinical trials. Liposomal nanovectors are adequate for a parenteral delivery, indicated in cases of complicated malaria, those at risk of developing severe disease, or if the patient is vomiting and unable to take oral antimalarials. Parenteral treatment can also be required in the *last mile* of a malaria eradication protocol for the single-dose, individualized administration of highly toxic drugs specifically targeted to pRBCs with good accuracy with the objective of eliminating remaining multiresistant strains. The nanovector prototype described here can improve *ca*. tenfold the activity of hydrosoluble antimalarial drugs, and it is amenable to improvement or adaptation through modification of some of its parts, e.g., better antibodies or targeting molecules, different nanocapsule structures, or new antimalarial drugs. Finally, BM1234 immunoliposomes can also be an efficient drug delivery vessel for the administration of liposoluble drugs against *P. falciparum*; unlike chloroquine and fosmidomycin, the solubility of hydrophobic compounds will be low when free in plasma, but can be significantly increased when incorporated in the lipid bilayers of liposomes.

Acknowledgements

This work was supported by grants BIO2008-01184, and CSD2006-00012 from the Ministerio de Ciencia e Innovación, Spain, which included FEDER funds, and by grant 2009SGR-760 from the Generalitat de Catalunya, Spain. A fellowship of the Instituto de Salud Carlos III (Spain) is acknowledged by Patricia Urbán. We acknowledge the support of the Scientific and Technological Centres from the University of Barcelona (CCiT-UB: cytometry, confocal microscopy, cryo-electron microscopy, and liquid chromatography units).

Author details

[1]Nanobioengineering Group, Institute for Bioengineering of Catalonia, Baldiri Reixac 10-12, Barcelona, E08028, Spain [2]Nanoscience and Nanotechnology Institute (IN2UB), University of Barcelona (UB), Martí i Franquès 1, Barcelona, E08028, Spain [3]Barcelona Centre for International Health Research (CRESIB), Hospital Clínic-Universitat de Barcelona, Rosselló 132, Barcelona, E08036, Spain [4]Departament de Fisicoquímica, Facultat de Farmàcia, University of Barcelona, Av. Joan XXIII, s/n, Barcelona, E08028, Spain [5]Scientific and Technological Centres, University of Barcelona, Baldiri Reixac 10-12, Barcelona, E08028, Spain [6]Institute for Research in Biomedicine, Barcelona Science Park, Baldiri Reixac 10-12, Barcelona, E08028, Spain [7]Institució Catalana de Recerca i Estudis Avançats (ICREA), Passeig Lluís Companys 23, Barcelona, E08018, Spain

Authors' contributions

PU carried out the inhibition assays, performed the microscopy analysis, participated in the design of the study and data analysis, and drafted the manuscript. JE participated in the liposome design and assembly and in the

data analysis. AA carried out the chloroquine and fosmidomycin determination. AC participated in the *P. falciparum* culture preparation and in the analysis of subcellular localizations. XF-B conceived and coordinated the study, participated in the design of the study and data analysis, and drafted the manuscript. All authors read and approved the final manuscript.

Competing interests
The authors declare that they have no competing interests.

Received: 9 September 2011 Accepted: 7 December 2011
Published: 7 December 2011

References

1. World Malaria Report 2009. [http://www.who.int/malaria/world_malaria_report_2009/en/].
2. Kappe SH, Vaughan AM, Boddey JA, Cowman AF: **That was then but this is now: malaria research in the time of an eradication agenda.** *Science* 2010, **328**:862-866.
3. Vangapandu S, Jain M, Kaur K, Patil P, Patel SR, Jain R: **Recent advances in antimalarial drug development.** *Med Res Rev* 2007, **27**:65-107.
4. Okiro EA, Al Taiar A, Reyburn H, Idro R, Berkley JA, Snow RW: **Age patterns of severe paediatric malaria and their relationship to *Plasmodium falciparum* transmission intensity.** *Malar J* 2009, **8**:4.
5. Wells TN, Alonso PL, Gutteridge WE: **New medicines to improve control and contribute to the eradication of malaria.** *Nat Rev Drug Discov* 2009, **8**:879-891.
6. Tuteja R: **Malaria - an overview.** *FEBS J* 2007, **274**:4670-4679.
7. Griffith KS, Lewis LS, Mali S, Parise ME: **Treatment of malaria in the United States: a systematic review.** *JAMA* 2007, **297**:2264-2277.
8. Enserink M: **Malaria's drug miracle in danger.** *Science* 2010, **328**:844-846.
9. Na-Bangchang K, Karbwang J: **Current status of malaria chemotherapy and the role of pharmacology in antimalarial drug research and development.** *Fundam Clin Pharmacol* 2009, **23**:387-409.
10. White NJ: **Assessment of the pharmacodynamic properties of antimalarial drugs *in vivo*.** *Antimicrob Agents Chemother* 1997, **41**:1413-1422.
11. Orive G, Hernández RM, Rodríguez Gascón A, Domínguez-Gil A, Pedraz JL: **Drug delivery in biotechnology: present and future.** *Curr Opin Biotechnol* 2003, **14**:659-664.
12. Zhang Z, Cao W, Jin H, Lovell JF, Yang M, Ding L, Chen J, Corbin I, Luo Q, Zheng G: **Biomimetic nanocarrier for direct cytosolic drug delivery.** *Angew Chem Int Ed Engl* 2009, **48**:9171-9175.
13. Santos-Magalhaes NS, Mosqueira VC: **Nanotechnology applied to the treatment of malaria.** *Adv Drug Deliv Rev* 2010, **62**:560-575.
14. Farokhzad OC, Langer R: **Impact of nanotechnology on drug delivery.** *ACS Nano* 2009, **3**:16-20.
15. Date AA, Joshi MD, Patravale VB: **Parasitic diseases: liposomes and polymeric nanoparticles versus lipid nanoparticles.** *Adv Drug Deliv Rev* 2007, **59**:505-521.
16. Storm G, Wilms HP, Crommelin DJ: **Liposomes and biotherapeutics.** *Biotherapy* 1991, **3**:25-42.
17. Maurer N, Fenske DB, Cullis PR: **Developments in liposomal drug delivery systems.** *Expert Opin Biol Ther* 2001, **1**:923-947.
18. Barenholz Y: **Liposome application: problems and prospects.** *Curr Opinion Coll Interface Sci* 2001, **6**:66-77.
19. Robinson AM, Creeth JE, Jones MN: **The specificity and affinity of immunoliposome targeting to oral bacteria.** *Biochim Biophys Acta* 1998, **1369**:278-286.
20. Owais M, Varshney GC, Choudhury A, Chandra S, Gupta CM: **Chloroquine encapsulated in malaria-infected erythrocyte-specific antibody-bearing liposomes effectively controls chloroquine-resistant *Plasmodium berghei* infections in mice.** *Antimicrob Agents Chemother* 1995, **39**:180-184.
21. Postma NS, Hermsen CC, Zuidema J, Eling WM: ***Plasmodium vinckei*: optimization of desferrioxamine B delivery in the treatment of murine malaria.** *Exp Parasitol* 1998, **89**:323-330.
22. Postma NS, Crommelin DJ, Eling WM, Zuidema J: **Treatment with liposome-bound recombinant human tumor necrosis factor-alpha suppresses parasitemia and protects against *Plasmodium berghei* k173-induced experimental cerebral malaria in mice.** *J Pharmacol Exp Ther* 1999, **288**:114-120.
23. Robertson RT, Baratta JL, Haynes SM, Longmuir KJ: **Liposomes incorporating a *Plasmodium* amino acid sequence target heparan sulfate binding sites in liver.** *J Pharm Sci* 2008, **97**:3257-3273.
24. Longmuir KJ, Robertson RT, Haynes SM, Baratta JL, Waring AJ: **Effective targeting of liposomes to liver and hepatocytes in vivo by incorporation of a *Plasmodium* amino acid sequence.** *Pharm Res* 2006, **23**:759-769.
25. Urbán P, Estelrich J, Cortés A, Fernàndez-Busquets X: **A nanovector with complete discrimination for targeted delivery to *Plasmodium falciparum*-infected versus non-infected red blood cells in vitro.** *J Control Release* 2011, **151**:202-211.
26. MacDonald RC, MacDonald RI, Menco BP, Takeshita K, Subbarao NK, Hu LR: **Small-volume extrusion apparatus for preparation of large, unilamellar vesicles.** *Biochim Biophys Acta* 1991, **1061**:297-303.
27. Martin FJ, Papahadjopoulos D: **Irreversible coupling of immunoglobulin fragments to preformed vesicles. An improved method for liposome targeting.** *J Biol Chem* 1982, **257**:286-288.
28. Koppenhagen FJ, Storm G, Underberg WJ: **Development of a routine analysis method for liposome encapsulated recombinant interleukin-2.** *J Chromatogr B Biomed Sci Appl* 1998, **716**:285-291.
29. Cranmer SL, Magowan C, Liang J, Coppel RL, Cooke BM: **An alternative to serum for cultivation of *Plasmodium falciparum* in vitro.** *Trans R Soc Trop Med Hyg* 1997, **91**:363-365.
30. Lambros C, Vanderberg JP: **Synchronization of *Plasmodium falciparum* erythrocytic stages in culture.** *J Parasitol* 1979, **65**:418-420.
31. Leivar P, González VM, Castel S, Trelease RN, López-Iglesias C, Arró M, Boronat A, Campos N, Ferrer A, Fernàndez-Busquets X: **Subcellular localization of Arabidopsis 3-hydroxy-3-methylglutaryl-coenzyme A reductase.** *Plant Physiol* 2005, **137**:57-69.
32. Yayon A, Ginsburg H: **The transport of chloroquine across human erythrocyte membranes is mediated by a simple symmetric carrier.** *Biochim Biophys Acta* 1982, **686**:197-203.
33. Ashley CE, Carnes EC, Phillips GK, Padilla D, Durfee PN, Brown PA, Hanna TN, Liu J, Phillips B, Carter MB, Carroll NJ, Jiang X, Dunphy DR, Willman CL, Petsev DN, Evans DG, Parikh AN, Chackerian B, Wharton W, Peabody DS, Brinker CJ: **The targeted delivery of multicomponent cargos to cancer cells by nanoporous particle-supported lipid bilayers.** *Nat Mater* 2011, **10**:389-397.

doi:10.1186/1556-276X-6-620
Cite this article as: Urbán *et al.*: Study of the efficacy of antimalarial drugs delivered inside targeted immunoliposomal nanovectors. *Nanoscale Research Letters* 2011 **6**:620.

ARTICLE 3

Demonstration of specific binding of heparin to Plasmodium falciparum-infected red blood cells by single-molecule force spectroscopy

RBCs infected with the mature stages of *P. falciparum* bind to the endothelial cells of capillaries and post-capillary venules of several tissues in a phenomenon known as sequestration, which allows parasites to replicate while evading splenic clearance. The cytoadherence of pRBCs is suggested to be mediated by *P. falciparum* erythrocyte membrane protein 1 (PfEMP1), and different receptors, including both proteins and glycosaminoglycans (GAGs) on endothelial cells and platelets have been described for PfEMP1. Binding of PfEMP1 to the GAGs chondroitin 4-sulfate (CS), heparan sulfate (HS) and heparin has been reported, the last two molecules being involved in sporozoite attachment to hepatocytes during the primary stage of malaria infection in the liver. Soluble CSA, heparin, HS, heparin/ HS derivatives and other sulfated glycoconjugates can either inhibit pRBC sequestration, disrupt rosettes, or block sporozoite adhesion to hepatocytes; these results are the basis of the proposal of GAG-based therapies against malaria.

In this article we have quantitatively explored by fluorescence microscopy and flow cytometry the targeting specificity of heparin to pRBCs vs RBCs (work performed by P. Urbán), and we have analyzed by atomic force microscopy (AFM) force spectroscopy the binding of heparin to pRBCs (work performed by J.J. Valle-Delgado), as a pioneering nanotechnological approach to understanding the mechanisms underlying GAG-pRBC interactions.

Heparin fluorescence was exclusively observed on infected erythrocytes, proving that heparin specifically bound to pRBCs, and not to RBCs. Fluorescence-assisted cell sorting assays (Figure 16) revealed that the amount of heparin bound

to pRBCs depends on heparin concentration and the developmental stage of *P. falciparum*, with a maximum heparin binding observed at schizont phase. In the light of these results, heparin and erythrocytes infected with mature forms of *P. falciparum* 3D7 were considered as a model system to study GAG-pRBC interactions at the single-molecule level, and AFM force spectroscopy was applied to measure the binding forces between heparin and pRBCs or non-infected RBCs. Results obtained showed an average between 28 and 46 pN, depending on the loading rate, for the binding force between individual heparin molecules and pRBCs.

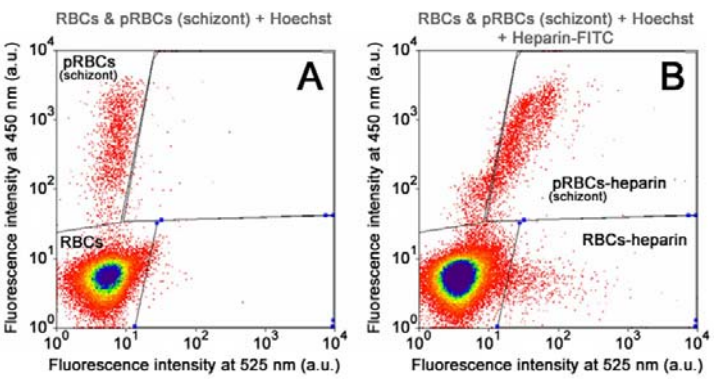

Figure 16. FACS analysis of the binding of heparin to schizont-containing-pRBCs, corresponding to Figure 2A and B in the article. A) Hoechst-stained pRBCs are distributed in the upper left area, whereas non-infected RBCs appear in the lower left area. B) After incubation with 40 µg/ml heparin-FITC, pRBCs showing heparin attachment (positive FITC fluorescence) are collected in the upper right area. Non-parasitized RBCs exhibiting association with heparin are located in the lower right area.

Heparin had been used in the treatment of malaria, but it was abandoned because of its strong anticoagulant action, with side effects such as intracranial bleeding. However, the use of either heparin as a targeting molecule covalently attached to nanocarriers for antimalarial drug delivery could be a viable therapeutic approach that would reduce the risk of anticoagulation and internal bleeding induced by soluble heparin. Comparing the heparin-pRBC binding force between 28 and 46 pN obtained in this work with the antibody-antigen interaction values reported in the literature, it can be suggested that low amounts of heparin as targeting molecule might be sufficient for future antimalarial-containing nanovectors.

Nanoscale

RSC Publishing

PAPER

View Article Online
View Journal

Demonstration of specific binding of heparin to *Plasmodium falciparum*-infected *vs.* non-infected red blood cells by single-molecule force spectroscopy†

Cite this: DOI: 10.1039/c2nr32821f

Juan José Valle-Delgado,[abc] Patricia Urbán[abc] and Xavier Fernàndez-Busquets*[abc]

Received 19th September 2012
Accepted 5th December 2012

DOI: 10.1039/c2nr32821f

www.rsc.org/nanoscale

Glycosaminoglycans (GAGs) play an important role in the sequestration of *Plasmodium falciparum*-infected red blood cells (pRBCs) in the microvascular endothelium of different tissues, as well as in the formation of small clusters (rosettes) between infected and non-infected red blood cells (RBCs). Both sequestration and rosetting have been recognized as characteristic events in severe malaria. Here we have used heparin and pRBCs infected by the 3D7 strain of *P. falciparum* as a model to study GAG–pRBC interactions. Fluorescence microscopy and fluorescence-assisted cell sorting assays have shown that exogenously added heparin has binding specificity for pRBCs (preferentially for those infected with late forms of the parasite) *vs.* RBCs. Heparin–pRBC adhesion has been probed by single-molecule force spectroscopy, obtaining an average binding force ranging between 28 and 46 pN depending on the loading rate. No significant binding of heparin to non-infected RBCs has been observed in control experiments. This work represents the first approach to quantitatively evaluate GAG–pRBC molecular interactions at the individual molecule level.

Introduction

Red blood cells (RBCs) infected with mature stages of the malaria parasite, *Plasmodium falciparum*, bind to the endothelial cells of capillaries and post-capillary venules of tissues such as brain, heart, lung, kidney, placenta and small intestine. This phenomenon, known as sequestration, allows replication of parasites while evading splenic clearance.[1] *P. falciparum*-infected RBCs (pRBCs) can also adhere to non-infected RBCs giving rise to rosettes,[2,3] and they can form clumps through platelet-mediated binding to other pRBCs.[4] These events, which may lead to occlusion of the microvasculature, are thought to play a major role in the fatal outcome of severe malaria.[1] The cytoadherence of pRBCs is suggested to be mediated by *P. falciparum* erythrocyte membrane protein 1 (PfEMP1), a parasite-derived, antigenically diverse protein expressed at the surface of pRBCs.[5,6] Different receptors have been described for PfEMP1 on endothelial cells and platelets, including both proteins and glycosaminoglycans (GAGs).[4,7–17] Binding of PfEMP1 to the GAG chondroitin 4-sulfate (CSA) is thought to cause pRBC sequestration in the placenta, which has been linked to the severe disease outcome of pregnancy-associated malaria.[18–21] PfEMP1 has also been identified as the rosetting ligand that binds to heparan sulfate (HS), or a HS-like molecule, exposed on RBCs.[15,22–24] The GAGs heparin and HS are also targets for the circumsporozoite protein in the sporozoite attachment to hepatocytes during the primary stage of malaria infection in the liver.[25–29] GAG-based therapies against malaria have been proposed in the wake of the results from different assays showing that soluble CSA, heparin, HS, heparin–HS derivatives and other sulfated glycoconjugates can either inhibit pRBC sequestration,[9–12,16,18–20,30,31] disrupt rosettes,[3,15,16,22–24,31–35] or block sporozoite adhesion to hepatocytes.[25–28]

Thus, a detailed study of GAG–pRBC adhesion from a biophysical point of view has a potential impact on the development of new nanomedical strategies against malaria, because unraveling the mechanisms and quantifying the forces involved in the binding of pRBCs to GAGs could lead to the design of competitors against pRBC sequestration and rosetting. Alternatively, GAGs could be also used as targeting agents to direct antimalarial-carrying nanocapsules towards pRBCs with high specificity. Within this therapeutical approach, we have recently developed liposomal nanovectors for the targeted delivery of antimalarial drugs specifically to pRBCs. Our current prototype, based on antibodies as targeting molecules, has complete discrimination *in vitro* for pRBCs *vs.* non-infected erythrocytes,[36] and it increases tenfold the activity of the antimalarial drugs chloroquine and fosmidomycin.[37] Improvement of the immunoliposomal nanovector performance can foreseeingly be achieved by optimizing the liposome formulation and also by increasing the amount of targeting antibody and the concentration of encapsulated drugs. However, although antibodies

[a]*Nanobioengineering Group, Institute for Bioengineering of Catalonia (IBEC), Baldiri Reixac 10-12, Barcelona E08028, Spain. E-mail: xfernandez_busquets@ub.edu*
[b]*Barcelona Centre for International Health Research (CRESIB, Hospital Clínic-Universitat de Barcelona), Rosselló 149-153, Barcelona E08036, Spain*
[c]*Biomolecular Interactions Team, Nanoscience and Nanotechnology Institute (IN2UB), University of Barcelona, Martí I Franquès 1, Barcelona E08028, Spain*

† Electronic supplementary information (ESI) available. See DOI: 10.1039/c2nr32821f

have an exquisite recognition of their corresponding antigens, some of their properties limit their role as targeting elements in antimalarial therapeutic strategies. First, antibodies are relatively expensive to produce, which is an undesirable characteristic when designing medicines to be used in developing countries. Secondly, they are highly immunogenic unless genetically engineered humanized forms are used. Finally, as a result of the high variability of *Plasmodium* proteins exposed on pRBC surfaces, any antibody will likely lose targeting efficacy as the parasite switches to new antigenic repertoires.

The combination of high sensitivity at force detection (of the order of piconewtons), subnanometric location resolution, and the possibility to operate in liquid environments has made the atomic force microscope (AFM) a very useful tool for the characterization of biological samples. In single-molecule force spectroscopy (SMFS) experiments, the AFM has been successfully applied to measure the binding forces between ligand–receptor, antibody–antigen or enzyme–substrate,[38–49] and to analyze the mechanical properties of polymeric molecules like proteins, polysaccharides or DNA upon stretching.[50–59] Cell adhesion and elasticity have also been probed by AFM,[60–62] with special attention to RBCs,[63–66] whereas lectin–glycoprotein interactions on RBCs[67,68] and binding of the endothelial receptor proteins thrombospondin (TSP) and CD36 to pRBCs have been also studied by SMFS.[69] Here we have quantitatively explored by fluorescence microscopy the targeting specificity of heparin to pRBCs *vs.* RBCs, and we have analyzed by AFM force spectroscopy the binding of heparin to pRBCs, as a pioneering nanotechnological approach to understanding the mechanisms underlying GAG–pRBC interactions.

Results

Living *P. falciparum* 3D7 cultures containing *ca.* 5% pRBCs were treated with 10 μg ml^{-1} of fluorescein-labeled heparin (heparin–FITC), and after 90 minutes of incubation the samples were prepared for fluorescence microscopy examination. Because RBCs are anucleated cells, the DNA-binding fluorophore 4′,6-diamino-2-phenylindole (DAPI) was used to provide a clear identification of pRBCs. Remarkably, FITC emission was exclusively observed on infected erythrocytes, proving that heparin specifically binds to pRBCs, and not to RBCs (Fig. 1). The resolution of the images did not permit unequivocal determination of whether heparin was being taken up by the targeted cells but cross-reactivity of DAPI and FITC was ruled out in control assays (Fig. S1†). Fluorescence-assisted cell sorting (FACS) assays revealed that the amount of heparin bound to pRBCs depends on the heparin concentration and the developmental stage of *P. falciparum* (Fig. 2). 13.0%, 16.3% and 24.4% of pRBCs at the ring stage showed heparin binding after incubation with 10, 20 and 40 μg ml^{-1} heparin–FITC, respectively. Those percentage values increased to 19.5%, 33.7% and 55.4%, respectively, in the case of pRBCs at the trophozoite stage. Maximum heparin binding was observed at the schizont phase, where up to 76.6% of pRBCs significantly bound heparin after incubation with 40 μg ml^{-1} heparin–FITC. Only a marginal proportion of about 0.5% of non-infected RBCs exhibited an association with heparin. However, it must be mentioned that the difficulty in achieving perfectly synchronized pRBC cultures and the continuous development of *P. falciparum* parasites inside erythrocytes complicate the obtention of pure pRBC populations at the same stage of infection during the preparation and performance of FACS experiments. Microscopic examination of Giemsa-stained smears showed that cultures of pRBCs which had been synchronized at the ring phase contained about 10% of trophozoite-infected pRBCs, and that in schizont-enriched preparations about 7% and 10% of pRBCs were parasitized by rings and trophozoites, respectively. Therefore, an overestimation of heparin binding to ring-infected pRBCs is expected in the data presented in Fig. 2C; in contrast, the results shown in the same figure would underestimate the heparin attachment to schizont-infected pRBCs. Visual inspection of pRBC cultures by fluorescence microscopy corroborated the trend of heparin binding observed in FACS experiments (rings < trophozoites < schizonts); however, the percentage of schizont-infected pRBCs showing heparin fluorescence was significantly higher (94%), because ring stages could be easily identified and discarded.

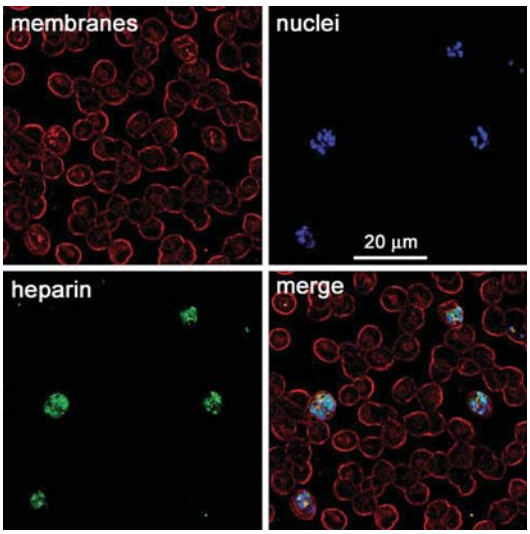

Fig. 1 Confocal fluorescence microscopy study of the specific interaction of heparin with pRBCs. Fluorescein-labeled heparin was added to a living pRBC culture and incubated for 90 minutes before sample preparation. The fluorescence of labeled heparin (green) co-localizes with the four late form-containing pRBCs in the microscope field, detected by the DAPI staining of *Plasmodium* DNA (blue). Erythrocyte membranes were stained with WGA (red).

The pRBC membrane is modified as the intraerythrocytic cycle of the parasite proceeds from the ring to trophozoite and schizont phases, and different proteins of *Plasmodium* origin arrange on the membrane of pRBCs giving rise to the formation of small bumps called knobs,[70–73] with a typical height of 20 to 30 nm (Fig. 3A and B). Knobs appear during the trophozoite stage, and their number increases to a maximum in schizonts,[71,72] in close correlation with the trend of heparin binding

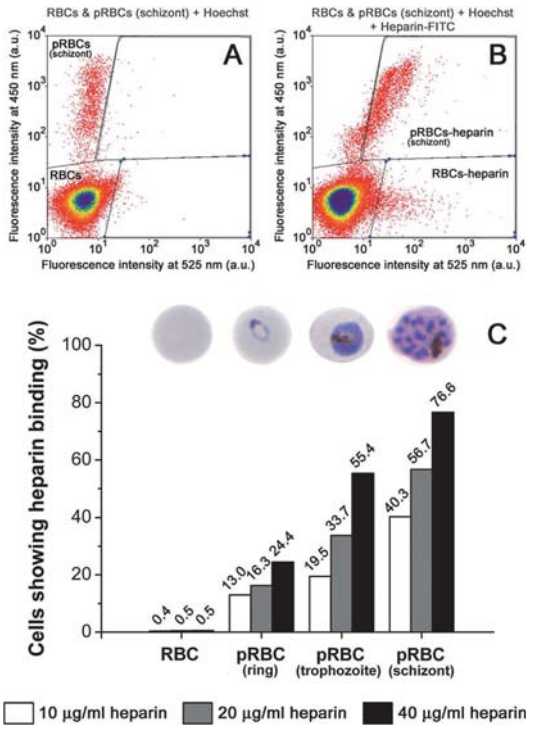

Fig. 2 FACS analysis of the binding of heparin to pRBCs at different stages of parasite development. Data from a typical FACS experiment are presented in (A) and (B), where the fluorescence at 450 nm (Hoechst 33342 emission) and 525 nm (FITC emission) is plotted for every single erythrocyte of a coculture of RBCs and pRBCs at the schizont stage. (A) In the absence of heparin–FITC, Hoechst-stained pRBCs are distributed in the upper left area, whereas anucleated non-infected RBCs appear in the lower left area. (B) After incubation for 90 minutes with 40 µg ml^{-1} heparin–FITC, pRBCs showing heparin attachment (positive FITC fluorescence) are collected in the upper right area. Non-parasitized RBCs exhibiting association with heparin are located in the lower right area. (C) Percentage of RBCs and pRBCs at different stages of parasite development showing heparin binding. Data were obtained from the analysis of FACS experiments carried out with RBC and pRBC samples previously incubated with 10, 20 and 40 µg ml^{-1} heparin–FITC for 90 minutes at 37 °C. Percentage values are indicated above each bar. Illustrative microscope images of Giemsa-stained RBC and pRBCs at different stages are shown.

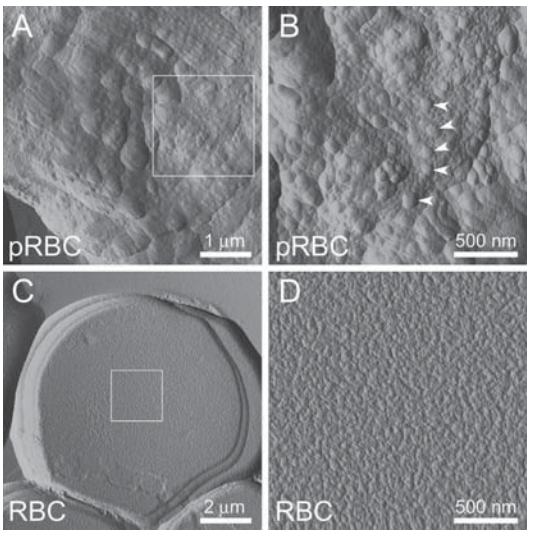

Fig. 3 High resolution images of infected and non-infected red blood cells. AFM images of a pRBC (A and B) and a RBC (C and D). (B) and (D) are magnified images of the square areas framed in (A) and (C), respectively. The small round bumps in (A) and (B) correspond to knobs on the pRBC membrane (arrowheads point to some of them in (B)), which are not present on the smoother RBC membrane (C and D).

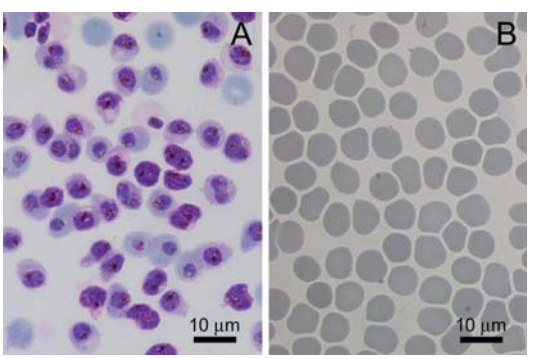

Fig. 4 Light microscope images of Giemsa-stained red blood cell samples. (A) Percoll-purified red blood cells infected by mature stages of *P. falciparum* 3D7. (B) Non-infected red blood cells.

presented in Fig. 2. Fig. 3C and D show AFM images of the membrane of a RBC, where no knob structures can be observed. Addition of heparin to pRBCs or RBCs did not induce structural changes on the cell membrane that could be identified by AFM imaging (data not shown).

In the light of the results presented above, heparin and erythrocytes infected with mature forms of *P. falciparum* 3D7 were considered as a model system to study GAG–pRBC interactions at the single-molecule level. AFM force spectroscopy was applied to measure the binding forces between heparin molecules immobilized on the tip of force sensors and Percoll-purified pRBCs (Fig. 4A) or non-infected RBCs (Fig. 4B) deposited on poly-L-lysine-coated glass slides. Fig. 5 shows a scheme of this experimental set-up, whereby force curves were obtained in phosphate buffered saline (PBS) by approaching the heparin-functionalized cantilever tip to the adsorbed erythrocytes until contact, followed by its retraction. Single-molecule heparin–pRBC adhesion forces were evaluated from the unbinding events observed in the retraction force curves. Between 5% and 15% of the force curves obtained in different experiments showed unbinding events similar to those presented in Fig. 6A. As the heparin-coated tip withdrew, a decompression of the pRBC was observed in the retraction force curves for distances between 1 and 2.5 µm, which were similar to the compression

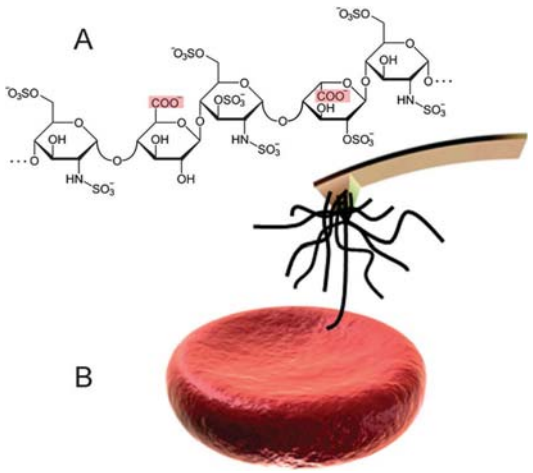

Fig. 5 Scheme of the experimental set-up for force spectroscopy experiments. (A) Heparin sequence region corresponding to the antithrombin pentasaccharide binding site; the carboxyl groups used for the covalent crosslinking of heparin to AFM cantilevers are shaded. (B) Cartoon of a binding event between an erythrocyte and one of the heparin chains crosslinked to the AFM cantilever tip. RBC and heparin images were adapted from http://en.wikipedia.org/wiki/File:Erythrocyte_deoxy.jpg and from http://en.wikipedia.org/wiki/Fondaparinux, respectively.

range distances observed in the approach force curves (data not shown). The pRBC decompression was followed by a vertical jump (arrows in Fig. 6A) corresponding to the detachment of the tip from the cell membrane. A flat baseline was finally reached, reflecting no interaction between the cell and tip after their complete separation. Unbinding events were absent in typical retraction force curves on non-infected RBCs (Fig. 6B). A representative histogram for the heparin–pRBC adhesion is shown in Fig. 6C. The Gaussian fits of the histograms from seven independent experiments yielded an average value of 43 ± 5 pN for the binding force between heparin and pRBC at a loading rate of 17.5 nN s^{-1}. From that value it could be inferred that binding forces around 90 and 125 pN observed in a small proportion of force curves could correspond to the simultaneous unbinding of, respectively, 2 and 3 interacting groups on the same or different heparin molecules. Control experiments with non-infected RBCs showed non-significant adhesion to heparin (Fig. 6C). Dynamic force spectroscopy data derived from experiments at different loading rates (Fig. 6D) yielded binding forces between 28 and 46 pN. A linear relationship between the binding force and the logarithm of loading rate was observed (Fig. 6D), which is in agreement with the predictions from the Bell–Evans model for binary interactions.[74,75]

Discussion

Specific binding of heparin to pRBCs infected by late forms of the *P. falciparum* 3D7 strain has been proved here by fluorescence microscopy, FACS, and SMFS. This result joins previous experimental evidence suggesting binding of heparin and heparin derivatives to pRBCs.[3,15,16,22–24,31–35] Duffy-binding-like domain 1 (DBL-1), a lysine-rich region next to the *N*-terminal segment of PfEMP1, has been proposed as the ligand receptor

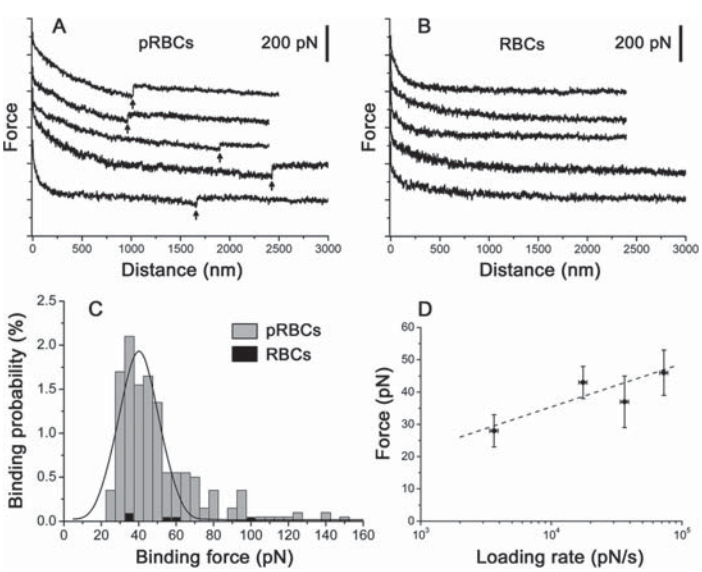

Fig. 6 AFM force spectroscopy results. (A and B) Typical force curves from independent experiments obtained when retracting heparin-functionalized cantilever tips from (A) pRBCs and (B) RBCs. Arrows in (A) indicate individual heparin–pRBC unbinding events. For the sake of clarity, the force curves were shifted vertically to avoid overlapping. (C) Representative force histograms for the binding of heparin to pRBCs (grey) and RBCs (black) at a loading rate of 17.5 nN s^{-1}. Heparin–pRBC binding data were fitted to a Gaussian curve. (D) Average binding forces between heparin and pRBCs at different loading rates.

for heparin binding.[15,16,22,24,76] PfEMP1 is located in the knobs,[77] whose formation is closely associated with the intraerythrocytic cycle of *P. falciparum*: knobs are absent during the ring stage, begin to form on the pRBC membrane at the early trophozoite stage, and reach a maximum number during late trophozoite and schizont phases.[71,72] In good correlation with knob formation, pRBCs show higher adherent properties after 16 hours of parasite invasion,[20,78] and our results are consistent with heparin binding to PfEMP1 present on the knobs. An important role of knobs in the adherence of pRBCs to vascular endothelial cells under physiological flow conditions has also been observed.[79,80] The presence of PfEMP1 DBL-1 domains on knobs, rich in positively charged residues, is supported by surface potential spectroscopy experiments revealing that knobs have a positive electrical charge, in contrast to the negatively charged pRBC membrane.[81] These positively charged patches on pRBCs could favour the binding of highly sulfated heparin, since it has been observed that the sulfation degree of heparin affects the affinity of the polysaccharide for pRBCs.[15,34] Similarly, *P. falciparum*-infected RBCs bind to CSA in the placenta *via* the VAR2CSA protein, a member of the PfEMP1 family. CSA binding occurs through a cluster of conserved positively charged residues on subdomains 2 and 3 of the DBL3x domain in VAR2CSA.[82]

SMFS has offered new opportunities for probing the adhesion and mechanics of polysaccharides on live cells.[83] Understanding the molecular interaction between GAGs and pRBCs is essential for elucidating the mechanisms of malarial pathogenesis. The specific binding force range between 28 and 46 pN obtained in this work for the heparin–pRBC adhesion is comparable to that of many protein-mediated cell interactions, such as the binding between mycobacterial adhesins and HS proteoglycan receptors on A549 pneumocytes, which was found to be 57 ± 16 pN.[84] Similar binding forces of about 50 pN were also observed between mycobacterial adhesins and heparin.[85] Li *et al.* have recently applied SMFS to study the binding interactions between pRBCs and the endothelial receptors involved in pRBC sequestration[8] TSP and CD36 anchored on cantilever tips.[69] Forces in the range 30–90 pN were required to rupture TSP–pRBC and CD36–pRBC bonds,[69] values within the same order of magnitude as those for heparin–pRBC presented here. Using micropipette manipulation techniques, it has been reported that forces of about 440 pN were necessary to detach an erythrocyte from a rosette,[86] a phenomenon thought to be due to interactions between heparin-related HS (or a HS-like molecule) on RBCs and PfEMP1 on pRBCs. That value is tenfold higher than the single-molecule heparin–pRBC binding force observed by us, but it must be noted that when studying the total adhesion between two cells with the micropipette technique, higher forces are expected due to the simultaneous measurement of several binding contacts.

Heparin had been used in the treatment of severe malaria[87–91] but it was abandoned because of its strong anticoagulant action, with side effects such as intracranial bleeding.[92] However, depolymerized heparin lacking anticoagulant activity has been found to disrupt rosette formation and pRBC cytoadherence *in vitro* and *in vivo* in animal models and in fresh parasite isolates,[31,35] and there is also evidence for non-anticoagulant activity of heparin when covalently immobilized on a substrate.[93] Surface plasmon resonance biosensor studies showed that covalent binding of heparin through its carboxyl groups dramatically reduced the interaction of heparin with antithrombin III (ATIII),[94] whereas attachment through the reducing amino terminus did not significantly affect it and heparin immobilized *via* intrachain naturally occurring unsubstituted amine residues had intermediate binding capacity. Here, heparin has been bound to AFM cantilevers through its carboxyl groups, a situation in which heparin maintains its specific binding to pRBCs; the corresponding low ATIII binding would minimize the otherwise undesirable anticoagulation activity of exogenously added heparin. Thus, the use of either heparin or depolymerized heparin as a targeting molecule covalently attached to nanocarriers for antimalarial drug delivery could be a viable therapeutic approach that would reduce the risk of internal bleeding induced by soluble heparin. In a previous work,[36] we showed that antimalarial-encapsulating immunoliposomes studded with an estimated 5 antibody molecules per liposome improved *ca.* tenfold the efficacy of the drugs. By comparing the heparin–pRBC binding force with the antibody–antigen interaction values reported in the literature (ranging from 40 to 250 pN),[44–46] it can be suggested that relatively low amounts of heparin as a targeting molecule might substitute for antibodies in future antimalarial nanotherapies.

Experimental section

P. falciparum culture and purification

P. falciparum 3D7 was grown *in vitro* in rinsed human RBCs of blood group type B prepared as described elsewhere[36] using previously established conditions.[95] Briefly, parasites (thawed from glycerol stocks) were cultured at 37 °C in petri dishes containing RBCs in Roswell Park Memorial Institute (RPMI) complete medium under a gas mixture of 92% N_2, 5% CO_2, and 3% O_2. Synchronized cultures were obtained by 5% sorbitol lysis[96] and cytoadherent parasites were selected by gelatin flotation using gelafundin (B. Braun, Melsungen, Germany).[97] For culture sustainment, parasitemias were kept below 5% late forms by diluting with washed RBCs and the medium was changed every 2 days maintaining 3% hematocrit. Parasitemia was estimated by examination of Giemsa-stained smears with a Zeiss Primo Star microscope. Synchronized cultures at mature stages for AFM imaging and force spectroscopy experiments were enriched using Percoll (GE Healthcare, UK) purification[98] to obtain late trophozoite- and schizont-containing pRBC suspensions at *ca.* 90% parasitemia.

Fluorescence microscopy

Living *P. falciparum* cultures with mature stages of the parasite were incubated in the presence of 10 μg ml^{-1} fluorescein-labeled heparin (heparin–FITC, Invitrogen, Carlsbad, CA, USA) for 90 minutes at 37 °C with gentle stirring. After washing, blood smears were prepared and cells were fixed in acetone : methanol (90 : 10). Parasite nuclei were stained with

4′,6-diamino-2-phenylindole (DAPI, Invitrogen) and the RBC membrane was labeled with wheat germ agglutinin (WGA)–tetramethylrhodamine conjugate (Molecular Probes, Eugene, OR, USA). Slides were finally mounted with Mowiol (Calbiochem, Merck Chemicals, Darmstadt, Germany), and analyzed with a Leica TCS SP5 laser scanning confocal microscope. DAPI, FITC, reflection (hemozoin), and WGA–rhodamine images were acquired sequentially using 405, 488, 488 and 561 laser lines, and emission detection ranges 415–480 nm, 500–550 nm, 480–500 nm, and 571–625 nm, respectively, with the confocal pinhole set at 1 airy units. Bright field transmitted light images were acquired simultaneously.

FACS analysis

Cultures of *P. falciparum* at approximately 4% parasitemia synchronized at ring, trophozoite and schizont stages were incubated with heparin–FITC at final concentrations of 10, 20 and 40 μg ml^{-1} for 90 minutes at 37 °C. After washing, parasite nuclei were stained with Hoechst 33342 (Sigma-Aldrich, St Louis, MO, USA). For FACS analysis, pRBCs were diluted to a final concentration of 1–10 × 10^6 cells per ml. Samples were analyzed using a Gallios multi-color flow cytometer instrument (Beckman Coulter, Inc, Fullerton, CA, USA) set up with the 3-laser 10 color standard configuration. The single-cell population was selected on a forward-side scatter scattergram. FITC was excited using a blue laser (488 nm), and its fluorescence collected through a 525/40 nm filter. Hoechst was excited with a violet laser (405 nm), and its fluorescence collected using a 450/40 nm filter. Between 50 000 and 200 000 cells (cocultures of RBCs and pRBCs) were analyzed in every experiment. Control tests of heparin binding in the absence of Hoechst were also carried out (Fig. S2†).

Atomic force microscopy

50 μl of RBC or Percoll-purified pRBC solutions were deposited on poly-L-lysine-coated glass slides, which were prepared in advance by exposing the glass slides (StarFrost, Waldemar Knittel Glasbearbeitungs GmbH, Braunschweig, Germany) to 0.01% poly-L-lysine solution (Sigma-Aldrich) for 30 minutes followed by rinsing with double deionised water (Milli-Q) and evaporation. After about half an hour of adsorption, the glass slides were rinsed several times with 100 μl PBS, carefully added and removed with an automatic pipette, to take away weakly and non-attached cells. 50 μl of fixation solution (4% paraformaldehyde, 0.0125% glutaraldehyde, in PBS) were then added and, 20 minutes later, the glass slides were rinsed with water using an automatic pipette and dried by evaporation. A Dimension 3100 atomic force microscope (Veeco Instruments Inc., Santa Barbara, CA, USA) was used to obtain images of the fixed RBCs and pRBCs in air. NSC15 probes (Mikromasch, Tallinn, Estonia), with a nominal spring constant of 46 N m^{-1}, were used to scan the samples in tapping mode at 0.2–0.5 Hz scan rates.

Force spectroscopy

A MFP-3D atomic force microscope (Asylum Research, Santa Barbara, CA, USA) was used to measure the binding forces between pRBCs deposited on poly-L-lysine-coated glass slides and heparin molecules immobilized on the silicon nitride tip of NP–S cantilevers (Veeco Instruments Inc.; spring constants in the range 0.05–0.08 N m^{-1} obtained by the thermal method). The cantilevers were previously silanized in the vapour phase with 3-aminopropyl triethoxysilane (APTES, Fluka, Buchs, Switzerland) to provide them with amine groups, which were crosslinked with the carboxyl groups of heparin by immersing the cantilevers in a solution of 100 μg ml^{-1} heparin (Sigma-Aldrich) containing 2.5 mM *N*-(3-dimethylaminopropyl)-*N*′-ethylcarbodiimide hydrochloride (EDAC, Fluka) and 10 mM *N*-hydroxysuccinimide (NHS, Fluka). After about one hour of reaction, the cantilevers were rinsed with PBS. In parallel to heparin immobilization, 50 μl of a Percoll-purified pRBC solution in RPMI medium were deposited on poly-L-lysine-coated glass slides prepared as described above. After about one hour of adsorption, weakly and non-attached pRBCs were discarded by rinsing the glass slides several times with 100 μl PBS using an automatic pipette. Force curves were acquired in PBS at room temperature by approaching the cantilever tip with immobilized heparin to the pRBCs adsorbed on the glass slide until contact and then retracting them. The approaching velocity was kept constant at 2.5 μm s^{-1}, whereas the retraction speed was varied between 0.7 and 14 μm s^{-1} (dynamic force spectroscopy). The corresponding loading rates were calculated by multiplying the retraction velocities by the effective spring constant of the system,[99] which was *ca.* 10% of the spring constants of the cantilevers. Maximum applied forces were below 0.5 nN to prevent cell lysis.[63] In a typical experiment, about 2000 force curves were collected in at least 100 different spots on the same or different cells. Adhesion between heparin and pRBC was evaluated from the unbinding events in the retraction force curves. When several unbinding events were observed, only the last one was considered for analysis. Force histograms were fitted to Gaussian curves to obtain the average binding forces. Control experiments with non-infected RBCs were also accomplished.

Conclusion

Within the framework of our search for pRBC-specific targeting molecules that could represent an alternative to the use of antibodies, here we have explored the GAG heparin based on previous data suggesting pRBC binding to certain GAGs. Heparin is cheap, of low immunogenicity due mainly to its endogenous nature, and it might bind pRBCs through electrostatic interactions with relatively large positively charged regions in the knobs, a target that *Plasmodium* will likely not be able to modify as readily as it can do with the small antigenic determinants recognized by antibodies. The high specificity of heparin binding to pRBCs infected with late forms of *P. falciparum* opens the way for the design of heparin-based nanotherapies for the targeted delivery of antimalarial drugs.

Acknowledgements

This work was supported by grant BIO2011-25039 from the Ministerio de Ciencia e Innovación, Spain, which included

FEDER funds, and by grant 2009SGR-760 from the Generalitat de Catalunya, Spain. J.J.V.-D. acknowledges the financial support from Juan de la Cierva Programme of the Ministerio de Ciencia e Innovación, Spain. A fellowship of the Instituto de Salud Carlos III (Spain) is acknowledged by P.U. The AFM force spectroscopy experiments were carried out in the Nanometric Techniques unit of the Scientific and Technological Centers of the University of Barcelona (CCiTUB). The support of Jaume Comas from the Cytometry unit of the CCiTUB is also acknowledged.

References

1 L. H. Miller, D. I. Baruch, K. Marsh and O. K. Doumbo, *Nature*, 2002, **415**, 673.
2 S. M. Handunnetti, P. H. David, K. L. R. L. Perera and K. N. Mendis, *Am. J. Trop. Med. Hyg.*, 1989, **40**, 115.
3 R. Udomsangpetch, B. Wåhlin, J. Carlson, K. Berzins, M. Torii, M. Aikawa, P. Perlmann and M. Wahlgren, *J. Exp. Med.*, 1989, **169**, 1835.
4 A. Pain, D. J. P. Ferguson, O. Kai, B. C. Urban, B. Lowe, K. Marsh and D. J. Roberts, *Proc. Natl. Acad. Sci. U. S. A.*, 2001, **98**, 1805.
5 D. I. Baruch, B. L. Pasloske, H. B. Singh, X. Bi, X. C. Ma, M. Feldman, T. F. Taraschi and R. J. Howard, *Cell*, 1995, **82**, 77.
6 K. Flick and Q. Chen, *Mol. Biochem. Parasitol.*, 2004, **134**, 3.
7 G. B. Nash, B. M. Cooke, K. Marsh, A. Berendt, C. Newbold and J. Stuart, *Blood*, 1992, **79**, 798.
8 D. I. Baruch, J. A. Gormley, C. Ma, R. J. Howard and B. L. Pasloske, *Proc. Natl. Acad. Sci. U. S. A.*, 1996, **93**, 3497.
9 C. Robert, B. Pouvelle, P. Meyer, K. Muanza, H. Fujioka, M. Aikawa, A. Scherf and J. Gysin, *Res. Immunol.*, 1995, **146**, 383.
10 B. M. Cooke, S. J. Rogerson, G. V. Brown and R. L. Coppel, *Blood*, 1996, **88**, 4040.
11 J. Gysin, B. Pouvelle, M. Le Tonquèze, L. Edelman and M. C. Boffa, *Mol. Biochem. Parasitol.*, 1997, **88**, 267.
12 B. Pouvelle, T. Fusaï, C. Lépolard and J. Gysin, *Infect. Immun.*, 1998, **66**, 4950.
13 J. C. Reeder, A. F. Cowman, K. M. Davern, J. G. Beeson, J. K. Thompson, S. J. Rogerson and G. V. Brown, *Proc. Natl. Acad. Sci. U. S. A.*, 1999, **96**, 5198.
14 C. J. McCormick, C. I. Newbold and A. R. Berendt, *Blood*, 2000, **96**, 327.
15 A. Barragan, V. Fernandez, Q. Chen, A. von Euler, M. Wahlgren and D. Spillmann, *Blood*, 2000, **95**, 3594.
16 A. M. Vogt, A. Barragan, Q. Chen, F. Kironde, D. Spillmann and M. Wahlgren, *Blood*, 2003, **101**, 2405.
17 C. F. Ockenhouse, N. N. Tandon, C. Magowan, G. A. Jamieson and J. D. Chulay, *Science*, 1989, **243**, 1469.
18 M. Fried and P. E. Duffy, *Science*, 1996, **272**, 1502.
19 J. G. Beeson, K. T. Andrews, M. Boyle, M. F. Duffy, E. K. Choong, T. J. Byrne, J. M. Chesson, A. M. Lawson and W. Chai, *J. Biol. Chem.*, 2007, **282**, 22426.
20 S. V. Madhunapantula, R. N. Achur and D. C. Gowda, *Infect. Immun.*, 2007, **75**, 4409.
21 A. Muthusamy, R. N. Achur, M. Valiyaveettil, J. J. Botti, D. W. Taylor, R. F. Leke and D. C. Gowda, *Am. J. Pathol.*, 2007, **170**, 1989.
22 Q. Chen, A. Barragan, V. Fernandez, A. Sundström, M. Schlichtherle, A. Sahlén, J. Carlson, S. Datta and M. Wahlgren, *J. Exp. Med.*, 1998, **187**, 15.
23 A. Barragan, D. Spillmann, P. G. Kremsner, M. Wahlgren and J. Carlson, *Exp. Parasitol.*, 1999, **91**, 133.
24 A. Juillerat, S. Igonet, I. Vigan-Womas, M. Guillotte, S. Gangnard, G. Faure, B. Baron, B. Raynal, O. Mercereau-Puijalon and G. A. Bentley, *Mol. Biochem. Parasitol.*, 2010, **170**, 84.
25 S. J. Pancake, G. D. Holt, S. Mellouk and S. L. Hoffman, *J. Cell Biol.*, 1992, **117**, 1351.
26 U. Frevert, P. Sinnis, C. Cerami, W. Shreffler, B. Takacs and V. Nussenzweig, *J. Exp. Med.*, 1993, **177**, 1287.
27 C. Pinzon-Ortiz, J. Friedman, J. Esko and P. Sinnis, *J. Biol. Chem.*, 2001, **276**, 26784.
28 D. Rathore, T. F. McCutchan, D. N. Garboczi, T. Toida, M. J. Hernáiz, L. A. LeBrun, S. C. Lang and R. J. Linhardt, *Biochemistry*, 2001, **40**, 11518.
29 J. B. Ancsin and R. Kisilevsky, *J. Biol. Chem.*, 2004, **279**, 21824.
30 K. T. Andrews, N. Klatt, Y. Adams, P. Mischnick and R. Schwartz-Albiez, *Infect. Immun.*, 2005, **73**, 4288.
31 A. M. Vogt, F. Pettersson, K. Moll, C. Jonsson, J. Normark, U. Ribacke, T. G. Egwang, H.-P. Ekre, D. Spillmann, Q. Chen and M. Wahlgren, *PLoS Pathog.*, 2006, **2**, e100.
32 J. Carlson, H.-P. Ekre, H. Helmby, J. Gysin, B. M. Greenwood and M. Wahlgren, *Am. J. Trop. Med. Hyg.*, 1992, **46**, 595.
33 S. J. Rogerson, J. C. Reeder, F. Al-Yaman and G. V. Brown, *Am. J. Trop. Med. Hyg.*, 1994, **51**, 198.
34 M. A. Skidmore, A. F. Dumax-Vorzet, S. E. Guimond, T. R. Rudd, E. A. Edwards, J. E. Turnbull, A. G. Craig and E. A. Yates, *J. Med. Chem.*, 2008, **51**, 1453.
35 A. M. Leitgeb, K. Blomqvist, F. Cho-Ngwa, M. Samje, P. Nde, V. Titanji and M. Wahlgren, *J. Med. Chem.*, 2011, **84**, 390.
36 P. Urbán, J. Estelrich, A. Cortés and X. Fernàndez-Busquets, *J. Controlled Release*, 2011, **151**, 202.
37 P. Urbán, J. Estelrich, A. Adeva, A. Cortés and X. Fernàndez-Busquets, *Nanoscale Res. Lett.*, 2011, **6**, 620.
38 E. L. Florin, V. T. Moy and H. E. Gaub, *Science*, 1994, **264**, 415.
39 A. Vinckier, P. Gervasoni, F. Zaugg, U. Ziegler, P. Lindner, P. Groscurth, A. Plückthun and G. Semenza, *Biophys. J.*, 1998, **74**, 3256.
40 P. P. Lehenkari and M. A. Horton, *Biochem. Biophys. Res. Commun.*, 1999, **259**, 645.
41 I. Lee and R. E. Marchant, *Ultramicroscopy*, 2003, **97**, 341.
42 H. Yang, J. Yu, G. Fu, X. Shi, L. Xiao, Y. Chen, X. Fang and C. He, *Exp. Cell Res.*, 2007, **313**, 3497.
43 I. H. Kim, H. Y. Lee, H. D. Lee, Y. J. Jung, S. J. B. Tendler, P. M. Williams, S. Allen, S. H. Ryu and J. W. Park, *Anal. Chem.*, 2009, **81**, 3276.
44 P. Hinterdorfer, W. Baumgartner, H. J. Gruber, K. Schilcher and H. Schindler, *Proc. Natl. Acad. Sci. U. S. A.*, 1996, **93**, 3477.

45 F. Kienberger, G. Kada, H. Mueller and P. Hinterdorfer, *J. Mol. Biol.*, 2005, **347**, 597.
46 J. Morfill, K. Blank, C. Zahnd, B. Luginbühl, F. Kühner, K.-E. Gottschalk, A. Plückthun and H. E. Gaub, *Biophys. J.*, 2007, **93**, 3583.
47 M. Sletmoen, G. Skjåk-Bræk and B. T. Stokke, *Biomacromolecules*, 2004, **5**, 1288.
48 X. Wang, D. Zhou, K. Sinniah, C. Clarke, L. Birch, H. Li, T. Rayment and C. Abell, *Langmuir*, 2006, **22**, 887.
49 X. Sisquella, K. de Pourcq, J. Alguacil, J. Robles, F. Sanz, D. Anselmetti, S. Imperial and X. Fernàndez-Busquets, *FASEB J.*, 2010, **24**, 4203.
50 M. Rief, M. Gautel, F. Oesterhelt, J. M. Fernandez and H. E. Gaub, *Science*, 1997, **276**, 1109.
51 P.-F. Lenne, A. J. Raae, S. M. Altmann, M. Saraste and J. K. H. Hörber, *FEBS Lett.*, 2000, **476**, 124.
52 W. Zhang, Q. Xu, S. Zou, H. Li, W. Xu, X. Zhang, Z. Shao, M. Kudera and H. E. Gaub, *Langmuir*, 2000, **16**, 4305.
53 J. M. Fernandez and H. Li, *Science*, 2004, **303**, 1674.
54 A. Jollymore, C. Lethias, Q. Peng, Y. Cao and H. Li, *J. Mol. Biol.*, 2009, **385**, 1277.
55 P. E. Marszalek, H. Li and J. M. Fernandez, *Nat. Biotechnol.*, 2001, **19**, 258.
56 Q. Zhang, Z. Lu, H. Hu, W. Yang and P. E. Marszalek, *J. Am. Chem. Soc.*, 2006, **128**, 9387.
57 G. Francius, S. Lebeer, D. Alsteens, L. Wildling, H. J. Gruber, P. Hols, S. D. Keersmaecker, J. Vanderleyden and Y. F. Dufrêne, *ACS Nano*, 2008, **2**, 1921.
58 A. Noy, D. V. Vezenov, J. F. Kayyem, T. J. Meade and C. M. Lieber, *Chem. Biol.*, 1997, **4**, 519.
59 M. Rief, H. Clausen-Schaumann and H. E. Gaub, *Nat. Struct. Mol. Biol.*, 1999, **6**, 346.
60 M. Benoit and H. E. Gaub, *Cells Tissues Organs*, 2002, **172**, 174.
61 T. G. Kuznetsova, M. N. Starodubtseva, N. I. Yegorenkov, S. A. Chizhik and R. I. Zhdanov, *Micron*, 2007, **38**, 824.
62 J. Helenius, C.-P. Heisenberg, H. E. Gaub and D. J. Muller, *J. Cell Sci.*, 2008, **121**, 1785.
63 A. Hategan, R. Law, S. Kahn and D. E. Discher, *Biophys. J.*, 2003, **85**, 2746.
64 M. Lekka, M. Fornal, G. Pyka-Fosciak, K. Lebed, B. Wizner, T. Grodzicki and J. Styczen, *Biorheology*, 2005, **42**, 307.
65 S. Strasser, A. Zink, G. Kada, P. Hinterdorfer, O. Peschel, W. M. Heckl, A. G. Nerlich and S. Thalhammer, *Forensic Sci. Int.*, 2007, **170**, 8.
66 Y. Wu, Y. Hu, J. Cai, S. Ma, X. Wang, Y. Chen and Y. Pan, *Micron*, 2009, **40**, 359.
67 R. Afrin and A. Ikai, *Biochem. Biophys. Res. Commun.*, 2006, **348**, 238.
68 C. Yan, A. Yersin, R. Afrin, H. Sekiguchi and A. Ikai, *Biophys. Chem.*, 2009, **144**, 72.
69 A. Li, T. S. Lim, H. Shi, J. Yin, S. J. Tan, Z. Li, B. C. Low, K. S. W. Tan and C. T. Lim, *PLoS One*, 2011, **6**, e16929.
70 J. Gruenberg, D. R. Allred and I. W. Sherman, *J. Cell Biol.*, 1983, **97**, 795.
71 E. Nagao, O. Kaneko and J. A. Dvorak, *J. Struct. Biol.*, 2000, **130**, 34.
72 A. Li, A. H. Mansoor, K. S. W. Tan and C. T. Lim, *J. Microbiol. Methods*, 2006, **66**, 434.
73 L. M. Joergensen, A. Salanti, T. Dobrilovic, L. Barfod, T. Hassenkam, T. G. Theander, L. Hviid and D. E. Arnot, *Malar. J.*, 2010, **9**, 100.
74 G. I. Bell, *Science*, 1978, **200**, 618.
75 E. Evans and K. Ritchie, *Biophys. J.*, 1997, **72**, 1541.
76 A. Juillerat, A. Lewit-Bentley, M. Guillotte, S. Gangnard, A. Hessel, B. Baron, I. Vigan-Womas, P. England, O. Mercereau-Puijalon and G. A. Bentley, *Proc. Natl. Acad. Sci. U. S. A.*, 2011, **108**, 5243.
77 B. M. Cooke, N. Mohandas and R. L. Coppel, *Adv. Parasitol.*, 2001, **50**, 1.
78 J. P. Gardner, R. A. Pinches, D. J. Roberts and C. I. Newbold, *Proc. Natl. Acad. Sci. U. S. A.*, 1996, **93**, 3503.
79 B. S. Crabb, B. M. Cooke, J. C. Reeder, R. F. Waller, S. R. Caruana, K. M. Davern, M. E. Wickham, G. V. Brown, R. L. Coppel and A. F. Cowman, *Cell*, 1997, **89**, 287.
80 M. Rug, S. W. Prescott, K. M. Fernandez, B. M. Cooke and A. F. Cowman, *Blood*, 2006, **108**, 370.
81 M. Aikawa, K. Kamanura, S. Shiraishi, Y. Matsumoto, H. Arwati, M. Torii, Y. Ito, T. Takeuchi and B. Tandler, *Exp. Parasitol.*, 1996, **84**, 339.
82 K. Singh, A. G. Gittis, P. Nguyen, D. C. Gowda, L. H. Miller and D. N. Garboczi, *Nat. Struct. Mol. Biol.*, 2008, **15**, 932.
83 G. Francius, D. Alsteens, V. Dupres, S. Lebeer, S. De Keersmaecker, J. Vanderleyden, H. J. Gruber and Y. F. Dufrêne, *Nat. Protoc.*, 2009, **4**, 939.
84 V. Dupres, C. Verbelen, D. Raze, F. Lafont and Y. F. Dufrêne, *ChemPhysChem*, 2009, **10**, 1672.
85 V. Dupres, F. D. Menozzi, C. Locht, B. H. Clare, N. L. Abbott, S. Cuenot, C. Bompard, D. Raze and Y. F. Dufrêne, *Nat. Methods*, 2005, **2**, 515.
86 G. B. Nash, B. M. Cooke, J. Carlson and M. Wahlgren, *Br. J. Haematol.*, 1992, **82**, 757.
87 T. W. Sheehy and R. C. Reba, *Ann. Intern. Med.*, 1967, **66**, 807.
88 H. Smitskamp and F. H. Wolthuis, *Br. Med. J.*, 1971, **1**, 714.
89 N. Jaroonvesama, *Lancet*, 1972, **299**, 221.
90 M. Munir, H. Tjandra, T. H. Rampengan, I. Mustadjab and F. H. Wulur, *Paediatr. Indones.*, 1980, **20**, 47.
91 T. H. Rampengan, *Paediatr. Indones.*, 1991, **31**, 59.
92 World health organization malaria action program, *Trans. R. Soc. Trop. Med. Hyg.*, 1986, **80**, suppl. 3.
93 Y. Miura, S. Aoyagi, Y. Kusada and K. Miyamoto, *J. Biomed. Mater. Res.*, 1980, **14**, 619.
94 R. I. W. Osmond, W. C. Kett, S. E. Skett and D. R. Coombe, *Anal. Biochem.*, 2002, **310**, 199.
95 S. L. Cranmer, C. Magowan, J. Liang, R. L. Coppel and B. M. Cooke, *Trans. R. Soc. Trop. Med. Hyg.*, 1997, **91**, 363.
96 C. Lambros and J. P. Vanderberg, *J. Parasitol.*, 1979, **65**, 418.
97 J. B. Jensen, *Am. J. Trop. Med. Hyg.*, 1978, **27**, 1274.
98 A. R. Dluzewski, I. T. Ling, K. Rangachari, P. A. Bates and R. J. M. Wilson, *Trans. R. Soc. Trop. Med. Hyg.*, 1984, **78**, 622.
99 A. Fuhrmann, D. Anselmetti, R. Ros, S. Getfert and P. Reimann, *Phys. Rev. E: Stat., Nonlinear, Soft Matter Phys.*, 2008, **77**, 031912.

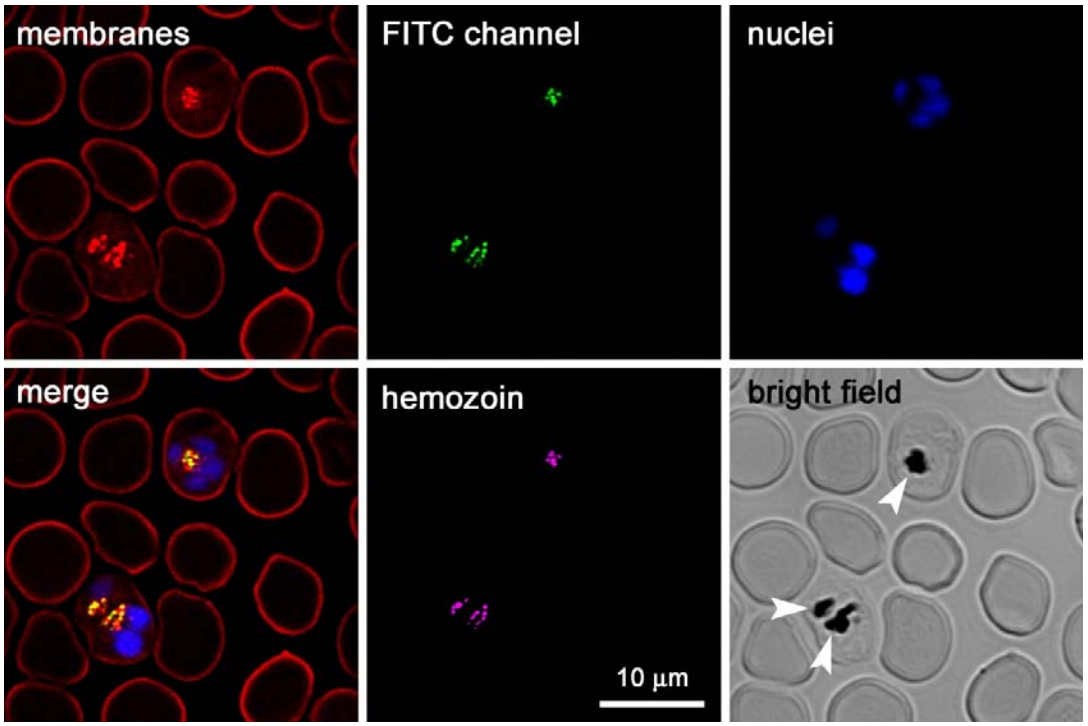

Supplementary Figure 1. Confocal fluorescence microscopy control of the absence of cross-reactivity of DAPI with FITC. In the absence of heparin-FITC, emission could be observed in the FITC channel only at a very high laser intensity, well above that used for heparin detection. This emission was due to reflection of the laser beam by hemozoin crystals and was not colocalizing with DAPI stain. In every experiment it was routinely checked that at the used laser intensities hemozoin reflection was not being collected in the FITC channel. Erythrocyte membranes were stained with WGA (red), *Plasmodium* nuclei with DAPI (blue), and hemozoin was detected by collecting the reflection of the 488 laser line at 480–500 nm. Arrowheads in the bright field image indicate hemozoin crystals inside pRBCs.

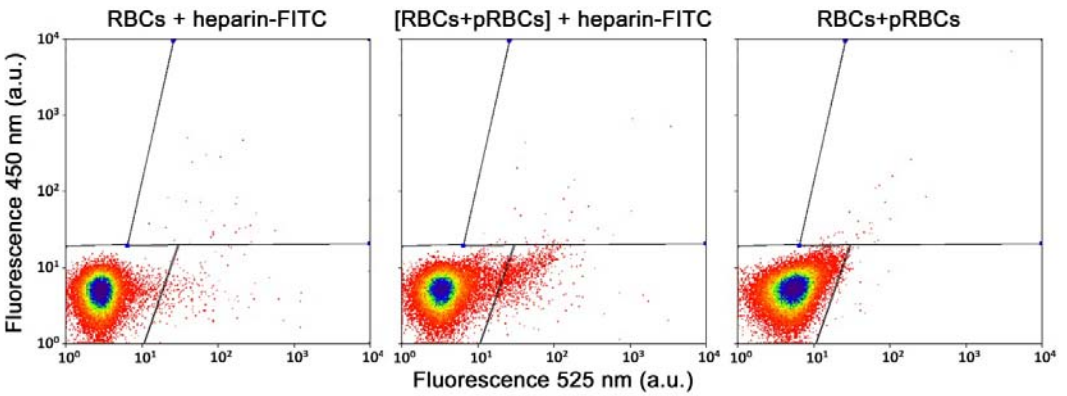

Supplementary Figure 2. FACS control of the binding of heparin to pRBCs in the absence of Hoechst staining.

ARTICLE 4

Nanomedicine against malaria: use of poly(amidoamine)s for the targeted drug delivery to *Plasmodium*

In this work we have explored the use of polymers for the targeted drug delivery of antimalarials. Three polymers from the poly(amidoamine)s family: ISA1, ISA23 and AGMA1 have been tested for their ability to inhibit *Plasmodium* growth *in vitro*, unespecific toxicity and hemolytic activity. AGMA1 has antimalaric activity *per se*, with an approximate IC_{50} of 2.5 μM for the 50-100 kDa fraction (Figure 17). ISA1 has been left aside since toxicity in mice has been detected.

Fluorescence-assisted cell sorting, confocal immunofluorescence and transmission electron microscopy indicate that AGMA1 and ISA23 have specific targeting to pRBCs, and subcellular targeting to the parasite itself. Chloroquine and primaquine have been encapsulated inside AGMA1 and ISA23 and the activity of polymer-drug conjugates has been evaluated *in vitro* and *in vivo*. The *in vitro* activity of encapsulated CQ was modest in comparison with its *in vivo* performance. In a 4-day suppressive test, *P. yoelii*-infected mice were freed of parasites and cured after intraperitoneal administration of 4 x 0.8 mg/kg doses of CQ encapsulated in AGMA1 or ISA23, whereas the same amount of free CQ was unable to cure the animals.

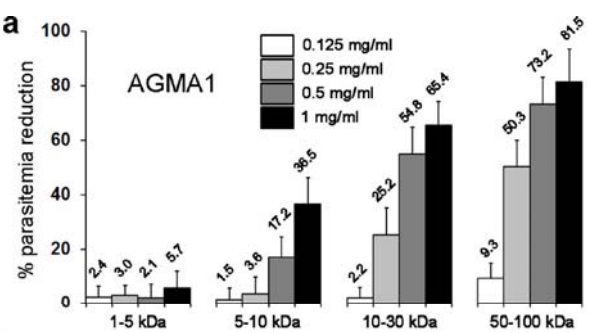

Figure 17. Effect of AGMA1 on the growth of *P. falciparum*, corresponding to figure 5A in Article 4. Polymers were added at the ring stage and incubated for 48 h before determining parasitemias.

Nanomedicine against malaria: use of poly(amidoamine)s for the targeted drug delivery to *Plasmodium*

Patricia Urbán[1-3], Fabio Fenili[4], Juan José Valle-Delgado[1-3], Mauro Nicolò[4], Amedea Manfredi[4], Elisabetta Ranucci[4], Paolo Ferruti[4], and Xavier Fernàndez-Busquets[1-3]*

[1]Nanobioengineering Group, Institute for Bioengineering of Catalonia (IBEC), Baldiri Reixac 10-12, Barcelona E08028, Spain,

[2]Barcelona Centre for International Health Research (CRESIB, Hospital Clínic-Universitat de Barcelona), Rosselló 149-153, Barcelona E08036, Spain,

[3]Biomolecular Interactions Team, Nanoscience and Nanotechnology Institute (IN2UB), University of Barcelona, Martí i Franquès 1, Barcelona E08028, Spain,

[4]Chemistry Department, Università degli Studi di Milano, Via Golgi 19, Milano 20133, Italy.

*e-mail: xfernandez_busquets@ub.edu

Abstract

Here we have explored the poly(amidoamine)-based polymers AGMA1 and ISA23 for the targeted delivery of antimalarial drugs to *Plasmodium*-infected red blood cells (pRBCs). AGMA1 has antimalarial activity *per se* as shown by its inhibition of the in vitro growth of *P. falciparum*, with an IC_{50} of 2.3 μM. Both polymers have specific targeting to pRBCs, and subcellular targeting to the parasite itself. 10- to 40-nm nanoparticles formed by AGMA1 and ISA23 show a high capacity for the encapsulation of the antimalarial drugs primaquine and chloroquine, with drug:polymer ratios around 0.25. Intraperitoneal administration of 0.8 mg kg^{-1} chloroquine encapsulated into either polymer cured *P. yoelii*-infected mice, whereas control animals treated with twice as much free drug did not survive. These nanovectors combining into a single chemical structure drug encapsulating capacity, antimalarial activity, specific pRBC targeting, and affordable synthesis cost are good candidates for oral administration formulations that can bring nanomedicine into the antimalarial therapeutic arena.

Introduction

More than 40% of the world's population lives with some risk of contracting malaria, with most recent estimates indicating several hundred million clinical cases and 665,000 deaths in 2010 [1, 2], of which the large majority are children below 5 years[3, 4]. The recent call for the elimination and eradication of the disease requires research from multiple fronts, including developing strategies for the efficient delivery of new medicines[5]. Five *Plasmodium* species cause disease in humans: *P. vivax*, *P. ovale*, *P. malariae*, *P. knowlesi*[6], and *P. falciparum*, with the latter being responsible for the most deadly and severe cases. When taking a blood meal, the female *Anopheles* mosquito inoculates *Plasmodium* sporozoites that in the liver infect hepatocytes and proliferate into thousands of merozoites[7]; these invade red blood cells (RBCs), where they develop first into rings, and then into the late forms trophozoites and schizonts. Schizont-infected RBCs burst and release more merozoites, which start the blood cycle again. Because the blood-stage infection is responsible for all symptoms and pathologies of malaria, *Plasmodium*-infected RBCs (pRBCs) are a main chemotherapeutic target[8].

Because antimalarial drug delivery currently relies on soluble compounds with little or no specificity for pRBCs, the administration of most drugs requires high doses. However, unspecificity of toxic drugs demands low concentrations to minimize undesirable side-effects, thus incurring the risk of sublethal doses favouring the appearance of resistant pathogen strains[9]. Targeted nanovector systems can fulfill the objective of achieving the intake of total amounts sufficiently low to be innocuous for the patient but that locally are high enough to be lethal for the parasite. The development of novel drug delivery systems is not only less expensive than developing new drugs, but may also improve delivery of antimalarials at the desired rates[10]. Nanomedicine, which uses nanosized tools for treatment of disease[11], has not yet been extensively applied to malaria, but the administration of antimalarial compounds would largely benefit from an economically affordable method based on nanoparticles of sufficiently small size to be formulated for oral intake. Ideally, such nanoparticles should be able to penetrate pRBCs with the aid of targeting molecules small and of low cost. The nanoparticles themselves must be economically affordable since the final product is expected to be used in malaria endemic regions, which in most cases are located in developing areas with low per capita incomes. Finally, the nanovector must be capable of carrying antimalarial compounds.

Polymers offer effectively unlimited diversity in chemistry, dimensions and topology, rendering them a class of materials that is particularly suitable for applications in nanoscale drug delivery systems[12]. Polymeric nanoparticles are made of natural or artificial polymers that range in size between 10 and 1000 nm, and if adequately targeted they can be used to deliver highly localized drug doses into specific cell types or tissues[13]. In the case of biodegradable polymers, which decompose into products that can be completely eliminated by the body, significant advantages are their history of safe use, proven biocompatibility, a high surface/volume ratio, and ability to control the time and rate of polymer degradation and drug release, thus increasing the half-life of bioactives[14]. Poly(amidoamine)s[15] (PAAs) are a family of synthetic polymers exhibiting a combination of properties imparting them a considerable potential in the biomedical field, being usually biocompatible, degradable in water and bioeliminable[16, 17]. They display membrane disruptive properties in response to a decrease in pH, conferring endosomolytic properties *in vitro* and *in vivo*[18]. These characteristics led us to explore PAAs as nanovectors for the targeted delivery of antimalarial drugs.

Results

AGMA1 (Fig. 1), a prevailingly cationic amphoteric PAA obtained by polyaddition of (4-aminobutyl)guanidine (agmatine) to 2,2-bis(acrylamido)acetic acid (BAC), was studied as a potential DNA carrier and transfection promoter[19]. In spite of its cationic character (Supplementary Table 1), AGMA1 is neither toxic (MTD ca. 500 mg kg^{-1}) nor hemolytic in the pH range 4.0-7.4[19-21] and circulates in the blood for a long time without preferentially localizing in the liver. A second amphoteric PAA exhibiting an interesting combination of properties is ISA23, derived from the polyaddition of 2-methylpiperazine to BAC. ISA23 is approximately as biocompatible as dextran, and after intravenous injection it is not captured by the reticulo-endothelial system and has also a prolonged permanence in the blood[22]. The polycationic polymer ISA 1 is formed by Michael type polyaddition of bis(acryloyl)piperazine, 2-methylpiperazine and bis(hydroxyethyl-ethylenediamine)[23].

Atomic force microscopy (AFM) imaging in liquid on mica substrates of 0.1 ng ml^{-1} solutions of AGMA1, ISA23, and ISA1 showed landscapes with regular features (Fig. 2a-f), suggesting homogeneous polymer solutions without significant aggregation. 10-30- and 50-100-kDa AGMA1 samples contained almost exclusively circular

structures with a height of around 1 nm and an estimated diameter of ca. 9 nm after deconvolution analysis[24]. AFM images of ISA1 and ISA23 fractions showed similar structures (data not shown). Conjugation to antimalarial drugs did not significantly increase polymer size (Fig. 2g). In diluted samples, the circular shapes could be observed to form beads-on-a-string alignments (Fig. 2h,i), suggestive of a polymer structured in a number of domain-like regions. Cryo-transmission electron microscopy (cryo-TEM) analysis of the AGMA1 10-30 kDa fraction (Fig. 3) revealed circular shapes ranging from ca. 20 to 40 nm in diameter, often found in associations of two or three in a row. Dynamic light scattering analysis of the 10-30 and 50-100 kDa AGMA1 fractions indicated that, respectively, 94.9% and 73.4% of the molecules had a mean hydrodynamic diameter of 7.4 and 8.7 nm (Supplementary Fig. 2).

Fluorescence-assisted cell sorting (FACS) analysis revealed that fluorescein-labeled AGMA1 specifically targets pRBCs, although also a significant number of non-infected RBCs (Fig. 4c,d). Both pRBC and RBC targeting increase with polymer size, and for >30 kDa AGMA1 we have observed an almost complete pRBC binding (Fig. 4e,f). On the other hand, ISA1 and ISA23 polymers exhibit a highly specific targeting towards pRBCs (Fig. 4g-j), with non-significant binding to non-infected RBCs.

In *P. falciparum* growth inhibition assays (GIAs), only AGMA1 showed significant antimalarial activity *in vitro* (Fig. 5a and Supplementary Table 2). Inhibition of *P. falciparum* growth augmented with polymer size, in good correlation with the increased binding of higher molecular mass AGMA1 to pRBCs observed in FACS assays. The highest antimalarial AGMA1 activity corresponded to the 50-100-kDa fraction, which at a concentration of 1 mg ml^{-1} (10 μM for a 100-kDa polymer) reduced parasitemia by 81.5%. AGMA1 IC_{50} in *P. falciparum* GIAs is around 0.23 mg ml^{-1} for the 50-100 kDa fraction. ISA1 did not have significant antimalarial activity (Fig. 5b), whereas the 30-100 kDa ISA23 fraction was observed to reduce parasitemia by 34.8% at 2 mg ml^{-1} (Fig. 5c). When, in a modified GIA, AGMA1 was added to trophozoites, i.e. 24 h after pRBC culture synchronization, and incubated for a further 48 h before parasitemia determination, the antimalarial activity of the smaller polymer fractions was observed to increase significantly (Fig. 5d). This result is in agreement with a toxicity mechanism working on late parasite stages, which might have its basis on a facilitated polymer entry in pRBCs due to the altered plasma membrane of these cells[25]. In this scenario, AGMA1 would lose antimalarial activity if added 24 h before trophozoites

appear, possibly through a degradation process which would be exacerbated in the smaller fractions.

Neither AGMA1 nor ISA23 nor ISA1 have detectable hemolytic activity (data not shown). Unspecific cytotoxicity of the polymers was observed to depend on their molecular mass (Supplementary Fig. 1): AGMA1 and ISA1 toxicity on HUVEC was significant for the 50-100 kDa fraction above 0.5 mg ml^{-1}, and for the AGMA1 10-30 kDa fraction at 1 mg ml^{-1}; on the other hand, only minor cytotoxicity was observed for the 1-3 kDa ISA23 fraction at concentrations above 5 mg ml^{-1}. Toxicity assays in mice indicated that ISA23 and AGMA1 did not have observable pernicious effects on the animals up to an intraperitoneal dose of 200 mg kg^{-1}, and ISA1 was toxic at 50 mg kg^{-1}, where all the animals died before 1 h after polymer administration. Based on these data ISA1 was left aside at this point.

Cell targeting was also examined by confocal fluorescence microscopy analysis of living pRBC cultures treated with FITC-labeled polymers (Fig. 6). The fluorescence of both AGMA1 (Fig. 6a) and ISA23 (Fig. 6b) was clearly found inside pRBCs infected by *P. falciparum* trophozoites and schizonts, but not in ring-infected pRBCs or in non-infected erythrocytes. Assays done with FITC-labeled 50-100 kDa AGMA1 showed an increased fluorescence signal for both pRBCs and RBCs (data not shown), but with a poor intracellular localization for the latter, suggesting that AGMA1 binds healthy erythrocytes (as clearly indicated by FACS) but does not enter them easily. The observed increased pRBC binding of >30 kDa AGMA1 is consistent with the higher antimalarial activity of the larger polymers. After 90 min both PAAs were detected inside target cells, in the close vicinity of *Plasmodium* DNA. This targeting to pRBCs and to the parasite itself could also be observed for the mouse malaria parasite *P. yoelii*, where the binding of ISA23 to merozoites was particularly striking (Fig. 6c). This result offers interesting perspectives for PAAs as targeting elements not only towards pRBCs but also towards free merozoites.

TEM images of pRBCs that had been incubated for 90 min in the presence of AGMA1 or ISA23 prior to fixation revealed the localization of both polymers in the pRBC cytosol and inside the area enclosed by the parasitophorous vacuole membrane (PVM) (Fig. 7). Whereas ISA23 was more abundant in the pRBC cytosol than beyond the PVM, the opposite was observed for AGMA1. The polymers were not surrounded by a lipid bilayer, thus suggesting a membrane trespassing mechanism not based on the formation of endocytic vesicles, although the differences observed in their intracellular

distribution suggest different entry routes for both structures. AGMA1 was often found associated to Maurer's clefts, Golgi-like organelles which are part of an exomembrane system that the parasite establishes in the host cell cytoplasm[26]. The cytosolic areas around small bumps on the pRBC membrane called knobs were enriched in AGMA1, suggesting that these structures, assembled by the parasite molecular machinery and involved in cytoadhesion events, might be entry gates for this polymer.

Microscopic observation of 10-30 kDa AGMA1-treated samples >48 h after PAA addition showed a remarkable amount of free merozoites outside RBCs (Fig. 8a). This suggested some type of perturbation in the invasion capacity of *Plasmodium*, since control untreated samples completed the invasion step following merozoite egression from mature schizonts, and consisted mostly of ring stages (Fig. 8b). Because invasion proceeds normally when non-infected RBCs are pretreated with AGMA1 prior to their incorporation into pRBC cultures (data not shown), any alteration of invasion is likely due to a direct effect of AGMA1 on the merozoite.

In standard GIAs, the non-covalent conjugation of AGMA1 and ISA23 with the antimalarial drugs primaquine (AGMA1-PQ, ISA23-PQ) and chloroquine (AGMA1-CQ, ISA23-CQ) did not significantly modify the in vitro antimalarial activity of the drugs relative to their free forms (Fig. 9). Covalent conjugation, on the other hand, almost eliminated drug activity (data not shown). Addition of drugs and non-covalent PAA-drug conjugates at trophozoite stage in a modified GIA or incubation with either ring or trophozoite stage for 1 h before removing the drugs and incubating for another 48 h before parasitemia determination did not improve nanovector performance *in vitro*. This last result suggests that the polymers must have some affinity also for ring-infected pRBCs, although this could not be confirmed by fluorescence microscopy. The data obtained also indicate that either PAA nanocarriers do not increase the amount of drug inside pRBCs in comparison to a similar concentration of free drug, or, if a large amount of PAA-drug is indeed entering the cell, a significant part of it does not leave the polymer and thus its antimalarial activity is not manisfested. PAA-CQ conjugate stability assays indicate that after 10 h in PBS about 60% of the drug has leaked from AGMA1 and ISA23 (Figure 10), suggesting that PAA-drug conjugates do indeed enter the target cell in sufficient amounts to kill *Plasmodium*. However, in *in vitro* assays, the slow release of the drug once inside the cell seems to cancel out the improved targeting mediated by PAAs. As suggested above, such release is also due in part to polymer breakdown.

In a 4-day suppressive test (Fig. 11), *P. yoelii*-infected mice were freed of parasites and cured after intraperitoneal administration of 4 × 0.8 mg kg^{-1} doses of CQ encapsulated in AGMA1 or ISA23, whereas a larger amount of free CQ was unable to cure the animals. PQ and CQ conjugates of AGMA1 and ISA23 showed no toxicity in mice after intraperitoneal administration up to a dose of 200 mg kg^{-1}.

Discussion

Several polymeric nanocarriers have been proposed for the delivery of antimalarials *in vivo*[10], including quinine[27], halofantrine[28], curcumin[29], artemisinin derivatives[30], chloroquine[31, 32], and primaquine[33-35]. However, most of these reports are pharmacokinetic studies and only four cases in the literature describe in malaria-infected animals the efficacy of polymer-encapsulated drugs compared with the free compounds. Orally administered lipid nanoemulsions of primaquine at a dose of 1.5 mg kg^{-1} day^{-1} improved the mean survival time of *P. berghei*-infected mice from 13 to 39 days, and reduced parasitemia 4-fold relative to free drug[35]; oral delivery of curcumin bound to chitosan nanoparticles cured all *P. yoelii*-infected mice when administered at 100 mg kg^{-1}, whereas the same amount of the free drug cured only one third of the animals[29]; intravenous administration to *P. berghei*-infected rats of several doses of 75 mg kg^{-1} day^{-1} quinine enclosed in nanocapsules prepared with poly(ε-caprolactone) and Polysorbate 80 improved by 30% the efficacy of free quinine; finally, a single intravenous dose of 1 mg kg^{-1} halofantrine encapsulated in poly(D,L-lactide)-based polymer cured 80% of *P. berghei*-infected mice, when the same dose of the free drug was unable to arrest the infection or to prolong the survival of the animals[28]. Here, we have shown that intraperitoneal administrarion of 0.8 mg kg^{-1} day^{-1} chloroquine encapsulated in AGMA1 and ISA23 cured all *P. yoelii*-infected mice treated and eliminated parasitemia from the blood, whereas the same or even a higher amount of free drug (1.9 mg kg^{-1} day^{-1}) was unable to cure the animals and only reduced parasitemia by 16%. Taking as reference our *in vitro* IC_{50} data for CQ in *P. falciparum* and assuming for the mice used a mean weight of 20 g and about 2 ml of blood volume, only about 0.3% of intraperitoneally administered drug reaches the blood vessels. Taking into account the respective IC_{50} of the drugs used in the aforementioned works (1.4 μM for primaquine, 5 μM for curcumin, 195 nM for quinine, 1.7 nM for halofantrine, and 141 nM for chloroquine)[36, 37], the doses used, and the expected blood

drug levels according to the administration routes chosen, the best performance corresponds to AGMA1 encapsulation of chloroquine, which lowered IC_{50} *in vivo* around 10-fold. This represents an improvement of several orders of magnitude in comparison with previous reports, only matched by lipid-encapsulated primaquine[35], whose concentration would be about twice its IC_{50} assuming that only one tenth of the orally administered drug reached the blood circulation. The good performance of PAA-targeted CQ is highlighted by the challenge of improving CQ therapy, given the fast action of the drug in blood stage parasites, its low toxicity, good bioavailability in oral administration, water solubility, high volume of distribution in the body and low cost.

It is likely that a significant part of the increase in drug efficacy provided by its encapsulation comes from the specific targeting of the polymers towards and penetration into pRBCs, since the concentrations of AGMA1 and ISA23 used for *in vitro* and *in vivo* tests are way below their IC_{50} determined for *P. falciparum*. The specific cell targeting observed for AGMA1 and ISA23 in both *P. yoelii* and *P. falciparum* offers good perspectives regarding an ample activity of PAA-derived polymers against different *Plasmodium* species. In a previous work[38], we had shown a 10-fold improvement in the *in vitro* activity of immunoliposome-encapsulated antimalarial drugs, whereas PAAs have been found not to improve drug activity *in vitro*. Because the amount of drug encapsulated in a 200-nm liposome is much larger than that contained in a 10-nm polymer particle, and since equal amounts of drug are being delivered with each system, it is likely that, *in vitro*, the immediate release of a large amount of drug provided by a liposome has a better antimalarial activity than the slow release provided by PAAs.

However, the *in vitro* activity of encapsulated CQ was modest in comparison with its *in vivo* performance. This result could be explained because the random encounters between pRBCs and polymers required for targeting specificity to be manifested are favored by the turbulent mixing in the blood circulation, although this would also apply for free CQ, which has an endogenous carrier across human erythrocyte membranes that accumulates the drug selectively in these cells[39]. More likely, drug release could be facilitated by some blood factor accelerating polymer breakdown.

The subcellular localization of AGMA1 inside the PV is consistent with its observed antimalarial activity and with its suspected mechanism of action directly on the merozoite, perhaps blocking the invasion step. Encapsulation of drugs in this polymer can thus result in nanoparticles entering the target cells and having a

synergistic antimalarial effect by adding the activity of AGMA1 and the drug. ISA23, on the other hand, has an exquisite specific targeting towards pRBCs, similar to that obtained with monoclonal antibodies [40]. However, unlike antibodies, ISA23 has been observed to penetrate pRBCs *in vivo* and colocalize with *Plasmodium* itself, a property opening interesting perspectives regarding the use of this polymer for the delivery of drugs directly to the parasite. RBC infection by *Plasmodium* increases the permeability of the host cell membrane to low molecular mass solutes[41], and macromolecules up to 70 nm in diameter have been found to have direct access to intraerythrocytic *Plasmodium* through areas of apparent membrane continuity between the RBC membrane and the PVM[42].

Although the receptor for AGMA1 and ISA23 in pRBCs has not been elucidated, the observation that cell binding increases with polymer size suggests that the underlying mechanism is likely to be based on multiple low-affinity interactions, perhaps of electrostatic nature, over a large area. If this were the case, it would take longer for the parasite modifying a large antigenic region than changing the small epitopes which antibodies target. The efficacy of nanovectors whose targeting would be based on this type of recognition could be expected to be less affected by the high antigenic variability of *Plasmodium*[43], which complicates vaccination and targeted drug delivery strategies.

The low unspecific toxicity of the polymers makes them adequate for the administration of antimalarial drugs encompassing a wide IC_{50} span, as we have demonstrated in *in vitro* assays with encapsulated PQ and CQ. Finally, an issue which has not been considered for other polymeric systems addressed to antimalarial drug delivery is their cost, an essential aspect taking into account that malaria medicines have to be deployed in low per capita income areas. According to our calculations, eliminating 50% of the parasitemia from 1 l of *P. falciparum*-infected blood with a single dose of a CQ-encapsulating immunoliposomal nanovector would cost around 50 €[38, 40]. According to the *in vivo* data presented here, a complete elimination of *P. yoelii* parasitemia from 1 l of blood could be achieved with four intraperitoneal doses of CQ-encapsulating AGMA1, for a total cost of 40 cents, a figure likely to be cut down for batch sizes larger than 1 kg, whose current synthesis cost is 9 € g^{-1}.

AGMA1 and ISA23 intrinsic pRBC targeting without the need for including bulky and often expensive ligands such as specific antibodies will contribute to the design of smaller nanovectors, apt for oral formulation, and of lower cost, a desirable

characteristic when designing medicines to be used in developing areas. PAAs are platforms for a new generation of low-cost antimalarial nanovectors combining into a single chemical structure drug encapsulating capacity, antimalarial activity, and specific pRBC targeting.

Methods

Unless otherwise indicated, all reagents were purchased from Sigma-Aldrich (St. Louis, MO, USA).

Polymer synthesis and FITC labeling. Linear AGMA1 and ISA23 were prepared following previously reported procedures[20, 22]. The resulting polymers were filtered (Amicon, Millipore) in order to obtain fractions with defined molecular mass ranges. FITC-labeled 10-30 kDa AGMA1 was prepared as described elsewhere[19]. FITC-labeled 10-30 kDa ISA23 was prepared by treating with a 0.2 mg ml^{-1} FITC solution in methanol a 10 mg ml^{-1} solution in buffer pH 7.4 of an ISA23 10-30 kDa sample carrying amine groups as side substituents (ISA23-NH_2). ISA23-NH_2 was obtained by substituting on a molar basis 7% of mono(*tert*-butoxycarbonyl)ethylenediamine for 2-methyl-piperazine[44]. The mixture was stirred overnight at room temperature and then centrifuged to eliminate insoluble impurities. The resultant clear solution was then dialyzed and the fluorescein-labeled polymer isolated by freeze-drying the retained portion. The recovery was quantitative. The conjugation of PAA-NH_2 with FITC was confirmed by NMR and fluorescence microscopy and the efficiency of the labeling procedure was determined by measuring the fluorescence intensity at λ_{ex}=480 nm and λ_{ex}=520 nm of a solution of PAA-FITC versus a standard FITC solution of known concentration. On a molar basis, FITC content was 7.2% and 6.5% for AGMA1-FITC and ISA23-FITC, respectively.

Preparation of drug-polymer conjugates. 10-30 kDa ISA23 at its isoelectric point (pH 5.2) was synthesized as previously reported[44]. PQ free base was prepared as reported elsewhere[45]; briefly, a 10 mg^{-1} ml^{-1} PQ diphosphate aqueous solution was brought to pH 12 by addition of 0.1 M NaOH, whereby PQ free base separated as an oil which was extracted 4× with ether. The combined ether extracts were dried over Na_2SO_4 and evaporated *in vacuo*, leaving PQ as a dark brown oil with a yield of 50.9%.

CQ free base was prepared following the same procedure, except for the initial dissolution of CQ diphosphate in an emulsion of 1:1 H_2O:ether; CQ free base was recovered, after separation and evaporation of the ether phase, as a white solid with a yield of 59.1%. A 0.1 mg ml^{-1} methanol solution of PQ or CQ free base was added drop-wise to a 10 mg ml^{-1} 10-30 kDa AGMA1 or 10-30 kDa ISA23 solutions at respective pH of 5.5 and 5.2 until pH 7-7.4 was obtained. The resultant clear solutions were freeze-dried and the polymer salts retrieved as a white powder. PQ and CQ loading was determined by UV measurements in PBS at 352 and 340 nm, respectively (ε_{PQ} = 3,254 M^{-1} cm^{-1}; ε_{CQ} = 18,570 M^{-1} cm^{-1}). The corresponding drug payload for each conjugate was (w/w) 15.1% for ISA23-PQ, 29.4% for AGMA1-PQ, 32.9% for ISA23-CQ, and 14.2% for AGMA1-CQ.

***Plasmodium falciparum* cell culture and growth inhibition assays**

P. falciparum 3D7 was grown *in vitro* in rinsed human RBCs of blood group type B prepared as described elsewhere[40] using previously established conditions[46]. Briefly, parasites (thawed from glycerol stocks) were cultured at 37 °C in Petri dishes containing RBCs in RPMI complete medium under a gas mixture of 92% N_2, 5% CO_2, and 3% O_2. Synchronized cultures were obtained by 5% sorbitol lysis[47], and the medium was changed every 2 days maintaining 3% hematocrit. For culture maintenance, parasitemias were kept below 5% late forms by dilution with washed RBCs. For standard growth inhibition assays, parasitemia was adjusted to 1.5% with more than 90% of parasites at ring stage after sorbitol synchronization. For modified growth inhibition assays, synchronized cultures were incubated for 24 h before addition of drug to allow for the appearance of late forms. 200 µl of these living *Plasmodium* cultures were plated in 96-well plates and incubated for 48 h at 37 °C in the presence of free drugs and PAA-encapsulated drugs. Parasitemia was determined by microscopic counting of blood smears or by FACS. Smears were fixed in methanol for a few seconds and then stained for ten minutes with Giemsa (Merck Chemicals, Germany) diluted 1:10 in Sorenson's Buffer, pH 7.2. After washing with distilled water and drying, the ratio of infected versus non-infected RBCs was determined by microscopic analysis.

Confocal fluorescence microscopy. Living *P. falciparum* 3D7 cultures were incubated in the presence of 0.2-0.5 mg ml^{-1} ISA 23- FITC or AGMA1-FITC for 90 minutes at

37°C with gentle stirring. After washing, blood smears were prepared and cells were fixed in acetone:methanol (90:10). Parasite nuclei were stained with 4'6-diamino-2-phenylindole (DAPI, Invitrogen) and the RBC membrane was labeled with wheat germ agglutinin (WGA)-tetramethylrhodamine conjugate (Molecular Probes, Eugene, OR, USA). Slides were finally mounted with Mowiol (Calbiochem, Merck Chemicals, Darmstadt, Germany), and analyzed with a Leica TCS SP5 laser scanning confocal microscope.

Dynamic light scattering. Polymers were dissolved in PBS to a 1 mg ml^{-1} concentration. The size of polymers was determined by dynamic light scattering at 90º with a Zetasizer NanoZS90 (Malvern Ltd, Malvern, UK) at 25ºC.

Hemolysis assays. RBCs were diluted in PBS to yield a solution with 3% hematrocrit. 200 µl of RBCs from this suspension and 2 µl of each PAA solution were added to a 96-well plate. Each assay was performed in triplicate, including positive (1% Triton X-100) and negative (PBS) controls. After incubating for 3 h, 6h and 24h at 37 °C, samples were collected in eppendorf tubes, spun at 16,000 g for 5 min, and the supernatant absorbance was measured at 541 nm.

Unspecific cytotoxicity assays. Human umbilical vein endothelial cells (5000 cells/well) were plated in 96-well plates and after 24 h at 37 °C in 5% CO_2 the medium was substituted by 100 µl of PAA-containing culture medium without FBS, and incubation was resumed for 48 h. 10 µl of 4-[3-(4-iodophenyl)-2-(4-nitrophenyl)-2H-5-tetrazolio]-1,3-benzene disulfonate labeling reagent (WST-1) was added to each well, and the plate was incubated in the same conditions for 3 h. After thoroughly mixing for 1 min on a shaker, the absorbance of the samples was measured at 440 nm using a Benchmark Plus microplate reader. WST-1 in the absence of cells was used as blank and samples were prepared in triplicate for each experiment.

Fluorescence-assisted cell sorting (FACS) analysis. Synchronized cultures at mature stages of *P. falciparum* at an approximate parasitemia of 4% were incubated with PAA-FITC at a final concentration of 0.5 mg ml^{-1} for 90 minutes at 37 °C. After washing, parasite nuclei were stained with Hoechst 33342 (Sigma-Aldrich, St. Louis, MO, USA). For FACS analysis, pRBCs were diluted to a final concentration of $1\text{-}10\times10^{6}$ cells ml^{-1}.

Samples were analyzed using a Gallios multi-color flow cytometer instrument (Beckman Coulter, Inc, Fullerton, CA) set up with the 3-lasers 10 colors standard configuration. The single-cell population was selected on a forward-side scatter scattergram. FITC was excited using a blue laser (488 nm), and its fluorescence collected through a 525/40 nm filter. Hoechst was excited with a violet laser (405 nm), and its fluorescence collected using a 450/40 nm filter.

Atomic force microscopy (AFM). 10 µl of 0.1 ng ml^{-1} polymer solutions were deposited on cleaved mica substrates and, after an adsorption time of about 5 minutes, 50 µl of double deionised water (Milli-Q) were added. A Dimension 3100 atomic force microscope (Veeco Instruments Inc., Santa Barbara, CA, USA) and NP-S probes (Veeco) with nominal spring constants of 0.06 N m^{-1} were used to obtain images of the polymer samples in liquid in tapping mode at scan rates of 1 or 2 Hz. For images taken in air, mica substrates were gently rinsed with double deionised water and dried with nitrogen flow after depositing 10 µl of 0.1 ng ml^{-1} polymer solutions on them. Images were then taken by AFM in air using NSC15 probes (Mikromasch, Tallinn, Estonia) with nominal spring constants of 46 N m^{-1} in tapping mode at 1 Hz scan rate. The diameter of the polymers was estimated from AFM images by applying the following deconvolution equation[48]: $w' = w - 2\sqrt{2hR}$, where w' is the real diameter, w the apparent diameter obtained in AFM images, h is the height of the polymer, and R is the radius of curvature of the AFM tip (nominal value of 10 nm according to the supplier).

Transmission electron microscopy. Gelatin-purified pRBCs were incubated with free FITC or 0.5 mg ml^{-1} FITC-labeled polymers for 90 minutes at 37 ºC. After washing, cells were chemically fixed at 4 ºC with a mixture of 4% paraformaldehyde and 0.1% glutaraldehyde (both from Electron Microscopy Sciences, Hatfield, PA, USA) in PB buffer. Prior to embedding in 12% gelatine (Calbiochem, Merck, Germany) and infusion in 2.3 M sucrose, cells were washed with PB containing 50 mM glycine. Mounted gelatine blocks were frozen in liquid nitrogen. Thin sections were prepared in an ultracryomicrotome (Leica EM Ultracut UC6/FC6, Vienna, Austria). Ultrathin cryosections were collected with 2% methylcellulose in 2.3 M sucrose.
Cryosections were incubated at room temperature on drops of 2% gelatin in PBS for 20 min at 37ºC, followed by 50 mM glycine in PBS during 15 min and 10% FBS in PBS during 10 min and 5% FBS in PBS 5 min. Then they were incubated with anti-

FITC (Rockland antibodies, PA, USA) at a final concentration of 3μg antibody ml^{-1} in 5% FBS in PBS for 30 min. After three washes with drops of PBS for 10 min, sections were incubated for 20 min using IgG anti-goat coupled to 6 nm diameter colloidal gold particles (Jackson ImmunoResearch) using a 1:30 dilution in 5% FBS in PBS. This was followed by three washes with drops of PBS for 10 min and two washes with distilled water. The observations were done in an Electron Microscope Jeol J1010 (Jeol, Japan) with a CCD camera SIS Megaview III and a Tecnai Spirit (FEI Company, Eindhoven, The Netherlands) with the same CCD camera. Controls included omission of polymer-FITC, omission of anti-FITC antibody, and inclusion of free FITC plus detection with anti-FITC antibody.

Cryo-TEM of polymers. A thin aqueous film was formed by dipping and withdrawing a bare glow-discharged holey carbon grid from a 1 mg ml^{-1} polymer solution. After withdrawal the grid was blotted against filter paper, leaving thin sample films spanning the grid holes. These films were vitrified by plunging the grid into ethane, which was kept at its melting point by liquid nitrogen, using a Vitrobot (FEI Company) and keeping the sample before freezing at 100% humidity. The temperature at which the thin films and from which vitrification was initiated was room temperature. The vitreous sample films were transferred to a microscope Tecnai F20 (FEI Company, Eindhoven, Netherlands) using a Gatan Cryo Transfer. The images were taken at 200 kV with a 4096 × 4096 pixel CCD Eagle camera (FEI Company) at a temperature between -170ºC and -175ºC and using low-dose imaging conditions.

Antimalarial activity assay in vivo. The *in vivo* antimalarial activity of free chloroquine, ISA23-CQ and AGMA1-CQ was analyzed by using a 4-day-blood suppressive test as previously described[49]. Briefly, mice were inoculated 2×10^6 RBC from *P. yoelii yoelii* 17XL (PyL) MRA-267-infected mice by intraperitoneal injection. Treatment started 2 hours later (day 0) with a single dose of 1.9 ± 0.3 or 0.8 ± 0.2 mg kg^{-1} day^{-1} chloroquine (n=3) administered as free chloroquine, ISA23-CQ or AGMA1-CQ by an intraperitoneal injection followed by identical dose administration for the following 3 days. Tested compounds were prepared at appropriate doses in PBS. The control groups received PBS (n=3). Parasitemia was monitored daily by microscopic examination of Wright's-stained thin-blood smears. Activity was calculated by microscopic counting of blood smears from day 4.

Statistical analysis. Data are presented as the mean ± standard error of at least three independent experiments, and the corresponding standard errors in histograms are represented by error bars. Statistical analyses were performed using Stata Software version 12. Concentrations were transformed using natural log for linear regression. Regression models were adjusted for replicates and assay data. Molecular mass was treated as a categorical variable with 1-5 kDa (for AGMA1 and ISA1) or 1-3 kDa sample (for ISA23) as reference.

Figures

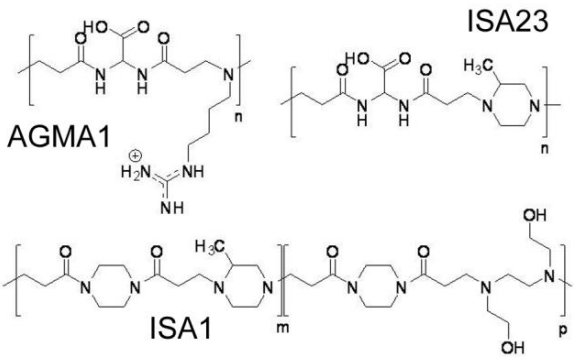

Figure 1 | Chemical structures of AGMA1, ISA1, and ISA23.

		% charged units (charge)		
polymer	IP	pH 5.5	pH 7.4	IC_{50} (cell type)
AGMA1	10.0	90% (+)	55% (+)	> 10 mg ml^{-1} (HUVEC)
ISA1	>10.0	95% (+)	55% (+)	3.1 ± 0.7 mg ml^{-1} (B16F10)
ISA23	5.5	40% (–)	2% (–)	> 10 mg ml^{-1} (HUVEC)

Supplementary Table 1 | Isoelectric point (IP), overall charge at pH 5.5 and 7.4, and IC_{50} for AGMA1, ISA1, and ISA23.

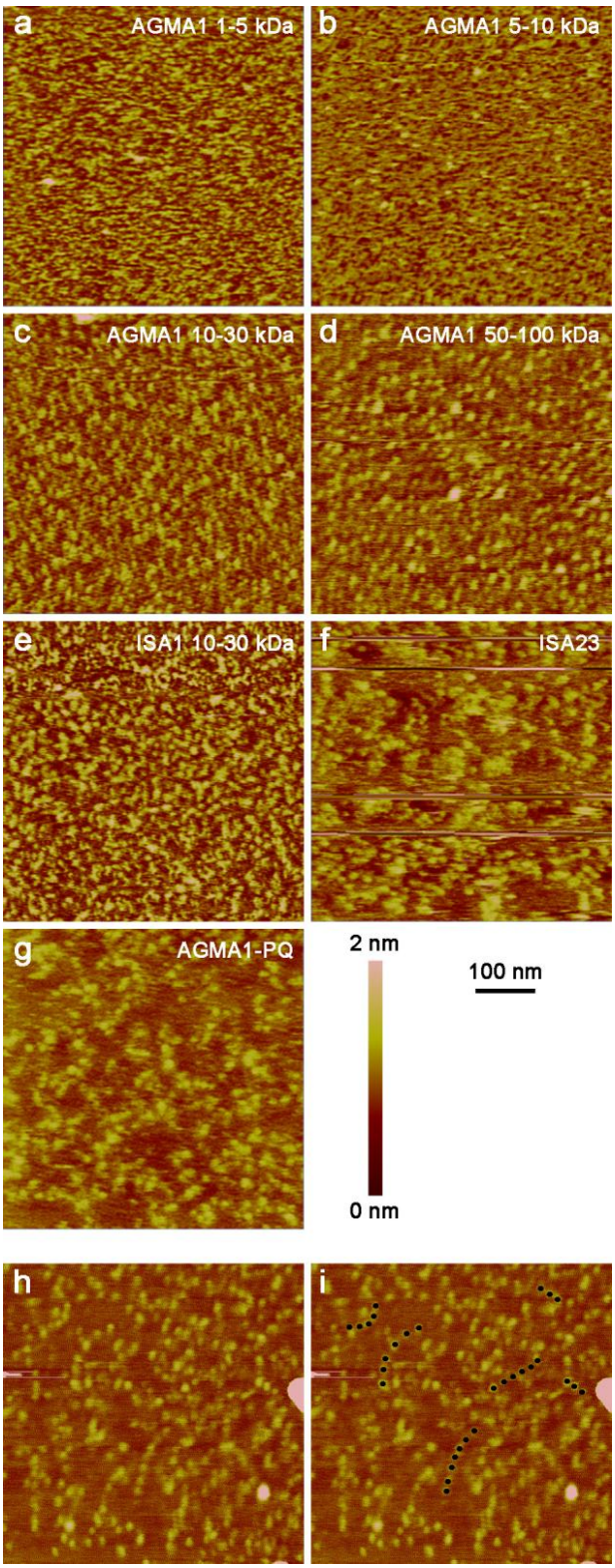

Figure 2 | Atomic force microscope images of different fractions of AGMA1 (a-d) and ISA1 (e), and of non-fractionated ISA23 (f) and AGMA1-primaquine (g). h,i, Diluted 50-100 kDa AGMA1 sample. Suggested beads-on-a-string AGMA1 structures are indicated by dots in panel **i**. Images a-g were taken in liquid and image h in air.

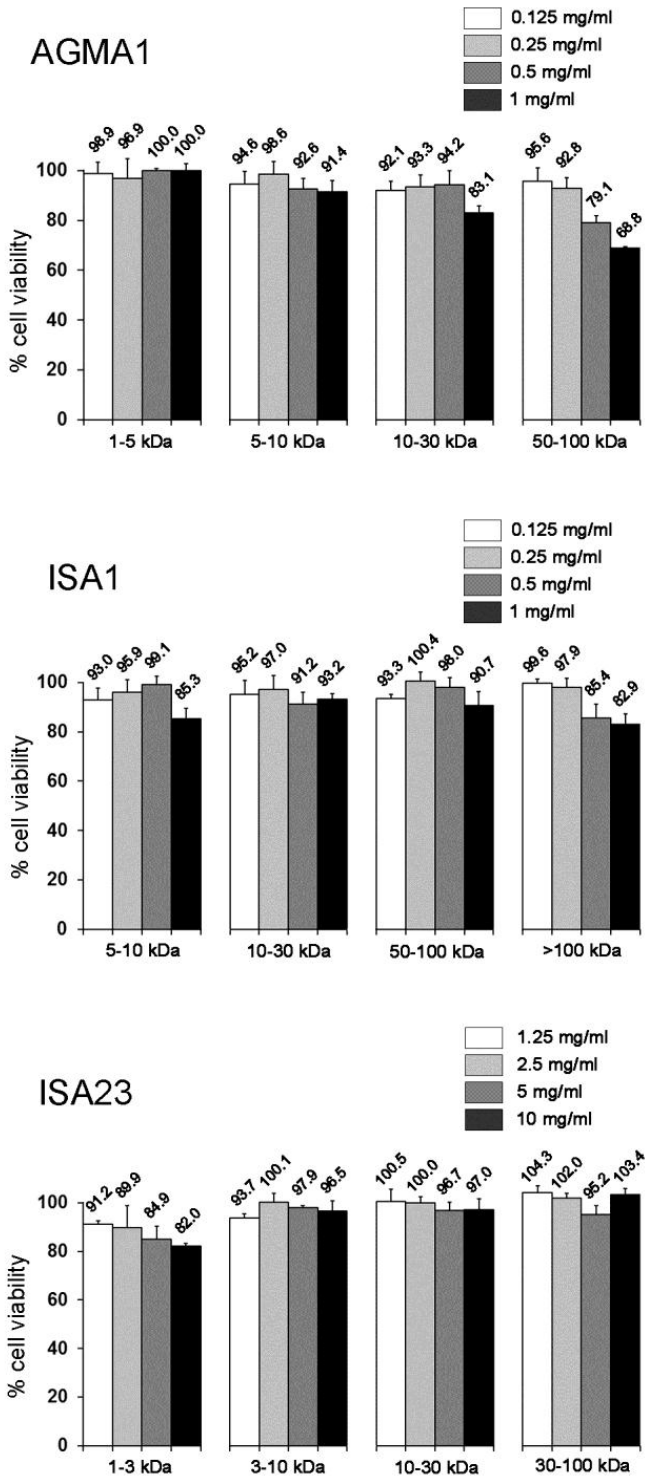

Supplementary Figure 1 | Unspecific cytotoxicity analysis of the different fractions of AGMA1, ISA1, and ISA23. The values indicate the percentage of viable cells relative to the control.

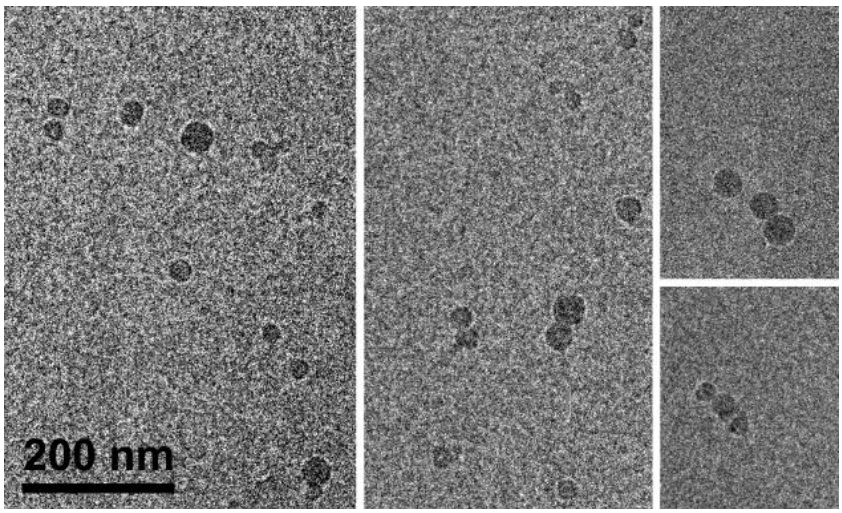

Figure 3 | Cryo-TEM analysis of 10-30 kDa AGMA1.

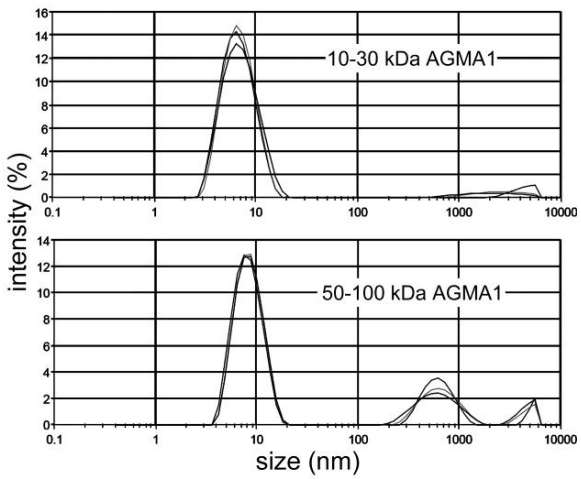

Supplementary Figure 2 | Dynamic light scattering analysis of 10-30 and 50- 100 kDa AGMA1.

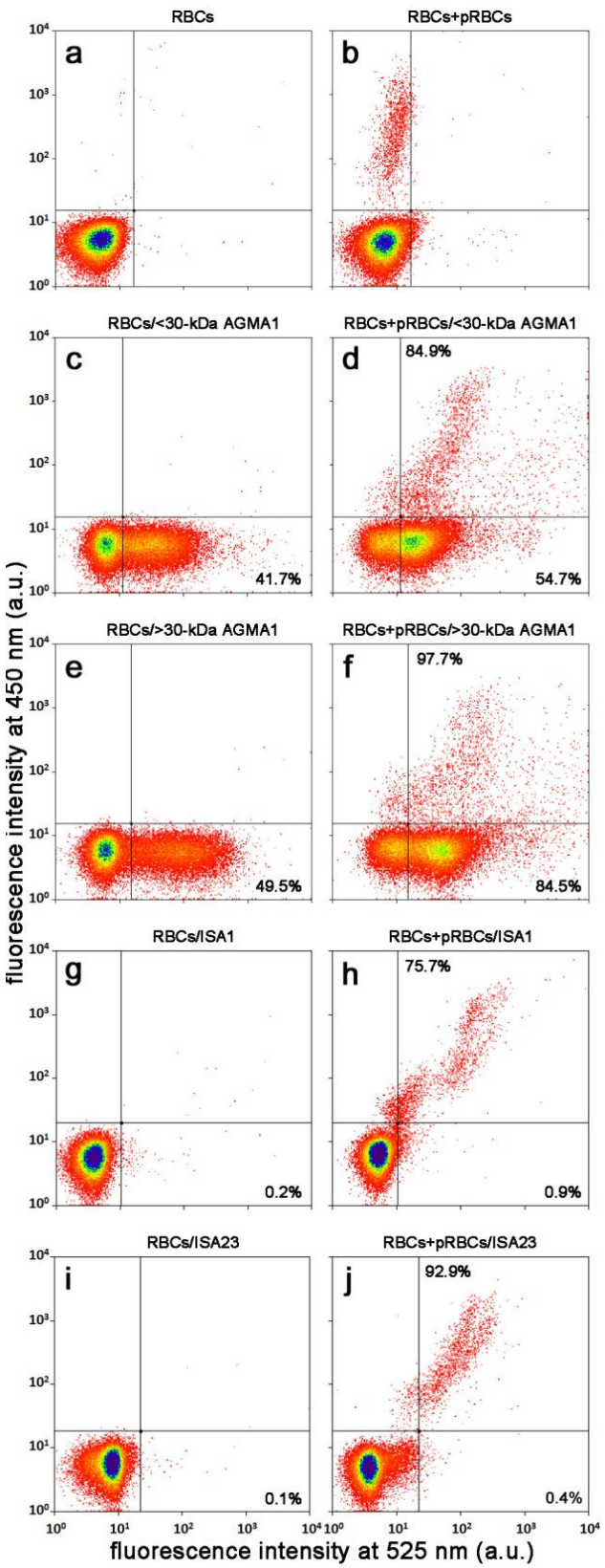

Figure 4 | FACS analysis of the interaction with RBCs and pRBCs of AGMA1, ISA1, and ISA23. The upper areas contain pRBCs (Hoechst fluorescence) and the right hand areas contain PAA-bound cells (FITC fluorescence). Percentage values indicate the fraction of PAA-bound pRBCs (upper right areas) and RBCs (lower right areas).

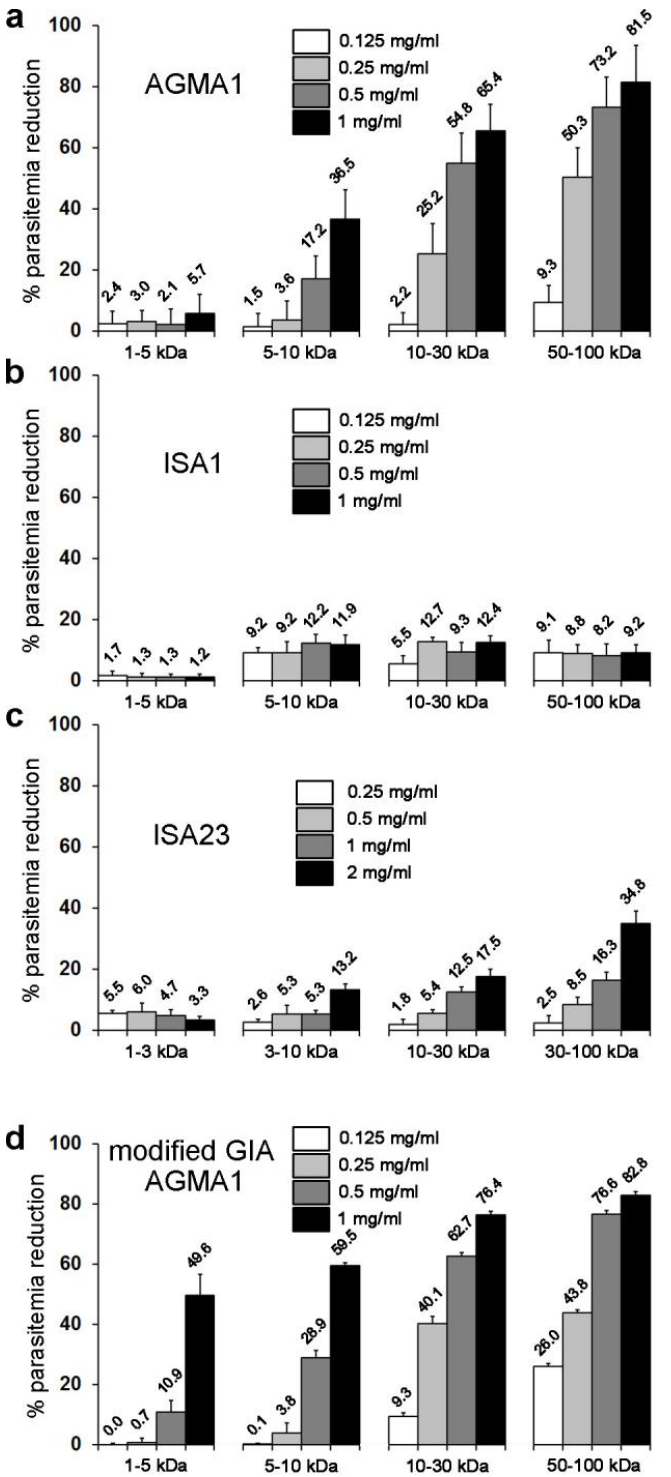

Figure 5 | Effect of AGMA1, ISA1, and ISA23 on the growth of *P. falciparum*. a-c, Conventional GIAs, where the polymers were added to *P. falciparum* cultures synchronized at the ring stage, and incubated for 48 h before determining parasitemia. **d**, Modified GIA, where AGMA1 was added 24 h after pRBC culture synchronization, and incubated for a further 24 h before parasitemia determination.

Sample	Coefficient	p-value	95% confidence interval
AGMA1 5-10 kDa	12.4	<0.001	7.1–17.7
AGMA1 10-30 kDa	30.2	<0.001	24.9–35.4
AGMA1 50-100 kDa	46.4	<0.001	39.6–53.1
ISA1 5-10 kDa	8.6	<0.001	7.0-10.1
ISA1 10-30 kDa	7.3	<0.001	5.8-8.9
ISA1 50-100 kDa	6.9	<0.001	5.4-8.4
ISA23 3-10 kDa	0.0	0.996	-3.5-3.5
ISA23 10-30 kDa	4.1	0.023	0.6-7.7
ISA23 30-100 kDa	8.5	<0.001	4.9-12.2

Supplementary Table 2A | Statistical analysis of the significance of differences in *in vitro* antimalarial activity between AGMA1, ISA1, and ISA23 polymers of different molecular mass. Each value corresponds to the comparison with the smallest size fraction for each polymer (1-5 kDa for AGMA1 and ISA1 and 1-3 kDa for ISA23). The less significant differences are shaded.

Compared samples	Coefficient	p-value	95% confidence interval
AGMA1 10-30 kDa vs AGMA 5-10 kDa	17.7	<0.001	13.0-22.4
AGMA1 10-30 kDa vs AGMA1 50-100 kDa	16.2	<0.001	10.2-22.3
AGMA1 50-100 kDa vs AGMA 5-10 kDa	33.9	<0.001	27.9-40.0
ISA1 10-30 kDa vs ISA1 5-10 kDa	4.1	0.002	1.6-6.7
ISA1 10-30 kDa vs ISA1 50-100 kDa	4.4	0.016	0.8-7.9
ISA1 50-100 kDa vs ISA1 5-10 kDa	8.5	<0.001	4.9-12.1
ISA23 10-30 kDa vs ISA23 3-10 kDa	4.1	0.002	1.6-6.7
ISA23 10-30 kDa vs ISA23 30-100 kDa	4.4	0.016	0.8-7.9
ISA23 30-100 kDa vs ISA23 3-10 kDa	8.5	<0.001	4.9-12.1

Supplementary Table 2B | Statistical analysis of the significance of differences in *in vitro* antimalarial activity between AGMA1, ISA1, and ISA23 polymers of different molecular mass. The less significant differences are shaded.

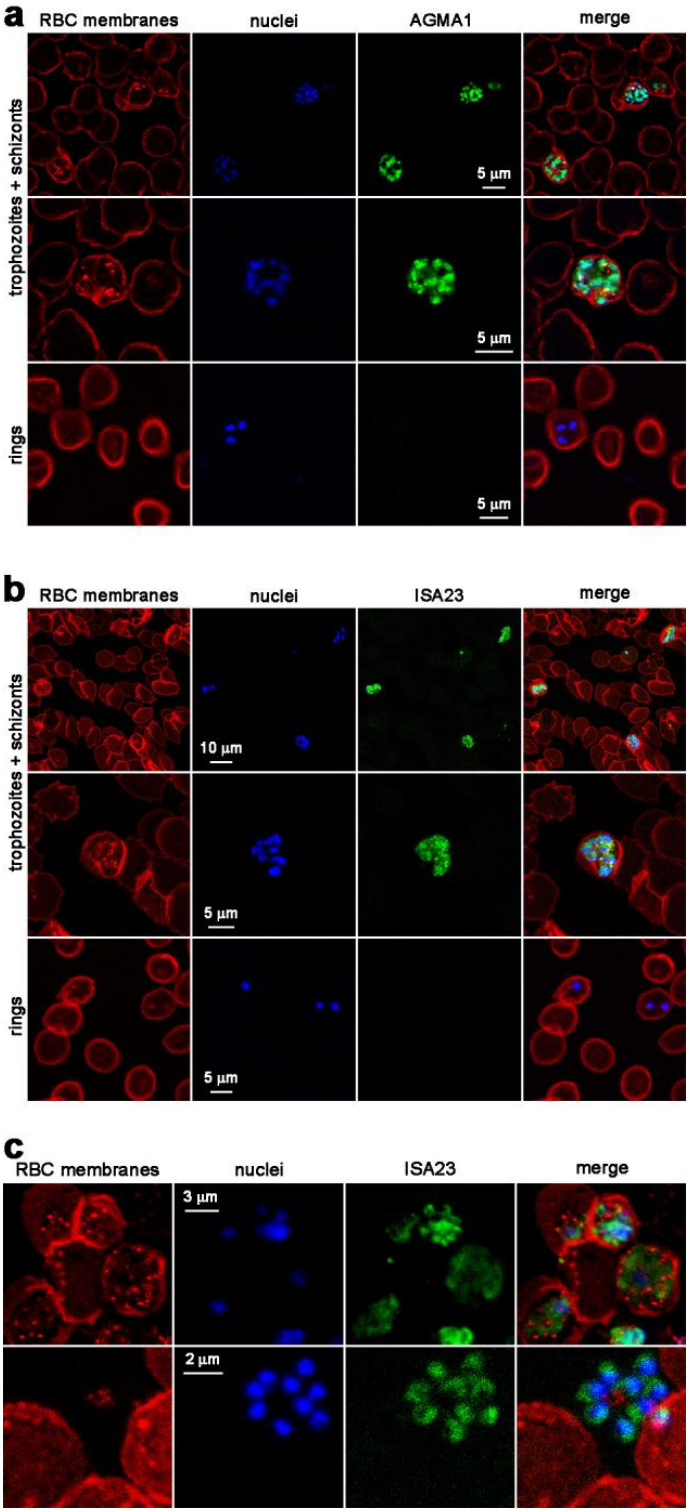

Figure 6 | Confocal fluorescence microscopy study of the targeting of AGMA1 and ISA23. FITC-labeled 30-100 kDa AGMA1 (**a**) or 10-30 kDa ISA23 (**b**,**c**) was added to *P. falciparum* cultures of the 3D7 strain (**a**,**b**) or to *P. yoelii*-infected mouse blood (**c**), and after 90 min of incubation PAA localization (green) was detected by confocal fluorescence on cells parasitized by trophozoites, schizonts, or rings. DAPI (blue) staining of *Plasmodium* nuclei is used to indicate pRBCs. The RBC plasma membrane is shown in red.

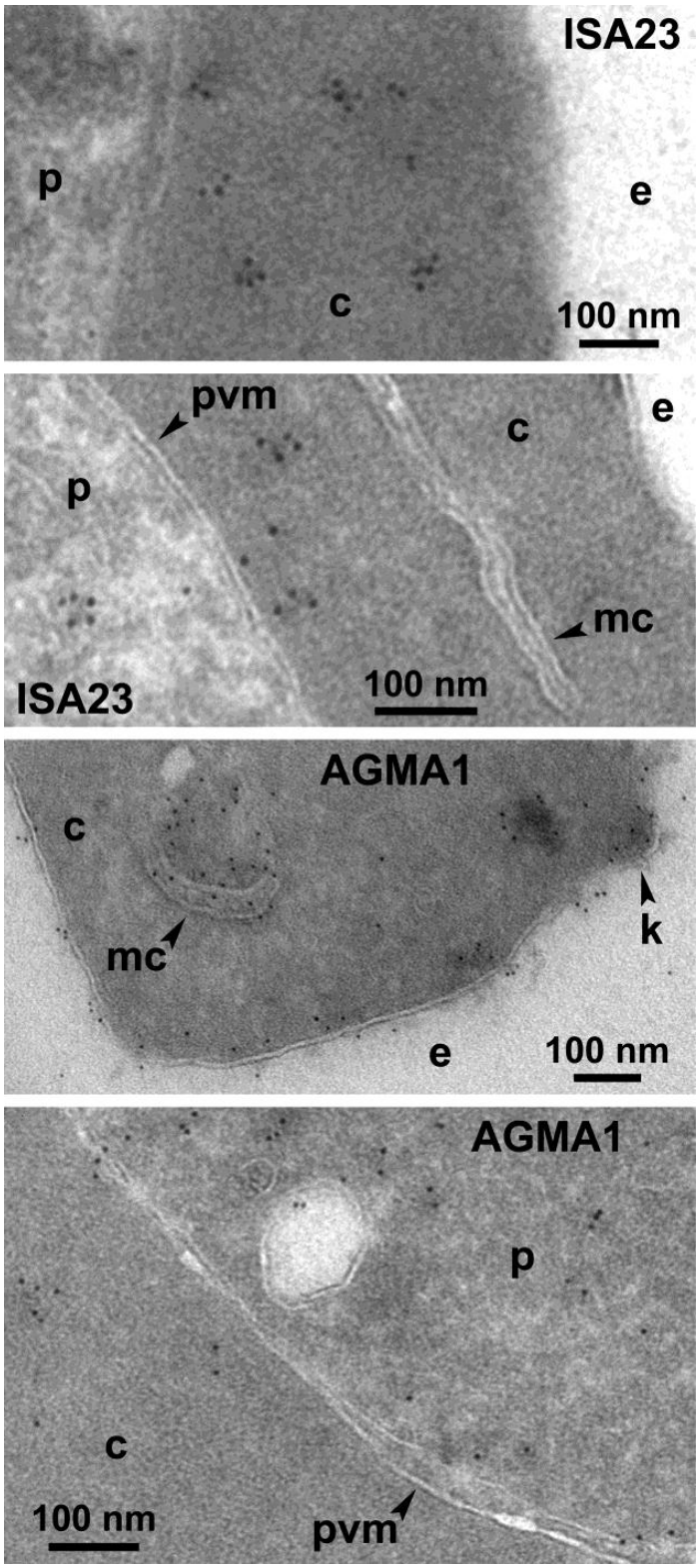

Figure 7 | TEM analysis of the subcellular localization of AGMA1 and ISA23. Living pRBCs were treated with FITC-labeled 10-30 kDa AGMA1 or ISA23 for 90 min before TEM processing. e, extracellular area; c, pRBC cytosol; p, *Plasmodium*; pvm, parasitophorous vacuole membrane; mc, Maurer's cleft; k, knob.

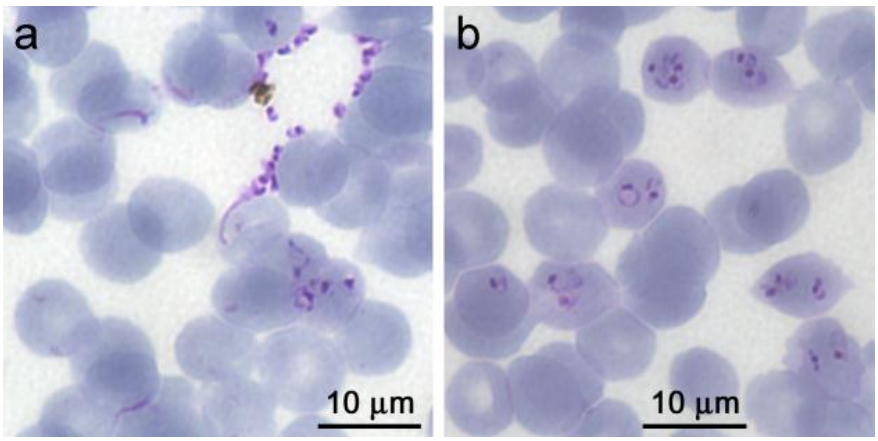

Figure 8 | Microscopy images of Giemsa-stained smears of 10-30 kDa AGMA1-treated *P. falciparum* cultures at ring stage after a complete cycle. a, 1 mg ml^{-1}AGMA1-treated sample. **b**, Control sample without AGMA1.

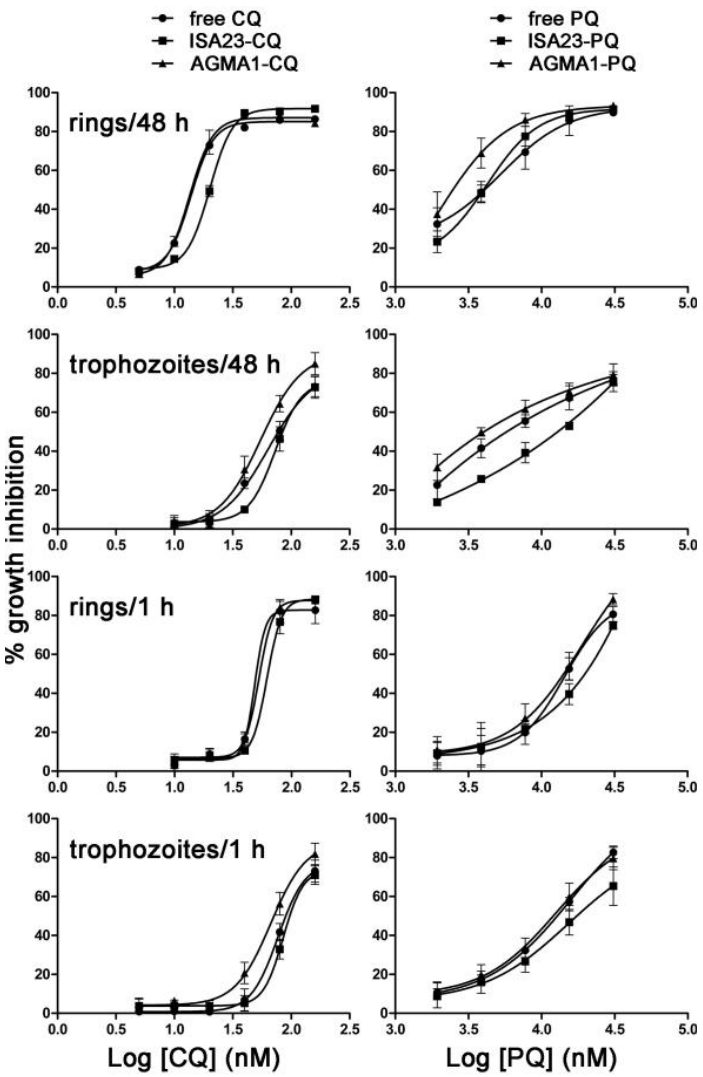

Figure 9 | *In vitro* antimalarial activity of PAA-drug conjugates.

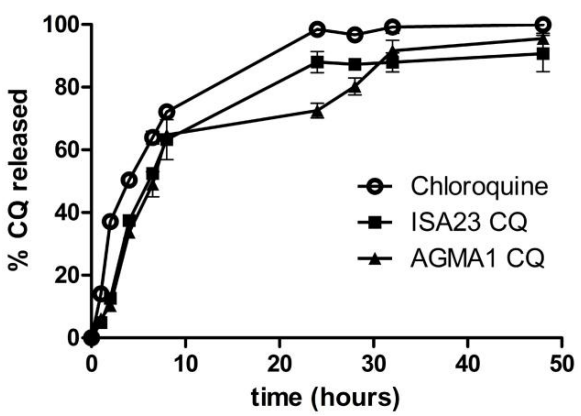

Figure 10 | Temporal release profile in PBS of CQ from PAA-drug conjugates.

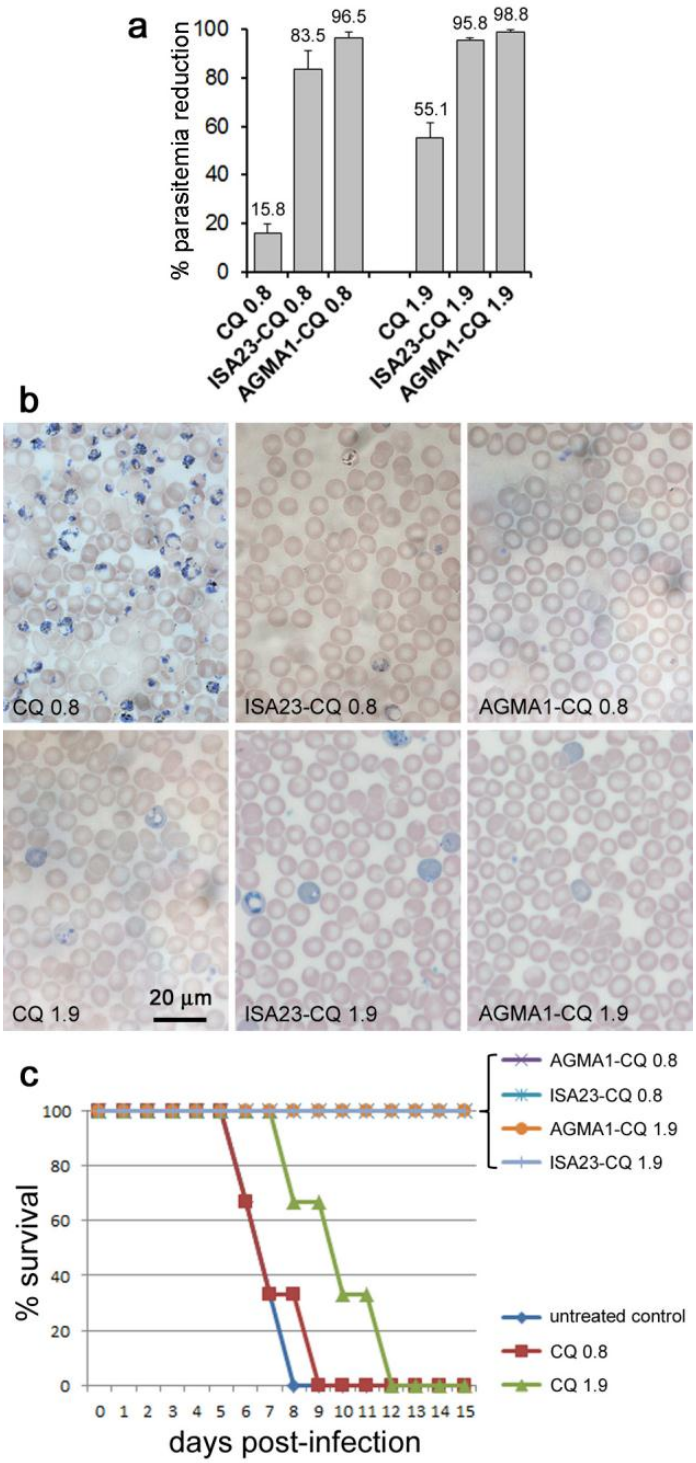

Figure 11 | *In vivo* antimalarial activity of PAA-drug conjugates. a, Percentage of parasitemia reduction relative to untreated control at day 4 in *P. yoelii*-infected mice treated with 0.8 or 1.9 mg kg^{-1} day^{-1} CQ, either free or encapsulated in ISA23 or AGMA1. **b**, Microscopy images of Giemsa-stained smears of the same samples. **c**, Mice survival graph of *P. yoelii*-infected mice treated with 0.8 or 1.9 mg kg^{-1} day^{-1} CQ, either free or encapsulated in ISA23 or AGMA1.

Reference List

1. WHO. World Malaria Report 2011. http://www.who.int/malaria/world_malaria_report_2011/9789241564403_eng.pdf . 2011. Ref Type: Electronic Citation

2. Kappe,S.H., Vaughan,A.M., Boddey,J.A., & Cowman,A.F. That was then but this is now: malaria research in the time of an eradication agenda. *Science* **328**, 862-866 (2010).

3. Vangapandu,S. *et al.* Recent advances in antimalarial drug development. *Med. Res. Rev.* **27**, 65-107 (2007).

4. Okiro,E.A. *et al.* Age patterns of severe paediatric malaria and their relationship to *Plasmodium falciparum* transmission intensity. *Malar. J* **8**, 4 (2009).

5. Wells,T.N., Alonso,P.L., & Gutteridge,W.E. New medicines to improve control and contribute to the eradication of malaria. *Nat. Rev. Drug Discov.* **8**, 879-891 (2009).

6. White,N.J. *Plasmodium knowlesi*: the fifth human malaria parasite. *Clin. Infect. Dis.* **46**, 172-173 (2008).

7. Tuteja,R. Malaria - an overview. *FEBS J* **274**, 4670-4679 (2007).

8. Griffith,K.S., Lewis,L.S., Mali,S., & Parise,M.E. Treatment of malaria in the United States: a systematic review. *JAMA* **297**, 2264-2277 (2007).

9. Baird,J.K. Effectiveness of Antimalarial Drugs. *N Engl J Med* **352**, 1565- 1577 (2005).

10. Murambiwa,P., Masola,B., Govender,T., Mukaratirwa,S., & Musabayane,C.T. Anti-malarial drug formulations and novel delivery systems: A review. *Acta Tropica* **118**, 71-79 (2011).

11. Duncan,R. & Gaspar,R. Nanomedicine(s) under the Microscope. *Mol. Pharmaceutics* **8**, 2101-2141 (2011).

12. Paleos,C.M., Tsiourvas,D., Sideratou,Z., & Tziveleka,L.A. Drug delivery using multifunctional dendrimers and hyperbranched polymers. *Expert. Opin. Drug Deliv.* **7**, 1387-1398 (2010).

13. Sukhorukov,G.B. *et al.* Multifunctionalized polymer microcapsules: novel tools for biological and pharmacological applications. *Small* **3**, 944-955 (2007).

14. Tiwari,A.K., Gajbhiye,V., Sharma,R., & Jain,N.K. Carrier mediated protein and peptide stabilization. *Drug Deliv.* **17**, 605-616 (2010).

15. Ferruti,P., Marchisio,M.A., & Duncan,R. Polyamidoamines: biomedical applications. *Macromol. Rapid. Commun.* **23**, 332-355 (2002).

16. Ferruti,P. *et al.* Recent results on functional polymers and macromonomers of interest as biomaterials or for biomaterial modification. *Biomaterials* **15**, 1235-1241 (1994).

17. Ferruti,P. *et al.* Degradation behaviour of ionic stepwise polyaddition polymers of medical interest. Journal of Biomaterials Science, Polymer Edition 6[9], 833-844. 1995.
Ref Type: Abstract

18. Pattrick,N.G., Richardson,S.C., Casolaro,M., Ferruti,P., & Duncan,R. Poly(amidoamine)-mediated intracytoplasmic delivery of ricin A-chain and gelonin. *J Control Release* **77**, 225-232 (2001).

19. Ferruti,P. *et al.* Prevailingly cationic agmatine-based amphoteric polyamidoamine as a nontoxic, nonhemolytic, and "stealthlike" DNA complexing agent and transfection promoter. *Biomacromolecules* **8**, 1498-1504 (2007).

20. Franchini,J., Ranucci,E., Ferruti,P., Rossi,M., & Cavalli,R. Synthesis, physicochemical properties, and preliminary biological characterizations of a novel amphoteric agmatine-based poly(amidoamine) with RGD-like repeating units. *Biomacromolecules* **7**, 1215-1222 (2006).

21. Cavalli,R. *et al.* Amphoteric agmatine containing polyamidoamines as carriers for plasmid DNA *in vitro* and *in vivo* delivery. *Biomacromolecules* **11**, 2667-2674 (2010).

22. Richardson,S., Ferruti,P., & Duncan,R. Poly(amidoamine)s as potential endosomolytic polymers: evaluation in vitro and body distribution in normal and tumour-bearing animals. *J Drug Target* **6**, 391-404 (1999).

23. Ranucci,E., Spagnoli,G., Ferruti,P., Sgouras,D., & Duncan,R. Poly(amidoamine)s with potential as drug carriers: degradation and cellular toxicity. Journal of Biomaterials Science, Polymer Edition 2[4], 303-315, 1991. Ref type: Abstract.

24. Podestà,A., Tiana,G., Milani,P., & Manno,M. Early events in insulin fibrillization studied by time-lapse atomic force microscopy. Biophysical Journal 90[2], 589-597. 2006.
Ref Type: Abstract

25. Zuccala,E.S. & Baum,J. Cytoskeletal and membrane remodelling during malaria parasite invasion of the human erythrocyte. *British Journal of Haematology* **154**, 680-689 (2011).

26. Hanssen,E. *et al.* Whole cell imaging reveals novel modular features of the exomembrane system of the malaria parasite, Plasmodium falciparum. *International Journal for Parasitology* **40**, 123-134 (2010).

27. Haas,S.E., Bettoni,C.C., de Oliveira,L.K., Guterres,S.l.S., & Dalla Costa,T. Nanoencapsulation increases quinine antimalarial efficacy against Plasmodium berghei in vivo. International journal of antimicrobial agents 34[2], 156-161. 2009.
Ref Type: Abstract

28. Mosqueira,V.C.F. *et al.* Efficacy and pharmacokinetics of intravenous nanocapsule formulations of halofantrine in *Plasmodium berghei*-infected mice. *Antimicrobial Agents and Chemotherapy* **48**, 1222-1228 (2004).

29. Akhtar,F., Rizvi,M.M.A., & Kar,S.K. Oral delivery of curcumin bound to chitosan nanoparticles cured Plasmodium yoelii infected mice. *Biotechnology Advances* **30**, 310-320 (2012).

30. Bhadra,D., Bhadra,S., & Jain,N.K. Pegylated lysine based copolymeric dendritic micelles for solubilization and delivery of artemether. *J. Pharm. Pharm. Sci.* **8**, 467-482 (2005).

31. Bhadra,D., Bhadra,S., & Jain,N.K. PEGylated peptide dendrimeric carriers for the delivery of antimalarial drug chloroquine phosphate. *Pharm. Res.* **23**, 623-633 (2006).

32. Agrawal,P., Gupta,U., & Jain,N.K. Glycoconjugated peptide dendrimers-based nanoparticulate system for the delivery of chloroquine phosphate. *Biomaterials* **28**, 3349-3359 (2007).

33. Green,M.D., D'Souza,M.J., Holbrook,J.M., & Wirtz,R.A. In vitro and in vivo evaluation of albumin-encapsulated primaquine diphosphate prepared by nebulization into heated oil. *Journal of Microencapsulation* **21**, 433-444 (2004).

34. Bhadra,D., Yadav,A.K., Bhadra,S., & Jain,N.K. Glycodendrimeric nanoparticulate carriers of primaquine phosphate for liver targeting. *Int. J Pharm.* **295**, 221-233 (2005).

35. Singh,K.K. & Vingkar,S.K. Formulation, antimalarial activity and biodistribution of oral lipid nanoemulsion of primaquine. *International Journal of Pharmaceutics* **347**, 136-143 (2008).

36. Basco,L.K., Bickii,J., & Ringwald,P. In-vitro activity of primaquine against the asexual blood stages of Plasmodium falciparum. Annals of Tropical Medicine and Parasitology 93[2], 179-182. 1999.
Ref Type: Abstract

37. Reddy,R.C., Vatsala,P.G., Keshamouni,V.G., Padmanaban,G., & Rangarajan,P.N. Curcumin for malaria therapy. *Biochemical and Biophysical Research Communications* **326**, 472-474 (2005).

38. Urbán,P., Estelrich,J., Adeva,A., Cortés,A., & Fernàndez-Busquets,X. Study of the efficacy of antimalarial drugs delivered inside targeted immunoliposomal nanovectors. *Nanoscale Research Letters* **6**, 620 (2011).

39. Yayon,A. & Ginsburg,H. The transport of chloroquine across human erythrocyte membranes is mediated by a simple symmetric carrier. *Biochim. Biophys. Acta* **686**, 197-203 (1982).

40. Urbán,P., Estelrich,J., Cortés,A., & Fernàndez-Busquets,X. A nanovector with complete discrimination for targeted delivery to *Plasmodium falciparum*-infected versus non-infected red blood cells in vitro. *J Control Release* **151**, 202-211 (2011).

41. Kirk,K. & Saliba,K.J. Targeting nutrient uptake mechanisms in *Plasmodium*. *Curr Drug Targets* **8**, 75-88 (2007).

42. Goodyer,I.D., Pouvelle,B., Schneider,T.G., Trelka,D.P., & Taraschi,T.F. Characterization of macromolecular transport pathways in malaria-infected erythrocytes. *Mol. Biochem. Parasitol.* **87**, 13-28 (1997).

43. Rovira-Graells,N.+. *et al.* Transcriptional variation in the malaria parasite Plasmodium falciparum. *Genome Research* **22**, 925-938 (2012).

44. Richardson,S.C.W., Pattrick,N.G., Lavignac,N., Ferruti,P., & Duncan,R. Intracellular fate of bioresponsive poly(amidoamine)s in vitro and in vivo. *Journal of Controlled Release* **142**, 78-88 (2010).

45. Allahyari,R., Strother,A., Fraser,I.M., & erbiscar,A.J. Synthesis of certain hydroxy analogues of the antimalarial drug primaquine and their in vitro methemoglobin-producing and glutathione-depleting activity in human erythrocytes. *J. Med. Chem.* **27**, 407-410 (1984).

46. Cranmer,S.L., Magowan,C., Liang,J., Coppel,R.L., & Cooke,B.M. An alternative to serum for cultivation of *Plasmodium falciparum* in vitro. *Trans. R. Soc. Trop. Med. Hyg.* **91**, 363-365 (1997).

47. Lambros,C. & Vanderberg,J.P. Synchronization of *Plasmodium falciparum* erythrocytic stages in culture. *J Parasitol.* **65**, 418-420 (1979).

48. Odin,C., Aimeé,J.P., El Kaakour,T., & Bouhacina,T. Tip finite size effects on atomic force microscopy in the contact mode: simple geometrical considerations for rapid estimation of apex radius and tip angle based on the study of polystyrene latex ball. *Surface Science* **317**, 321-340 (1994).

49. Fidock,D.A., Rosenthal,P.J., Croft,S.L., Brun,R., & Nwaka,S. Antimalarial drug discovery: efficacy models for compound screening. *Nat. Rev. Drug Discov.* **3**, 509-520 (2004).

OTHER RESULTS

Study of the stability of immunoliposomes

Liposomes encapsulating chloroquine were synthesized as previously described[197] in order to study their physical and chemical stability at 4ºC and 37ºC for a period of 90 days. The size of the liposome population was determined by dynamic light scattering at 90º with a Zetasizer NanoZS90 (Malvern Ltd, Malvern, UK) at 25ºC. The particle size distribution was defined by the polydispersity index (PDI), which ranges from 0.0 for an entirely monodisperse sample to 1.0 for a polydisperse sample. The amount of chloroquine inside liposomes was quantified using HPLC-MS/MS at different time points after lipid extraction with chloroform and methanol. Data are presented as the mean ± standard error, represented by error bars, of at least three independent samples. Statistical analyses were performed using the GraphPad Prism5 data analysis and statistical software. The parametric Student's t test was used to compare two independent groups with data following a Gaussian distribution.

Physical stability results are shown in Figure 18. No differences are observed for Z-average and PDI measures between liposomes stored at 4ºC or at 37ºC. These results were confirmed by HPLC quantification of chloroquine content in liposomes (data not shown).

Results obtained indicate that liposomes can be stored for at least 3 months without aggregation or loss of drug content. Although liposomes are stable at 37ºC, storage at 4ºC is recommended due to the presence of half-antibodies in the case of immunoliposomes.

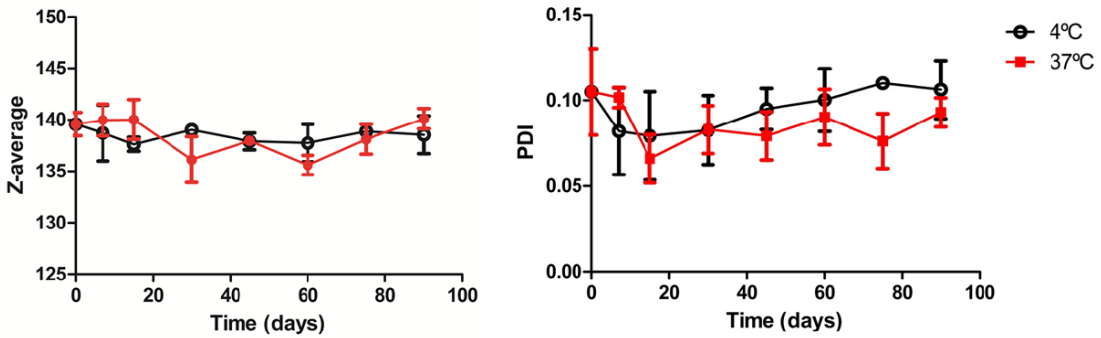

Figure 18. Determination of the physical stability of liposomes using dynamic light scattering. Z-average (left) and polydispersity index (right) were measured at 4ºC and 37ºC at different time points for a period of 90 days.

Study of the efficacy of immunoliposomes in *P. yoelii*-infected mice

These experiments were performed during a 6-month stay in the group of Prof. José Manuel Bautista at the Universidad Complutense de Madrid under the supervision of Dr. Patricia Marín. The objective of this collaboration was to learn how to study the efficacy of nanovectors *in vivo* and bring the know-how to our laboratory in Barcelona. The experiments performed were aimed at assessing the efficacy of free drugs and (immuno)liposomal drugs using a 4-day blood suppressive test in *P. yoelii*-infected mice before testing immunoliposomal nanovectors in a *P.falciparum*-animal model.

(Immuno)liposomes encapsulating different doses of chloroquine were synthesized as previously described[197] and a PEG-lipid derivative (1,2-distearoyl-sn-glycero-3-phosphoethanolamine-N-[methoxy(polyethyleneglycol)-2000 from Avanti Polar Lipids Inc., Alabaster, AL, USA.) was included in liposomal formulation in order to increase blood half-life of liposomes. Immunoliposomes were functionalized with specific antibodies against *P. falciparum*-infected RBCs.

The lethal rodent malaria parasite *Plasmodium yoelii yoelii 17XL* MRA-267 was obtained from the Malaria Research and Reference Resource Center, maintained by serial blood passage in mice, and stored in liquid N_2. Inbred BALB/c female, 6-8 weeks old, were purchased from Harlan Laboratories and housed under standard conditions of light and temperature at the Animal Housing Facility from the Universidad Complutense de Madrid. All mice were fed *ad libitum* on a commercial diet. All animal work was conducted at the Universidad Complutense de Madrid according to the relevant national and international guidelines for animal experimentation.

The *in vivo* antimalarial activity of chloroquine or (immuno)liposomal chloroquine was assessed using a 4-day-blood suppressive test as previously described[109]. Briefly, mice were inoculated $2x10^7$ red blood cells from *P. yoelii*-

infected mice by intraperitoneal (i.p.) injection. The chemotherapy treatment started 2 h later (day 0) with a single dose of 1, 2.5 or 5 mg/kg/day of chloroquine or (immuno)liposomal chloroquine by an i.p. injection, followed by identical dose administration for the following 3 days, whereas control groups received PBS. The parasitemia was monitored daily by microscopic examination of Wright's-stained thin-blood smears. Activity was calculated on day 4 (first day without treatment) comparing parasitemias of treated and control mice. Data are presented as the mean ± standard error represented by error bars of at least three independent experiments. Statistical analyses were performed using GraphPad Prism5 data analysis and statistical software. Data obtained for CQ, liposomes-CQ and immunoliposomes-CQ was compared using the nonparametric Kruskal-Wallis test, and Mann-Whitney test was used to compare two unpaired groups. Differences were considered significant when the p value was ≤ 0.05.

Activity results on first day without chemotherapy indicate that significant differences were observed when comparing the three groups for 1 and 2.5 mg/kg/day of CQ, but no differences were observed when comparing the activity of liposomes-CQ and immunoliposomes-CQ (Table 3). Differences between CQ and (immuno)liposomes were higher for 1 mg/kg/day dose ($p \leq 0.005$) because at 2.5 mg/kg/day the activity of free CQ is closer to 100%. At 5 mg/kg/day no differences were observed in the activity values, no parasites were detected at day 4 in mice treated with CQ 5 mg/kg/day either as free drug or immuno(liposomal) (Figure 19).

	CQ	**Liposomes-CQ**	**Immunoliposomes-CQ**
1 mg/kg	12.8 ± 12.3	78.8 ± 20.6	72.3 ± 10.1
2.5 mg/kg	85.2 ± 12.5	94.5 ± 6.4	90.7 ± 12.1
5 mg/kg	100.0 ± 0.0	100.0 ± 0.0	100.0 ± 0.0

Table 3. Activity expressed as % of parasitemia reduction vs control mice of CQ, liposomes-CQ and immunoliposomes-CQ at three different doses in *P. yoelii*-infected mice. The percentages of activity are expressed as mean ± standard error of at least three independent experiments.

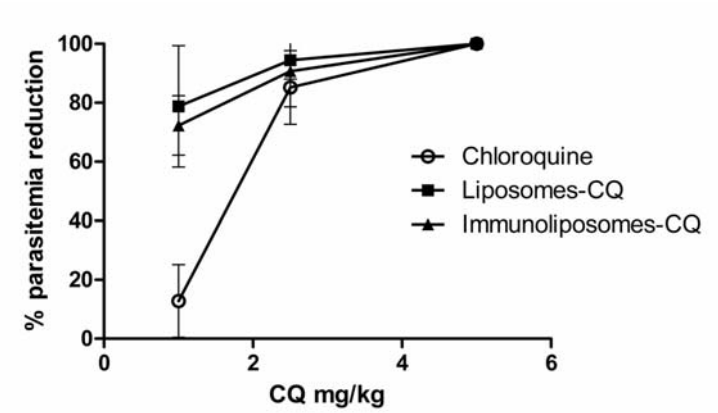

Figure 19. Activity expressed as % of parasitemia reduction vs control mice treated with free CQ, liposomal and immunoliposomal CQ in *P. yoelii*-infected mice at day 4 in a 4-day-blood suppressive test.

However, treatment at 1 and 2.5 mg CQ/kg/day, either free or liposomal, does not protect mice from death in 100% of the cases; percentages of mice that died and survived after infection and treatment are shown in Table 4. Mice treated with 1 mg CQ/kg/day did not present differences in the day of death when compared to control animals, but significant differences were observed when mice were treated either with liposomes or immunoliposomes encapsulating 1mg CQ/kg/day, these mice died later than animals treated with the same dose of free CQ. No differences in the day of death were observed between liposomes and immunoliposomes at this dose. Mice treated with free or (immuno)liposomal CQ at 2.5 mg/kg/day presented significant differences in the mean day of death in comparison with control animals, but differences between CQ and (immuno)liposomes were only observed for immunoliposomal treatment, which lead to a 50% of survival vs a 20% survival in CQ-treated mice.

	% dead mice	Day of death	% survived mice
control (n=16)	100	5.7 ± 0.6	0
CQ 1 (n=16)	100	5.7 ± 0.6	0
LPS-CQ1 (n=16)	100	7.3 ± 1.4	0
iLPS-CQ1 (n=10)	90	6.7 ± 0.8	10
CQ 2.5 (n=15)	80	9.0 ± 2.6	20
LPS-CQ 2.5 (n=14)	73	8.8 ± 1.4	27
iLPS-CQ 2.5 (n=8)	50	9.8 ± 3.1	50

Table 4. Percentages of dead and survived mice in in *P. yoelii*-infected mice treated with free CQ, liposomal and immunoliposomal CQ at two different doses: 1 and 2.5 mgCQ/kg/day. Statistical analysis has been performed using the mean and standard deviation of the day of death of non-cured mice.

Results obtained show an increase of activity of liposome-encapsulated drugs compared to free drugs and a prolonged survival rate of the animals, but no significant differences in the activity of encapsulated CQ have been observed between liposomes and immunoliposomes, probably because the antigen recognized by the antibody used for liposomes functionalization is not present in *P. yoelii*-infected mice. However, experiments were performed with a lethal strain of *Plasmodium* and if parasitemia was detected at day 4, as no more drug will be administered, parasites can replicate and mice die if they cannot control infection. Mice treated with immunoliposomes-CQ presented higher survival rates than CQ or liposomal CQ at the same dose, but animals treated with immunoliposomes could survive even if activity at day 4 was not significantly different. Key factors such as degree of parasitemia, clearance capacity, immune system and medular exhaustion are determinant for mice survival once treatment is removed.

In vivo therapeutic eficacy of liposomal cloroquine in humanized mice

The goal of this study was to measure the *in vivo* therapeutic efficacy of immunoliposomal drugs against *P. falciparum* growing in peripheral blood of NODscidIL2Rγ^{null} mice engrafted with human erythrocytes[198]. These experiments were performed under the supervision of María Belén Jiménez-Díaz in Diseases of the Developing World, GlaxoSmithKline (GSK), Tres Cantos, Spain.

Liposomes encapsulating chloroquine, primaquine and artesunate were prepared as previously described[199]. All drugs were incorporated in the aqueous compartment of the liposome, except artesunate that was also incorporated in the lipid bilayer. The amount of encapsulated drug was adjusted in order to administer the ED_{50} of each drug once a day. ED_{50} is defined as the dose in mg/Kg that reduces parasitemia at day 7 after infection by 50 % with respect to vehicle-treated mice, and had been previously in GSK (Table 5).

Compound	ED_{50} (mg/Kg)
Artesunate	5.3 (3.7-7.2)
Primaquine	1.8 (1.3-2.5)
Chloroquine	3.5 (2-5)

Table 5. ED_{50} values for artesunate, primaquine and chloroquine obtained with *P.falciparum*-infected mice in GSK.

The antimalarial efficacy of chloroquine, primaquine and artesunate encapsulated in immunoliposomes was assessed using a 4-day test. Female immunodeficient NSG mice, enfrafted with human RBCs were infected i.v. with $2x10^7$ *P. falciparum*-infected erythrocytes on day 0. The treatment was administered intravenously once a day and started at day 3 and finished at day 6 after infection. Parasitemia was measured on days 3, 4, 5, 6 and 7 after

infection by flow cytometry. A vehicle-treated group is used as control of infection. The effect of treatments is determined by reduction of parasitemia with respect to vehicle-treated group (control) 24 hours after last dose of liposomal drug.

Results obtained indicate that in the aforementioned experimental conditions, chloroquine and artesunate have an increased activity when administered inside inmunoliposomes (Figure 20). When chloroquine is administered inside inmunoliposomes at the dose that reduces parasitemia at day 7 after infection by 50%, the reduction of parasitemias is more than 95%. This increased effect is also observed for artesunate, either in immunoliposomes encapsulating artesunate or when artesunate is incorporated in the membrane. However, immunoliposomes containing primaquine have not increased the activity of free drug.

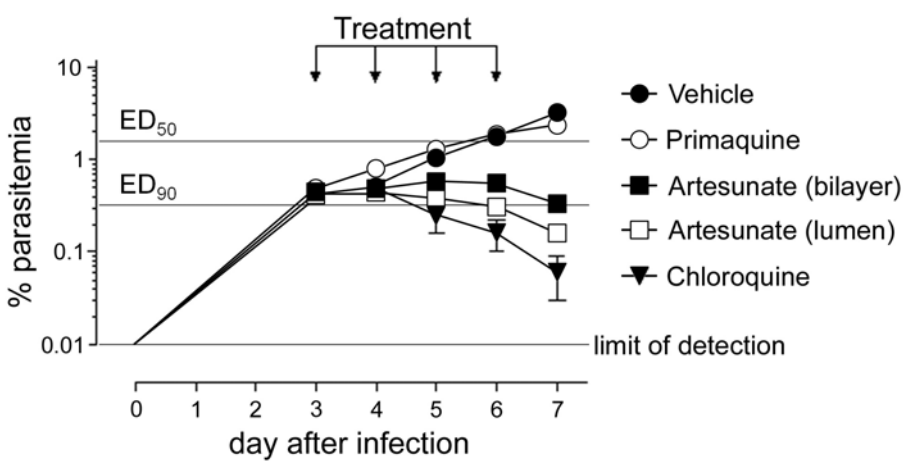

Figure 20. Effect of liposomal drugs on the parasitemias of *P. falciparum*-infected mice. Doses of each drug were adjusted to the ED_{50}, the dose that reduces parasitemia at day 7 after infection by 50 % with respect to vehicle-treated mice.

Encapsulation of antimalarial drugs with dendritic derivatives

This work has been performed in collaboration with the group of José Luis Serrano at the Instituto de Nanociencia de Aragón (INA), Zaragoza, Spain. Dendritic derivatives have been synthesized and characterized at INA. The biological studies of polymers in terms of unspecific toxicity, antimalarial activity and interaction with pRBCs have been performed by Julie Movellan and Patricia Urbán at the Centre de Recerca en Salut Internacional de Barcelona.

After preliminary tests, dendritic products A, B, C and D were synthesized by J. Movellan as potential carriers of antimalarial drugs. Dendrimers A and B were formed from bis-MPA dendrons, with one polar part from the dendron functionalized with amine groups and one apolar part from the second or third generation dendron of functionalized with apolar chains ($C_{17}H_{35}$). Dendritic-linear-dendritic polymers C and D were synthesized with Pluronic® F127 modified by *bis*-MPA dendrons, that were functionalized by amine groups.

The unspecific cytotoxicity of dendritic derivatives was studied in Human Umbilical Vein Endothelial Cells in a WST-1 toxicity assay. Percentages of viability were obtained using non-treated cells as control of survival and IC_{50} values were calculated by nonlinear regression with an inhibitory dose-response model using GraphPad Prism5 software. Results obtained (Table 6 and Figure 21) indicate that the precursor of compounds A and B and polymer D present significant unspecific cytotoxicity, with IC_{50} values of 2 mg/ml and 0.47 mg/ml respectively. IC_{50} for derivative C is above 10 mg/ml. None of the polymers presented hemolytic activity at these concentrations (data not shown).

Dendritic derivatives	1250 µg/ml	625 µg/ml	312.5 µg/ml	156.2 µg/ml	78.1 µg/ml	39.1 µg/ml
A and B precursor	75.8 ± 10.7	91.4 ± 4.2	97.1 ± 6.2	99.6 ± 3.5	99.3 ± 6.5	99.9 ± 3.2
C	98.9 ± 4.9	100.0 ± 1.9	97.7 ± 2.3	99.8 ± 3.3	100.0 ± 3.7	100.0 ± 3.9
D	45.7 ± 3.2	55.9 ± 6.3	68.8 ± 6.1	81.1 ± 5.9	87.3 ± 8.6	93.8 ± 4.5

Table 6. Unspecific cytotoxicity analysis of A and B precursor, C and D dendritic derivatives in HUVEC cells. Values indicate the percentage of viable cells relative to the control.

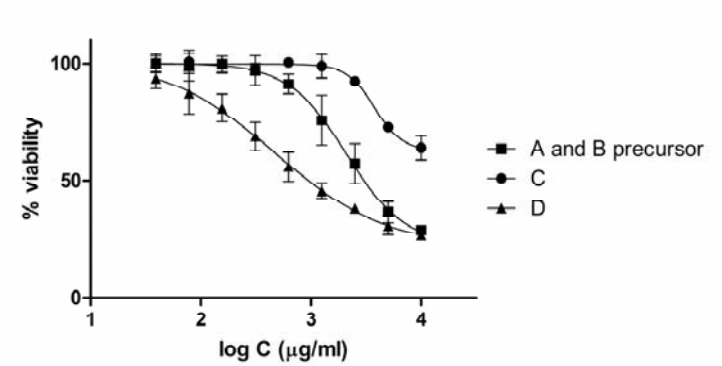

Figure 21. Percentages of viability of HUVEC cells incubated with different concentrations of A and B precursor, C and D for 48 h.

Dendritic derivatives were tested for their activity against *P. falciparum in vitro* in a growth inhibition assay. Briefly, parasitemia of *P. falciparum* 3D7 cultures was adjusted to 1.5% with more than 90% of parasites at ring stage after sorbitol synchronization. *Plasmodium* culture was incubated in the presence of each polymer solution for 48 h at 37°C under a gas mixture of 92% N_2, 5% CO_2, and 3% O_2. Parasitemia was determined by microscopic counting of blood smears, or by fluorescence-assisted cell sorting (FACS) and growth inhibition was calculated comparing parasitemias of polymer-treated and control samples. Results obtained are shown in Figure 22 and indicate that derivatives C and D present intrinsic antimalarial activity with IC_{50} values of 6.9 µg/ml and 151.5 µg/ml respectively.

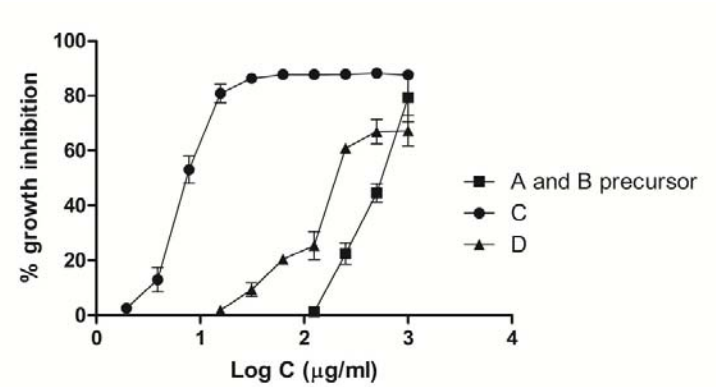

Figure 22. Effect of dendritic derivatives on the growth of *P. falciparum*. Polymers were added to *P. falciparum* cultures and incubated for 48 h before determining parasitemia.

For the encapsulation of CQ and PQ we used the oil/water emulsion method, which is based on the emulsification of an organic phase (organic volatile solvent + dendrimers) and an aqueous phase (H_20 + drug). Drugs were solubilized in water and the polymer was added in a small amount of dichloromethane to a molar ratio drug:polymer (5:1). After one hour, dichloromethane had been completely evaporated and the sample was dialysed against deionized water in order to eliminate free drug and the amount of encapsulated CQ and PQ was quantified by measuring the absorbance at 345 nm or 340 nm, respectively. Encapsulation yields are shown in Table 7 and indicate that derivatives A and B have a higher encapsulating capacity than C and D, and that CQ is encapsulated with higher efficacy than PQ in A and B dendritic structures in these conditions.

Chloroquine		**Primaquine**	
Derivative	% encapsulated	Derivative	% encapsulated
A	89.4	A	45.9
B	77.9	B	43.2
C	14.9	C	15.6
D	16.3	D	12.9

Table 7. Percentages of CQ and PQ encapsulated in polymers A-D.

Scanning Electron Microscopy (SEM) analyses were performed with gold-coated samples in order to study the size and shape of the conjugates (Table 8). The nano-objects formed after encapsulation of drugs presented different shapes depending on the drug used (Figure 23). The shape of the structures depending on the encapsulated drug would suggest that the drug contained changes the shape of the nano-object formed. When the drug encapsulated is CQ, nanospheres (C-CQ) and ovals are observed. With PQ, the compound A-PQ appears to form non-spheric structures of length between 100 nm and 500 nm. The compound B-PQ forms elongated or rod-like structures of approx. 600 nm in length. The structures formed by C-PQ and D-PQ are spherical to rod-like with smaller lengths (between 200 nm and 300 nm).

Compound	**A-CQ**	**B-CQ**	**C-CQ**	**D-CQ**	**A-PQ**	**B-PQ**	**C-PQ**	**D-PQ**
X (nm)	415	500	172	360	386	641	290	178
SD	109	226	87	131	257	277	78	53
Shape	Spheres	Spheres	Oval	Spheres	Oval	Rods	Spheres	Oval
AR	1.13	1.17	1.46	1.3	1.71	4.66	1.23	1.73
SD	0.16	0.11	0.25	0.15	0.28	1.83	0.17	0.15

Table 8. Size and shape of structures formed by dendritic derivatives A, B, C and D encapsulating CQ or PQ by analysis of SEM images. X (nm) is the average size and aspect ratio (AR) is the ratio of the major axis to the minor axis of the structures calculated from more than 50 structures.

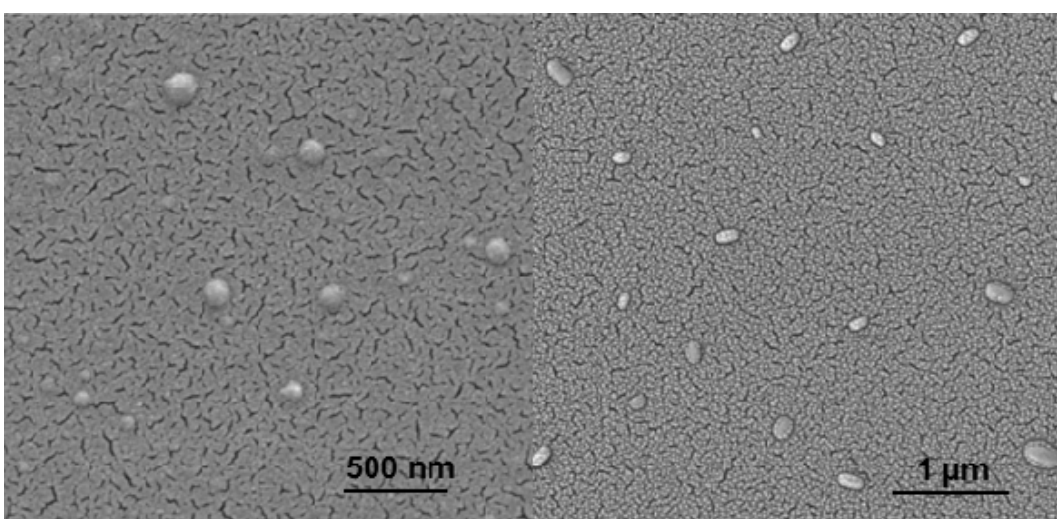

Figure 23. SEM pictures of the structures formed by dendritic derivatives D after the encapsulation of chloroquine (left) and primaquine (right).

Equal concentrations of free drugs and drug-containing dendritic derivatives were tested for their ability to inhibit the growth of *P. falciparum in vitro.* After 48 hours of incubation, parasitemia was determined by fluorescence-assisted cell sorting (FACS) and the percentage of growth inhibition was calculated relative to the control. Results obtained for polymers encapsulating chloroquine (Table 9) show that derivative A-CQ presents a similar activity than free CQ, indicating that CQ can be released from this polymer. With derivatives B-CQ and C-CQ a decrease in the antimalarial activity of polymers vs free chloroquine is appreciated, particularly in the case of derivative C-CQ, probably due a strong entrapment of CQ inside the nanocarrier difficulting its release.

The opposite is seen with derivative D: at all tested concentrations D-CQ presents higher antimalarial activity than free CQ. Since the IC_{50} for this polymer is higher than the concentrations of it, the antimalarial effect observed is likely due mainly to the activity of chloroquine, which is significantly increased when the drug is delivered inside derivative D-CQ. As shown in Figure 24, *Plasmodium* cultures that had been incubated with D-CQ were almost free of pRBCs, supporting the notion that derivative D is promising as a drug carrier for the delivery of chloroquine. Derivative A is also worth exploring for the delivery of chloroquine; its encapsulation efficacy is high and *in vitro* experiments indicate that CQ can be released quantitavely from this carrier. *In vivo* tests are required in order to further study the potentiality of these dendritic derivatives.

CQ (nM)	CQ	A-CQ	B-CQ	C-CQ	D-CQ
40	83.4 ± 7.2	82.4 ± 8.2	70.6 ± 4.4	2.9 ± 3.4	83.4 ± 8.0
20	81.5 ± 5.0	87.4 ± 0.2	3.9 ± 1.6	4.3 ± 4.8	83.7 ± 8.0
10	12.6 ± 5.1	5.9 ± 4.8	2.5 ± 2.2	2.4 ± 2.8	84.2 ± 7.4

Table 9. *Plasmodium* growth inhibition assays with free chloroquine and derivatives encapsulating CQ. The data shown represents the mean and standard deviation in the percentages of growth inhibition.

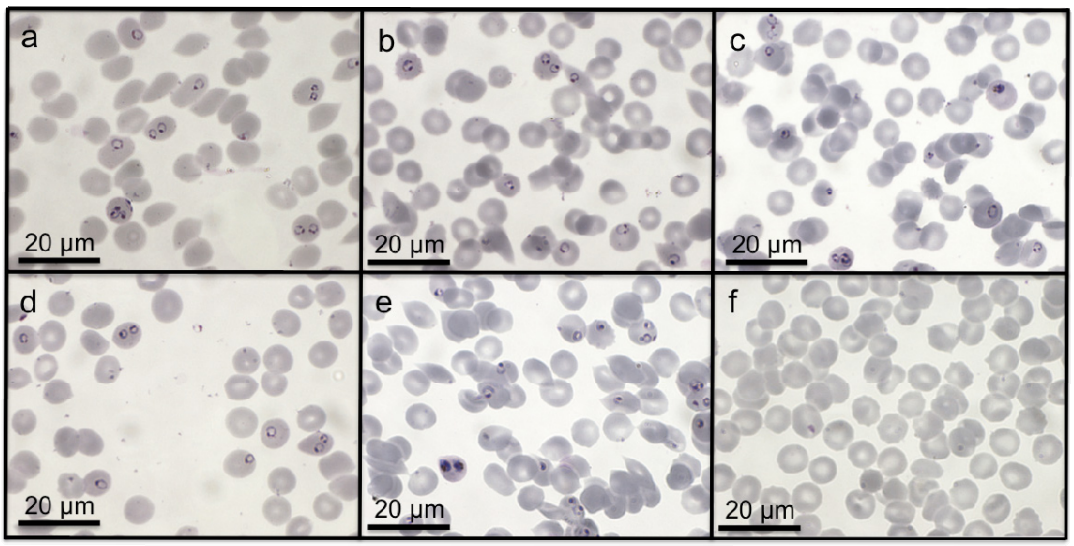

Figure 24. Microscope images of *Plasmodium*-infected RBCs treated with for 48h with 10 nM CQ either free or encapsulated in dendritic derivatives. (a) non-treated pRBCs (control); (b) chloroquine; (c) A-CQ; (d) B-CQ; (e) C-CQ and (f) D-CQ.

Results obtained with dendritic derivatives encapsulating primaquine (Table 10 and Figure 25) indicate that in derivatives A-PQ, B-PQ and D-PQ the activity of the nanocarriers is lower than that of free primaquine, likely due to a difficult release of the drug from the polymer. Derivative C-PQ shows an increased antimalarial activity compared to primaquine.

PQ (µM)	PQ	A-PQ	B-PQ	C-PQ	D-PQ
15.5	80.7 ± 5.5	10.7 ± 4.3	74.3 ± 0.4	80.3 ± 6.9	21.0 ± 5.2
7.8	69.1 ± 2.3	3.9 ± 3.9	45.7 ± 2.8	79.0 ± 7.1	8.4 ± 2.3
3.9	26.4 ± 2.6	1.1 ± 1.3	25.7 ± 4.1	86.0 ± 0.9	2.2 ± 1.5
1.9	18.4 ± 9.7	1.2 ± 1.2	6.6 ± 4.1	83.4 ± 0.6	1.5 ± 1.6

Table 10. *Plasmodium* growth inhibition assays in the presence of PQ, free or encapsulated in dendritic derivatives. The data shown represent the mean and standard error in the percentages of growth inhibition.

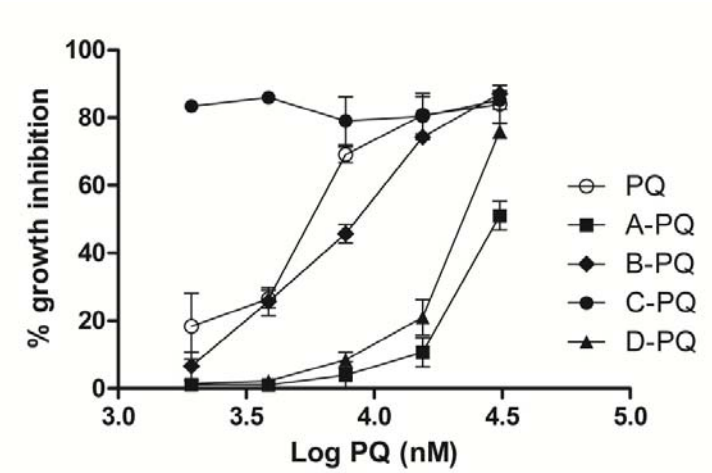

Figure 25. Activity of free primaquine and of dendritic derivatives encapsulating PQ in *Plasmodium* growth inhibition assays.

The best results have been obtained with dendritic derivatives C and D, which are Pluronic® derivatives that have been previously reported to form micelles[200] and to interact with cell membranes facilitating the internalization of compounds[201]. Moreover, the primary amine groups present in compound D could facilitate the interaction with the negatively charged cell membrane and would also be responsible for the unspecific toxicity of this dendrimer. As growth inhibition results indicate, the antimalarial effect of different drugs is not equally increased when delivered by the same dendritic structure, because the interaction between each drug and its carrier is unique and the engineering of the most adequate carrier is required for the design of efficacious delivery systems.

In order to study the interaction of dendritic derivatives with pRBCs, rhodamine B base (rho) was encapsulated inside the nano-objects formed by A, B, C and D. Encapsulation efficacy was calculated by measuring the fluorescence emission of rhodamine. SEM analyses confirmed the formation of spherical nano-objects of different sizes (data not shown). A-rho dendrimers were highly polydisperse, ranging in size from ca. 50 to 400 nm. The structures formed by B-rho were more regular, with a diameter between 90 and 120 nm. The compounds derived from Pluronic® polymer presented more spherical and

smaller morphologies, with diameters of approximately 80 nm in the case of C-rho and 50 nm in the case of D-rho.

Living *P. falciparum* cultures with mature stages of the parasite were incubated for 90 minutes at 37ºC with gentle stirring in the presence of 100 µg/ml of nano-objects containing rhodamine. After washing, blood smears were prepared and cells were fixed in acetone:methanol (90:10). Parasite nuclei were stained with 4'6-diamino-2-phenylindole (DAPI, Invitrogen) and the RBC membrane was labeled with wheat germ agglutinin (WGA)-Alexa 488 conjugate (Molecular Probes, Eugene, OR, USA). Slides were finally mounted with Fluoroprep Mounting Medium (BioMérieux), and analyzed with a Leica TCS SP5 laser scanning confocal microscope. DAPI, reflection (hemozoin), WGA-Alexa 488 and rhodamine images were acquired sequentially using 405, 488, 488 and 561 laser lines, and emission detection ranges 415-480 nm, 500-550 nm, 480-500 nm, and 571-625 nm, respectively, with the confocal pinhole set at 1 Airy units. Bright field transmitted light images were acquired simultaneously.

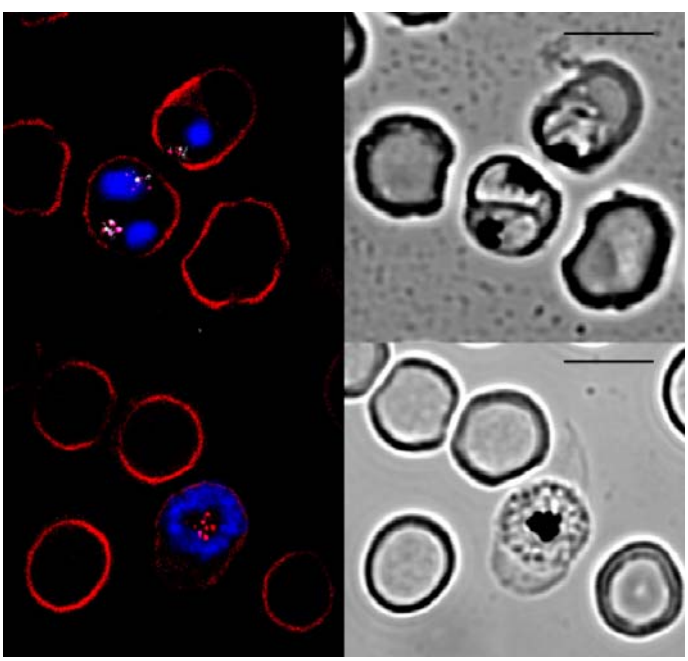

Figure 26. Confocal fluorescence microscopy study of the specific interaction and internalization in pRBCs of dendrimers A (upper images) and B (bottom images) encapsulating rhodamine. Fluorescence images (left) and bright field images (right). Color code: RBC membranes (red), *Plasmodium* nuclei (blue), hemozoin (parasite pigment) is shown in pink and rhodamine fluorescence in white. Scale bar: 5 µm.

Results obtained with dendrimers A and B encapsulating rhodamine are shown in Figure 26. A-rho ranged in size between 50 and 400 nm. When pRBCs were incubated with dendrimer A-rho, the fluorescence of rhodamine was detected inside pRBCs near the pigment of the parasite. Goodyer et al[193], using a variety of latex beads, showed that macromolecules up to 50-80 nm in diameter could have a direct access to the intracellular *Plasmodium* parasites. The fluorescence of dendrimer B-rho could not be detected by confocal microscopy. B-rho dendrimers are bigger, ranging in size between 90 and 120 nm, dimensions above the upper limit previously reported for internalization.

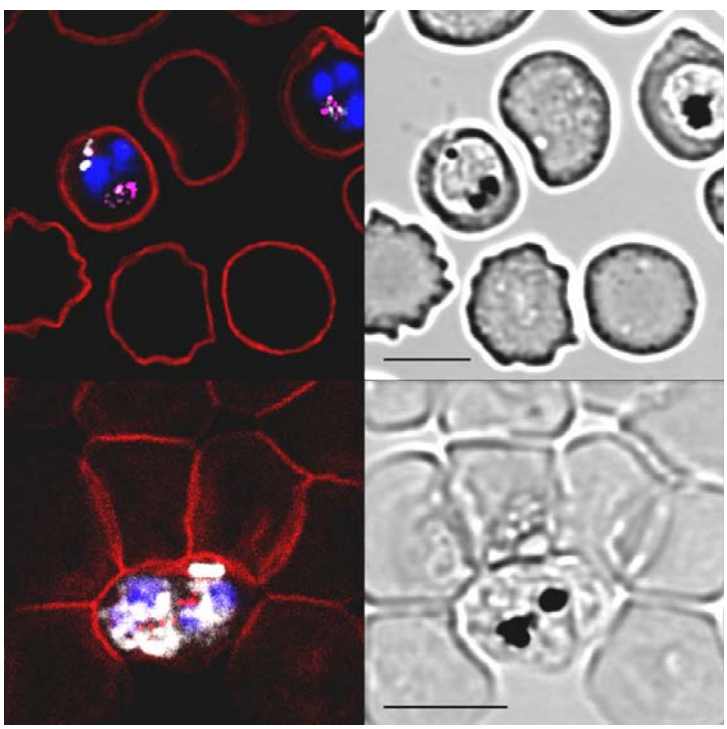

Figure 27. Confocal fluorescence microscopy study of the specific interaction and internalization in pRBCs of dendritic derivatives C (upper images) and D (bottom images) encapsulating rhodamine. Fluorescence images (left) and bright field images (right). Color code: RBC membranes (red), *Plasmodium* nuclei (blue), hemozoin (parasite pigment) is shown in pink and rhodamine fluorescence in white. Scale bar: 5 μm.

Dendritic derivatives C and D encapsulating rhodamine are smaller, with an average size of 80 nm for C-rho and 50 nm for D-rho. C-rho can be internalized, but the highest internalization is seen with the smaller dendrimer D-rho (Figure 27), which in addition presents primary amino groups that would favor the interaction with cell membranes. The fluorescence of C-rho polymer is observed next to hemozoin deposits and is less intense whereas in the case of D-rho, the fluorescent pattern is distributed thoughout the cytoplasm of the parasite (Figure 28). The specificity towards pRBCs of D-rho could also explain the good performance in growth inhibition assays of this derivative when encapsulating chloroquine.

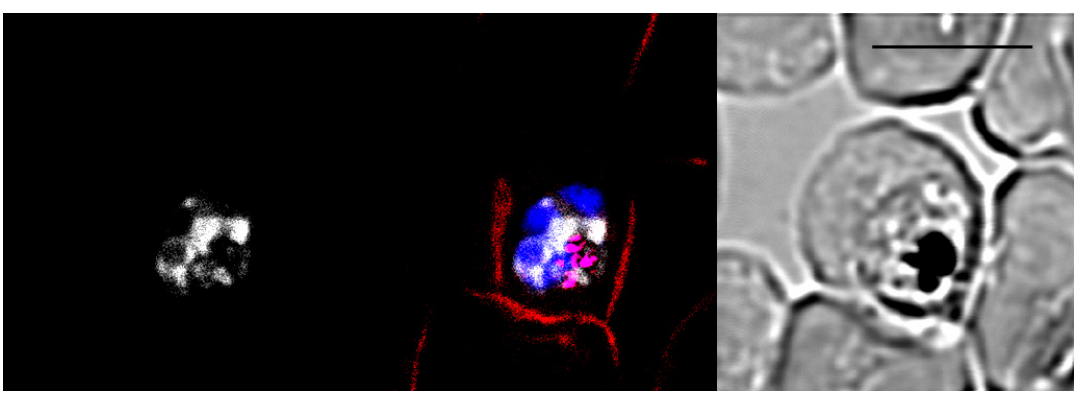

Figure 28. Confocal fluorescence microscopy study of the subcellular localization of D-rho derivatives in pRBCs. Color code: RBC membranes (red), *Plasmodium* nuclei (blue), hemozoin (parasite pigment) is shown in pink and rhodamine fluorescence in white. Scale bar: 5 μm.

Taken all together, the results indicate that dendritic derivatives A, C and D are the best candidates for the targeted delivery of antimalarials because they can release their cargo selectively into pRBCs. At the concentrations required for CQ and PQ exhibit good antimalarial activity, the polymers are neither cytotoxic nor hemolytic. Pluronic® derivatives C-PQ and D-CQ present higher activity against the parasite *in vitro* than free drugs when the hydrophilic drugs PQ and CQ are encapsulated in nano-objects formed by these nanocarriers. Interestingly, derivatives with higher activity than free drugs have an aspect ratio closer to 1 (corresponding to a more spherical shape). It has been shown

that the shape of the nanoparticles influences their targeting ability, internalization capacity and degradation to release therapeutic drug[202,203], demonstrating the complexity of the interactions between nanoparticles and cells. Hydrophobic antimalarials, such as artemether or lumefantrin, could be encapsulated inside dendritic derivatives in order to exploit the solubility enhancement property of polymeric carriers. As a next step, we propose *in vivo* experiments with C-PQ and D-CQ in order to study if *in vitro* results could be improved due to polymer protection of their encapsulated drugs from fast degradation in the physiological environment and to a progressive and temporally expanded drug release.

DISCUSSION

Malaria is one of the main medical concerns worldwide because of the number of people affected, the severity of the disease, and the complexity of the life cycle of its causative agent, the protist *Plasmodium*. Strategies used until now include fighting the mosquito vector with insecticides, distributing mosquito nets, desiccating paludic areas, using drugs against the parasite, and developing vaccination approaches; none of these strategies has been capable yet of claiming victory and there is a wide consensus that, with the currently available tools, it is unlikely that malaria will be eradicated. The future of malaria control and eradication depends on a very large extent on sustained financial investments and efforts, efficient health systems, and on the outcomes of research to produce a steady pipeline of new and improved tools to fight the disease. Malaria represents the paradigm of the vicious circle of disease and poverty and highlights the critical role of research as a strategic component of international cooperation. Recent efforts in research have been dedicated in particular to the development of efficient vaccines and to the discovery of new antimalarial drugs. However, investigating new delivery methods for currently used drugs is cheaper than developing new ones.

One of the main drawbacks of conventional malaria chemotherapy is the nonspecificity of most antimalarials. Commonly used formulations provide an immediate release of the drug, which ends up in the blood stream where it can be taken up by any cell, diseased or not, resulting in loss of drug efficacy (Figure 29). Consequently, the current way to achieve therapeutic levels that extend over time is using a high initial concentration of the drug, often adjusted to stay just below known levels of toxicity, that gradually diminish over time to an ineffective concentration. This peak and valley delivery is known to cause toxic side effects and, in consequence, low overall doses are generally administered to minimize this undesirable scenario. In the case of malaria treatment this approach has a significant drawback, because it risks to deliver a dose that is sublethal for the parasite population, which would favor the appearance of resistant *Plasmodium* strains. In this way, resistance to chloroquine has spread to the vast majority of

malaria endemic areas rendering this drug increasingly ineffective, and emerging resistance has been reported even to the highly effective artemisinin-based combination therapies. Thus, any new drug will always be exposed to efficacy loss due to resistance development, unless lethal doses can be delivered directly to the parasite.

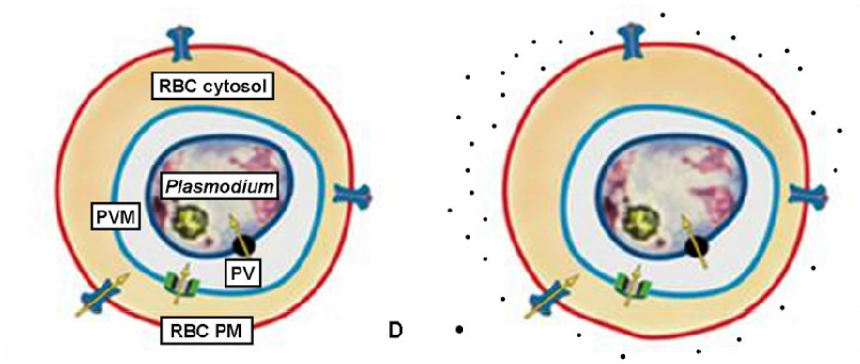

Figure 29. Scheme of a RBC infected by *Plasmodium* (left). Currently available strategy for antimalarial drug delivery where the drugs are free in the plasma. RBC drug intake is usually poor in this situation (right). Plasma membrane (PM).

Nanomedicine is a rapidly evolving area of science that aims at providing advances in drug discovery and delivery, as well as in the continued miniaturization of analytical and diagnostic procedures. Recent progress in drug delivery deals with the development of nanometer-sized targeted delivery systems for therapeutic agents. In the case of malaria, targeted drug delivery strategies would allow the increase of the bioavailability of antimalarial drugs, permiting the administration of localized doses that are sufficiently high to be lethal to the parasite but innocuous for the patient, representing a turning point in the search for a safe and effective treatment of the disease, with a minimized risk of resistance onset. The availability of such a delivery system, capable of delivering locally high (overall low) doses of antimalarials to pRBCs would be an important element in a coordinated global strategy addressed to eradicate malaria.

The work presented in this PhD thesis has as main objective the development of an innovative nanovector for improving the efficacy of existing antimalarial drugs

and the understanding of the role and the importance of the main nanovector design parameters that determine the ultimate nanocarrier performance. This research constitutes the first qualitative and quantitative study at the cellular and subcellular level of the performance of liposomes and polymers specifically targeted to *P. falciparum*-infected RBCs, and demonstrates the feasibility of constructing a carrier able to completely discriminate RBCs from pRBCs, and of releasing its contents into the latter.

Understanding at the cellular and molecular level why nanovectors have a good performance or not is one of the main points of this thesis. Previous published works on drug delivery of antimalarials are mainly focused on the synthesis of different types of nanocapsules, the study of the pharmacokinetic properties of these vectors and, especially in the case of liposomes, the assessment of the *in vivo* efficacy without previous studies of the interaction of these nanovectors with pRBCs *in vitro*. We have adopted a rational design approach, where we have made an effort to characterize the key elements that control nanovector efficacy in terms of specificity towards target cells, capacity of drug release and study of the *in vitro* efficacy; the information obtained from these experiments enters a feed-back process for the establishment of the best strategies and the engineering of candidate nanovectors that would be selected for *in vivo* assays.

This work has been divided in 3 main phases:

Phase 1 – Prototype design and initial development

Preparation of immunoliposomes and characterization of their targeting towards pRBCs and content release. In this phase we tested different antibodies for their ability to bind pRBCs, selected the commercial antibody BM1234 for the functionalization of liposomes, and studied the targeting of immunoliposomes and the delivery of liposomal cargo inside pRBCs.

Phase 2 – Test of the performance of the immunoliposomal nanovector as antimalarial drug carrier *in vitro* and *in vivo*

Immunoliposomes encapsulating chloroquine or fosmidomycin were assayed for

their ability to inhibit the growth of *P. falciparum* in comparison to free drugs *in vitro*. In order to obtain the best performance of the prototype nanovector, several parameters were adjusted in the design of the liposomes and the experimental protocols. The efficacy of liposomal nanocarriers was also tested *in vivo*, in *P. yoelii* and *P. falciparum*-infected mice.

Phase 3 – Evolution and refinement of the immunoliposome prototype

One of the approaches used in order to deal with the drawbacks of the immunoliposomal model was testing polymers as drug delivery systems. Two of the polymers synthesized presented specific targeting towards pRBCs, constituting promising candidates for the targeted delivery of antimalarials. Polymers were conjugated to chloroquine or primaquine and tested *in vitro* and *in vivo* for their efficacy vs soluble drugs. We have also explored the use of other specific pRBC-binding molecules and propose the use of heparin as an alternative to antibodies for pRBC targeting purposes.

We started from the abstract concept of a *Russian doll nanovector*, which consisted of an immunoliposomal capsule targeted with specific antibodies to *Plasmodium*-infected red blood cells, containing biodegradable dendrimers or polymeric nanoparticles encapsulating compounds with antimalarial activity (Figure 30). This first theoretical prototype was conceived deliberately as a complex model, with several different elements that could be either assembled to obtain a highly specific and efficacious nanovector, or discarded if preliminary data indicated that some of them were superfluous or were not adding a quantitative value. The sought-after nanovector for malaria therapy should achieve maximum efficacy with minimal complexity in order to reduce costs and gain commercial feasibility. Immunoliposomes were chosen for the delivery of their cargo to the RBC cytosol through membrane fusion and the selected size was 200 nm because it had been described as optimal size for increased blood residence times. Dendrimers and polymeric nanoparticles, with a very scarce application in the drug delivery of antimalarials, represented innovative nanocarriers full of potential. If required, dendrimers or polymers could be coupled to specific

antibodies or cell penetrating peptides, which are interesting targeting agents for nanoparticle functionalization due to their ability to translocate across cellular membranes, in order to deliver the drug inside the PV.

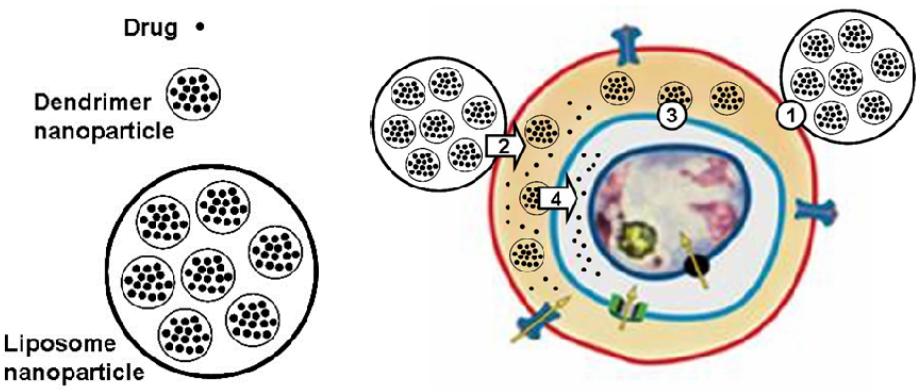

Figure 30. Cartoon depicting the *Russian doll* targeted drug delivery strategy. The four basic steps are (1) specific *Plasmodium*-infected RBC recognition and docking of liposomes to the pRBC plasma membrane, (2) membrane fusion and liberation into the pRBC cytosol of liposome-encapsulated polymers/dendrimers carrying the antimalarial drug, (3) specific PVM recognition and docking of polymers/dendrimers, and (4) liberation of drug in the pRBC cytosol and inside the PV.

Our research began with the preparation of immunoliposomes, where the choice of the proper antibody is a key element for the discrimination between pRBCs and RBCs. For this purpose, we made polyclonal antibodies raised in rabbits against certain regions of the anion transporter band 3 protein (Article 1, Supplementary data, Fig. S1), which had been described as good pRBC markers. It had been reported that infection by *P. falciparum* causes structural modifications to band 3 protein[204] that can be recognized using specific antibodies, binding specifically to pRBCs but not to RBCs. Although our polyclonal antibodies bound preferentially pRBCs, a significant background fluorescence was observed for RBCs, indicating a certain level of unspecific binding. For this reason we searched commercially available monoclonal antibodies prepared using as immunogen *P. falciparum* fractions, and after a first screening using fluorescence microscopy, we selected BM1234 and BM1232 as candidates for the assembly of a prototype nanovector. In our hands, a *Plasmodium*-encoded antigen was more specific for the selective recognition of pRBCs than an endogenous RBC antigen which changes

conformation upon infection.

Immunofluorescence assays showed that BM1234 was highly specific for mature trophozoite- and schizont-infected RBCs, with a peripheral spotted pattern which is an essential requirement for targeting strategies. However, when pRBCs were fixed with acetone/methanol prior to immunocytochemistry, the fluorescence pattern of the antibody was observed to bind internal pRBC structures too. These could be regions in the endomembrane system built by *Plasmodium* that delineate the trafficking of the BM1234 antigen from its synthesis towards its final location in the pRBC plasma membrane, or could also correspond to internalization routes of externally exposed antigens. The preferential binding of BM1234 to pRBCs containing trophozoites and schizonts suggested a differential localization of the corresponding antigen throughout the intraerythrocytic cycle of *P. falciparum*. High-resolution confocal fluorescence microscopy studies revealed in early trophozoites a dominant spotted pattern, consistent with the binding to pRBC intracellular membranous structures termed Maurer's clefts, whereas in late trophozoites and especially in schizonts, BM1234 binds structures on the periphery of the pRBC. BM1234 recognized pRBCs infected with *P. falciparum* 3D7 and D10 strains, and this suggests that its epitope might be relatively conserved, an important factor for a widespread use of the nanovector and for a lasting efficacy before resistances appear within the parasite's distribution range. BM1232 reacted specifically with pRBCs infected by all forms of the parasite, likely binding to *Plasmodium* itself. BM1234 was selected for immunoliposome preparation, and BM1232 was kept as a backup antibody that could be used for the functionalization of polymers or dendrimers if a direct targeting of the parasite would be required to increase the performance of the nanovector.

Goodyer et al[193] provided evidence that macromolecules internalized in *P. falciparum* through the cytostome, via new permeation pathways induced by the parasite, are transported to the food vacuole and that this process starts earlier than previously estimated, being evident in late ring stage parasites. A second macromolecular transport pathway has been proposed, where macromolecules

and other membrane-impermeable compounds in the external medium could bypass the erythrocyte cytosol through a duct left as a remnant of merozoite invasion, whereby the erythrocyte membrane and the PVM would fuse prior to parasite internalization by a process resembling fluid-phase endocytosis[205]. Using a variety of latex beads, it was determined that molecules up to 50–80 nm in diameter can access intracellular parasites. This size exclusion is consistent with the dimensions of the parasitophorous duct pathway revealed by electron microscopy[193]. The existence of such an anomalous membrane, which becomes leaky prior to rupture[206], has been proposed as an explanation for the observed permeability of pRBCs to antibodies[207].

Whatever the antibody used, reducing its amount will contribute to minimizing the risk of triggering immune responses leading to nanovector elimination. Targeting specificity requires oriented antibody molecules able to recognize its antigen. Most generally used methods for the covalent immobilization of antibody molecules are through free primary amino groups and have the risk of chemically modifying functionally important amino acid residues in the antigen-binding region, ending up in a significant amount of defective antibody conjugates that would demand using higher antibody concentrations[208]. An alternative strategy for the oriented immobilization of antibodies is the preparation of immunoconjugates using the oligosaccharide moieties in the antibody Fc region which are distal from the antigen-binding region, but this involves oxidation steps and the use of heterobifunctional crosslinkers that make it a longer and more complex process[209]. We chose the fast and efficient strategy of functionalizing liposomes with half-antibodies. Half-antibodies can be obtained by treatment with 2-mercaptoethylamine, a mild reducing agent which cleaves the disulfide bridges in the Fc region by preserving the antigen binding site; the resulting free thiol groups can react with maleimide groups present in one of the lipids included in the liposomal formulation, leading to oriented antibodies able to bind target cells, as shown in Article 1.

In addition to specific docking, the planned antimalarial targeted drug delivery system required the release of the liposome cargo inside target cells. Covalently functionalized with specific half-antibodies against pRBCs liposomes were loaded with quantum dots and characterized by cryo-TEM. Variable numbers of quantum dots that were either associated with the membrane or free in the liposomal lumen were observed, with approximately half of the liposomes containing at least one quantum dot. Quantum dot-loaded immunoliposomes were added to living cultures of *P. falciparum*, where we have assessed the *in vitro* efficacy for the delivery of their contents exclusively to pRBCs using fluorescence microscopy[199]. In less than 90 minutes, targeted immunoliposomal nanovectors dock to pRBC plasma membranes and deliver their contents to 100% of mature trophozoite- and schizont-containing pRBCs and to 0% of non-infected RBCs. The almost exclusively peripheral BM1234 localization and the homogeneous intracellular quantum dot fluorescence are in agreement with a process of liposome fusion and delivery of its contents inside the cell. When incubating immunoliposomes with co-cultures of pRBCs and endothelial cells, the latter do not interfere significantly with the delivery of quantum dots into pRBCs after 90 minutes of incubation. Endothelial cells forming the walls of blood vessels are by far, due to their large numbers, the main competitor of pRBCs (after RBCs) to incorporate liposomal contents. This result indicates that immunoliposomes will quantitatively deliver the encapsulated drug to pRBCs and not to other cell types.

Liposomes docked to pRBCs do no seem to be internalized, but to fuse with the erythrocyte plasma membrane and deliver their contents inside the cell. The capacity of liposomes to inject their cargo into pRBCs could presumably have its basis on alterations of the pRBC plasma membrane after malaria infection. Since erythrocytes have limited biosynthetic capabilities, the generation and regulation of pathways responsible for molecular transport in malaria-infected erythrocytes are probably under parasite control. As the parasite matures, the RBC membrane suffers a profound increase in permeability to a wide range of low-molecular mass solutes[210] and becomes less elastic, thus limiting the rebounding of randomly colliding liposomes. The resulting slightly longer interactions, a phenomenon that

is intensified if targeting antibodies are present, could allow enough time for the physical phenomenon of lipid bilayer fusion to occur. This hypothesis could also explain why liposomes devoid of antibody can deliver their contents inside pRBCs and do perform better when added at trophozoite stage, since the membrane of ring-containing pRBCs is more similar to uninfected erythrocytes than that of pRBCs infected by later forms.

Pharmacokinetics results obtained in our group indicate that 95% of administered immunoliposomes are present in the blood 90 minutes after intravenous injection in mice and that about 15% of the initial dose is still circulating 24 h later. Because less than 90 minutes are required to achieve 100% targeting specificity *in vitro*, immunoliposomes *in vivo* were expected to dock pRBCs and deliver encapsulated antimalarials, even in the presence of other cell types, before being cleared from blood by macrophages or spleen filtration. These results open good perspectives regarding the development of an immunoliposomal nanovector for the specific drug delivery to *Plasmodium*-parasitized cells without containing additional subcellular targeting or encapsulating elements. Thus, with the aim of designing the simplest working model, we decided to incorporate antimalarial drugs into the immunoliposomal nanocapsule and to study the efficacy of the nanovector vs free drugs *in vitro*. However, the nanoparticulate nature of quantum dots suggest that immunoliposomes could also be used for the delivery of smaller nanoparticles targeted to intracellular pRBC specific sites. Thus, a generation of *Trojan horse* prototypes can be envisaged where, if required, different types of antimalarial drug-containing polymeric nanoparticles can be delivered to specific organelles inside pRBCs.

Chloroquine and fosmidomycin were chosen as model drugs for encapsulation experiments in immunoliposomes. Both drugs are hydrophilic, are contained in the liposome lumen and have very different IC_{50} values, which would allow testing the prototype with drugs in the nano- and micromolar concentration range. CQ has been the gold standard for the treatment of malaria for many years, but nowadays CQ resistance has spread to the vast majority of malaria-endemic areas,

rendering this drug increasingly ineffective. Fosmidomycin has been proven to be efficacious in the treatment of *P. falciparum* malaria by inhibiting 1-deoxy-D-xylulose-5-phosphate reductoisomerase, an enzyme of the non-mevalonate pathway, which is absent in humans. The discovery of the non-mevalonate pathway in malaria parasites has indicated the use of fosmidomycin and other such inhibitors as very specific antimalarial drugs.

Chloroquine or fosmidomycin were incorporated during the hydration phase of liposome synthesis. BM1234 half-antibodies were used for immunoliposome preparation and the activity of free drugs and of their liposomal and immunoliposomal formulations was tested *in vitro* in *P. falciparum* growth inhibition assays. In preliminary experiments, chloroquine showed improved efficacy as an antimalarial when delivered inside targeted immunoliposomes. However, difficulties in determining the exact concentration of the drug with spectrophotometric techniques due to the low amount of compound in the sample prevented an accurate estimation of the nanovector performance. In order to assess the efficacy of any drug delivery system is fundamental to compare the same dose of soluble and encapsulated drug, so we recommend the establishment of a reliable method, like HPLC-MS/MS, to quantify the amount of drug contained in the nanovector.

The targeting antibody BM1234 has high specificity for pRBCs infected by trophozoite and schizont forms, but it does not bind significantly to ring-stage pRBCs. For this reason, we speculated that BM1234 immunoliposomes containing chloroquine or fosmidomycin would have a higher efficacy if administered to trophozoites rather than to rings[197]. In a classical *Plasmodium* growth inhibition assay, the drug is added at the ring stage, and after 48 h of incubation throughout a complete erythrocytic cycle, parasitemia is determined. We have also assayed the addition of targeted nanovectors at the trophozoite stage (24 h later than in the standard protocol), determining parasitemia by FACS analysis and Giemsa-stained blood smears after a further 48 h of incubation. The best results have been obtained with immunoliposomes administered at the

trophozoite stage. On average, encapsulation in immunoliposomes as described here improves drug efficacy by an order of magnitude: similar drug amounts kill 10 times more parasites if encapsulated, reducing the IC_{50} of the antimalarial drugs at least 10-fold. When added at the trophozoite stage, 20 nM soluble chloroquine kills 28.1 ± 0.6% of parasites vs 26.5 ± 0.5% for the immunoliposome-encapsulated drug at 1.6 nM final concentration. This good performance suggests that the complexity of the original *Russian doll* prototype will not be required, and that immunoliposomes themselves are strong candidates for the treatment of malaria, deserving further studies and *in vivo* testing.

The efficacy of the nanovector is particularly relevant in the case of chloroquine, which has an endogenous carrier across human erythrocyte membranes that accumulates the drug selectively in these cells[211]. Chloroquine is accumulated in the digestive vacuole of the parasite, where it interferes with the polymerization of the toxic heme monomers resulting from hemoglobin digestion, leading to parasite death by heme poisoning. CQ-resistant *Plasmodium* strains accumulate fewer amounts of drug due to mutations on CQ transporters present in the digestive vacuole[83]. Under continued drug exposure, resistant strains become dominant over time. CQ transporters could be probably bypassed by drugs encapsulated in nanovectors, which would give an alternative route of internalization for drugs, such as membrane fusion[212]. Alternatively, nanocarriers containing antisense nucleotides that inhibit the expression of CQ-resistance phenotype of membrane transporters could be designed.

Since the role of targeting antibodies is most likely anchoring liposomes to pRBCs when a random collision occurs, the *in vitro* efficacy of these drug delivery systems can foreseeingly be increased by incorporating more antibodies on their surfaces. As shown in Article 2, increasing the antibody concentration on immunoliposomes containing chloroquine results in a corresponding significant increase of nanovector performance, reaching a clearance of 50% parasitemia for liposomes functionalized with an estimated number of 250 antibody molecules vs 10% of that activity for the same amount of free chloroquine. Keeping the antibody

concentration as low as possible will contribute to reduce the immune response towards plasma-circulating immunoliposomes, even if camouflage elements such as PEG are used. We expect that the turbulent mixing in the bloodstream will facilitate random encounters between liposomes and pRBCs, permitting the use of low targeting antibody amounts. Thus, when designing *in vivo* assays, a balance has to be reached between a sufficiently high density of targeting antibody for efficient drug delivery and levels below those triggering fast lymphocyte uptake. We expected to approach 100% of parasitemia reduction when using the immunoliposomal prototype in a murine model for *P. falciparum* malaria.

These findings open perspectives for the use in antimalarial therapy of already existing drugs that are not being tested because of their high toxicity and/or elevated unspecificity. If these drugs were correctly delivered to targeted cells, the interaction with other cell types would be minimized and the required effective dose of these compounds would be lower, making possible their use in malaria therapy or for the treatment of other diseases. When administered inside nanocapsules, halofantrine presented a reduced cardiotoxic profile when compared to the free drug at the same high doses[213], probably due a modification in drug distribution. Such reduction in side effects represents a potential interest in the future production of safer intravenous malaria treatments. Our immunoliposomal prototype could also be an interesting tool for the delivery of antimalarials that present a promising activity *in silico* but which are inactive when tested *in vitro* or *in vivo* because they can not cross the pRBC membrane and reach the parasite in order to carry out their action. If these compounds were encapsulated inside immunoliposomes, they could be specifically delivered inside pRBCs and would not be discarded for malaria therapy.

The immunoliposomal prototype described here is restricted to the recognition of RBCs infected by trophozoites and schizonts due to the specificity of the antibody chosen for targeting. This limits its potential use as antimalarial encapsulating device to an administration timed to the phase of *Plasmodium* intraerythrocytic cycle when late forms are present. Structural changes in pRBCs and the resulting

increase in adhesiveness are major contributors to the virulence of *P. falciparum* malaria[214]. Owing to the increased adhesiveness, RBCs infected with late stages of *P. falciparum* (during the second half of the 48 hour life cycle) adhere to the capillary and postcapillary venular endothelium in the deep microvasculature and sequester in various organs such as the heart, lung, brain, liver, kidney, intestines, adipose tissue, subcutaneous tissues, and placenta[215]. Sequestration of the growing *P. falciparum* parasites in these tissues provides them the microaerophilic venous environment that is better suited for their maturation and allows them to escape splenic clearance and to better hide from the immune system. These factors help *Plasmodium* to undergo unbridled multiplication, thereby increasing the parasite load to very high numbers. Due to sequestration of the growing parasites, only the ring and early trophozoite stages of *P. falciparum* are found in circulation in the peripheral blood, while the more mature trophozoites and schizonts are bound in the deep microvasculature. Whereas the BM1234 immunoliposomal prototype can target trophozoites in circulation, specific antibodies raised against the ring stage or against all intraerythrocytic forms will be required to cover a wider span of the blood cycle. Furthermore, the use of antibodies, the encapsulating structure and the antimalarial compound itself in chloroquine and fosmidomycin-containing immunoliposomes have characteristics that restrict their use to certain particular situations.

Antibodies used for liposome functionalization are a limitation for the application of targeted delivery systems to malaria therapy since proteins expressed in the pRBC membrane are highly variable, and antibodies are expensive and difficult to formulate for oral administration. *Plasmodium* presents a remarkable capacity for adaptating to its highly heterogeneous natural environment. Antigenic variation in the proteins displayed on the surface of the infected red blood cell is one of the adaptive mechanisms that the parasite uses to survive and transmit within a highly selective and ever-changing host environment. As the infection progresses, variant-specific antibodies against the expressed antigen are developed by the host and confer a competitive advantage to a new parasite variant. This variant rises in frequency until it, too, induces production of specific

antibody against itself, thus causing a diversifying selection[12]. Due to the high variability of antigens in the membrane of pRBCs, the good performance of an antibody-targeted nanovector can be compromised by the appearance of *Plasmodium* strains that are no longer recognized by the targeting antibody. Antibodies can be engineered to modify their binding site for continuous adaptation to antigen variability, and also to obtain the smallest region preserving an active antigen binding site which facilitates their formulation for oral administration[216]. Nanovectors targeted with these minimal antibody versions are more adequate to be formulated into nanoparticles up to 1000 nm, which are able to penetrate the intestinal mucosa and have been assayed for the oral delivery of insulin[119]. Some studies indicate that the continuity of parts of the *Plasmodium*-built endomembrane network with the pRBC plasma membrane seems to provide occasional access to certain intracellular antigens to the outside of the cell, thus antigens that are expressed preferentially in the endomembrane system of pRBCs might be adequate for extracellular recognition by specific antibodies in certain situations. Because these internal antigens are likely less prone to variation than externally exposed epitopes, they can be interesting candidates for targeted delivery strategies.

Although antibodies can be very useful as a proof of concept in order to test the efficacy of targeted liposomes encapsulating antimalarial drugs, their production process is relatively lengthy and costly. These two characteristics are an obstacle because, as mentioned above, most *Plasmodium*-encoded antigens useful in malaria therapy are highly variable and will most likely require a continued development of active targeting agents, which is an expensive process. A main limitation in the development of antimalarial agents is their cost, being the recommended limit price 1 USD per dose if a potential drug has to reach the malaria market. Commercial feasibility, which is governed by the cost of the components and the ease of manufacturing and scaling up, is one of the most desired characteristics of any novel drug delivery system. Our calculations indicate that a single dose of our best immunoliposomal prototype

able to eliminate 50% of the parasitemia from 1 l of blood would cost 50 €, which is far away from the 1 USD recommendation.

As an alternative to antibodies, we have investigated the use of other targeting molecules. In the 3rd article presented in this PhD thesis, specific binding of heparin to pRBCs infected by late forms of the *P. falciparum* 3D7 strain has been proved by fluorescence microscopy, FACS, and SMFS. Comparing the heparin-pRBC binding force between 28 and 46 pN obtained in this work with the antibody-antigen interaction values reported in the literature (ranging from 40 to 250 pN),[44-46] it can be suggested that low amounts of heparin as targeting molecule might be sufficient for future antimalarial-containing nanovectors, directed towards pRBCs with high specificity. Heparin binding specificity has already been explored in some studies; Ma and colleagues have used the heparin-binding domain of the protein neuregulin[217], showing that this domain may be a useful targeting vector for tissues that express and/or bind to this protein and that modifications in this sequence could modulate glycosaminoglycan and tissue-specific targeting specificity in many pathologies, including neurodegenerative diseases and cancers.

The use of DNA aptamers is at the moment under investigation in our group as another attractive alternative to antibody and peptide-based drug delivery systems. Aptamers present high affinity binding, selectivity, low immunogenicity, and can be conjugated to nanomaterials easily. Binding specificities and affinities comparable to those of monoclonal antibodies can be obtained with aptamers, but they can be produced much faster and cheaper and can be identified by *in vitro* selection against almost any target, including antigens which do not induce immune responses in host animals for antibody production[218]. As a result, this novel class of ligands is highly promising for the development of therapeutics, biotechnological tools and also for clinical diagnosis.

The administration route is also an important aspect to be considered when designing malaria therapies. The oral route is a first choice for uncomplicated malaria whereas our immunoliposomal nanovector is adequate for parenteral delivery, indicated in all patients with severe or complicated malaria, those at high risk of developing severe disease, or if the patient is vomiting and cannot take oral antimalarials. In these cases, malaria requires treatment in hospitals or health centres that have the refrigerating storage facilities required to preserve liposomes for long periods. Parenteral treatment in the form of a vaccine or of targeted liposomal delivery can be a useful weapon for the *last mile* in a malaria eradication strategy, using single-dose, individualized administration of highly toxic drugs specifically targeted to pRBCs with good accuracy with the objective of eliminating remaining multiresistant strains.

Liposomes and whole antibodies are difficult to formulate for oral administration, but nanosystems adequate for this administration route would be a valuable contribution to malaria treatment in endemic areas far from health centres. During the last part of this thesis we have focused on the development of new and innovative polymeric nanovectors for antimalarial drugs capable of selectively delivering them to pRBCs. As antimalarial drug delivery systems, polymeric nanoparticles provide several advantages over liposomes, prominent among them their capability to be more easily formulated for oral administration. We have focused our research on three polymers from the polyamidoamine family: ISA23, ISA1 and AGMA1. ISA23 is a prevailingly anionic amphoteric PAA, ISA 1 is cationic and the peptidomimetic AGMA1 is amphoteric and shows a strong structural resemblance to the RGD sequence, known to play a role in integrin-mediated adhesion to the extracellular matrix.

The observation that PAAs can target pRBCs infected by different species of *Plasmodium* and that AGMA1 pRBC binding and antimalarial activity increase with polymer size suggest that the underlying mechanism of targeting is likely to be based on multiple low affinity interactions, perhaps of electrostatic nature, over a large area. If this was the case, the evolution of parasite strains that are

no longer recognized by polymers would take longer, because the parasite would probably need to modify the structure of a large antigenic area. The development of a system without a classical targeting element such as a peptide or an antibody was not considered in our first prototype design but confers important advantages in key aspects previously discussed such as cost, stability and ease for oral formulation of the nanovector. The preliminary results obtained indicated that polymers could target and release their cargo into pRBCs, but experiments with polymers containing antimalarials were required in order to assess the potential of these promising nanocarriers.

ISA23 and AGMA1 were conjugated to primaquine and chloroquine via covalent and non-covalent interactions. The *in vitro* activity of encapsulated CQ was modest in comparison with its *in vivo* performance; this result could be explained because the random encounters between pRBCs and polymers required for targeting specificity are favored by the turbulent mixing in the blood circulation. *In vitro*, good PAA-mediated targeting might cancel out with slow drug release from the polymers, resulting in no clear increase in encapsulated drug efficacy *vs.* its free form. Our *in vitro* experiments indicate that the highest increase of CQ activity is observed when it is encapsulated inside immunoliposomes, suggesting that the delivery of a larger amount of drug as a single dose to the pRBC seems to be better than delivery of the same amount as many small doses, as in the case of polymers. However, chloroquine encapsulated in AGMA1 and ISA23 cured all *P. yoelii*-infected mice treated and eliminated parasitemia from the animals, when the same amount of free drug was unable to cure the animals. It is likely that a significant part of the increase in drug efficacy provided by its encapsulation comes from the specific targeting of the polymers towards and penetration into pRBCs, since the concentrations of AGMA1 and ISA23 used for *in vitro* and *in vivo* tests are way below their IC_{50}. The specific cell targeting observed for AGMA1 and ISA23 in both *P. yoelii* and *P. falciparum* and the presence of highly functional groups in the polymers offers good perspectives regarding an ample activity of PAA-derived polymers against different *Plasmodium* species encapsulating different antimalarials.

Dendrimers are also interesting candidates for the targeted drug delivery of antimalarials. Results obtained in collaboration with the Instituto de Nanociencia de Aragón indicate that Pluronic® derivatives present intrinsic antimalarial activity and specific targeting towards pRBCs. Dendrimers encapsulating CQ and PQ showed an increased activity of the drugs depending on the dendrimer used and *in vivo* experiments are needed to fully characterize the potential of these promising carriers for malaria treatment. But dendrimers are more expensive and difficult to synthesize than polymers.

A balance between complexity, efficacy, and cost is necessary to obtain the simplest and cheapest system capable of significantly reducing or eliminating detectable parasitemia in people living in malaria-endemic areas. Optimization and design of a sufficiently cheap (≤1€/dose) and stable nanovector (≥50% of original activity after ≥1 month at 37°C would be a minimal requirement) that can be used as treatment for uncomplicated malaria in rural areas lacking health care centres is a must for a realistic therapy intended to treat malaria. The commercial feasibility of any delivery system is governed by the cost of its component elements and the ease of manufacturing and scale up, because malaria medicines have to be deployed in low per capita income areas.

Considering these facts, in the case of synthetic PAA polymers the scenario is promising, as they are made of easily available and cheap materials and polymerization is simple and scalable. Furthermore, PAAs do not need to be functionalized with specific antibodies to target pRBCs, which entails that the cost of the product will be reduced and that its shelf-live will be increased and no refrigeration facilities will be required in order to storage the nanovector. According to the *in vivo* data presented here, a complete elimination of *P. yoelii* parasitemia from 1 l of blood could be achieved with four intraperitoneal doses of CQ-encapsulating AGMA1, for a total cost of 40 cents, a figure likely to be cut down for batch sizes larger than 1 kg, whose current synthesis cost is 9 €/g and that is comparable to the cost of chloroquine treatment.

However, polymer prototype has some limitations that should be considered in order to obtain the sought after nanovector. The synthesis of larger polymeric nanoparticles, of ca. 100 nm would permit the delivery of larger amounts of drug to a single cell, increasing the activity of the encapsulated drugs and would also avoid renal filtration (which affects small nanoparticles), resulting in an increased blood residence time *in vivo*. An important experiment that we are performing at the moment is the study of the oral bioability of PAAs containing CQ. If orally administered PAAs-CQ were active against the parasite it would mean that they are stable enough to tolerate the acidic pH of the stomach, cross the intestinal barrier to the blood, and reach and enter the target cells in order to exert their action.

Orally available polymers would be our most promising candidates for the treatment of uncomplicated malaria in rural areas from endemic countries, which are far away from hospitals and would be the starting point for the improvement in future prototypes, however results obtained with liposomes encourage their use for the treatment of complicated malaria, which requires parenteral administration of drugs and the hospitalization of the patient. Another potential use of targeted immunoliposomes is vaccine development, where encapsulation of poorly immunogenic peptides liposomes has been reported as a successful adjuvant strategy in humans for inducing high levels of specific antibody production with strong antigen-specific T-cell responses for adequate protection [219,220].

Immunoliposomes present higher activity when incubated with late stages of the parasite, and that would be the optimal scenario for nanovector administration. Even if monitorization of the cycle of the parasite would be possible in order to choose the best moment to treat malaria, it would be tedious and inconvenient for malaria endemic countries. In order to overcome this limitation, we propose the functionalization of liposomes with targeting molecules that recognize all stages of the parasite, and if possible, different species of *Plasmodium*. Liposomes encapsulating primaquine would be useful for the treatment of *P. vivax* infections because liposomes without a PEG coating accumulate in the

liver and could eliminate latent hypnozoites in order to achieve a complete cure of malaria. Primaquine kills mature *P. falciparum* gametocytes and hypnozoites of *P. vivax* and *P. ovale* and had been included previously in mass drug administration programmes, but serious haemolytic anaemia in areas with high levels of glucose-6 phosphate dehydrogenase deficiency has limited the use of this drug. If encapsulated inside targeted nanovectors we expect to use lower drug amounts that currently used, that would be innocuous for all the patients.

When evaluating the potential of nanovectors, we have to keep in mind that we have chosen the worst possible context for the performance of the nanovector: the asexual phase of the parasite is the point of the cycle of *Plasmodium* in humans with more infected cells (up to 10^{11} pRBCs) and most of our experiments have been performed with chloroquine, which has been for many years the gold standard for malaria treatment due to its high efficacy against the parasite. We propose the development of nanovectors targeting bottleneck stages such as gametocytes, which are present in the blood in small numbers. Gametocyte-targeted delivery systems containing primaquine could reach pRBCs and eliminate this phase of the parasite, blocking malaria passage to the mosquito and protecting the population by preventing onward transmission of infection. New drugs, with limited efficacy, could be tested inside nanovectors in order to benefit from the advantages of targeted drug delivery, as previously discussed. At the moment, our group is working on the encapsulation of different commercial antimalarials, either hydrophilic or lipophilic, in order to optimize the use of compounds with different properties and on the increase of the amount of drug in the prototypes for the obtention 100% efficacy either *in vitro* or *in vivo*.

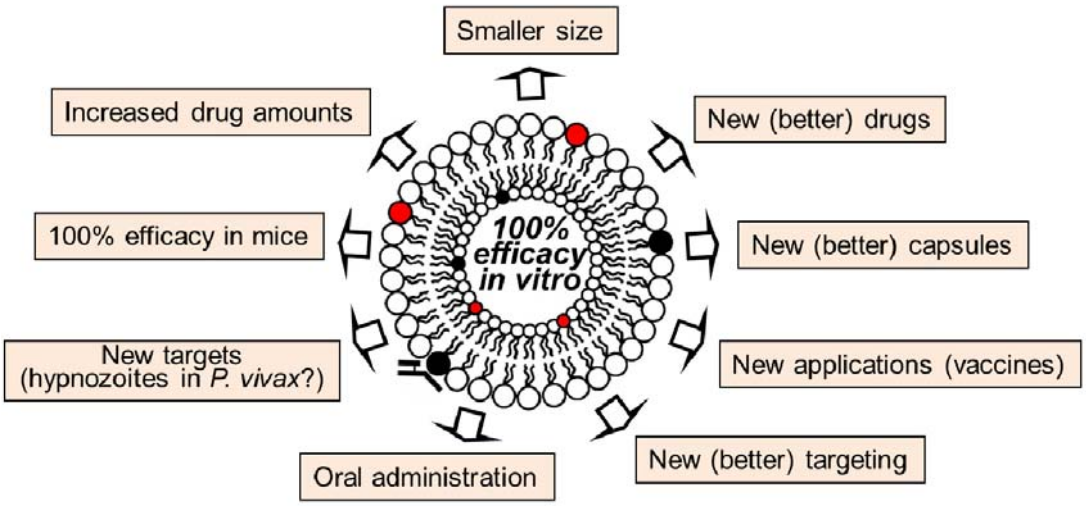

Figure 31. Scheme that summarizes the limitations and future perspectives of immunoliposomal prototype.

The different parts of future nanocarriers (targeting molecule, lipid formulation, external coating, and containing drug) must be so that they can be substituted by new elements, to assemble nanovessels tailored to fit the specificity of different encapsulated antimalarial agents and the delivery to different *Plasmodium* species or intracellular targets. This ***Lego-like* nanovectors** technology, with exchangeable components, can foreseeingly be also applied to the targeted drug delivery of compounds for the treatment of a wide array of diseases triggered by intracellular parasites such as viruses, protozoans, and bacteria, including hepatitis, leishmaniasis, listeriosis, or tuberculosis, among many others and opens promising perspectives for a new generation of nanomedicines.

Most of the advances in the field of nanomedicine are mainly related to pathologies such as cancer and Alzheimer's. Nanomedicine should not only be associated to expensive treatments. Diseases of poverty, like malaria, also deserve the attention of nanomedicine for the development of effective, cheap and affordable drug delivery systems.

CONCLUSIONS

1. Targeted immunoliposomal nanovectors deliver their contents to 100% pRBCs and to 0% non-infected RBCs in less than 90 minutes even in the presence of other cell types.

2. Immunoliposomes encapsulating antimalarial drugs have been shown to increase 10-fold the activity of free drugs *in vitro*.

3. Heparin has been demonstrated to have strong binding and highly specific targeting towards pRBCs infected by late stages vs non-infected RBCs.

4. New polymeric nanovectors which target specifically pRBCs in the absence of antibodies have been synthesized. Polymers have been successfully conjugated to the antimalarial drugs chloroquine and primaquine.

5. *In vivo* experiments show that AGMA1 and ISA23 polymers containing chloroquine can cure P. *yoelii*-infected mice whereas animals treated with the same dose of free drug die.

6. Preliminary *in vitro* data suggest that Pluronic® derivatives are a promising type of nanocarriers for the targeted delivery of antimalarials.

ANNEX I: RESUMEN

INTRODUCCIÓN

Malaria y *Plasmodium*

La malaria o paludismo es la enfermedad infecciosa que produce mayor mortalidad, morbilidad, e impacto socio-económico en la población humana. Actualmente alrededor de la mitad de la población mundial vive en zonas de riesgo de infección, que se distribuyen mayoritariamente en las regiones tropicales y subtropicales del planeta. Cada año se diagnostican alrededor de 250 millones de casos de malaria en todo el mundo y se contabilizan casi un millón de muertes, principalmente en niños menores de 5 años y mujeres embarazadas[1]. Esta enfermedad es la principal causa de muerte en los países más pobres del mundo, especialmente en África, sudeste asiático y Latinoamérica. Como consecuencia de la aparición de resistencia de los parásitos frente a los distintos fármacos que se utilizan para su tratamiento, esta enfermedad ha resurgido recientemente en zonas donde se había erradicado, lo que pone de manifiesto las dificultades que existen para el control de la misma.

La malaria se produce por un parásito protozoario del género *Plasmodium* que se transmite mediante la picadura de mosquitos hembra de algunas especies del género *Anopheles,* que han sido previamente infectadas[11]. De las especies de *Plasmodium* conocidas, solamente cuatro son capaces de infectar al hombre: *P. vivax, P. malariae, P. ovale* y *P. falciparum*. Recientemente se ha descubierto que *P. knowlesi*, una especie que infecta simios del sudeste asiático, es también patógena para humanos. *P. falciparum* es el más letal y causa los casos más severos, predominando en África. *P. vivax* produce malaria no severa, pero está más diseminado y presenta formas latentes en el hígado, los llamados hipnozoítos, que pueden reactivarse incluso cuando el sujeto ha abandonado el área con riesgo de malaria. De manera que para conseguir curar totalmente la enfermedad es fundamental tratar con fármacos específicos contra estas fases del parásito.

La malaria presenta un amplio abanico de manifestaciones clínicas. Los niños menores de 5 años, las mujeres embarazadas y los viajeros procedentes de zonas no endémicas son los más susceptibles de presentar las formas graves de la misma y sufrir sus complicaciones. La sintomatología clínica puede incluir fiebre, escalofríos y anemia; pero cuando la enfermedad es grave puede generar delirio, acidosis metabólica, anemia severa, malaria cerebral, afección de múltiples órganos, coma y finalmente la muerte.

La problemática de la malaria se ha acentuado en los últimos años debido a la creciente resistencia tanto de cepas de *Plasmodium* a los fármacos convencionalmente utilizados en su tratamiento como de los mosquitos vectores a los insecticidas. El complejo ciclo biológico de *Plasmodium* y su elevada variabilidad antigénica le permite unos extraordinarios mecanismos de evasión del sistema inmunitario[12], factores que dificultan la obtención de una vacuna eficaz en el 100% de los casos. Los hallazgos obtenidos a partir de investigación en genómica, proteómica y transcriptómica del parásito están empezando a revelar sus complejos que utiliza el parásito, y con ellos, la necesidad de búsqueda de nuevas dianas moleculares con las que formular futuras vacunas que induzcan respuestas inmunes totalmente eficaces.

El ciclo vital del parásito es complejo y se desarrolla en dos huéspedes. Consta de una fase sexual en el mosquito, que actúa como vector, y una fase asexual en el humano. El ciclo comienza cuando el humano se infecta a través de la picadura de la hembra del mosquito *Anopheles*, que porta *Plasmodium* en el estado de esporozoíto en las glándulas salivares, inoculando éstos en la dermis y en el torrente sanguíneo. Aunque el número de esporozoítos depositados puede variar, se estima que es aproximadamente de 15 a 200. Los esporozoítos abandonan el sistema vascular penetrando en las células del hígado, comenzando la fase hepática donde cada esporozoíto invade una célula hepática, convirtiéndose en un parásito intracelular. En las cuatro especies se observa entonces una multiplicación asexual; pero en el caso de *P. vivax* y *P. ovale* algunos esporozoítos pueden pasar por una fase de latencia

(hipnozoíto) capaz de permanecer durante meses en el hígado antes de iniciar la división asexual. La multiplicación asexual en el hígado permite la maduración del esporozoíto hasta la formación de un esquizonte hepático (5-15 días post-infección, según la especie), el cual produce miles de merozoítos en cada célula infectada (10.000 para *P. falciparum* y hasta 30.000 para *P. vivax*). El hepatocito infectado se rompe y libera los merozoítos a la sangre, que invaden los glóbulos rojos en cuyo interior se desarrolla el ciclo asexual del parásito. Esta fase sanguínea es la causante de la patología clínica asociada a la malaria.

La fase de invasión comienza cuando el merozoíto interacciona con la membrana del eritrocito, produciéndose la fusión entre ambos[16]. El merozoíto penetra en el interior de la célula, desarrollándose así una vacuola parasitófora en la cual el parásito evoluciona a una forma llamada de anillo que posteriormente se convierte en trofozoíto. La fase de trofozoíto es metabólicamente muy activa, el parásito madura mediante la ingestión del citoplasma del eritrocito y como resultado de la degradación proteolítica de la hemoglobina aparece el pigmento del parásito: la hemozoína. *Plasmodium* además comienza a dividir su cromatina de manera asexuada, dando lugar a una forma más madura denominada esquizonte, que posee entre 16 y 32 merozoítos (en función de la especie), que se liberan al torrente sanguíneo para volver a invadir otros hematíes. Junto con los merozoítos, se liberan los productos metabólicos del parásito, que son los responsables de las crisis de fiebre cíclicas típicas de la malaria. Paralelamente, algunos merozoítos se desarrollan dentro del eritrocito hacia un estadio sexual llamado gametocito. Cuando una hembra de *Anopheles* pica a un humano infectado por *Plasmodium*, ingiere la sangre parasitada que contiene los gametocitos. Comienza así la fase sexual, en la que los parásitos pasan al estómago del mosquito, donde mediante un proceso denominado exflagelación liberan los gametos. La fecundación de los gametos origina el cigoto, la única forma diploide del ciclo parasitario. El cigoto se alarga, y se convierte en una forma móvil denominada ooquineto, que atraviesa el intestino del mosquito y se

enquista en la pared exterior, formando un ooquiste. El ooquiste crece y mediante división celular por meiosis forma esporozoítos, con complejo apical. Entre 7 y 15 días post-infección, dependiendo de la especie de *Plasmodium* y de la temperatura ambiental, un sólo ooquiste forma más de 10.000 esporozoítos. El ciclo se cierra cuando se liberan los esporozoítos, que migran hasta las glándulas salivales desde donde se inocularán en un nuevo huésped humano.

El parásito se caracteriza por su gran variabilidad, tanto de las proteínas de superficie en la fase de merozoíto como de las que expone en la membrana de los eritrocitos infectados en las fases de anillo, trofozoíto y esquizonte. Esta variabilidad dificulta que el sistema inmunitario reconozca al parásito y es un obstáculo a la hora de desarrollar vacunas eficaces o marcadores específicos de eritrocitos infectados por *Plasmodium*.

Herramientas para combatir la malaria

Desde que en 1955 empezó la primera campaña de la Organización Mundial de la Salud para erradicar la malaria se han realizado muchos progresos en la lucha contra la enfermedad. 79 países la han eliminado y la proporción de la población mundial que vive en áreas endémicas ha disminuido más del 50%. En la actualidad existen varias coaliciones públicas y privadas que tienen el objetivo de acelerar el proceso de eliminación de la enfermedad en muchos países, estableciendo un gran compromiso global en la lucha contra la enfermedad[26].

Existen tres grandes herramientas para combatir la malaria[27]: el control del vector, las vacunas y los fármacos antimaláricos. La detección temprana de la enfermedad y la vigilancia de su desarrollo se han convertido en requisitos claves para el control eficaz de las infecciones por *Plasmodium*. Además, la rápida adquisición de resistencia por parte del parásito a los antimaláricos convencionales hace necesarias nuevas estrategias terapéuticas que contribuyan a la erradicación de la malaria.

El objetivo principal del control del mosquito es la reducción de la morbilidad y mortalidad asociadas a la malaria a través de la reducción de los niveles de transmisión. Para controlar de forma efectiva al mosquito se utilizan insecticidas (preferentemente para impregnar telas mosquiteras y para rociar el interior de las casas), tratamiento que puede ser efectivo hasta durante 6 meses en función del tipo de compuesto utilizado. A nivel individual, los sistemas de protección personal contra el mosquito representan la primera línea de defensa en la prevención contra la malaria. La problemática actual de esta herramienta es que depende del uso de una única clase de insecticidas, los piretroides, y en los últimos años el mosquito ha desarrollado resistencia en varios países a estos compuestos. Afortunadamente, este fenómeno de resistencia ha sido raramente asociado a una disminución en la eficacia de los sistemas de control del vector, que siguen siendo unas herramientas muy efectivas.

Los primeros estudios para desarrollar una vacuna contra la malaria comenzaron hace más de 50 años, pero aún no se ha conseguido una que confiera un 100% de protección. Actualmente RTS,S/AS01 es la vacuna más avanzada contra *P. falciparum*, está dirigida contra los esporozoítos y se encuentra en ensayos clínicos en varios países de África, presentando una eficacia del 50% en niños menores de 5 años y del 30% en niños menores de 6 meses[31].

Un diagnóstico a tiempo y un tratamiento adecuado reducen la morbilidad de la enfermedad y disminuyen las muertes causadas por malaria. Las herramientas para el diagnóstico (principalmente detección del parásito por microscopía y tests rápidos para el diagnóstico) y los fármacos antimaláricos permiten un control efectivo de la enfermedad y si se utilizan correctamente pueden reducir tanto su incidencia como el riesgo de aparición de parásitos resistentes.

Los agentes antimaláricos disponibles en la actualidad pueden clasificarse en función de su actividad biológica o de su estructura química[53]. Desde el punto de vista biológico y en función de su eficacia frente a las diversas etapas del ciclo de vida de *Plasmodium*, se clasifican como: esquizonticidas eritrocitarios, esquizonticidas tisulares, gametocidas y esporonticidas.

- **Esquizonticidas eritrocitarios:** actúan en la fase asexual intraeritrocítica del parásito de la malaria, inhibiendo la proliferación del parásito en el interior de los eritrocitos. Los fármacos que pertenecen a esta clase son de *acción rápida*: cloroquina, quinina, mefloquina, halofantrina, artemisinina o de *acción lenta*: pirimetamina, sulfadoxina, sulfonas, las tetraciclinas y atovacuona.
- **Esquizonticidas tisulares:** actúan contra las formas de *Plasmodium* en el hígado, evitando el desarrollo del esquizonte hepático. Son profilácticos, ya que previenen la invasión de los eritrocitos, pero como en esa fase de la infección aún no se presentan síntomas, no suelen utilizarse. Los fármacos con esta actividad son: primaquina, pirimetamina, proguanil y sulfonamidas.
- **Hipnozoiticidas:** actúan sobre las formas latentes (hipnozoítos) de *P. vivax* y *P. ovale* en el hígado. La primaquina es el único fármaco disponible para esta etapa.
- **Gametocidas:** destruyen las formas sexuales del parásito en la sangre, y previenen la transmisión de la infección del humano al mosquito. Primaquina y artemisinina tienen actividad gametocida frente a todas las especies de *Plasmodium*, mientras que cloroquina, quinina y mefloquina sólo frente a *P. vivax*, *P. ovale* y *P. malariae*.
- **Esporonticidas:** bloquean el desarrollo de los ooquistes en los mosquitos infectados, anulando así la transmisión de la malaria. Los fármacos que poseen actividad frente a esta etapa del ciclo son primaquina, cloroquina y cloroguadina.

Desde el punto de vista de su estructura química, los fármacos antimaláricos se clasifican en: quinolinas y antimaláricos relacionados, artemisinina y derivados, antifolatos y otros antimaláricos. En este resumen se explicarán detalladamente solamente los fármacos que han sido utilizados durante esta tesis doctoral:

- **Cloroquina:** antimalárico de la familia de las 4-aminoquinolinas, derivadas de la quinina, ha sido el tratamiento estándar para la malaria durante muchos años. Las bases moleculares de su acción se basan en la inhibición de la formación de la hemozoína, formada a partir de la digestión de la hemoglobina en la vacuola del parásito para evitar la acumulación de sustancias tóxicas. La cloroquina impide la desintoxicación de las especies reactivas de oxígeno, matando al parásito con sus propios desechos metabólicos. Estudios recientes demuestran además que la cloroquina genera daño oxidativo específico en el proteoma de *Plasmodium falciparum* en los diferentes estadios de su ciclo eritrocitario. La eficacia de la cloroquina se ha visto disminuida en los últimos años, principalmente como resultado de la propagación de la resistencia del parásito.
- **Primaquina:** pertenece al grupo de las 8-aminoquinolinas, es efectiva contra los hipnozoítos y los gametocitos. Su mecanismo de acción es desconocido, pero se sabe que inhibe la polimerización del grupo hemo. Los metabolitos hidroxilados de primaquina estimulan la vía de las hexosas monofosfato, aumentando así la producción de compuestos que generan estrés oxidativo en el parásito. Desafortunadamente, esta misma propiedad de la primaquina, es también responsable de su efecto hemolítico y de su toxicidad, especialmente en personas con deficiencia en glucosa-6-fosfato dehidrogenasa.
- **Fosmidomicina:** antibiótico que es un inhibidor de la enzima principal de la vía de biosíntesis de isoprenoides alternativa a la del mevalonato. Esta ruta metabólica se localiza en el apicoplasto del parásito y no está presente en humanos. La fosmidomicina

administrada junto a clindamicina se ha probado para el tratamiento de la malaria no severa.

La resistencia en *Plasmodium* está causada por mutaciones aleatorias que confieren una susceptibilidad reducida a fármacos antimaláricos. Las mutaciones son aleatorias y poco frecuentes, pero una vez presentes están sujetas al proceso de selección, que ocurre cuando una población que contiene parásitos mutantes se expone a una concentración de fármaco suficientemente elevada para eliminar a los parásitos susceptibles pero no a los resistentes, que serán seleccionados y se transmitirán. La aparición de parásitos resistentes depende de múltiples factores, entre los que se encuentran: la tasa de mutación del parásito, la carga parasitaria en el huésped, la fuerza de selección del fármaco, el seguimiento del tratamiento por parte del paciente y el grado de endemicidad de la zona. El fenómeno de la resistencia a antimaláricos es un grave problema que afecta a la salud pública ya que hace peligrar las estrategias actuales de control de la malaria.

El uso indiscriminado de antimaláricos ejerce una fuerte presión selectiva en los parásitos que favorece el desarrollo de resistencia. La resistencia se puede prevenir, o al menos se puede reducir considerablemente si se combinan antimaláricos con diferentes mecanismos de acción y si se ajustan las dosis de tratamiento a seguir. La cloroquina, el fármaco de referencia para el tratamiento de la malaria durante más de medio siglo, no es efectiva en la mayoría de regiones endémicas de malaria. Se ha documentado resistencia para todos los fármacos antimaláricos usados en la actualidad, incluso para el tratamiento recomendado por la Organización Mundial de la Salud. Esta situación alarmante de desarrollo de resistencias plantea muchas cuestiones sobre si los fármacos que existen en la actualidad permitirán erradicar la enfermedad, y pone de manifiesto la necesidad de buscar nuevos compuestos antimaláricos y de mejorar los mecanismos de liberación de los fármacos que existen actualmente.

Debido a la baja especificidad hacia las células diana, los métodos actuales de administración para la mayoría de antimaláricos requieren múltiples dosis. Sin embargo, una baja especificidad de fármacos tóxicos exige concentraciones reducidas, aumentando así el riesgo de administrar dosis subletales que favorecen la aparición de resistencias. En esta tesis doctoral, se propone el desarrollo de estrategias basadas en la liberación dirigida de fármacos a través de nanovectores, con el objetivo de conseguir la administración de dosis suficientemente bajas como para ser inocuas para el paciente pero que localmente sean elevadas y letales hacia el parásito.

Nanotecnología y malaria

La nanotecnología engloba una amplia variedad de técnicas y métodos que permiten el control y manipulación de materiales a una escala menor que el micrómetro. Gracias al control del tamaño y la forma con la nanotecnología se pueden crear materiales y sistemas novedosos con propiedades únicas y que presentan múltiples aplicaciones. La nanotecnología es una de las áreas de la ciencia que está evolucionando más rápidamente, pero al mismo tiempo despierta las mismas cuestiones que cualquier nueva tecnología, incluyendo inquietudes sobre una posible toxicidad y el impacto medioambiental de los nanomateriales. Debido a la potencialidad de la nanotecnología en medicina son necesarios un mejor conocimiento de las implicaciones toxicológicas de los nanomateriales y una regulación adecuada, que permitirá asegurar una transferencia segura y fiable de los nuevos avances desde el laboratorio a su aplicación médica.

La nanomedicina es la aplicación de la nanotecnología a la medicina y ha sido definida por la Fundación Europea de la Ciencia del siguiente modo: “La nanomedicina utiliza herramientas de medida nanométrica para el diagnóstico, prevención y tratamiento de enfermedades, permitiendo así obtener un mejor entendimiento de la complejidad que reside debajo de la patofisiología de la enfermedad y mejorando la calidad de vida del paciente”.

Las tres áreas principales que pueden distinguirse en el campo de la nanomedicina son:

- **Diagnóstico, sensores y herramientas de visualización**: La nanotecnología permite el desarrollo de nuevos sistemas analíticos con mayor sensibilidad, coste reducido y dimensiones menores.
- **Tecnologías y biomateriales innovativos** que se utilizan en ingeniería de tejidos para promover la reparación, mantenimiento o recuperación de la función tisular o de un órgano.
- **Sistemas de liberación dirigidos** para mejorar los métodos de administración de fármacos con el objetivo de conseguir mejores efectos terapéuticos.

El desafío de los sistemas de liberación dirigida es la dispensación de fármacos en el momento adecuado de una manera segura y reproducible, normalmente a células diana, de manera que el resto de tejidos tienen una mínima exposición al compuesto en cuestión y se consigue un efecto terapéutico mejorado. En el momento de diseñar un nanovector para una aplicación específica, hay que tener en cuenta que las características del sistema no serán debidas tan sólo a la naturaleza de las moléculas que componen el nanovector, sino también a su tamaño y morfología. Además, habrá que considerar el método de administración a utilizar y las barreras biológicas que el nanovector deba atravesar para poder ejercer su acción.

Un sistema de liberación óptimo debe presentar una amplia variedad de propiedades útiles para el desarrollo de su acción, como pueden ser:

- Capacidad de transportar una elevada cantidad de fármaco y más de un tipo de compuesto.
- Protección del fármaco hasta que se libere en el lugar de acción.
- Elevado tiempo de circulación en sangre, sin ser eliminado por el sistema inmunitario, ni por filtración en el bazo o en los riñones.
- Direccionamiento específico a su lugar de acción, gracias a la presencia de ligandos unidos a su superficie.

- Penetración intracelular incrementada, a través de moléculas en su superficie que favorecen la internalización.
- Facilidad para ser visualizado *in vitro* e *in vivo* gracias a sistemas de marcaje con agentes de contraste.

Los materiales que componen el nanovector deberían ser biocompatibles y biodegradables. Una vez se ha encapsulado un fármaco en el interior de un nanovector, la biodistribución del compuesto vendrá determinada por las características del sistema de liberación, alterando la distribución del fármaco en cuestión. Esto puede comportar cambios en los efectos secundarios producidos por un compuesto, como es el caso de la toxicidad dérmica observada en pacientes tratados con doxorubicina liposomal, ausente en pacientes tratados con doxorubicina libre.

Otro factor muy importante a tener en cuenta en el diseño de un nanovector es el tamaño, ya que determina si una nanopartícula será internalizada y el mecanismo de internalización, y por tanto, la posterior localización subcelular. Nanopartículas de entre 70 y 200 nm presentan los tiempos de vida media más prolongados en sangre.

El direccionamiento de los sistemas de liberación de fármacos puede ser pasivo o activo. En el direccionamiento pasivo los nanovectores se acumulan un lugar en concreto debido a características anatómicas de esa zona, como es el caso de los endotelios con permeabilidad incrementada en tumores. En cambio, el direccionamiento activo se consigue gracias a la presencia de moléculas en la superficie del nanovector que son capaces de unirse a las células diana, evitando uniones indeseadas con otras células. La desventaja de estos sistemas activos es que las moléculas direccionalizadoras pueden ser reconocidas por el sistema inmunitario como extrañas, provocando respuestas indeseadas. Para evitar el reconocimiento por parte del sistema inmunitario, se han diseñado elementos de camuflaje como por ejemplo el polietilenglicol, que permiten alargar el tiempo de residencia extracelular de los nanovectores.

Hay una gran variedad de sistemas de liberación de fármacos, entre los que podemos encontrar: nanopartículas inorgánicas, liposomas, protocélulas, nanoemulsiones, nanopartículas poliméricas, micelas y dendrímeros. Aproximadamente una docena de productos para la liberación de fármacos han sido aprobados y comercializados para uso clínico, pero a pesar de su enorme potencial, aún no ha sido aprobado ningún sistema de liberación dirigido, aunque actualmente hay algunos en ensayos clínicos. Esto se debe principalmente a la dificultad en la elección de la molécula direccionadora adecuada, que debe ser altamente específica, fácilmente modificable y debe permitir su producción a gran escala.

Los liposomas son vesículas esféricas con una membrana formada por una doble capa de fosfolípidos alrededor de un compartimento acuoso, que es capaz de contener compuestos hidrofílicos en su interior o hidrofóbicos en su bicapa lipídica. Los liposomas funcionan como reservorios, protegiendo a los compuestos que tienen encapsulados de la degradación, interaccionando con las células a través de diferentes mecanismos y liberando su contenido en el interior celular. Los liposomas pueden recubrirse de polietilenglicol para incrementar su vida media en sangre y pueden funcionalizarse con moléculas direccionadoras para conseguir una liberación dirigida de las sustancias encapsuladas en su interior. Utilizando liposomas, se ha conseguido incrementar la eficacia de numerosos fármacos, incluyendo antifúngicos, antivirales, antibióticos y antiparasíticos.

Los polímeros son una prometedora aproximación para la liberación dirigida de fármacos: son pequeños, biocompatibles, pueden penetrar en el interior de las células, pueden ser funcionalizados con ligandos para conseguir direccionarlos y existe una amplia variedad de materiales y estructuras moleculares para su síntesis. Los polímeros pueden encapsular fármacos, protegerlos de la degradación, y conseguir una liberación controlada del compuesto, incrementando su vida media en sangre.

Las poliamidoaminas (PAAs) constituyen una familia de polímeros biodegradables y biocompatibles cuya síntesis es simple y fácilmente escalable. Las PAAs presentan una baja citotoxicidad y han sido estudiadas para diferentes aplicaciones, entre las que se incluyen la formación de complejos polielectrolíticos con heparina, la conjugación con fármacos anticancerígenos y la terapia génica.

La nanotecnología ha sido aplicada en varias áreas de investigación contra la malaria, como son el desarrollo de nuevos sistemas de diagnóstico, el descubrimiento de nuevos fármacos o el desarrollo de sistemas de liberación de antimaláricos. Los beneficios de la liberación de fármacos pueden jugar un papel importante en el tratamiento de la malaria, ya que:

- Permitirían la liberación de dosis elevadas a nivel local que minimizarían el desarrollo de parásitos resistentes.
- Incrementarían la eficacia de los antimaláricos usados en la actualidad.
- Posibilitarían el uso de fármacos huérfanos que no han sido utilizados para terapia debido a su elevada toxicidad inespecífica.

A pesar de las ventajas que supondrían los sistemas de liberación de fármacos para el tratamiento de la malaria, la mayoría de esfuerzos para la aplicación de la nanomedicina han sido destinados a la terapia del cáncer, ya que representa una enfermedad con mayores posibilidades lucrativas para las compañías farmacéuticas.

Tal y como se ha descrito anteriormente, las estrategias de liberación dirigida de fármacos pueden ser pasivas o activas. El direccionamiento pasivo es adecuado para células diana con propiedades fagocíticas como pueden ser los macrófagos, pero los eritrocitos son inactivos a nivel de endocitosis y fagocitosis. No obstante, el direccionamiento pasivo podría aplicarse para la liberación de fármacos a hipnozoítos (formas latentes en el hígado), que están

situados al lado de las células de Kupffer, que son muy activas a nivel de fagocitosis, lo cual comportaría una acumulación local de los nanovectores. La modificación de los nanovectores con elementos de camuflaje para incrementar su tiempo de permanencia en sangre, incrementaría la posibilidad de interacción de los vectores con las células infectadas por *Plasmodium*. El direccionamiento activo se consigue gracias a la presencia de ligandos en la superficie de los nanovectores, que son los que se encargan de que se produzca una acumulación preferente del fármaco en las células diana, ya sean glóbulos rojos infectados o hepatocitos. La elección de una diana adecuada es un requisito imprescindible para el éxito de este tipo de liberación dirigida, las moléculas direccionadoras utilizadas son normalmente péptidos o anticuerpos y los sistemas de liberación de fármacos que se han investigado en el campo de la malaria son liposomas, emulsiones, polímeros y dendrímeros.

Los liposomas constituyen un sistema eficaz para la liberación de fármacos en el interior de los eritrocitos ya que pueden fusionarse con su membrana, liberando sus contenidos al interior celular sin necesidad de endocitosis o fagocitosis, ambas ausentes en los glóbulos rojos. Resultados previos de otros grupos indican que la encapsulación de cloroquina y primaquina en liposomas podría prolongar la vida media del compuesto en sangre, disminuir su toxicidad e incrementar su eficacia[179]. Se han funcionalizado liposomas con elementos direccionadores para conseguir su acumulación preferencial en hepatocitos y en eritrocitos infectados[221]. En el caso de los derivados de artemisinina, se han utilizado los vehículos liposomales para incrementar el tiempo de permanencia en sangre de éstos compuestos[184], y utilizando emulsiones se ha conseguido una eficaz administración oral de los mismos[186].

A pesar de estos prometedores ensayos, la terapia antimalárica basada en liposomas no ha avanzado hacia ensayos clínicos, probablemente debido a la ausencia en el momento de realización de los estudios de un elemento direccionalizador adecuado que pudiera ser utilizado para una liberación dirigida de fármacos. Además la mayoría de los estudios publicados se centran

en la eficacia *in vivo* de los vehículos liposomales, sin haber estudios *in vitro* que caractericen la interacción de los eritrocitos infectados por *Plasmodium* y liposomas y la liberación del contenido de éstos al interior de las células diana en cultivos *in vitro* o en presencia de otros tipos celulares.

Los polímeros tienen la ventaja sobre los liposomas de una formulación más sencilla para administración oral, requisito indispensable para el tratamiento de la malaria no severa en áreas endémicas, alejadas de centros sanitarios. Varios derivados poliméricos han sido sintetizados para la administración de antimaláricos, aunque existen pocos ejemplos del estudio de su eficacia tanto *in vitro* como *in vivo*. La encapsulación de primaquina se ha probado en nanopartículas de gelatina, albúmina, glutaraldehído y poliacrilamida, pero estas nanopartículas no han sido ensayadas contra el parásito. Nanopartículas de ácido poliláctico con halofantrina en su interior, con o sin recubrimiento de polietilenglicol, han sido testadas en ratones con malaria; los resultados obtenidos muestran que los dos tipos de nanopartículas (con y sin recubrimiento) actúan de manera complementaria, de manera que se propone su administración combinada[222]. Nanopartículas de quitosano se han ensayado para la administración oral de curcumina, fármaco prometedor para el tratamiento de varias enfermedades pero que tiene limitaciones a nivel de difícil formulación oral, baja hidrosolubilidad y rápida degradación. Los resultados obtenidos indican que estas nanopartículas pueden curar a ratones infectados por malaria, pero sólo si las parasitemias iniciales son bajas[194].

Se han probado varios tipos de dendrímeros para la liberación de los antimaláricos artemeter y cloroquina. Con el objetivo de reducir la toxicidad asociada a los grupos amino terminales de estos sistemas, se han recubierto de galactosa, PEG o lisina. Se han caracterizado a nivel de toxicidad inespecífica, liberación de fármaco y estabilidad, pero sólo en el caso de los dendrímeros de polilisina recubiertos con PEG y conjugados a sulfato de condroitina A se ha estudiado su actividad *in vitro*[191]. No hemos encontrado resultados publicados sobre la eficacia *in vivo* de estos sistemas.

La liberación dirigida es una herramienta prometedora para la mejora de la eficacia, especificidad, tolerabilidad e índice terapéutico de los fármacos existentes. Además permite la administración oral de compuestos con poca estabilidad o baja hidrosolubilidad. La formulación y evaluación de posibles sistemas de liberación de fármacos ya existentes no es sólo más económica que el descubrimiento de nuevos compuestos, sino que permite ajustar la dosis necesaria para el tratamiento, reduciendo así los casos de fracaso en el tratamiento de la malaria debido a dosis inadecuadas o abandono por parte del paciente. Un nanovector ideal contra la malaria debería ser pequeño, específico y económico. También debería contener una molécula direccionadora que fuera de obtención fácil y rápida y que reconociera varias especies del parásito. Algunos de los nanovectores presentados en esta tesis doctoral reunen estos requisitos y podrían formar parte de una nueva generación de nanovectores que pudieran entrar en ensayos preclínicos como parte de una terapia asequible para la malaria.

OBJETIVOS

El objetivo de esta tesis doctoral es el desarrollo de un nanovector para la liberación dirigida de antimaláricos exclusivamente a hematíes infectados por *Plasmodium* y la comprensión de los parámetros principales en el diseño de dicho nanovector, que determinan su eficacia.

Este objetivo general se conseguirá a través de los siguientes pasos experimentales:

1. Diseño e ingeniería de un nanovector inmunoliposomal capaz de (i) encapsular fármacos antimaláricos, (ii) unirse específicamente a eritrocitos infectados, y (iii) liberar sus contenidos en el interior de estas células pero no en los eritrocitos sanos.
2. Síntesis y evaluación de los polímeros como nanovectores direccionados de antimaláricos hacia glóbulos rojos con el parásito.
3. Caracterización de la eficacia *in vitro* de fármacos antimaláricos cuando se administran en el interior de inmunoliposomas y polímeros.
4. Estudios *in vivo* con nanovectores liposomales y poliméricos.
5. Exploración de nuevas moléculas direccionadoras para futuros nanovectores que contengan antimaláricos.

RESULTADOS

ARTÍCULO 1:

Nanovector con completa discriminación para la liberación dirigida a eritrocitos infectados por *Plasmodium falciparum in vitro*

Con los métodos actuales de administración de antimaláricos, los compuestos son liberados al torrente sanguíneo, donde pueden ser internalizados por todas las células y no sólo por los glóbulos rojos infectados con *Plasmodium*. Los sistemas de liberación de fármacos podrían minimizar los efectos secundarios de los antimaláricos ya que permitirían incrementar su biodisponibilidad y selectividad. Se han ensayado sistemas liposomales para la liberación de compuestos en el tratamiento de la malaria en ratones, pero no hay estudios que caractericen la eficacia de liposomas dirigidos de manera específica a eritrocitos infectados a nivel de interacción específica y liberación de su contenido en el interior celular.

Hemos determinado la eficacia *in vitro* de liposomas en el direccionamiento específico de sus contenidos al interior de eritrocitos infectados por *P. falciparum* mediante microscopía de fluorescencia. Liposomas que encapsulan *quantum dots*, funcionalizados con anticuerpos contra formas tardías del parásito se unen en menos de 90 minutos a eritrocitos infectados por *Plasmodium* y liberan su contenido en el interior de las células diana. *In vitro* los inmunoliposomas reconocen el 0% de los eritrocitos sanos mientras que el 100% de los eritrocitos infectados con las formas tardías del parásito son reconocidos y presentan el contenido liposomal en su interior. Este reconocimiento y liberación del contenido liposomal no se ve afectado por la presencia de otros tipos celulares. Liposomas no funcionalizados con anticuerpos específicos también se dirigen a los eritrocitos infectados, pero con menos afinidad que los inmunoliposomas. En ensayos preliminares el antimalárico cloroquina a una concentración de 2 nM, 10 inferior superior a su IC_{50} en solución, eliminó al 26,7±1,8% de los eritrocitos infectados cuando fue administrado en forma de inmunoliposomas.

ARTÍCULO 2:

Estudio de la eficacia de fármacos antimaláricos cuando se administran en nanovectores inmunoliposomales dirigidos

La implementación de los sistemas de liberación dirigida de fármacos es actualmente un reto debido a tres limitaciones: la identificación de las dianas moleculares o celulares para la enfermedad en cuestión, la necesidad de un fármaco que sea eficaz y la búsqueda de una estrategia de liberación que permita la acumulación del fármaco de manera selectiva en las células de interés.

En nuestro trabajo anterior propusimos un nanovector inmunoliposomal para la liberación dirigida de sus contenidos a eritrocitos infectados con *P. falciparum*. En este trabajo nos hemos centrado en el estudio de la actividad de los fármacos cloroquina y fosmidomicina cuando se administran en dicho prototipo inmunoliposomal y en la determinación de la cantidad exacta de fármaco encapsulada mediante el desarrollo de un método de HPLC-MS/MS.

Los resultados obtenidos indican que la encapsulación de fármacos en nuestras condiciones experimentales incrementa su eficacia unas diez veces. Con el objetivo de conseguir la máxima eficacia del nanovector, hemos modificado el ensayo para la determinación de actividad *in vitro* y hemos funcionalizado el inmunoliposoma con cantidades crecientes de anticuerpo, llegando a un 50% de reducción de la parasitemia *in vitro*. Estos resultados indican que con las modificaciones adecuadas, el nanovector liposomal puede contribuir a la mejora de la actividad de los fármacos antimaláricos existentes.

ARTÍCULO 3:
Demostración mediante espectroscopía de molécula única de la unión específica de la heparina a eritrocitos infectados por *Plasmodium falciparum*

Los glucosaminoglucanos (GAGs) juegan un papel importante en varios procesos asociados con la malaria severa como son el secuestro de eritrocitos infectados por *P. falciparum* en el endotelio vascular de varios órganos y su adhesión a la placenta. En este trabajo se ha usado la heparina como modelo para estudiar las interacciones entre GAGs y eritrocitos infectados por *Plasmodium*.

Los resultados obtenidos mediante microscopía de fluorescencia y citometría de flujo indican que la heparina presenta unión específica a eritrocitos infectados, preferentemente aquellos contienen formas tardías del parásito. Los estudios realizados con el microscopio de fuerzas atómicas indican que la adhesión de los eritrocitos infectados a la heparina está caracterizada por una fuerza de entre 28 y 46 pN, mientras que no se ha detectado unión significativa de la heparina a eritrocitos sanos. Este trabajo representa la primera aproximación para la cuantificación de la interacción entre GAGs y eritrocitos infectados a nivel de moléculas y células individuales.

ARTÍCULO 4:
Nanotecnología contra la malaria: uso de poliamidoaminas para la liberación dirigida de fármacos a *Plasmodium*

En este trabajo hemos explorado el uso de dos polímeros de la familia de las poliamidoaminas, AGMA1 e ISA23, para la liberación dirigida de fármacos antimaláricos a eritrocitos con *Plasmodium*. Ensayos de inhibición del crecimiento de *P. falciparum in vitro* han demostrado que el polímero AGMA1 tiene actividad antimalárica *per se*, con una IC_{50} de 2,5 μM para la fracción de 50-100 kDa. Los resultados obtenidos mediante citometría de flujo, microscopía confocal y microscopía electrónica indican que AGMA1 e ISA23 tienen un direccionamiento específico hacia eritrocitos infectados por *Plasmodium*, reconociendo al parásito en el interior de los hematíes.

AGMA1 e ISA23 presentan una elevada capacidad para encapsular los antimaláricos cloroquina y primaquina mediante uniones electrostáticas. La administración intraperitoneal de 0,8 mg/kg/día de cloroquina encapsulada en los polímeros curó a ratones infectados por la cepa letal de *Plasmodium yoelii*, mientras que los animales control y los tratados con el doble de cantidad de fármaco libre no sobrevivieron.

El tamaño de los polímeros, con un radio hidrodinámico estimado en 8 nm aproximadamente, hace que sean buenos candidatos para ser formulados para administrarse por vía oral. AGMA1 e ISA23 son unas prometedoras plataformas para una nueva generación de nanovectores contra la malaria de bajo coste, combinando en una única estructura química capacidad de encapsular fármacos, actividad antimalárica y direccionamiento específico a hematíes infectados por *Plasmodium*.

DISCUSIÓN

La malaria representa el paradigma del círculo vicioso de la enfermedad y la pobreza y pone de manifiesto el papel clave de la investigación como componente estratégico de la cooperación internacional. Recientemente los esfuerzos en investigación se han dedicado sobretodo al desarrollo de vacunas y al descubrimiento de nuevos fármacos, no obstante, el desarrollo de nuevos métodos de liberación para los antimaláricos ya existentes es más económico que la búsqueda de nuevos compuestos.

El trabajo presentado en esta tesis doctoral tiene como objetivo principal el desarrollo de un nanovector para la mejora de la eficacia de los antimaláricos existentes y la comprensión de los parámetros fundamentales de su diseño que determinan la eficacia de dicho nanovector. Entender a nivel molecular y celular por qué los nanovectores mejoran o no el efecto de los fármacos actuales es uno de los puntos clave de esta tesis. En cambio, los trabajos publicados hasta el momento en liberación dirigida de antimaláricos se basan sobretodo en la síntesis de diferentes tipos de nanovectores, el estudio de su capacidad para encapsular y liberar fármacos y, en algunos casos, la determinación de su efecto antimalárico *in vivo*, sin estudios previos de la interacción de estos nanovectores con pRBCs *in vitro*. Nosotros hemos adoptado una estrategia de diseño racional, donde se ha priorizado la caracterización de la eficacia del sistema a nivel de especificidad por las células diana, capacidad de liberación de fármaco y estudio de la eficacia *in vitro*; la información obtenida a partir de estos experimentos se ha utilizado para desarrollar nuevas estrategias y optimizar los candidatos que serán probados en ratones.

Este trabajo puede ser dividido en tres fases principales:

Fase 1 – Diseño del prototipo y desarrollo inicial.

Preparación de inmunoliposomas y caracterización de su direccionamiento hacia eritrocitos infectados por *Plasmodium*. En esta fase se seleccionó el anticuerpo comercial BM1234 para la funcionalización de liposomas y se

estudió mediante microscopía de fluorescencia la capacidad del modelo inmunoliposomal para liberar sus contenidos en el interior de las células diana.

Fase 2 – Test del nanovector inmunoliposomal *in vitro* e *in vivo*.
Inmunoliposomas con cloroquina o fosmidomicina en su interior se probaron en ensayos de inhibición del crecimiento del parásito. La eficacia del modelo inmunoliposomal también se testó *in vivo*.

Fase 3 – Evolución y refinamiento del prototipo inmunoliposomal.
Se probaron polímeros como alternativa al modelo inmunoliposomal, dos de los polímeros sintetizados presentan un direccionamiento específico hacia eritrocitos con *Plasmodium*, siendo buenos candidatos para el diseño de sistemas de liberación dirigida de antimaláricos. Se conjugaron estos polímeros a cloroquina y primaquina y se testaron *in vitro* e *in vivo* para estudiar su efecto en comparación con los fármacos solubles. Hemos explorado también el uso de la heparina como alternativa a los anticuerpos como moléculas de direccionamiento específico.

La búsqueda del nanovector más idóneo para nuestra aplicación empezó a partir del concepto abstracto de un vector basado en las *Muñecas rusas* (o matriuskas), que consistía en una cápsula inmunoliposomal que estaba funcionalizada con anticuerpos específicos contra eritrocitos infectados por *Plasmodium*, y que contenía en su interior dendrímeros o nanopartículas poliméricas que encapsulaban fármacos antimaláricos. Este primer prototipo teórico, fue concebido deliberadamente como un modelo complejo, con diferentes elementos que pudieran utilizarse para conseguir un sistema altamente específico y eficaz, o que pudieran ser descartados si no añadían un valor cuantitativo al sistema. El nanovector deseado para el tratamiento de la malaria debería conseguir el máximo efecto con la mínima complejidad posible, para poder tener un coste reducido que le permitiera tener perspectivas favorables a nivel de comercialización. Los inmunoliposomas, que ya habían sido utilizados como sistemas de liberación específica de antimaláricos, se

escogieron debido a su capacidad de fusionarse con la membrana de los hematíes, y los dendrímeros y nanopartículas poliméricas representan sistemas innovadores y muy prometedores, que podrían funcionalizarse si fuera necesario con anticuerpos específicos para liberar el fármaco en el interior de la vacuola parasitófora.

Nuestros estudios empezaron con la preparación de inmunoliposomas, donde la elección del anticuerpo adecuado es un punto clave para la discriminación entre hematíes sanos e infectados. Los primeros estudios los realizamos con nuestros propios anticuerpos producidos contra ciertas regiones de Banda 3 de la membrana del hematíe, que habían sido publicadas como buenos marcadores de pRBCs, ya que la infección por el parásito causa modificaciones estructurales en esta proteína que pueden ser reconocidas por anticuerpos específicos. A pesar de que los anticuerpos policlonales se unían preferentemente a pRBCs, se detectó también unión inespecífica a eritrocitos sanos, y por esa razón realizamos un barrido de los anticuerpos comerciales preparados con fracciones de *P. falciparum*. Los anticuerpos BM1234 y 1232 fueron los candidatos para la preparación del nanovector.

En anticuerpo BM1234 es altamente específico para los eritrocitos que contienen formas maduras del parásito, con un patrón de reconocimiento alrededor de la membrana de los hematíes. El patrón de fluorescencia del anticuerpo va cambiando a lo largo del ciclo del parásito. En cambio BM1232 reconoce todas las fases del parásito, pero aparentemente reconoce al parásito directamente. BM1234 se escogió como anticuerpo para la preparación de inmunoliposomas y BM1232 se guardó por si fuera necesario funcionalizar con anticuerpo los dendrímeros o las nanopartículas poliméricas.

Independientemente del anticuerpo utilizado, la reducción de la cantidad utilizada en el nanovector contribuye a minimizar el riesgo de que el sistema inmunitario lo elimine. Un nanovector específico requiere moléculas de anticuerpos orientadas para que puedan reconocer las células diana. Los

métodos utilizados generalmente se basan en la modificación química del anticuerpo, que puede llevar a la generación de moléculas de anticuerpo defectuosas que no reconozcan su antígeno. Una alternativa es utilizar los oligosacáridos de la región Fc para unir los anticuerpos, pero esta estrategia requiere varias reacciones químicas y es un proceso largo. Hemos utilizado la eficiente y rápida alternativa de la utilización de hemi-anticuerpos, que se forman tras la reducción del anticuerpo con 2-mercaptoetilamina que separa los puentes disulfuro de la región Fc, dejando libres grupos tiol que pueden reaccionar con el grupo maleimido presente en uno de los fosfolípidos incluidos en la composición liposomal.

Además de una unión específica, los inmunoliposomas han de liberar su contenido en el interior de los pRBCs. Liposomas con quantum dots en su interior y que han sido funcionalizados con hemi-anticuerpos contra formas tardías del parásito se unen en menos de 90 minutos a eritrocitos infectados por *Plasmodium* y liberan su contenido en el interior de las células diana. En cultivos in vitro los inmunoliposomas reconocen el 0% de los eritrocitos sanos y el 100% de los eritrocitos con formas tardías del parásito, que presentan el contenido inmunoliposomal en su interior. Esta liberación del contenido de los nanovectores no se ve afectada por la presencia de otros tipos celulares como células endoteliales que forman las paredes de los vasos sanguíneos, indicando que los inmunoliposomas podrán liberar los fármacos encapsulados en su interior exclusivamente a pRBCs y no a otras células.

Los liposomas unidos a pRBCs no se internalizan, sino que se fusionan con la membrana del eritrocito y liberan sus contenidos al interior celular. La capacidad de los liposomas de inyectar su carga podría ser debida a las alteraciones en la membrana de los pRBCs como consecuencia de la infección por el parásito. A medida que *Plasmodium* madura en el interior del hematíe, la membrana de la célula sufre una permeabilidad incrementada a solutos de bajo peso molecular y se vuelve menos elástica, este hecho favorece la interacción con los liposomas y se acentúa si anticuerpos específicos están presentes, y

podría facilitar la fusión entre membranas. Esta hipótesis explica también por qué en el caso de liposomas sin anticuerpo se observa cierto grado de liberación de los contenidos liposomales.

Datos obtenidos en nuestro grupo indican que 90 minutos después de administración intravenosa, el 90% del contenido liposomal inyectado sigue en circulación. Teniendo en cuenta que se necesitan menos de 90 minutos para conseguir un direccionamiento 100% específico *in vitro*, esperamos que los liposomas *in vivo* puedan reconocer los pRBCs y liberar su contenido, incluso en presencia de otros tipos celulares. Estos resultados abren buenas perspectivas para el desarrollo de un nanovector inmunoliposomal para la liberación específica de antimaláricos a pRBCs sin la necesidad de que contenga otros elementos en su interior, de manera que siguiendo nuestro objetivo de diseñar un vector lo más simple posible, decidimos incorporar directamente los antimaláricos en el interior de inmunoliposomas y estudiar su eficacia respecto a los fármacos solubles.

Se encapsuló cloroquina y fosmidomicina en el interior de inmunoliposomas y se probaron en ensayos de inhibición del crecimiento del parásito. En experimentos preliminares, la cloroquina administrada en forma inmunoliposomal incrementó su eficacia como antimalárico, pero las dificultades en la cuantificación de la concentración de compuesto en el interior del nanovector constituían una limitación para el estudio de la actividad del inmunoliposoma, ya que es fundamental comparar las mismas cantidades de fármaco en forma soluble y en el nanovector. Recomendamos establecer una técnica de cuantificación, que sea fiable incluso a bajas concentraciones de compuesto, para poder determinar la eficacia de un sistema de liberación dirigido de fármacos.

Los mejores resultados *in vitro* con el modelo inmunoliposomal han sido obtenidos administrando los nanovectores en parásitos maduros, que son los que reconoce el anticuerpo 1234, mejorando la eficacia de la cloroquina soluble

al menos 10 veces. Al incrementar la cantidad de anticuerpo en la superficie del liposoma, aumenta también su actividad. Estos datos nos indican que el prototipo de las *Muñecas rusas* era demasiado complejo y que los inmunoliposomas son buenos candidatos para estudios *in vivo*. La eficacia del nanovector es particularmente relevante en el caso de la cloroquina, donde existen transportadores específicos para este fármaco. En parásitos resistentes a CQ se acumula menos cantidad de CQ debido a mutaciones en dichos transportadores, al administrar el fármaco en forma liposomal, habría una ruta alternativa para la internalización de CQ, posibilitando la acumulación de fármaco en cepas resistentes y facilitando su eliminación.

Estos hallazgos con el modelo inmunoliposomal abren la posibilidad de utilizar en la terapia contra la malaria fármacos ya existentes que no han sido comercializados debido a su elevada toxicidad inespecífica. Si estos compuestos se direccionalizan de manera adecuada a las células diana, se minimizaría su interacción con otros tipos celulares, posibilitando su uso para el tratamiento de la malaria o de otras enfermedades. El modelo inmunoliposomal, también sería interesante para la liberación de fármacos que *in silico* son muy prometedores, pero que *in vitro* carecen de actividad debido a su incapacidad para atravesar la membrana de los pRBCs.

El modelo inmunoliposomal descrito en esta tesis, está limitado al reconocimiento de formas tardías del parásito debido a la especificidad del anticuerpo utilizado, no obstante, el uso de anticuerpos en general, el antimalárico utilizado y los liposomas tienen características que restringen su uso en determinadas situaciones.

Los anticuerpos utilizados para la funcionalización de liposomas son una limitación para los sistemas de liberación dirigida ya que las proteínas expresadas por el parásito en hematíes infectados son muy variables y existe el riesgo de que se desarrollen cepas que ya no sean reconocidas por el parásito, además, la obtención de anticuerpos es un proceso costoso y su

formulación para ser administrados por vía oral es compleja. De manera que aunque los anticuerpos han sido muy útiles como prueba de concepto estas limitaciones dificultan la comercialización de un inmunoliposoma debido a su elevado coste. Como alternativa al uso de anticuerpos, en el Artículo 3 proponemos el uso de la heparina, que ha demostrado ser altamente específica para pRBCs, como elemento direccionalizador en futuros nanovectores. Otra alternativa al uso de anticuerpos que se está estudiando actualmente en nuestro grupo, es la utilización de aptámeros de DNA, que se caracterizan por una elevada afinidad de unión, una baja inmunogenicidad y una producción más rápida y económica que los anticuerpos.

La ruta de administración también es un factor importante a tener en cuenta en el diseño de terapias contra la malaria. La ruta oral es la de primera elección para el tratamiento de la malaria no severa. Nuestro nanovector inmunoliposomal es adecuado para la administración parenteral, que está indicada en el caso de malaria severa, donde los pacientes se encuentras en hospitales y centros médicos que tienen los recursos para almacenar los inmunoliposomas en neveras. Un tratamiento parenteral en forma de nanovector liposomal podría ser una herramienta muy útil para la última milla de la estrategia de erradicación de la malaria, donde utilizando una dosis de un fármaco direccionalizado a pRBCs se lograra la eliminación de cepas de parásito multiresistentes. La formulación para administración oral de anticuerpos y liposomas es complicada, nanovectores adecuados para esta vía de administración serían una contribución valiosa para el tratamiento de la malaria en zonas endémicas, alejadas de centros de salud.

Durante la última parte de esta tesis, nos hemos centrado en el desarrollo de nuevos nanovectores poliméricos que liberen de forma específica los fármacos a pRBCs, ya que las nanopartículas poliméricas pueden ser formuladas para administración oral más fácilmente que los liposomas. Hemos seleccionado tres polímeros de la familia de las poliamidoaminas: ISA1, ISA23 y AGMA1

para el estudio de su capacidad como nanovectores potenciales para la liberación de antimaláricos.

Los resultados obtenidos mediante microscopía de fluorescencia, citometría de flujo y microscopía electrónica con polímeros marcados con fluoresceína demuestran que estos tres polímeros presentan una interacción específica con pRBCs. Además, su caracterización mediante AFM y cryo-TEM indican que su tamaño oscila entre 10-40 nm, de manera que podrían ser internalizados en pRBCs y acceder al parásito intracelular, siendo a priori nanovectores interesantes para el direccionamiento específico de fármacos hacia pRBCs. ISA1 fue descartado de los siguientes experimentos debido a su elevada toxicidad *in vivo*.

El polímero AGMA1 presenta capacidad antimalárica *per se*, que incrementa con el peso molecular del polímero y que probablemente sea debida al aumento de interacción de este polímero con pRBCs y RBCs que se observa en las fracciones de elevada masa molecular mediante citometría de flujo y microscopía confocal. El direccionamiento se ha confirmado para otras especies de *Plasmodium*, y este resultado unido al efecto del peso molecular sugiere que el mecanismo de direccionamiento de los polímeros hacia pRBCs probablemente sea debido a muchas interacciones de baja afinidad, posiblemente de naturaleza electrostática. El desarrollo de un nanovector sin un elemento direccionalizador no fue considerado en nuestro primer prototipo, pero confiere ventajas importantes al sistema en aspectos ya discutidos como son el coste, estabilidad y facilidad para formulación oral.

Los polímeros AGMA1 e ISA23 fueron conjugados a cloroquina y primaquina mediante uniones electrostáticas, y los resultados obtenidos *in vitro* indican que los polímeros liberan el fármaco en las células dianas para que éste pueda ejercer su acción. Los resultados obtenidos *in vitro* son modestos comparados con los resultados *in vivo*, probablemente debido a que la circulación sanguínea favorece los encuentros aleatorios entre pRBCs y polímeros que se

requieren para el direccionamiento específico. Los resultados *in vivo* demuestran que ratones infectados con *P. yoelii* que han sido tratados con CQ unida a polímeros son capaces de curarse y sobrevivir a la infección con una cepa letal del parásito, mientras que los ratones tratados con la misma cantidad, o el doble, de fármaco libre mueren.

Los dendrímeros también son otros candidatos interesantes para el desarrollo de sistemas de liberación dirigida de antimaláricos. Los derivados dendríticos que se han testado a raíz de la colaboración con el INA, presentan actividad antimalárica *per se* y direccionamiento específico a pRBCs. Los ensayos preliminares *in vitro* con estos compuestos con CQ y PQ han sido muy prometedores ya que se ha mejorado la actividad antimalárica del fármaco soluble, no obstante, estos derivados son más caros y más difíciles de sintetizar que los polímeros de la familia de las poliamidoaminas.

Para obtener el nanovector más simple y más económico, pero que al mismo tiempo sea capaz de reducir y/o eliminar de un modo significativo la parasitemia de las personas que viven en áreas endémicas de malaria, es necesario encontrar un equilibrio entre complejidad, eficacia y coste. La optimización y el diseño de un sistema suficientemente barato (1 dólar por dosis) y estable (más del 50% de su actividad original después de un mes a 37ºC) que pueda ser utilizado como tratamiento para la malaria no severa son necesarios para el desarrollo de un tratamiento con posibilidades de ser utilizado en áreas endémicas, donde el precio y la facilidad del proceso de escalado de un producto gobiernan sus posibilidades de ser comercializado, sobretodo en el caso de la malaria. Considerando estos factores, el escenario para los polímeros es prometedor, ya que según nuestros cálculos para eliminar la parasitemia de un litro de sangre el coste del prototipo inmunoliposomal ascendería a 50€, mientras que el de los polímeros sería de poco más de 1€.

Las diferentes partes de futuros nanovectores (moléculas direccionalizadoras, formulación liposomal, recubrimiento exterior, fármaco encapsulado) están diseñadas de tal manera que puedan ser sustituidas por nuevos elementos para su utilización contra diferentes especies del parásito o para reconocer diferentes dianas intracelulares. Esta tecnología podría compararse a un sistema de tipo *Lego*, que podría aplicarse contra una gran variedad de patologías causadas por parásitos intracelulares o incluso otro tipo de enfermedades y permitiría aplicar los beneficios de la nanomedicina a los tratamientos utilizados actualmente.

CONCLUSIONES

1. Inmunoliposomas direccionalizados liberan su contenido al 100% de eritrocitos infectados por *Plasmodium* y al 0% de eritrocitos sanos en menos de 90 minutos, incluso en presencia de otros tipos celulares.
2. Se ha incrementado diez veces la actividad contra el parásito de antimaláricos encapsulados en inmunoliposomas respecto a fármacos libres.
3. Se ha demostrado el elevado direccionamiento y fuerza de unión de la heparina a eritrocitos infectados por las fases tardías del parásito.
4. Se han sintetizado nuevos nanovectores poliméricos que reconocen específicamente pRBCs y se han conjugado a los antimaláricos cloroquina y primaquina.
5. Experimentos *in vivo* han demostrado que los polímeros AGMA1 e ISA23 conjugados a cloroquina y administrados por vía intraperitoneal curan a ratones infectados con malaria, incrementando la actividad de la cloroquina libre.
6. Resultados preliminares indican que los derivados de Pluronic® son una clase prometedora de nanovectores para la liberación dirigida de antimaláricos.

ANNEX II: REVIEW

Nanotools for the Delivery of Antimicrobial Peptides

Patricia Urbán[#], Juan José Valle-Delgado[#], Ernest Moles, Joana Marques, Cinta Díez and Xavier Fernàndez-Busquets*

[1]*Nanobioengineering Group, Institute for Bioengineering of Catalonia, Baldiri Reixac 10-12, Barcelona E08028, Spain;* [2]*Barcelona Centre for International Health Research (CRESIB, Hospital Clínic-Universitat de Barcelona), Rosselló 149-153, Barcelona E08036, Spain;* [3]*Biomolecular Interactions Team, Nanoscience and Nanotechnology Institute (IN*^{2}*UB), University of Barcelona, Martí i Franquès 1, Barcelona E08028, Spain*

Abstract: Antimicrobial peptide drugs are increasingly attractive therapeutic agents as their roles in physiopathological processes are being unraveled and because the development of recombinant DNA technology has made them economically affordable in large amounts and high purity. However, due to lack of specificity regarding the target cells, difficulty in attaining them, or reduced half-lives, most current administration methods require high doses. On the other hand, reduced specificity of toxic drugs demands low concentrations to minimize undesirable side-effects, thus incurring the risk of having sublethal amounts which favour the appearance of resistant microbial strains. In this scenario, targeted delivery can fulfill the objective of achieving the intake of total quantities sufficiently low to be innocuous for the patient but that locally are high enough to be lethal for the infectious agent. One of the major advances in recent years has been the size reduction of drug carriers that have dimensions in the nanometer scale and thus are much smaller than —and capable of being internalized by— many types of cells. Among the different types of potential antimicrobial peptide-encapsulating structures reviewed here are liposomes, dendritic polymers, solid core nanoparticles, carbon nanotubes, and DNA cages. These nanoparticulate systems can be functionalized with a plethora of biomolecules providing specificity of binding to particular cell types or locations; as examples of these targeting elements we will present antibodies, DNA aptamers, cell-penetrating peptides, and carbohydrates. Multifunctional Trojan horse-like nanovessels can be engineered by choosing the adequate peptide content, encapsulating structure, and targeting moiety for each particular application.

Keywords: Antibodies, aptamers, dendrimers, liposomes, nanomedicine, nanoparticles, nanovectors, targeting.

ANTIMICROBIAL PEPTIDES

Some peptides are extremely potent *in vivo* antimicrobials that disrupt biological membranes or enter cells to interfere with pathogen metabolism [1]. Members of the cationic host defence peptide family are widely distributed in nature and vary substantially in their amino acid sequences, secondary structures, inducibility, potency, and activity spectra. In general, they have between 12 and 50 amino acids of which two to nine are positively charged lysine or arginine residues and as many as 50% are hydrophobic. Usually the peptides are expressed by innate immune cells as inactive propeptides that require cleavage by a protease. Although microbial and host structures share many components, antimicrobial polypeptides achieve specificity by exploiting differences between corresponding host and microbial structures, thus selectively concentrating themselves on microbial surfaces.

The mechanism of the direct antimicrobial activity of peptides is based on the folding of their processed, biologically active forms, into different secondary structures: amphipathic α-helices, β-hairpins, extended conformations, and cyclic species. Some of these structures fold after insertion into pathogen membranes such that the charged/polar and hydrophobic residues form patches on the surface of the cell, which in turn can lead to a rearrangement of the peptides to form one of four accepted models: barrel, carpet, toroidal pore, and aggregate. If this induces a substantial local perturbation of the lipid bilayer, cell membrane permeability is altered leading to cell death. An interesting example is that of the eosinophil cationic protein (ECP or RNase 3), a ribonuclease that is part of the human innate immune system [2], which has anti-pathogenic capabilities against viruses, bacteria [3], and protozoa [4, 5] and is involved in inflammatory processes mediated by eosinophils [6]. The antimicrobial activity of ECP has been associated primarily with its ability to disrupt membranes and it is dependent on both hydrophobic and cationic residues exposed on the surface of the protein [7]. ECP has been shown to partially insert into liposomes, promoting their aggregation and lysis according to a carpet-like mechanism [8].

Medicinal use of peptides has been often hampered by their rapid degradation by proteolytic enzymes in the gastrointestinal tract, which limits their administration to a parenteral route, although proteases in the bloodstream are also abundant. As a result, the biological half-life of peptides is short and demands frequent intake, whereas their transport across biological barriers is poor because of limited diffusivity and low partition coefficients. In the case of antimicrobial drugs it is essential to deliver sufficiently high local amounts

*Address correspondence to this author at the Nanomalaria Group, Centre Esther Koplowitz, 1st floor, CRESIB, Rosselló 149-153, Barcelona E08036, Spain; Tel: +34 93 227 5400 (ext 4276); Fax: + 34 93 403 7181;
E-mail: xfernandez_busquets@ub.edu

[#]*Both authors contributed equally*

1873-5592/12 $58.00+.00

to avoid creating resistant parasite strains [9], a common risk when using sustained low doses in order to limit the toxicity of the drug for the patient. In this context, nanoparticulate biodegradable systems have been proposed as an efficient means of peptide administration [10]. Rapidly increasing in the literature are reports on nanosized structures for the delivery of a number of therapeutic peptides, among which insulin, interferon, or the glycopeptide antibiotic vancomycin [11-15]. Here we will present an overview of nanoparticulate systems that can be applied to the targeted administration of antimicrobial peptides.

CONTROLLED DRUG DELIVERY

As stated in Paracelsus' Law of dose response, *There are no safe molecules nor toxic ones. It is the dose that makes the poison*. The challenge of antimicrobial drug delivery is the liberation of drug agents at the right time in a safe and reproducible manner, usually to a specific target site [16, 17]. Conventional dosage forms, such as orally administered pills and subcutaneous or intravenous injection, are the predominant administration routes, but they typically provide an immediate release. Consequently, to achieve therapeutic activity extending over time, the initial concentration of the drug in the body must be high, causing peaks (often adjusted to stay just below known levels of toxicity) that gradually diminish over time to an ineffective level. While the last three decades have seen considerable advances in drug delivery technology, major unmet needs remain. Among these are the broad categories of (i) continuous release of therapeutic agents over extended time periods and in accordance with a predetermined temporal profile [18, 19], (ii) targeted delivery at local sites to overcome systemic drug toxicity and ameliorate activity [20], and (iii) improved ease of administration, which would increase patient compliance while reducing the need for intervention by health care personnel and decreasing the length of hospital stays [21]. Success in addressing some or all of these challenges would lead to improvements in efficacy and limitation of side effects [22]. The potential therapeutic advantages of continuous-release antimicrobial drug delivery systems are significant and include minimized peak plasma levels, predictable and extended duration of action, and reduced inconvenience of frequent dosing [23, 24]. New drugs with ever increasing potency are being developed, many of them of peptidic nature and with a narrow therapeutic window (the concentration range outside the toxic regime where the drug is effective). Toxicity is observed for concentration spikes, which renders traditional methods of drug delivery ineffective [25]. In addition, conventional oral doses of these agents are frequently useless because the drugs are destroyed during intestinal transit or poorly absorbed. These limitations have fostered research in drug delivery systems providing a controlled release, which include transdermal patches, implants, inhalation systems, bioadhesive systems, and nanoencapsulation.

NANOVECTORS FOR TARGETED DRUG DELIVERY

The potential intersection between nanotechnology and the biological sciences is vast. The ability to assemble and study materials with nanoscale precision leads to opportunities in both basic biology (e.g., testing of biological hypotheses that require nanoscale manipulations) and development of new biomedical technologies such as drug delivery systems, imaging probes, or nanodevices [26-28]. It was Paul Ehrlich who popularized the *magic bullet* concept [29], according to which therapeutic agents would be directed specifically to destroy their diseased targets without harming any of the surrounding healthy cells. However, a century later the clinical implementation of this medical holy grail continues being a challenge in three main fronts [30]: identifying the right molecular or cellular targets for a particular disease, having a drug that is effective against it, and finding a strategy for the efficient delivery of sufficient amounts of the drug in an active state exclusively to the selected targets. This last requirement has to overcome the physiological mechanisms evolved to prevent the entry of alien structures into and clear them from the organism, namely physical barriers and the immune system. Nanovessels are one of the most promising structures being studied for their use in targeted drug delivery. Nanoparticulate systems are a miscellaneous family of submicron structures that can be inorganic, liposomal, polymeric, and even carbon nanotube-based. They are typically self-assembling and unable to self-replicate, and the main feature that makes them attractive drug carriers is their small size up to several hundred nm, which allows them to cross biological barriers. Since biological function depends heavily on units that have nanoscale dimensions, engineered devices at the nanoscale are small enough to interact directly with sub-cellular compartments and to probe intracellular events. Because many cells will internalize drug-loaded nanoscale particles, then nanoparticles can be used to deliver high drug doses into cells, and to release them in an environmentally controlled, temporally expanded profile. At the expense of lower drug loading capacity, the nanometer size range also reduces the risk of undesired clearance from the body through the liver or spleen and minimizes uptake by the reticuloendothelial system [31, 32]. Smaller particles have greater surface area/volume ratios, which increase dissolution rates, enabling them to overcome solubility-limited bioavailability [33]. Even within the nanoscale range, size variation strongly affects bioavailability and blood circulation time [34, 35]. Following systemic administration, particles below 10 nm are rapidly removed through extravasation and renal clearance [36] and those between 10 and 70 nm can penetrate even very small capillaries [37], whereas particles with diameters ranging from 70 to 200 nm show the most prolonged circulation times [34]. Larger particles are usually sequestered by the spleen and eventually removed by phagocytes [38].

A second essential characteristic of most nanoparticles is that their surface can be modified with appropriate molecules to dock them to specific target sites, and with camouflage elements designed to evade immune surveillance and to extend their blood residence time and half-life [39]. The most significant effect of functionalizing nanoparticles with targeting ligands is the increased intracellular uptake by target cells [40-42], which usually translates into a higher efficacy of encapsulated drugs [43]. Nanoparticles can also be modified to achieve efficient intracellular targeting to specific organelles: anionic particles usually remain in lysosomes whereas those positively charged become predominantly localized in the cytoplasm and within mitochondria [44].

Because of this combination of properties-subcellular size, controlled-release capability, and susceptibility to external activation— devices provided by nanotechnology will enable imminent new applications in biological and medical science [16, 45, 46].

TYPES OF NANOTOOLS FOR PEPTIDE TARGETED DELIVERY

As we have outlined above, several attempts have been made at delivering polypeptides as nanoparticulate systems. Proteins precipitated as spherical particles ranging in size from 100 to 500 nm were successfully prepared and used for aerosol delivery [47]. A biodegradable albumin core coated with fatty acids was assayed to encapsulate vancomycin for improved colon-specific release [13]. Administration of peptides inside biodegradable gelatin [12] or lipid nanoparticles has also been tested as a strategy to achieve a more efficient therapy through sustained release, e.g. for the administration of the antibiotic decapeptide polymyxin B [11]. Although these were successful approaches that represented an improvement when compared with the administration of free peptide, they had limited control over particle size and hardly any influence on the site of drug release at cell level. Here we are going to focus on encapsulation nanodevices of controlled dimensions and having the capability of being targeted to specific cell types or subcellular compartments.

Liposomes

Liposomes were first proposed as drug delivery vehicles by Gregoriadis in the 1970's [48]. They are self-assembling artificial lipid bilayer-bounded spheres up to several hundred nm in diameter, generally formed by amphiphilic phospholipids and cholesterol enclosing an aqueous inner cavity, and with a polar surface which can be neutral or charged. For drug delivery applications [49] liposomes are usually unilamellar and range in diameter from 50 to 200 nm, with larger liposomes being rapidly removed from the blood circulation. Encapsulation of hydrophobic or water-soluble drugs into, respectively, the bilayer or the hydrophilic core, can be done with a variety of loading strategies [50], which include the pH gradient [51] and ammonium sulfate [52] methods, and the direct drug entrapping simultaneously with liposome formation, or lipid film hydration [43]. Liposomes improve the delivery of bioactive molecules by functioning as circulating microreservoirs for sustained release because of their unique advantages which include the protection of drugs from degradation and the possibility of targeting them to the site of action and reducing their toxicity or side effects [53, 54]. The stability of the liposomal membrane, i.e., its mechanical strength as well as its function as a permeability barrier, depends on the packing of the hydrocarbon chains of lipid molecules. Neutral liposomes with tightly packed membranes exhibit increased drug retention and circulation half-life *in vivo*. The compact lipid association reduces binding of proteins which tend to destabilize the membrane and mark the liposomes for removal by phagocytic cells. The development of novel formulations with, e.g., polyethylene glycol (PEG) lipid derivatives resulted in sterically stabilized liposomes, termed stealth liposomes [55], with reduced mononuclear phagocyte system uptake and prolonged blood residence times [56, 57]. For conventional liposomes, circulation half-lives up to 12 h can be obtained, which are highly dependent on dose, whereas stealth liposomes have blood residence times above 24 h, with dose-independent clearance kinetics. Liposomes are naturally removed from the blood by resident macrophages mainly in the liver and spleen, an advantageous phenomenon when this cell type is the intended target, as is the case for many intracellular parasites localizing in phagocytic cells [50].

A drug carrier of clinical utility must be able to efficiently balance drug retention while in circulation with the ability to make the drug bioavailable at the disease site. Different liposome formulations provide passive control of drug release rates depending on lipid composition [50]. Active release, on the other hand, relies on a triggering mechanism to destabilize the liposomal bilayer once the drug reaches the pathogen. This can be a change in environmental factors encountered at disease sites such as a low pH or particular enzymes, or an external factor such as local heating or photochemical induction. Nanosized carriers have been receiving special attention with the aim of minimizing the side effects of malaria therapy by increasing bioavailability and selectivity of drugs [58]. Red blood cells (RBCs) have very poor endocytic processes, and for this reason liposomes docked by specific antibodies to RBCs can be an efficient system to deliver cargo into the cell by a simple membrane fusion process [43, 59-61], without the need for including fusogenic lipids in the liposome formulation. Many antibiotics are inactive against Gram-negative bacteria because of their inability to cross the outer membrane of these cells. Fusogenic liposomes have been used to localize vancomycin to the periplasmic space, showing an *in vitro* ability to inhibit to a certain extent the growth of Gram-negative bacterial strains when neither the free antibiotic nor vancomycin-loaded non-fusogenic liposomes had a significant antibacterial effect [62]. Liposomes encapsulating polymyxin B [63] have been proposed for the treatment of resistant Gram-negative bacterial infections due to the ability of the liposomal formulation to overcome the permeability and cell surface alterations responsible for the development of microbial resistance. When liposomal tobramycin or polymyxin B were tested against *Pseudomonas aeruginosa* in the cystic fibrosis sputum, the results obtained suggested their potential applications for the treatment of cystic fibrosis lung infections [64].

Liposomes bearing cell-specific recognition ligands on their surfaces have been widely considered as drug carriers in therapy due to their non-toxic and biodegradable character [65]. And yet, despite this versatility, major drawbacks to the use of liposomal nanocarriers in targeted drug delivery exist: limited control over release of the drug and thus potential leakage before reaching the target site, low encapsulation efficacy, relatively poor stability during storage, short *in vivo* circulation times, large size, and difficulty in formulation for oral administration. Most of these flaws can be overcome with the use of other types of nanocapsules.

Polymeric Structures

Polymers offer effectively unlimited diversity in chemistry, dimensions and topology, rendering them a class of materials that is particularly suitable for applications in

nanoscale drug delivery systems [66]. Biodegradable polymeric nanoparticles are made of natural or artificial polymers and range in size between 10 and 1000 nm, and if adequately targeted they can be used to deliver highly localized drug doses into specific cell types or tissues [67]. Nanoparticles can carry drugs in adsorbed, dissolved, entrapped, encapsulated, or covalently bound form. Drug loading into nanoparticles is generally done by one of three methods: incorporation of the drug at the time of nanoparticle synthesis, absorption after nanoparticles formation by incubating these in a solution of the drug, or chemical conjugation of drugs into preformed nanoparticles. Drug release from nanoparticles is a process governed by either cleavage or desorption of surface-bound or adsorbed drugs, respectively, diffusion through the nanosphere matrix or nanocapsule polymer wall, or biodegradation resulting in nanoparticle disintegration in a particular physiological environment. Long-circulating polymeric nanoparticles have been obtained mainly by two methods: surface coating with hydrophilic polymers/surfactants and development of biodegradable copolymers with hydrophilic segments [68]. Some widely used coating materials are PEG, polyethylene oxide, poloxamer, polysorbate (e.g. Tween-80), and lauryl ethers (e.g. Brij-35). Methods for the preparation of surface-modified sterically stabilized particles are reviewed in the literature [68, 69]. Properties of the nanoparticles are largely dependent on the polymer employed, and biocompatibility issues are a main concern. Polycations are often cytotoxic, haemolytic, and complement-activating, whereas polyanions are less cytotoxic but can induce anticoagulant activity and cytokine release [70]. An ever increasing number of biocompatible polymer blocks are being used to synthesize polymeric nanoparticles, among them poly(D,L-lactide-co-glycolide) [71], poly(alkylcyanoacrylate) [72], chitosan [73-75], gelatin [12], poly(methylidene malonate) [76], starch [77], alginate [78], or polyethylene carbonate [79]. Hydrogels are an interesting type of polymeric nanoparticles formed by three-dimensional networks composed of ionic or neutral hydrophilic polymers physically and/or chemically crosslinked [80, 81], whose common characteristic is their ability to swell by imbibing large amounts of water. Physiologically responsive hydrogels can exhibit dramatic changes in volume, network structure, permeability, or mechanical strength in response to different stimuli like variations in pH, ionic strength or temperature. This special behavior has inspired the design of biocompatible drug delivery systems [80-83] where the encapsulated drug is usually released during the swelling of the hydrogel [84-87], although drug delivery as a result of a squeezing mechanism has also been reported [88].

In the case of biodegradable polymers, which decompose into products that can be completely eliminated by the body, significant advantages are their history of safe use, proven biocompatibility, a high surface/volume ratio, and ability to control the time and rate of polymer degradation and peptide release, thus increasing the half-life of bioactives [89]. The most promising degradable synthetic polymers used in biomedical applications are poly(hydroxyacid)s, poly(caprolactone)s, poly(ether-ester)s, poly(orthoester)s, poly(anhydride)s, poly(phosphazene)s, and poly(aminoacid)s. Biodegradable polymers containing entrapped drugs can be used for localized delivery and/or controlled release over a period trolled release over a period of months. The release rates of drugs from biodegradable polymers can be controlled by a number of factors, such as biodegradation kinetics of the polymers, physicochemical properties of polymers and drugs, or thermodynamic compatibility between them. Hybrid polymer-based constructs have already shown that they can satisfy the requirements of industrial development and regulatory authority approval. Poly(amidoamine)s (PAAs), a family of biodegradable and biocompatible polymers, are promising materials for different pharmaceutical and biotechnological applications. They display membrane disruptive properties in response to a decrease in pH, conferring endosomolytic properties *in vitro* and *in vivo*, and are being studied as a synthetic alternative to fusogenic peptides as they display upon protonation at reduced pH conformational changes leading to membrane perturbation [90].

Some antimicrobial peptides have their targets in pathogens found inside the brain, such as the yeast *Cryptococcus neoformans* responsible for a form of meningitis [91]. Treatment in these cases is complicated by the poor penetration of most drugs across the blood-brain barrier (BBB). The BBB is formed by the tight endothelial cell junctions of the capillaries within the brain, which limits the ability of many molecules to enter the central nervous system (CNS). Surface-modified polymeric nanoparticles able to cross the BBB have been used to deliver chemicals acting on the CNS [92], and promising results have been obtained using such *Trojan horse* nanocapsules [93, 94]. The mechanism of enhancement of drug transport from the coated nanoparticles through the BBB is thought to be due to [68] (i) binding of the nanoparticles to the endothelium of brain capillaries and delivery of drugs to the brain by providing a large concentration gradient which enhances passive diffusion, and/or (ii) brain endothelial uptake by phagocytosis.

Dendritic Polymers

Dendrimers are a type of polymeric nanoparticles having definite molecular mass, shape, and size, formed by synthetic, highly branched, monodisperse macromolecules [95-97]. They possess three distinguishing architectural components, namely an initiator core, an interior layer radially attached to the initiator and composed of repeating units added in successive synthetic generations, and an outer functionalized layer bound to the outermost interior generation. The core is sometimes denoted generation zero (G0); the core for a polypropylene imine (PPI) dendrimer is 1,4-diaminobutane, whereas for a PAA dendrimer is ammonia. This type of architecture induces the formation of nanocavities, the environment of which determines their encapsulating properties, whereas the external groups primarily define solubility and chemical behavior. Hyperbranched polymers (Fig. **1**) are nonsymmetrical, polydisperse, and less expensive than dendrimers, which are prepared under tedious multistep reaction schemes [96]. Dendrimeric and hyperbranched polymers are called collectively dendritic polymers.

Dendritic polymers have a vacant inner core that can encapsulate drug molecules [98-101], often with high drug payloads [102]. Dendrimers are, despite their relatively large molecular size, structurally well defined, with a low polydispersity in comparison with traditional polymers. Highly

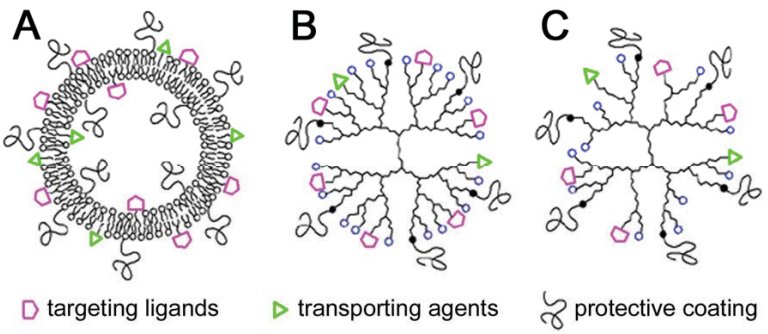

Fig. (1). Schematic representation of multifunctional (**A**) liposomal, (**B**) dendrimeric, and (**C**) hyperbranched polymeric systems. From the National Center of Scientific Research "Demokritos", Greece, web site (http://ipc.chem.demokritos.gr).

branched dendrimers such as PAA have been extensively studied for their biocompatible and non-immunogenic properties and for their ability to cross cell membranes with minimal perturbation [103]. Dendrimers of a sufficiently small size can be internalized by cells [104, 105], an attractive characteristic for drug delivery applications. Investigations using cationic and anionic PAA dendrimers in the size range 3-7 nm revealed that their uptake in everted rat intestinal systems most likely occurs across enterocytes by transcytosis [106]. Dendrimers protect their encapsulated drugs from fast degradation in the physiological environment and offer a continuous and temporally expanded release. In contrast to proteins, which consist of folded, linear polypeptide chains, the branched architecture of the dendrimer interior is to a large extent formed by covalent bonds, resulting in a somewhat less flexible structure. In addition, the dendrimer is on average less compact than a protein, and it contains a substantially higher number of surface functional groups than proteins of comparable molecular mass. However, polypeptide dendrimers have been synthesized [107], and glycoconjugated peptide dendrimers have been successfully assayed to encapsulate the antimalarial drugs chloroquine [108] and primaquine [109].

One of the advantages of dendrimers is the possibility of modulating their properties through modification of their large surface area [110]. This surface modification can be used for the covalent attachment of drugs, or to functionalize the dendrimer with targeting molecules such as cell penetrating peptides, carbohydrates [111], or antimicrobial peptides [112]. The multivalency of their surface provides a tighter binding than the low affinity of single ligands [100]. However, in spite of their broad applicability, associated toxicity due to the terminal amino groups and cationic charge of PAA and PPI dendrimers hampers their clinical applications [109]. One approach to improve dendrimer biocompatibility contemplates surface modifications [113], including capping of the terminal $-NH_2$ groups with neutral or anionic moieties such as PEG. It has been found that amino-terminated PAA dendrimers and their partially PEG-coated derivatives possess attractive antimicrobial properties, particularly against Gram-negative bacteria [114, 115]. Partial modification of amino-terminated PAA with PEG did not reduce toxicity to *P. aeruginosa*, while it greatly reduced toxicity to epithelial cells. Furthermore, G4-PAA-OH dendrimers have shown bactericidal effect and ability to treat *Escherichia coli* infections *in vivo* in pregnant guinea pigs. The G4-PAA-NH_2 dendrimer, known to be a potent antibacterial agent, was found to be highly cytotoxic in the μg/mL range whereas the G4-PAA-OH dendrimer was non-cytotoxic up to 1 mg/mL. This phenomenon could be attributed to the different interaction of G4-PAA-OH and G4-PAA-NH_2 with bacterial membranes [116].

Solid Core Nanoparticles

The term nanoparticle is a collective name for both nanospheres and nanocapsules. Nanospheres are dense polymeric matrices in which the drug may be dispersed within the particle or adsorbed on the sphere surface, whereas nanocapsules present a polymeric shell surrounding a liquid core where the active substances are usually dissolved, although they may also be adsorbed on the capsule surface. A common approach among nanobiosystem development is building around a core nanoparticle whose material offers good properties regarding stability and/or detection [27, 117]. One of the most extensively explored core nanoparticle material is metals, with gold, silver, iron, cobalt, nickel, platinum, and various metal composite nanoparticles being currently studied [118]. A particularly interesting characteristic of solid core nanocapsules is that they can combine different properties in individual particles, based on different compositions of the core and the shell. The core can be built to have a useful physical property (e.g. semiconductors, metals, magnetic oxides) that can make the nanoparticle responsive to mild external signals (such as light, ultrasounds, or magnetic fields) so that the movement of the particles could be directed from outside the body, or the particles could be activated at particular sites [119-121]. Liposomes can be combined with a large variety of nanomaterials, such as mesoporous silica nanoparticles [122] or superparamagnetic iron oxide nanocores. Because the unique features of both the magnetizable colloid and the versatile lipid bilayer can be joined, the resulting so-called magnetoliposomes [123] can be exploited in a great array of biotechnological and biomedical applications, including magnetic resonance imaging, hyperthermia cancer treatment and drug delivery.

The shell of solid core nanoparticles can be used to functionalize the nanoparticle with targeting molecules in order to direct it to the desired location in drug delivery applications. Gold colloids have been postulated as promising candidates in nanomedicine due to their bioinertness, cellular imaging ability, and presumed nontoxicity [124], and they have even been proposed for the delivery of drugs inside the brain [125]. In addition, conjugation to gold surfaces is readily performed for thiol-containing molecules in aqueous buffers. However, recent data have shown that in a human keratinocyte cell line gold nanoparticles induced changes in cellular morphology, mitochondrial function, mitochondrial membrane potential, intracellular calcium levels, DNA damage-related gene expression, and of p53 and caspase-3 expression levels [126]. Although metallic nanoparticles provide stability and enhanced detection capabilities of the nanobiosystem, some metals are toxic in elemental form. Nanotoxicology is an embryonic field and the dynamics and toxicity of these nanomaterials *in vivo* are not well understood at this time [27, 127]. Toxicity of nanomaterials is difficult to evaluate with the masking presence of hydrophilic coatings used to make these nanostructures biocompatible. Toxicity may well vary with nanoparticle size, and it could increase on an expanded timescale if the biocoatings are removed once inside the cell. Because the toxicity of metallic nanoparticles remains a largely unresolved issue, other biodegradable nanobiosystems threaten their development.

Carbon Nanotubes

Carbon nanotubes (CNT) are cylinders of 10-100 nm in diameter and up to several hundred microns in length, whose walls are formed by one (single-walled CNTs) or several (multi-walled CNTs) rolled-up graphene sheets [128]. Although CNT are insoluble in physiological conditions, the development of efficient methodologies for chemical modifications which increase solubility in aqueous environment has stimulated their application as drug delivery vessels. CNTs can be derivatized with bioactive peptides, proteins, nucleic acids and drugs, and used to deliver their cargoes to cells and organs [129, 130]. Because functionalized CNTs display low toxicity and immunogenicity and have a high propensity to cross cell membranes, they hold great potential as nanocarriers in biomedical applications [128, 131], particularly as vehicles for the delivery of small drug molecules [132-134]. Molecular dynamics simulation studies have been used to explore the chemical and physical interactions between model peptides and carbon nanotubes (Fig. **2**), showing that upon encapsulation peptides remain close to their native conformations [135]. Peptides were detected interacting with the outer walls of nanotubes, encapsulated into, and covalently bound to them. The results suggested that the confined space of the nanotube and its interaction with peptides stabilizes their structure, whereas covalent crosslinking to carbon nanotubes may lead to a change in the peptide conformation. No significant conformation changes were detected for peptides interacting non-covalently with nanotube outer walls.

However, as in the case of metallic nanoparticles, an important issue regarding the applicability of CNTs for antimicrobial peptide delivery is their biocompatibility. Actually, CNTs are not biodegradable at all, and the modification of their surface polarity by the introduction of charged groups results in better solubility but not in better biodegradability [136].

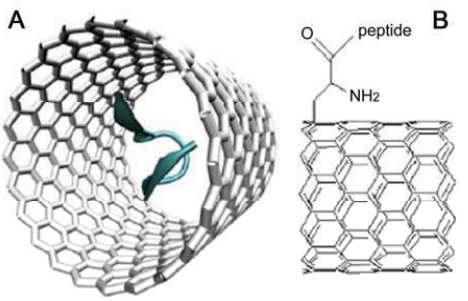

Fig. (2). Schematic representation of a beta-hairpin peptide (A) encapsulated in and (B) covalently linked to the outer wall of a carbon nanotube. From [135], with permission.

DNA Cages

The biological function, nanoscale geometry, low toxicity, biodegradability, and molecular recognition capacity of DNA make it a promising candidate as novel functional nanomaterial [137]. In particular, 3D DNA materials have tremendous potential applications in drug delivery systems. The so-called DNA *origami* technique has been applied to the construction of 3D boxes with controllable lids [138], where six DNA origami faces were designed to assemble into a hollow 3D box. The lid of the box was dynamically opened and closed by introducing *key* oligonucleotide sequences that displaced DNA duplexes holding the lid closed. Opening the box lid could be observed by changes in fluorescence resonance energy transfer between two fluorescent dyes placed on the DNA structure at strategic locations. Cage-like large three-dimensional structures made of DNA molecules have been successfully self-assembled from three different types of single-stranded DNA [139]. The three DNAs spontaneously formed three-point-star motifs, or tiles, that then progressed to polyhedral shapes in a one-pot process. By controlling the flexibility and concentration of the tiles, the molecular assembly yielded tetrahedra, dodecahedra, or buckyballs tens of nanometers across and having pores up to 20 nm (Fig. **3**). These two examples of DNA nanocages could be developed into carriers for controlled drug release.

Pharmacokinetics and Biodistribution of Nanoparticles

As discussed above for liposomes, a number of factors can influence nanoparticle blood residence time and organ-specific accumulation, which include interactions with biological barriers and nanoparticle composition, size, and surface modifications [140]. As a rule of thumb, reduction in the rate of mononuclear phagocyte system uptake and prolongation of the blood circulation half-life will be maximal for neutrally charged nanoparticles with a mean diameter of ca. 100 nm and surface-modified with PEG [141]. Interestingly, worm-shaped nanoparticles composed of a diblock copolymer circulate in the mouse blood with a very long

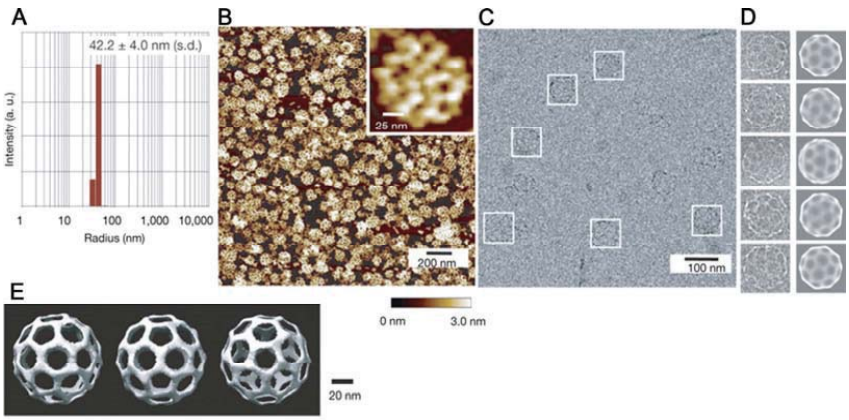

Fig. (3). A DNA cage. (**A**) Size histogram of the DNA buckyball measured by dynamic light scattering. (**B**) An AFM image and (**C**) a cryo-EM image of the DNA assemblies. (**D**) Individual raw cryo-EM images and the corresponding projections of the DNA buckyball 3D structure reconstructed from cryo-EM images. These particles are selected from different image frames to represent views at different orientations. (**E**) Three views of the DNA buckyball structure reconstructed from cryo-EM images. From [139], with permission.

half-life of ca. 5 days [142]. The underlying mechanism seems to be the strong drag force experienced in the fluid flow by the elongated structures such that the macrophages can not engulf them before they are carried away by the flow. Finally, to have pharmacological efficacy, the encapsulated antimicrobial peptide must be released from the nanovectors to the target cells. One strategy can make use of some type of local triggering mechanism to release the drug, such as pH [143]. Different organs, tissues, and subcellular compartments, as well as their pathophysiological states, can be characterized by their pH levels and gradients. Nanovessels can be designed to respond with physicochemical changes in their structure to such pH stimuli. These include swelling, dissociating, or surface charge switching, in a manner that favors drug release at the target sites. A second approach to increase the rate of intracellular delivery contemplates conjugating a targeting ligand on the nanovector surface.

TARGETING MOLECULES

In general, transport across biological barriers is determined by both the nature of carrier molecules such as size, charge, hydrophobicity, flexibility, and geometry, and the characteristics of the barrier itself such as location, function, and permeability. Mechanisms of uptake through the gastrointestinal tract include persorption, endocytosis by enterocytes, paracellular transport, uptake by intestinal macrophages, and passage through the gut-associated lymphoid tissue [144]. Oral delivery of drugs remains the most attractive mode of administration, but bioavailability of oral drugs is low due to the harsh grastrointestinal tract environment. A number of proposed microscale oral delivery devices have been based on the sequestering of the nanoparticles from the external environment [145-149]. Chitosan-containing particles, if smaller than 500 nm, have a greater capacity of being taken up in their original state through intercellular spaces between the enterocytes and M cells lining the Peyer's patches [150], and nanoparticles composed of mucoadhesive polymers have been proposed for oral delivery of peptide drugs [74]. Particles of size ranges up to 1000 nm can penetrate the intestinal mucosa within 30 to 60 min, and have been successfully assayed for the oral delivery of insulin [15, 148, 151]. However, unlike drug molecules, nanoparticles face additional delivery barriers even after systemic absorption, for instance in avoiding clearance by the reticuloendothelial system and overcoming intracellular barriers.

Active targeting of nanoparticles to the specific sites where pathogens are can be achieved by conjugating them to ligands which interact selectively with receptors present on the target cells. Biological molecules can be immobilized on nanoparticles through a variety of strategies that include physical adsorption, electrostatic binding, specific recognition, and covalent coupling [39]. Although any ligand specifically interacting with the intended delivery site can be used as targeting agent, here we will focus on the three types of biomacromolecules which carry specific binding information in their sequences and/or structures, namely proteins, nucleic acids, and polysaccharides.

Antibodies

The capacity of antibodies to recognize with high specificity virtually any new antigen with which they are presented has been long recognized as a useful tool for the targeting of drugs in therapeutic applications, especially in the case of monoclonal antibodies [152]. Monoclonal antibodies are biological products made in the laboratory that share with antisera made in animals the problem of immunogenicity: targeting antibodies are foreign proteins and elicit an immune response when injected into patients. Antibody engineering has provided a number of strategies to produce antibody forms that are sufficiently small or similar to human antibodies to be nonimmunogenic [153]. The simplest approach is to dispense with the protein domains that are not essential to antigen binding. Antibody fragments, such as antigen binding (Fab) and variable (Fv) region fragments retain the antigen-binding site, with much of the immuno-

genic protein removed. Other antibody subunits are minibodies, diabodies, and nanobodies [117]: minibodies are engineered to contain a fusion of single-chain Fv (scFv) and a C_H3 domain that self assembles into a bivalent dimer [154]; diabodies are covalently or non-covalently linked scFv dimers [155]; nanobodies, which are the smallest of all fully functional antigen-binding fragments, evolved from the variable domain of antibody heavy chains [156]. More recently, small antibody mimetics were formulated by fusing two complementarity-determining regions that retained the antigen recognition of their parent molecules [157]. These 3-kDa entities showed better biodistribution than the original antibodies, suggesting their potential as a new class of targeting ligands. The smaller size of antibody fragments makes them good elements for the targeting of nanovectors expected to diffuse rapidly into tissues and cells, although their single binding site might lead to a weaker interaction with the antigen.

Whatever the type of targeting antibody used, reducing its amount will contribute to minimizing the risk of triggering immune responses leading to nanovector elimination. A fast and efficient strategy for the covalent crosslinking of nanoparticles to antibodies involves the generation of half-antibodies (Fig. **4**), which allows the binding through thiol groups in the hinge regions of immunoglobulin heavy chains [158]. This represents an improvement over the most generally used method for the covalent immobilization of antibody molecules through free amino groups [159], which has the risk of chemically modifying functionally important amino groups in the antigen-binding region of an antibody, causing impairment or loss of function. The resulting significant amount of defective antibody conjugates demands using higher antibody concentrations that will increase the risk of detection by the immune system of the host. An alternative strategy for the oriented immobilization of antibodies is the preparation of immunoconjugates using the oligosaccharide moieties in the antibody Fc region [160].

Immunogenicity is not the only problem encountered when using antibodies for therapy [152]. Some of the biological effects of antibodies are inconvenient in a therapeutic setting, such as the cytokine release reaction triggering a cascade of immunological effects, although such reactions generally depend on crosslinking and are therefore not seen with Fab or Fv fragments.

Antibodies are difficult to formulate for oral administration, which will likely require smaller (but equally 100% specific) targeting agents and drug-containing structures. Orally administered antibodies have been described to be biologically active but only at a local level in the intestinal mucosa [161]. To facilitate intestinal intake, antibodies can be engineered as discussed above to obtain the smallest region preserving an active antigen binding site, still able to carry nanovectors to target cells. Besides their large size,

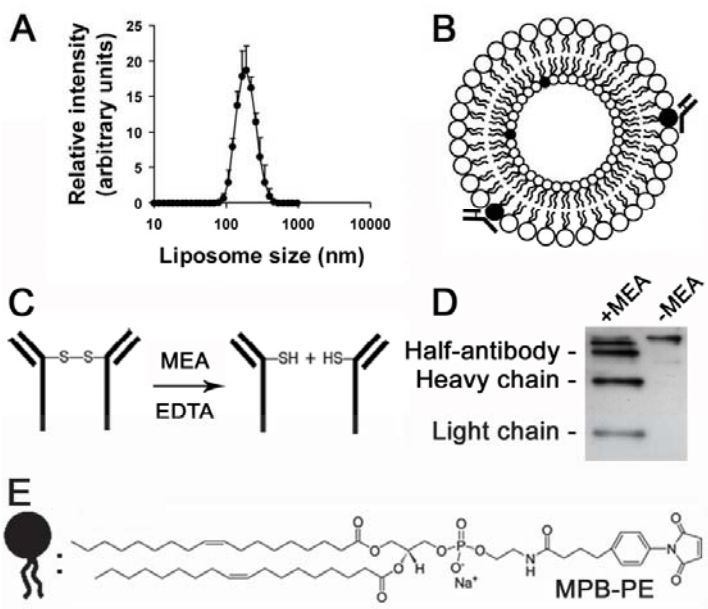

Fig. (4). Preparation of immunoliposomes. (**A**) Dynamic light scattering analysis of liposome size distribution. (**B**) Cartoon showing a liposome functionalized with half-antibodies bound to the thiol-reacting lipid 1,2-dipalmitoyl-sn-glycero-3-phosphoethanolamine-N-[4-(p-maleimidophenyl)butyramide] (MPB-PE), represented as black lipid molecules. (**C**) Scheme of the generation of half-antibodies through reduction with mercaptoethylamine (modified from Pierce Biotechnology catalog). (**D**) Western blot analysis of anti-glycophorin A IgGs (right lane) before and (left lane) after mercaptoethylamine treatment. (**E**) Structure of MPB-PE (extracted from Avanti Lipids catalog), represented as black lipid molecules in panel (**B**). From [43], with permission.

other limitations of antibodies as targeting agents are that they are relatively expensive to manufacture and their batch-to-batch variability.

Nucleic Acid Structures: DNA Aptamers

Most current methods addressed to the identification of molecular targets that could be used in antimicrobial drug delivery strategies rely on lengthy and costly approaches. These include detailed knowledge of the microbe's physiology and biochemistry or the development of immunological methods such as polyclonal and/or monoclonal antibody generation. However, binding specificities and affinities comparable to those of monoclonal antibodies can be obtained with short nucleic acids or peptides termed aptamers [162], much faster and cheaper to produce. DNA aptamers are small oligonucleotides that fold through intra-molecular interactions into unique conformations with ligand binding characteristics. Aptamers can bind to targets with high sensitivity and specificity, being able to distinguish between protein isoforms and different conformational forms of the same protein. Among their advantages as targeting ligands are a small size of up to ca. 15 kDa and a relatively low immunogenicity which leads to better biodistribution [117]. Aptamers can be identified by *in vitro* selection against almost any target, including toxins and antigens which do not induce immune responses for antibody production in host animals. As a result, this novel class of ligands is highly promising for the development of therapeutics and biotechnological tools. DNA oligomers can be identified that bind to biomarkers expressed only by target cells, e.g. cell surface epitopes that differ between two given cell types or between healthy and diseased cells. The potential utility of aptamers for *in vivo* applications and as therapeutic agents is considerably enhanced by the possibility to introduce chemical modifications that lend resistance to nuclease attack. Moreover, aptamers isolated from combinatorial libraries have low dissociation constants, ranging from nanomolar to femtomolar, similar to the best affinities of interactions between monoclonal antibodies and antigens. Aptamers are not only promising for therapy but also for clinical diagnosis: like antibodies, aptamers can be easily tagged with fluorescent reporters or nanoparticles for localization or pull-down experiments of target proteins. Nucleic acid aptamers can modulate the function of virtually any target of biological interest, making them a preferred method of choice for the identification of new bioactive ligands against essential pathogen targets.

The primary approach to obtain DNA aptamers is using Systematic Evolution of Ligands by EXponential enrichment (SELEX) technique [163, 164]. This procedure starts with a large pool of nucleic acid sequences (typically $\geq 10^{13}$), with fixed regions on either end and a randomized central sequence (commonly approximately 30-60 nucleotides). This DNA library is incubated with the ligand of interest, and oligonucleotides that bind it are isolated. These sequences are then amplified and the enriched nucleic acid pool is subjected to another round of binding and selection, repeating the cycle 6-12 times with increasingly stringent conditions until an aptamer (or set of aptamers) is discovered that binds the ligand with the desired specificity and affinity. The SELEX drawbacks of time requirement, relatively low-throughput nature of the counter-selection process and the necessity of cloning and sequencing have stimulated the appearance of microarray-based systems [165]. In this method, each feature of a microarray contains thousands to millions of a unique aptamer sequence. The microarray is overlaid with a solution of the ligand, whose binding after several stringency washes is detected fluorescently, e.g. with a labeled antibody.

Peptides

Cell adhesive proteins like fibronectin, collagen or laminin have been applied to coat biomaterials in order to ensure an adequate interaction with target cells, but the use of proteins has some important inconveniences for biomedical applications, such as a significant immunogenicity, which could be overcome with the use of small peptides as cell recognition motifs. The RGD sequence (R: arginine; G: glycine; D: aspartic acid) is the most widely employed cell adhesion motif. Different strategies for the immobilization of RGD peptides on polymers have been developed and RGD-functionalized polymers have been evaluated *in vitro* in order to test their effectiveness for cell adhesion, their influence on cell behaviour and their applicability for medical use [166].

Cell-penetrating peptides (CPPs) are interesting targeting agents for nanoparticle functionalization due to their ability to translocate across cellular membranes [167] *via* a mechanism independent of transporters and receptor-mediated endocytosis. CPPs are cationic or amphipathic sequences of, typically, upto 30 amino acids. Some of them are reviewed in [168]: the HIV-1-encoded nuclear trans-activating transcriptor (TAT) peptide YGRKKRRQRRR [169] and the regulator of virion expression Rep peptide TRQARR NRRRRWRERQR, the *Drosophila* Antennapedia protein-derived RQIKIYFQNRRMKWKK, the flock house virus coat-derived RRRRNRTRRNRRRVR, and small oligoarginine and oligolysine. Amphipathic CPPs have mainly lysine residues and a homogeneous content of hydrophobic and hydrophilic amino acids, and present an α-helical structure content as in the model amphipathic peptide MAP, KLALKLALKALKAALKLA [170]. Proline-rich CPPs such as Sweet Arrow Peptide (SAP), $(VRLPPP)_3$, are water-soluble, non-toxic peptides that also have the property of crossing lipid bilayers with high efficacy [171]. As mentioned above, a common limitation of the therapeutic use of peptides is their metabolic instability. In this regard, the use of all-D-peptide derivatives has been proposed as a strategy to obtain longer half-lives [172].

Functionalization with any of these peptides could represent a strategy to carry small drug-loaded nanoparticles through biological membranes [168, 173]. A potent cytotoxic peptide (R_7-KLA) was synthesized by joining a mitochondrial membrane disrupting peptide, KLA (KLAKLAKKLAKLAK), with a cell-penetrating domain, R_7 (RRRRRRR) [174]. The IC_{50} of R_7-KLA (3.54 ± 0.11 μM) was more than two orders of magnitude lower than that of KLA. R_7-KLA induced cell death both *in vitro* and *in vivo*, and showed rapid kinetics. Pharmaceutical carriers like liposomes and nanoparticles have also been modified with CPPs to increase their cellular uptake [175]. Although, as we have seen above, these vessels provide protection to their

payload and improve drug properties such as solubility, their size might hamper in some cases membrane trespassing. However, nanoparticles and liposomes can be functionalized with a higher amount of CPP per particle, and this surface density has been shown to affect the degree of cell entry and also the internalization pathway [176, 177]: low density of octaarginine on liposomes results in clathrin-mediated endocytosis, whereas a higher density results in macropinocytosis. Some reports suggest the existence of cell uptake *via* endocytic pathways for liposomal [178] and for cationic polymer-based TAT conjugates [179].

Interestingly, cationic CPPs contain clusters of arginine and lysine residues which make them very similar to antimicrobial peptides, suggesting that peptidic nanoparticles could be synthesized having both activities. A novel class of core-shell nanoparticles formed by the self-assembly of an amphiphilic peptide have been shown to have strong antimicrobial properties against a range of bacteria, yeasts and fungi [180]. These nanoparticles showed a high therapeutic index against *Staphylococcus aureus* infection in mice and were more potent than their unassembled peptide counterparts, being able to cross the BBB and suppress bacterial growth in infected brains. In another recent report, cholesterol-conjugated G_3R_6TAT, which contains the TAT sequence, formed self-assembled cationic nanoparticles which demonstrated strong *in vitro* activity against various types of microbes [91]. Biodistribution studies in rabbits revealed that fluorescently labeled peptide nanoparticles were also able to cross the BBB. The combined use of peptides and nanotechnology offers tremendous hope in the treatment of brain disorders [181].

Some peptides, despite not being *bona fide* cell penetrating, can virtually act as such in certain situations. Tuftsin is a natural macrophage activator tetrapeptide (TKPR) which is a part of the Fc portion of the IgG antibody heavy chain. The peptide is known to bind specifically to macrophages, potentiating phagocytosis, pinocytosis, motility, immunogenic response, and bactericidal activity [182]. The inherent tendency of liposomes to concentrate in the mononuclear phagocyte system can be exploited by encapsulating in them antibiotics against intracellular infections that reside in macrophages, e.g. leishmaniasis. This activity can be further enhanced by functionalizing the liposomes with ligands such as tuftsin, which besides binding specifically to phagocytes also enhances their natural killer activity [183].

Carbohydrates

Carbohydrates are emerging as highly versatile adhesion molecules due to the extraordinary plasticity of glycan chains, the low affinity and reversibility of individual binding sites, and the *cluster effect*, i.e. the capacity to form multivalent complexes leading to increased association forces [184]. Individual carbohydrate-mediated interactions are among the weakest biomolecular binding events and, to generate sufficient affinity, glycoconjugates tend to display polyvalent configurations. Glycoproteins and proteoglycans present repetitive epitopes on their carbohydrate chains, whereas glycosphingolipids are associated in clusters or patches. Carbohydrates are ideal for generating compact units with explicit informational properties, since the permutations on linkages are larger than can be achieved by amino acids or nucleotides [185]. The structural diversity of carbohydrates underlies the potential of this class of biomolecules for storing biological information. The resulting high-density coding capacity of oligosaccharides is established by variability in (i) anomeric status, (ii) linkage positions, (iii) ring size, (iv) branching, and (v) introduction of site-specific substitutions [186]. Recognition of carbohydrates by proteins has been shown to be central to a myriad of intra- and extracellular physiological and pathological processes [187], and thus carbohydrate-mediated targeted delivery of drugs is a promising new avenue just being opened. Numerous studies have shown that glycosylated dendrimers are good mimics of natural glycoconjugates and will interact efficiently with natural carbohydrate receptors, in many cases to an extent that allows competition with natural binding substances [100]. PAA dendrimers are easily modified with peptides and carbohydrates [111]. Galactose coating of poly-L-lysine formulations reduced 5 times phagocytosis by macrophages of dendrimers loaded with the antimalarial drug chloroquine [108]. Galactose coating of dendrimers drastically reduced their haemolytic activity and immunogenicity, has been shown to increase drug entrapment efficacy several fold depending upon generations, and extended the release period up to 3 times [109].

RBCs infected with the mature stages of the malaria parasite, *Plasmodium falciparum*, bind to the endothelial cells of capillaries and post-capillary venules of deep tissues such as the brain, heart, lung, and small intestine in a phenomenon called sequestration. Multiple receptors, including both proteins and carbohydrates, are known to be involved in this sequestration process which is thought to play a major role in the fatal outcome of severe malaria [188, 189], and the capacity of wild-type isolates of *Plasmodium*-infected RBCs (pRBCs) to bind glycosaminoglycans (GAGs) has been identified as a marker for severe disease. The sequestration of pRBCs is suggested to be mediated by *P. falciparum* erythrocyte membrane protein 1 (PfEMP1), a parasite-derived polypeptide expressed at the surface of the pRBC. Lectinlike interactions of PfEMP1 have been described with GAGs such as heparin [190] and heparan sulfate (HS) [191]. The GAG chondroitin 4-sulfate (CSA) has been found to act as a receptor for pRBC binding in the microvasculature [192] and the placenta [193, 194], and adhesion of *P. falciparum*-infected erythrocytes to placental CSA has been linked to the severe disease outcome of pregnancy-associated malaria [195]. Heparin and HS have also been implicated in the sporozoite attachment to hepatocytes mediated by the circumsporozoite protein that targets the liver for infection in the first step of developing malaria [196], and interactions with heparin-like molecules have been described during erythrocyte invasion by *P. falciparum* merozoites [197]. Thus, GAGs might be interesting candidates as targeting agents to direct antimicrobial peptide-carrying nanocapsules towards different stages of the malaria parasite.

MULTIFUNCTIONAL NANOVECTORS

Currently used pharmaceutical nanocarriers have a broad variety of useful properties, such as longevity in the blood, specific targeting to certain disease sites due to various targeting ligands attached to their surface, enhanced intracellu-

lar penetration with the help of bound cell-penetrating molecules, and ease of tracking by loading the carrier with various available contrast agents that can even permit *in vivo* visualization. The engineering of multifunctional pharmaceutical nanocarriers combining several of these characteristics in one particle can significantly enhance the efficacy of many therapeutic and diagnostic protocols [39, 100, 101, 198]. It is also possible to combine different types of nanocapsules into a composite structure, in a kind of *Russian doll* assembly at the molecular level. Many novel materials are being developed in nanotechnology laboratories that often require methodologies to enhance their compatibility with the biological milieu *in vitro* and *in vivo*. One such system could consist of a liposome encapsulating polymeric nanoparticles: liposomes are structurally suitable to make nanoparticles biocompatible and offer a clinically proven, versatile platform for the further enhancement of pharmacological efficacy. Although liposomes have a decade-long clinical presence as nanoscale delivery systems of encapsulated drugs, their use as delivery systems of nanoparticles is still in the preclinical development stages [199, 200]. However, parenterally administered liposome-nanoparticle hybrid constructs present great opportunities in terms of nanoscale delivery system engineering for combinatory therapeutic-imaging modalities.

A striking example of multicomponent nanovessels are porous nanoparticle-supported lipid bilayers termed protocells, which synergistically combine properties of liposomes and nanoporous particles [122]. Protocells can be loaded with combinations of therapeutic and diagnostic agents and modified to promote endosomal escape and nuclear accumulation of selected cargos. The enormous capacity of the nanoporous core combined with the enhanced targeting efficacy enabled by the fluid supported lipid bilayer allowed a *single* protocell loaded with a drug cocktail to kill a human hepatocellular carcinoma cell, representing a 10^6-fold improvement over classical drug-loaded liposomes of similar size. The foreseeable applications of protocell-like structures to the targeted delivery of antimicrobial peptides are obvious.

Once a nanovector prototype is assembled, its different parts can be exchanged by new elements to adapt to new parasite strains or to be used against entirely different microbes. In such LEGO-like structures better targeting molecules can easily substitute for those made obsolete by the disappearance of formerly exposed antigens, or the same CPP can be attached to either a liposome or a dendrimer, depending on the particular cell type to be targeted. Because each system has its own advantages and drawbacks a universal drug delivery platform may never be realized, but hybrid drug delivery systems that incorporate the benefits of various approaches will be tailored to address the needs of specific applications. However, a balance between complexity, efficacy, and cost will be necessary to obtain for each situation an efficient antimicrobial peptide delivery nanosystem as simple and economically affordable as possible.

CONFLICT OF INTEREST

The authors confirm that this article content has no conflict of interest.

ACKNOWLEDGEMENTS

This work was supported by grants BIO2008-01184, BIO2011-25039, and CSD2006-00012 from the Ministerio de Ciencia e Innovación, Spain, which included FEDER funds, and by grant 2009SGR-760 from the Generalitat de Catalunya, Spain. A fellowship of the Instituto de Salud Carlos III (Spain) is acknowledged by Patricia Urbán.

REFERENCES

[1] Brown KL, Mookherjee N, Hancock REW. Antimicrobial, host defence peptides and proteins. Encyclopedia of Life Sciences. Chichester: John Wiley & Sons, Ltd. 2007. DOI: 10.1002/9780470015902.a0001212.pub2.

[2] Boix E. Eosinophil cationic protein. Methods Enzymol 2001; 341: 287-305.

[3] Torrent M, Navarro S, Moussaoui M, Nogués MV, Boix E. Eosinophil cationic protein high-affinity binding to bacteria-wall lipopolysaccharides and peptidoglycans. Biochemistry 2008; 47(11): 3544-55.

[4] Waters LS, Taverne J, Tai PC, Spry CJ, Targett GA, Playfair JH. Killing of *Plasmodium falciparum* by eosinophil secretory products. Infect Immun 1987; 55(4): 877-81.

[5] Adu B, Dodoo D, Adukpo S, *et al.* Polymorphisms in the *RNASE3* gene are associated with susceptibility to cerebral malaria in Ghanaian children. PLoS One 2011; 6(12): e29465.

[6] Venge P, Byström J, Carlson M, *et al.* Eosinophil cationic protein (ECP): molecular and biological properties and the use of ECP as a marker of eosinophil activation in disease. Clin Exp Allergy 1999; 29(9): 1172-86.

[7] Torrent M, Cuyás E, Carreras E, *et al.* Topography studies on the membrane interaction mechanism of the eosinophil cationic protein. Biochemistry 2007; 46(3): 720-33.

[8] Torrent M, Sánchez D, Buzón V, Nogués MV, Cladera J, Boix E. Comparison of the membrane interaction mechanism of two antimicrobial RNases: RNase 3/ECP and RNase 7. Biochim Biophys Acta 2009; 1788(5): 1116-25.

[9] White NJ. Assessment of the pharmacodynamic properties of antimalarial drugs *in vivo*. Antimicrob Agents Chemother 1997; 41(7): 1413-22.

[10] Couvreur P, Puisieux F. Nano- and microparticles for the delivery of polypeptides and proteins. Adv Drug Deliv Rev 2005; 10(2-3): 141-62.

[11] Pattani AS, Mandawgade SD, Patravale VB. Development and comparative anti-microbial evaluation of lipid nanoparticles and nanoemulsion of Polymyxin B. J Nanosci Nanotechnol 2006; 6(9-10): 2986-990.

[12] Ofokansi K, Winter G, Fricker G, Coester C. Matrix-loaded biodegradable gelatin nanoparticles as new approach to improve drug loading and delivery. Eur J Pharm Biopharm 2010; 76(1): 1-9.

[13] Luppi B, Bigucci F, Cerchiara T, Mandrioli R, Di Pietra AM, Zecchi V. New environmental sensitive system for colon-specific delivery of peptidic drugs. Int J Pharm 2008; 358(1-2): 44-9.

[14] Hamidi M, Zarrin A, Foroozesh M. Novel delivery systems for interferons. Crit Rev Biotechnol 2007; 27(3): 111-27.

[15] Xiong XY, Li YP, Li ZL, *et al.* Vesicles from Pluronic/poly(lactic acid) block copolymers as new carriers for oral insulin delivery. J Control Release 2007; 120(1-2): 11-7.

[16] Saltzman M, Desai T. Drug delivery in the BME curricula. Ann Biomed Eng 2006; 34(2): 270-75.

[17] Orive G, Hernández RM, Rodríguez Gascón A, Domínguez-Gil A, Pedraz JL. Drug delivery in biotechnology: present and future. Curr Opin Biotechnol 2003; 14(6): 659-64.

[18] Sershen S, West J. Implantable, polymeric systems for modulated drug delivery. Adv Drug Deliv Rev 2002; 54(9): 1225-35.

[19] Kikuchi A, Okano T. Pulsatile drug release control using hydrogels. Adv Drug Deliv Rev 2002; 54(1): 53-77.

[20] Fleming AB, Saltzman WM. Pharmacokinetics of the carmustine implant. Clin Pharmacokinet 2002; 41(6): 403-19.

[21] Boudes P. Drug compliance in therapeutic trials: a review. Control Clin Trials 1998; 19(3): 257-68.

[22] Tao SL, Desai TA. Microfabricated drug delivery systems: from particles to pores. Adv Drug Deliv Rev 2003; 55(3): 315-28.
[23] Breimer DD. Future challenges for drug delivery. J Control Release 1999; 62(1-2): 3-6.
[24] Klausner EA, Eyal S, Lavy E, Friedman M, Hoffman A. Novel levodopa gastroretentive dosage form: *in-vivo* evaluation in dogs. J Control Release 2003; 88(1): 117-26.
[25] Davis SS, Illum L. Drug delivery systems for challenging molecules. Int J Pharm 1998; 176(1): 1-8.
[26] Goldberg M, Langer R, Jia X. Nanostructured materials for applications in drug delivery and tissue engineering. J Biomater Sci Polym Ed 2007; 18(3): 241-68.
[27] Seale-Goldsmith MM, Leary JF. Nanobiosystems. Wiley Interdiscip Rev Nanomed Nanobiotechnol 2009; 1(5): 553-67.
[28] Sahoo SK, Labhasetwar V. Nanotech approaches to drug delivery and imaging. Drug Discov Today 2003; 8(24): 1112-20.
[29] Tan SY, Grimes S. Paul Ehrlich (1854-1915): man with the magic bullet. Singapore Med J 2010; 51(11): 842-3.
[30] Fahmy TM, Fong PM, Goyal A, Saltzman WM. Targeted for drug delivery. Nano Today 2005; 8(8): 18-26.
[31] Qiu LY, Bae YH. Polymer architecture and drug delivery. Pharm Res 2006; 23(1): 1-30.
[32] Svenson S, Tomalia DA. Dendrimers in biomedical applications--reflections on the field. Adv Drug Deliv Rev 2005; 57(15): 2106-29.
[33] Rabinow BE. Nanosuspensions in drug delivery. Nat Rev Drug Discov 2004; 3(9): 785-96.
[34] Ishida O, Maruyama K, Sasaki K, Iwatsuru M. Size-dependent extravasation and interstitial localization of polyethyleneglycol liposomes in solid tumor-bearing mice. Int J Pharm 1999; 190(1): 49-56.
[35] Kong G, Braun RD, Dewhirst MW. Hyperthermia enables tumor-specific nanoparticle delivery: effect of particle size. Cancer Res 2000; 60(16): 4440-5.
[36] Vinogradov SV, Bronich TK, Kabanov AV. Nanosized cationic hydrogels for drug delivery: preparation, properties and interactions with cells. Adv Drug Deliv Rev 2002; 54(1): 135-47.
[37] Hawley AE, Davis SS, Illum L. Targeting of colloids to lymph nodes: influence of lymphatic physiology and colloidal characteristics. Adv Drug Deliv Rev 1995; 17(1): 129-48.
[38] Stolnik S, Illum L, Davis SS. Long circulating microparticulate drug carriers. Adv Drug Deliv Rev 1995; 16(2-3): 195-214.
[39] Katz E, Willner I. Integrated nanoparticle-biomolecule hybrid systems: synthesis, properties, and applications. Angew Chem Int Ed Engl 2004; 43(45): 6042-108.
[40] Farokhzad OC, Jon S, Khademhosseini A, Tran TN, Lavan DA, Langer R. Nanoparticle-aptamer bioconjugates: a new approach for targeting prostate cancer cells. Cancer Res 2004; 64(21): 7668-72.
[41] Gu F, Zhang L, Teply BA, *et al.* Precise engineering of targeted nanoparticles by using self-assembled biointegrated block copolymers. Proc Natl Acad Sci USA 2008; 105(7): 2586-91.
[42] Kim SH, Jeong JH, Chun KW, Park TG. Target-specific cellular uptake of PLGA nanoparticles coated with poly(L-lysine)-poly(ethylene glycol)-folate conjugate. Langmuir 2005; 21(19): 8852-7.
[43] Urbán P, Estelrich J, Cortés A, Fernàndez-Busquets X. A nanovector with complete discrimination for targeted delivery to *Plasmodium falciparum*-infected versus non-infected red blood cells *in vitro*. J Control Release 2011; 151(2): 202-11.
[44] Panyam J, Labhasetwar V. Biodegradable nanoparticles for drug and gene delivery to cells and tissue. Adv Drug Deliv Rev 2003; 55(3): 329-47.
[45] Rawat M, Singh D, Saraf S, Saraf S. Nanocarriers: promising vehicle for bioactive drugs. Biol Pharm Bull 2006; 29(9): 1790-8.
[46] Farokhzad OC, Langer R. Impact of nanotechnology on drug delivery. ACS Nano 2009; 3(1): 16-20.
[47] Bustami RT, Chan HK, Dehghani F, Foster NR. Generation of micro-particles of proteins for aerosol delivery using high pressure modified carbon dioxide. Pharm Res 2000; 17(11): 1360-6.
[48] Gregoriadis G. Drug entrapment in liposomes. FEBS Lett 1973; 36(3): 292-6.
[49] Jasmine D, Tushar T. Role of liposomes in nanotechnology and drug delivery. Int J Drug Dev Res 2011; 3(1): 341-50.
[50] Maurer N, Fenske DB, Cullis PR. Developments in liposomal drug delivery systems. Expert Opin Biol Ther 2001; 1(6): 923-47.
[51] Waterhouse DN, Madden TD, Cullis PR, Bally MB, Mayer LD, Webb MS. Preparation, characterization, and biological analysis of liposomal formulations of vincristine. Methods Enzymol 2005; 391: 40-57.
[52] Haran G, Cohen R, Bar LK, Barenholz Y. Transmembrane ammonium sulfate gradients in liposomes produce efficient and stable entrapment of amphipathic weak bases. Biochim Biophys Acta 1993; 1151(2): 201-15.
[53] Storm G, Wilms HP, Crommelin DJ. Liposomes and biotherapeutics. Biotherapy 1991; 3(1): 25-42.
[54] Kadir F, Zuidema J, Crommelin DJA. Liposomes as drug delivery systems for intramuscular and subcutaneous injections. In: Rolland A, Ed. Particulate Drug Carriers in Medical Applications. New York: Marcel Dekker 1993: 165-98.
[55] Čeh B, Winterhalter M, Frederik PM, Vallner JJ, Lasic DD. Stealth® liposomes: from theory to product. Adv Drug Deliv Rev 1997; 24(2-3): 165-77.
[56] Blume G, Cevc G. Liposomes for the sustained drug release *in vivo*. Biochim Biophys Acta 1990; 1029(1): 91-7.
[57] Kajiwara E, Kawano K, Hattori Y, Fukushima M, Hayashi K, Maitani Y. Long-circulating liposome-encapsulated ganciclovir enhances the efficacy of HSV-TK suicide gene therapy. J Control Release 2007; 120(1-2): 104-10.
[58] Santos-Magalhaes NS, Mosqueira VC. Nanotechnology applied to the treatment of malaria. Adv Drug Deliv Rev 2010; 62(4-5): 560-75.
[59] Singhal A, Gupta CM. Antibody-mediated targeting of liposomes to red cells *in vivo*. FEBS Lett 1986; 201(2): 321-26.
[60] Shillcock JC, Lipowsky R. Tension-induced fusion of bilayer membranes and vesicles. Nat Mater 2005; 4(3): 225-8.
[61] Wheeler JJ, Palmer L, Ossanlou M, *et al.* Stabilized plasmid-lipid particles: construction and characterization. Gene Ther 1999; 6(2): 271-81.
[62] Nicolosi D, Scalia M, Nicolosi VM, Pignatello R. Encapsulation in fusogenic liposomes broadens the spectrum of action of vancomycin against Gram-negative bacteria. Int J Antimicrob Agents 2010; 35(6): 553-8.
[63] Alipour M, Halwani M, Omri A, Suntres ZE. Antimicrobial effectiveness of liposomal polymyxin B against resistant Gram-negative bacterial strains. Int J Pharm 2008; 355(1-2): 293-8.
[64] Alipour M, Suntres ZE, Halwani M, Azghani AO, Omri A. Activity and interactions of liposomal antibiotics in presence of polyanions and sputum of patients with cystic fibrosis. PLoS One 2009; 4(5): e5724.
[65] Gregoriadis G. Liposomes as a drug delivery system: optimization studies. Adv Exp Med Biol 1988; 238: 151-9.
[66] Paleos CM, Tsiourvas D, Sideratou Z, Tziveleka LA. Drug delivery using multifunctional dendrimers and hyperbranched polymers. Expert Opin Drug Deliv 2010; 7(12): 1387-98.
[67] Sukhorukov GB, Rogach AL, Garstka M, *et al.* Multifunctionalized polymer microcapsules: novel tools for biological and pharmacological applications. Small 2007; 3(6): 944-55.
[68] Soppimath KS, Aminabhavi TM, Kulkarni AR, Rudzinski WE. Biodegradable polymeric nanoparticles as drug delivery devices. J Control Release 2001; 70(1-2): 1-20.
[69] Agnihotri SA, Mallikarjuna NN, Aminabhavi TM. Recent advances on chitosan-based micro- and nanoparticles in drug delivery. J Control Release 2004; 100(1): 5-28.
[70] Duncan R. The dawning era of polymer therapeutics. Nat Rev Drug Discov 2003; 2(5): 347-60.
[71] Kavanagh OV, Earley B, Murray M, Foster CJ, Adair BM. Antigen-specific IgA and IgG responses in calves inoculated intranasally with ovalbumin encapsulated in poly(DL-lactide-co-glycolide) microspheres. Vaccine 2003; 21(27-30): 4472-80.
[72] Andrieux K, Couvreur P. Polyalkylcyanoacrylate nanoparticles for delivery of drugs across the blood-brain barrier. Wiley Interdiscip Rev Nanomed Nanobiotechnol 2009; 1(5): 463-74.
[73] Fernández-Urrusuno R, Calvo P, Remuñán-López C, Vila-Jato JL, Alonso MJ. Enhancement of nasal absorption of insulin using chitosan nanoparticles. Pharm Res 1999; 16(10): 1576-81.

[74] Yin L, Ding J, He C, Cui L, Tang C, Yin C. Drug permeability and mucoadhesion properties of thiolated trimethyl chitosan nanoparticles in oral insulin delivery. Biomaterials 2009; 30(29): 5691-700.
[75] Prego C, Torres D, Alonso MJ. The potential of chitosan for the oral administration of peptides. Expert Opin Drug Deliv 2005; 2(5): 843-54.
[76] Lescure F, Seguin C, Breton P, Bourrinet P, Roy D, Couvreur P. Preparation and characterization of novel poly(methylidene malonate 2.1.2.)-made nanoparticles. Pharm Res 1994; 11(9): 1270-7.
[77] Wikingsson L, Sjoholm I. Polyacryl starch microparticles as adjuvant in oral immunisation, inducing mucosal and systemic immune responses in mice. Vaccine 2002; 20(27-28): 3355-63.
[78] Aynié I, Vauthier C, Chacun H, Fattal E, Couvreur P. Spongelike alginate nanoparticles as a new potential system for the delivery of antisense oligonucleotides. Antisense Nucleic Acid Drug Dev 1999; 9(3): 301-12.
[79] Bege N, Renette T, Jansch M, *et al.* Biodegradable poly(ethylene carbonate) nanoparticles as a promising drug delivery system with "stealth" potential. Macromol Biosci 2011; 11(7): 897-904.
[80] Peppas NA, Bures P, Leobandung W, Ichikawa H. Hydrogels in pharmaceutical formulations. Eur J Pharm Biopharm 2000; 50(1): 27-46.
[81] Peppas NA, Wood KM, Blanchette JO. Hydrogels for oral delivery of therapeutic proteins. Expert Opin Biol Ther 2004; 4(6): 881-7.
[82] Gupta P, Vermani K, Garg S. Hydrogels: from controlled release to pH-responsive drug delivery. Drug Discov Today 2002; 7(10): 569-79.
[83] Vinogradov SV. Colloidal microgels in drug delivery applications. Curr Pharm Des 2006; 12(36): 4703-12.
[84] Patel VR, Amiji MM. Preparation and characterization of freeze-dried chitosan-poly(ethylene oxide) hydrogels for site-specific antibiotic delivery in the stomach. Pharm Res 1996; 13(4): 588-93.
[85] Li JK, Wang N, Wu XS. Poly(vinyl alcohol) nanoparticles prepared by freezing-thawing process for protein/peptide drug delivery. J Control Release 1998; 56(1-3): 117-26.
[86] Salmaso S, Semenzato A, Bersani S, Matricardi P, Rossi F, Caliceti P. Cyclodextrin/PEG based hydrogels for multi-drug delivery. Int J Pharm 2007; 345(1-2): 42-50.
[87] Gupta NV, Shivakumar HG. Preparation and characterization of superporous hydrogels as pH-sensitive drug delivery system for Pantoprazole sodium. Curr Drug Deliv 2009; 6(5): 505-10.
[88] Gutowska A, Seok Bark J, Chan Kwon I, Han Bae Y, Cha Y, Wan Kim S. Squeezing hydrogels for controlled oral drug delivery. J Control Release 1997; 48(2-3): 141-8.
[89] Tiwari AK, Gajbhiye V, Sharma R, Jain NK. Carrier mediated protein and peptide stabilization. Drug Deliv 2010; 17(8): 605-16.
[90] Pattrick NG, Richardson SC, Casolaro M, Ferruti P, Duncan R. Poly(amidoamine)-mediated intracytoplasmic delivery of ricin A-chain and gelonin. J Control Release 2001; 77(3): 225-32.
[91] Wang H, Xu K, Liu L, *et al.* The efficacy of self-assembled cationic antimicrobial peptide nanoparticles against *Cryptococcus neoformans* for the treatment of meningitis. Biomaterials 2010; 31(10): 2874-81.
[92] Schröder U, Sabel BA. Nanoparticles, a drug carrier system to pass the blood-brain barrier, permit central analgesic effects of i.v. dalargin injections. Brain Res 1996; 710(1-2): 121-4.
[93] Kreuter J. Nanoparticulate systems for brain delivery of drugs. Adv Drug Deliv Rev 2001; 47(1): 65-81.
[94] Roney C, Kulkarni P, Arora V, *et al.* Targeted nanoparticles for drug delivery through the blood-brain barrier for Alzheimer's disease. J Control Release 2005; 108(2-3): 193-214.
[95] Al-Jamal KT, Ramaswamy C, Florence AT. Supramolecular structures from dendrons and dendrimers. Adv Drug Deliv Rev 2005; 57(15): 2238-70.
[96] Marcos M, Martín-Rapún R, Omenat A, Serrano JL. Highly congested liquid crystal structures: dendrimers, dendrons, dendronized and hyperbranched polymers. Chem Soc Rev 2007; 36(12): 1889-901.
[97] Liang C, Fréchet JMJ. Applying key concepts from nature: transition state stabilization, pre-concentration and cooperativity effects in dendritic biomimetics. Prog Polym Sci 2005; 30(3-4): 385-402.
[98] Ihre HR, Padilla De Jesús OL, Szoka FC, Jr., Fréchet JM. Polyester dendritic systems for drug delivery applications: design, synthesis, and characterization. Bioconjug Chem 2002; 13(3): 443-52.
[99] Padilla De Jesús OL, Ihre HR, Gagne L, Fréchet JM, Szoka FC Jr. Polyester dendritic systems for drug delivery applications: *in vitro* and *in vivo* evaluation. Bioconjug Chem 2002; 13(3): 453-61.
[100] Boas U, Heegaard PM. Dendrimers in drug research. Chem Soc Rev 2004; 33(1): 43-63.
[101] Paleos CM, Tsiourvas D, Sideratou Z. Molecular engineering of dendritic polymers and their application as drug and gene delivery systems. Mol Pharm 2007; 4(2): 169-88.
[102] Kolhe P, Khandare J, Pillai O, Kannan S, Lieh-Lai M, Kannan RM. Preparation, cellular transport, and activity of polyamidoamine-based dendritic nanodevices with a high drug payload. Biomaterials 2006; 27(4): 660-9.
[103] Kukowska-Latallo JF, Bielinska AU, Johnson J, Spindler R, Tomalia DA, Baker JR, Jr. Efficient transfer of genetic material into mammalian cells using Starburst polyamidoamine dendrimers. Proc Natl Acad Sci USA 1996; 93(10): 4897-902.
[104] Crespo L, Sanclimens G, Montaner B, *et al.* Peptide dendrimers based on polyproline helices. J Am Chem Soc 2002; 124(30): 8876-83.
[105] Farrera-Sinfreu J, Giralt E, Castel S, Albericio F, Royo M. Cell-penetrating cis-gamma-amino-l-proline-derived peptides. J Am Chem Soc 2005; 127(26): 9459-68.
[106] Wiwattanapatapee R, Carreño-Gómez B, Malik N, Duncan R. Anionic PAMAM dendrimers rapidly cross adult rat intestine *in vitro:* a potential oral delivery system? Pharm Res 2000; 17(8): 991-8.
[107] Crespo L, Sanclimens G, Pons M, Giralt E, Royo M, Albericio F. Peptide and amide bond-containing dendrimers. Chem Rev 2005; 105(5):1663-81.
[108] Agrawal P, Gupta U, Jain NK. Glycoconjugated peptide dendrimers-based nanoparticulate system for the delivery of chloroquine phosphate. Biomaterials 2007; 28(22): 3349-59.
[109] Bhadra D, Yadav AK, Bhadra S, Jain NK. Glycodendrimeric nanoparticulate carriers of primaquine phosphate for liver targeting. Int J Pharm 2005; 295(1-2): 221-33.
[110] Lee JW, Ko YH, Park SH, Yamaguchi K, Kim K. Novel pseudorotaxane-terminated dendrimers: Supramolecular modification of dendrimer periphery. Angew Chem Int Ed 2001; 40(4): 746-9.
[111] Mitchell JP, Roberts KD, Langley J, Koentgen F, Lambert JN. A direct method for the formation of peptide and carbohydrate dendrimers. Bioorg Med Chem Lett 1999; 9(19): 2785-8.
[112] Chamorro C, Boerman MA, Arnusch CJ, Breukink E, Pieters RJ. Enhancing membrane disruption by targeting and multivalent presentation of antimicrobial peptides. Biochim Biophys Acta 2012 Apr 14. [Epub ahead of print].
[113] Ciolkowski M, Petersen JF, Ficker M, *et al.* Surface modification of PAMAM dendrimer improves its biocompatibility. Nanomedicine 2012 Apr 26. [Epub ahead of print].
[114] Calabretta MK, Kumar A, McDermott AM, Cai C. Antibacterial activities of poly(amidoamine) dendrimers terminated with amino and poly(ethylene glycol) groups. Biomacromolecules 2007; 8(6): 1807-11.
[115] Lopez AI, Reins RY, McDermott AM, Trautner BW, Cai C. Antibacterial activity and cytotoxicity of PEGylated poly(amidoamine) dendrimers. Mol Biosyst 2009; 5(10): 1148-56.
[116] Wang B, Navath RS, Menjoge AR, *et al.* Inhibition of bacterial growth and intramniotic infection in a guinea pig model of chorioamnionitis using PAMAM dendrimers. Int J Pharm 2010; 395(1-2): 298-308.
[117] Wang AZ, Gu F, Zhang L, *et al.* Biofunctionalized targeted nanoparticles for therapeutic applications. Expert Opin Biol Ther 2008; 8(8): 1063-70.
[118] Veiseh O, Sun C, Gunn J, *et al.* Optical and MRI multifunctional nanoprobe for targeting gliomas. Nano Lett 2005; 5(6): 1003-8.
[119] Durán JD, Arias JL, Gallardo V, Delgado AV. Magnetic colloids as drug vehicles. J Pharm Sci 2008; 97(8): 2948-83.
[120] Xing Y, Smith AM, Agrawal A, Ruan G, Nie S. Molecular profiling of single cancer cells and clinical tissue specimens with semiconductor quantum dots. Int J Nanomedicine 2006; 1(4): 473-81.

[121] Hosseinkhani H, Hosseinkhani M. Biodegradable polymer-metal complexes for gene and drug delivery. Curr Drug Saf 2009; 4(1): 79-83.
[122] Ashley CE, Carnes EC, Phillips GK, *et al.* The targeted delivery of multicomponent cargos to cancer cells by nanoporous particle-supported lipid bilayers. Nat Mater 2011; 10(5): 389-97.
[123] Soenen SJ, Hodenius M, De Cuyper M. Magnetoliposomes: versatile innovative nanocolloids for use in biotechnology and biomedicine. Nanomedicine (Lond) 2009; 4(2): 177-91.
[124] Ghosh P, Yang X, Arvizo R, *et al.* Intracellular delivery of a membrane-impermeable enzyme in active form using functionalized gold nanoparticles. J Am Chem Soc 2010; 132(8): 2642-5.
[125] Guerrero S, Araya E, Fiedler JL, *et al.* Improving the brain delivery of gold nanoparticles by conjugation with an amphipathic peptide. Nanomedicine (Lond) 2010; 5(6): 897-913.
[126] Schaeublin NM, Braydich-Stolle LK, Schrand AM, *et al.* Surface charge of gold nanoparticles mediates mechanism of toxicity. Nanoscale 2011; 3(2): 410-20.
[127] Maynard AD, Warheit DB, Philbert MA. The new toxicology of sophisticated materials: nanotoxicology and beyond. Toxicol Sci 2011; 120(suppl 1): S109-S129.
[128] Bianco A, Kostarelos K, Prato M. Applications of carbon nanotubes in drug delivery. Curr Opin Chem Biol 2005; 9(6): 674-9.
[129] Sanz V, Coley H, Silva S, McFadden J. Modeling the binding of peptides on carbon nanotubes and their use as protein and DNA carriers. J Nanoparticle Res 2012; 14(2): 1-13.
[130] Bandaru NM, Voelcker NH. Glycoconjugate-functionalized carbon nanotubes in biomedicine. J Mater Chem 2012; 22(18): 8748-58.
[131] Beg S, Rizwan M, Sheikh AM, Hasnain MS, Anwer K, Kohli K. Advancement in carbon nanotubes: basics, biomedical applications and toxicity. J Pharm Pharmacol 2011; 63(2): 141-63.
[132] Pantarotto D, Briand JP, Prato M, Bianco A. Translocation of bioactive peptides across cell membranes by carbon nanotubes. Chem Commun 2004; (1): 16-7.
[133] Shi Kam NW, Jessop TC, Wender PA, Dai H. Nanotube molecular transporters: internalization of carbon nanotube-protein conjugates into mammalian cells. J Am Chem Soc 2004; 126(22): 6850-1.
[134] Heister E, Neves V, Lamprecht C, Silva SR, Coley HM, McFadden J. Drug loading, dispersion stability, and therapeutic efficacy in targeted drug delivery with carbon nanotubes. Carbon 2012; 50(2): 622-32.
[135] Trzaskowski B, Jalbout AF, Adamowicz L. Molecular dynamics studies of protein-fragment models encapsulated into carbon nanotubes. Chem Phys Lett 2006; 430(1-3): 97-100.
[136] Kümmerer K, Menz J, Schubert T, Thielemans W. Biodegradability of organic nanoparticles in the aqueous environment. Chemosphere 2011; 82(10): 1387-92.
[137] Yang D, Campolongo MJ, Nhi Tran TN, Ruiz RC, Kahn JS, Luo D. Novel DNA materials and their applications. Wiley Interdiscip Rev Nanomed Nanobiotechnol 2010; 2(6): 648-69.
[138] Andersen ES, Dong M, Nielsen MM, *et al.* Self-assembly of a nanoscale DNA box with a controllable lid. Nature 2009; 459(7243): 73-6.
[139] He Y, Ye T, Su M, *et al.* Hierarchical self-assembly of DNA into symmetric supramolecular polyhedra. Nature 2008; 452(7184): 198-201.
[140] Alexis F, Pridgen E, Molnar LK, Farokhzad OC. Factors affecting the clearance and biodistribution of polymeric nanoparticles. Mol Pharm 2008; 5(4): 505-15.
[141] Li SD, Huang L. Pharmacokinetics and biodistribution of nanoparticles. Mol Pharm 2008; 5(4): 496-504.
[142] Geng Y, Discher DE. Hydrolytic degradation of poly(ethylene oxide)-block-polycaprolactone worm micelles. J Am Chem Soc 2005; 127(37): 12780-1.
[143] Gao W, Chan JM, Farokhzad OC. pH-Responsive nanoparticles for drug delivery. Mol Pharm 2010; 7(6): 1913-20.
[144] Sakthivel T, Toth I, Florence AT. Distribution of a lipidic 2.5 nm diameter dendrimer carrier after oral administration. Int J Pharm 1999; 183(1): 51-5.
[145] Phua K, Leong KW. Microscale oral delivery devices incorporating nanoparticles. Nanomedicine (Lond) 2010; 5(2): 161-3.
[146] Yamanaka YJ, Leong KW. Engineering strategies to enhance nanoparticle-mediated oral delivery. J Biomater Sci Polym Ed 2008; 19(12): 1549-70.
[147] Lin YH, Mi FL, Chen CT, *et al.* Preparation and characterization of nanoparticles shelled with chitosan for oral insulin delivery. Biomacromolecules 2007; 8(1): 146-52.
[148] Wong TW. Design of oral insulin delivery systems. J Drug Target 2010; 18(2): 79-92.
[149] Damgé C, Maincent P, Ubrich N. Oral delivery of insulin associated to polymeric nanoparticles in diabetic rats. J Control Release 2007; 117(2): 163-70.
[150] Pan Y, Li YJ, Zhao HY, *et al.* Bioadhesive polysaccharide in protein delivery system: chitosan nanoparticles improve the intestinal absorption of insulin *in vivo*. Int J Pharm 2002; 249(1-2): 139-47.
[151] Carino GP, Mathiowitz E. Oral insulin delivery. Adv Drug Deliv Rev 1999; 35(2-3): 249-57.
[152] Zola H. Monoclonal antibodies: Therapeutic uses. Encyclopedia of Life Sciences. Chichester: John Wiley & Sons, Ltd. 2011. DOI: 10.1038/npg.els.0004018.
[153] Paul S, Planque S. Antibody engineering. Encyclopedia of Life Sciences. Chichester: John Wiley & Sons, Ltd. 2005. DOI: 10.1038/npg.els.0001278.
[154] Hu S, Shively L, Raubitschek A, *et al.* Minibody: A novel engineered anti-carcinoembryonic antigen antibody fragment (single-chain Fv-C_H3) which exhibits rapid, high-level targeting of xenografts. Cancer Res 1996; 56(13): 3055-61.
[155] Wu AM, Yazaki PJ. Designer genes: recombinant antibody fragments for biological imaging. Q J Nucl Med 2000; 44(3): 268-83.
[156] Cortez-Retamozo V, Backmann N, Senter PD, *et al.* Efficient cancer therapy with a nanobody-based conjugate. Cancer Res 2004; 64(8): 2853-7.
[157] Qiu XQ, Wang H, Cai B, Wang LL, Yue ST. Small antibody mimetics comprising two complementarity-determining regions and a framework region for tumor targeting. Nat Biotechnol 2007; 25(8): 921-9.
[158] Martin FJ, Papahadjopoulos D. Irreversible coupling of immunoglobulin fragments to preformed vesicles. An improved method for liposome targeting. J Biol Chem 1982; 257(1): 286-8.
[159] Owais M, Varshney GC, Choudhury A, Chandra S, Gupta CM. Chloroquine encapsulated in malaria-infected erythrocyte-specific antibody-bearing liposomes effectively controls chloroquine-resistant *Plasmodium berghei* infections in mice. Antimicrob Agents Chemother 1995; 39(1): 180-4.
[160] Vogel C-W. Preparation of immunoconjugates using antibody oligosaccharide moieties. In: Niemeyer CM, Ed. Methods in Molecular Biology. Totowa, NJ: Humana Press Inc., 2004: 87-108.
[161] Ishikawa H, Ochi H, Chen ML, Frenkel D, Maron R, Weiner HL. Inhibition of autoimmune diabetes by oral administration of anti-CD3 monoclonal antibody. Diabetes 2007; 56(8): 2103-9.
[162] Warren CL, Mohandas A, Chaturvedi I, Ansari AZ. Macromolecular interactions: aptamers. Encyclopedia of Life Sciences. Chichester: John Wiley & Sons, Ltd. 2009 DOI: 10.1002/9780470015902.a0003146.
[163] O'Sullivan CK. Aptasensors--the future of biosensing? Anal Bioanal Chem 2002; 372(1): 44-8.
[164] Abelson J. Directed evolution of nucleic acids by independent replication and selection. Science 1990; 249(4968): 488-9.
[165] Collett JR, Cho EJ, Ellington AD. Production and processing of aptamer microarrays. Methods 2005; 37(1): 4-15.
[166] Hersel U, Dahmen C, Kessler H. RGD modified polymers: biomaterials for stimulated cell adhesion and beyond. Biomaterials 2003; 24(24): 4385-415.
[167] Patel LN, Zaro JL, Shen WC. Cell penetrating peptides: intracellular pathways and pharmaceutical perspectives. Pharm Res 2007; 24(11): 1977-92.
[168] Futaki S. Arginine-rich peptides: potential for intracellular delivery of macromolecules and the mystery of the translocation mechanisms. Int J Pharm 2002; 245(1-2): 1-7.
[169] Rao KS, Reddy MK, Horning JL, Labhasetwar V. TAT-conjugated nanoparticles for the CNS delivery of anti-HIV drugs. Biomaterials 2008; 29(33): 4429-38.
[170] Fernández-Carneado J, Kogan MJ, Pujals S, Giralt E. Amphipathic peptides and drug delivery. Biopolymers 2004; 76(2): 196-203.
[171] Pujals S, Fernández-Carneado J, López-Iglesias C, Kogan MJ, Giralt E. Mechanistic aspects of CPP-mediated intracellular drug delivery: relevance of CPP self-assembly. Biochim Biophys Acta 2006; 1758(3): 264-79.

[172] Pujals S, Sabidó E, Tarragó T, Giralt E. all-D proline-rich cell-penetrating peptides: a preliminary *in vivo* internalization study. Biochem Soc Trans 2007; 35(Pt 4): 794-6.
[173] Chen L, Harrison SD. Cell-penetrating peptides in drug development: enabling intracellular targets. Biochem Soc Trans 2007; 35(Pt 4): 821-5.
[174] Law B, Quinti L, Choi Y, Weissleder R, Tung CH. A mitochondrial targeted fusion peptide exhibits remarkable cytotoxicity. Mol Cancer Ther 2006; 5(8): 1944-9.
[175] Dietz GP, Bähr M. Delivery of bioactive molecules into the cell: the Trojan horse approach. Mol Cell Neurosci 2004; 27(2): 85-131.
[176] Zhao M, Kircher MF, Josephson L, Weissleder R. Differential conjugation of tat peptide to superparamagnetic nanoparticles and its effect on cellular uptake. Bioconjug Chem 2002; 13(4): 840-4.
[177] Khalil IA, Kogure K, Futaki S, Harashima H. High density of octaarginine stimulates macropinocytosis leading to efficient intracellular trafficking for gene expression. J Biol Chem 2006; 281(6): 3544-51.
[178] Fretz MM, Koning GA, Mastrobattista E, Jiskoot W, Storm G. OVCAR-3 cells internalize TAT-peptide modified liposomes by endocytosis. Biochim Biophys Acta 2004; 1665(1-2): 48-56.
[179] Hashida H, Miyamoto M, Cho Y, *et al.* Fusion of HIV-1 Tat protein transduction domain to poly-lysine as a new DNA delivery tool. Br J Cancer 2004; 90(6): 1252-8.
[180] Liu L, Xu K, Wang H, *et al.* Self-assembled cationic peptide nanoparticles as an efficient antimicrobial agent. Nat Nanotechnol 2009; 4(7): 457-63.
[181] Teixidó M, Giralt E. The role of peptides in blood-brain barrier nanotechnology. J Pept Sci 2008; 14(2): 163-73.
[182] Fridkin M, Najjar VA. Tuftsin: its chemistry, biology, and clinical potential. Crit Rev Biochem Mol Biol 1989; 24(1): 1-40.
[183] Agrawal AK, Gupta CM. Tuftsin-bearing liposomes in treatment of macrophage-based infections. Adv Drug Deliv Rev 2000; 41(2): 135-46.
[184] Bucior I, Burger MM, Fernàndez-Busquets X. Carbohydrate-carbohydrate interactions. In: Gabius H-J, Ed. The Sugar Code. Weinheim: WILEY-VCH Verlag GmbH & Co. KGaA, 2009: 347-62.
[185] Winterburn PJ, Phelps CF. The significance of glycosylated proteins. Nature 1972; 236(5343): 147-51.
[186] Rüdiger H, Gabius H-J. The biochemical basis and coding capacity of the sugar code. In: Gabius H-J, Ed. The Sugar Code. Weinheim: WILEY-VCH Verlag GmbH & Co. KGaA, 2009: 3-13.
[187] Solís D, Romero A, Menéndez M, Jiménez-Barbero J. Protein-carbohydrate interactions: basic concepts and methods for analysis. In: Gabius H-J, Ed. The Sugar Code. Weinheim: WILEY-VCH Verlag GmbH & Co. KGaA, 2009: 233-45.
[188] Idro R, Jenkins NE, Newton CR. Pathogenesis, clinical features, and neurological outcome of cerebral malaria. Lancet Neurol 2005; 4(12): 827-40.
[189] Craig A, Scherf A. Molecules on the surface of the *Plasmodium falciparum* infected erythrocyte and their role in malaria pathogenesis and immune evasion. Mol Biochem Parasitol 2001; 115(2): 129-43.
[190] Barragan A, Fernandez V, Chen Q, von Euler A, Wahlgren M, Spillmann D. The duffy-binding-like domain 1 of *Plasmodium falciparum* erythrocyte membrane protein 1 (PfEMP1) is a heparan sulfate ligand that requires 12 mers for binding. Blood 2000; 95(11): 3594-9.
[191] Vogt AM, Barragan A, Chen Q, Kironde F, Spillmann D, Wahlgren M. Heparan sulfate on endothelial cells mediates the binding of *Plasmodium falciparum*-infected erythrocytes *via* the DBL1α domain of PfEMP1. Blood 2003; 101(6): 2405-11.
[192] Gysin J, Pouvelle B, Le Tonqueze M, Edelman L, Boffa MC. Chondroitin sulfate of thrombomodulin is an adhesion receptor for *Plasmodium falciparum*-infected erythrocytes. Mol Biochem Parasitol 1997; 88(1-2): 267-71.
[193] Singh K, Gittis AG, Nguyen P, Gowda DC, Miller LH, Garboczi DN. Structure of the DBL3x domain of pregnancy-associated malaria protein VAR2CSA complexed with chondroitin sulfate A. Nat Struct Mol Biol 2008; 15(9): 932-8.
[194] Fried M, Duffy PE. Adherence of *Plasmodium falciparum* to chondroitin sulfate A in the human placenta. Science 1996; 272(5267): 1502-4.
[195] Andrews KT, Klatt N, Adams Y, Mischnick P, Schwartz-Albiez R. Inhibition of chondroitin-4-sulfate-specific adhesion of *Plasmodium falciparum*-infected erythrocytes by sulfated polysaccharides. Infect Immun 2005; 73(7): 4288-94.
[196] Ancsin JB, Kisilevsky R. A binding site for highly sulfated heparan sulfate is identified in the N terminus of the circumsporozoite protein: significance for malarial sporozoite attachment to hepatocytes. J Biol Chem 2004; 279(21): 21824-32.
[197] Boyle MJ, Richards JS, Gilson PR, Chai W, Beeson JG. Interactions with heparin-like molecules during erythrocyte invasion by *Plasmodium falciparum* merozoites. Blood 2010; 115(22): 4559-68.
[198] Torchilin VP. Multifunctional nanocarriers. Adv Drug Deliv Rev 2006; 58(14): 1532-55.
[199] Al-Jamal WT, Kostarelos K. Construction of nanoscale multicompartment liposomes for combinatory drug delivery. Int J Pharm 2007; 331(2): 182-5.
[200] Al-Jamal WT, Kostarelos K. Liposome-nanoparticle hybrids for multimodal diagnostic and therapeutic applications. Nanomedicine (Lond) 2007; 2(1): 85-98.

Received: July 01, 2011 **Revised: February 02, 2012** **Accepted: May 23, 2012**

PMID: 22664075

ANNEX III: PATENT

Patent title**: Amphoteric polyamidoamines in the treatment of malaria**

Abstract: The present invention relates to the use of amphoteric polyamidoamines with MW of 10-100 kDa as antimalarial agents or carriers of antimalarial drugs and to formulations thereof.

Authors: Fabio Fenili, Paolo Ferruti, Amedea Manfredi, Nicolò Mauro, Elisabetta Ranucci, Patricia Urbán, Xavier Fernàndez-Busquets.

Application number: EP12192633.1

Date of filing: 14/11/ 2012

ANNEX IV: INFORME DEL DIRECTOR

Durant el seu doctorat sota la nostra direcció, la Sra. Patricia Urbán López ha contribuït en l'elaboració de quatre manuscrits publicats (un d'ells una revisió), un que serà enviat en les properes setmanes, i un altre en fase de redacció. La Patricia és la primera autora en cinc d'aquests articles, la qual cosa demostra la seva gran capacitat per a produir treball científic d'alta qualitat. A continuació resumirem la contribució de la Patricia en els manuscrits, que es presenten de forma cronològica.

1.

P. Urbán et al. J Control Release. 2011 Apr 30; 151(2):202-11. (IF 2011:6.499)

A nanovector with complete discrimination for targeted delivery to Plasmodium falciparum-infected versus non-infected red blood cells in vitro.

Patricia Urbán, Joan Estelrich, Alfred Cortés, and Xavier Fernàndez-Busquets.

Aquest treball tenia com a objectiu posar els fonaments per al disseny i construcció d'un primer prototip de nanovector que fos capaç d'encapsular fàrmacs antimalàrics i de dur-los amb total especificitat a eritròcits infectats pel paràsit de la malària, *Plasmodium falciparum*.

La Patricia va dur a terme la totalitat del treball experimental del manuscrit i va contribuir en la seva elaboració.

2.

P. Urbán et al. Nanoscale Res Lett. 2011; 6:620. doi: 10.1186/1556-276X-6-620. (IF 2011:2.726)

Study of the efficacy of antimalarial drugs delivered inside targeted immunoliposomal nanovectors.

Patricia Urbán, Joan Estelrich, Alberto Adeva, Alfred Cortés, and Xavier Fernàndez-Busquets.

L'objectiu d'aquest segon treball era, basant-se en els fonaments del primer, anar una passa més enllà i demostrar que el prototip d'immunoliposoma desenvolupat era capaç de millorar l'activitat antimalàrica de fàrmacs habitualment usats pel tractament de la malaltia, objectiu aquest que va ser assolit amb èxit.
La Patricia va dur a terme la totalitat del treball experimental del manuscrit i va contribuir en la seva elaboració.

3.

JJ. Valle-Delgado et al. Nanoscale 2012. In press. (IF 2011:5.914)
Demonstration of specific binding of heparin to Plasmodium falciparum-infected vs non-infected red blood cells by single-molecule force spectroscopy.
Juan José Valle-Delgado, Patricia Urbán, and Xavier Fernàndez-Busquets.

L'objectiu d'aquest tercer treball era explorar la capacitat de l'heparina pel reconeixement específic d'eritròcits infectats per *Plasmodium falciparum*, com a pas previ a la possible utilització de l'heparina com nou agent direccionador.
La Patricia va realitzar els experiments corresponents a les Figures 1, 2 i 4 i a les Figures Suplementàries. També va contribuir en l'elaboració del manuscrit.

4.

P. Urbán et al. Nature Nanotechnology. Preparing for submission
Nanomedicine against malaria: use of poly(amidoamine)s for the targeted drug delivery to Plasmodium.
Patricia Urbán, Fabio Fenili, Juan José Valle-Delgado, Elisabetta Ranucci, Paolo Ferruti, and Xavier Fernàndez-Busquets

L'objectiu d'aquest quart treball era avançar en l'evolució del model de nanovector per a l'alliberament dirigit de fàrmacs antimalàrics. Per a millorar les prestacions del model liposomal es va triar començar a assajar amb un tipus

radicalment nou de nanocàpsules de tipus polimèric. En aquest treball es van fer treballs de direccionament específic i d'activitat antimalàrica in vitro i es va arribar a fer assaigs in vivo amb models murins de malària.
La Patricia ha dut a terme la totalitat del treball experimental del manuscrit excepte l'encapsulament de fàrmacs antimalàrics dins dels polímers, i ha contribuit en la seva elaboració.
Aquest treball ha donat lloc a una sol·licitud de patent en la propietat intel·lectual de la qual figura la Patricia.

5.
P. Urbán et al. Curr Drug Targets. 2012 Aug;13(9):1158-72. (IF 2011: 3.553)
Nanotools for the delivery of antimicrobial peptides.
Patricia Urbán, Juan José Valle-Delgado, Ernest Moles, Joana Marques, Cinta Díez, and Xavier Fernàndez-Busquets.

La Patricia va participar en la redacció d'aquest treball de revisió.

Barcelona, a 18 de desembre de 2012.

Dr. Xavier Fernàndez-Busquets	Dr. Joan Estelrich Latràs
Director	Co-director

REFERENCES

1. WHO *World Malaria Report 2011*. http://www.who.int/malaria/world_malaria_report_20 (2011).

2. Gething, P. W. *et al.* A new world malaria map: Plasmodium falciparum endemicity in 2010. *Malaria Journal* **10**, 378 (2011).

3. Baird, J. K. Chloroquine Resistance in Plasmodium vivax. *Antimicrobial Agents and Chemotherapy* **48**, 4075–4083 (2004).

4. Price, R. N., Douglas, N. M. & Anstey, N. M. New developments in Plasmodium vivax malaria: severe disease and the rise of chloroquine resistance. *Current Opinion in Infectious Diseases* **22**, 430–5 (2009).

5. Rodrigues, T., Prudêncio, M., Moreira, R., Mota, M. M. & Lopes, F. Targeting the liver stage of malaria parasites: a yet unmet goal. *Journal of Drug Targeting* **55**, 995–1012 (2012).

6. Bannister, L. H., Hopkins, J. M., Fowler, R. E., Krishna, S. & Mitchell, G. H. A brief illustrated guide to the ultrastructure of Plasmodium falciparum asexual blood stages. *Parasitology Today* **16**, 427–33 (2000).

7. Sherman, I. W. *Malaria. Parasite Biology, Pathogenesis and Protection*. (American Society for Microbiology: 1998).

8. Goldberg, D. E. & Cowman, A. F. Moving in and renovating: exporting proteins from Plasmodium into host erythrocytes. *Nature reviews. Microbiology* **8**, 617–21 (2010).

9. Chen, Q., Schlichtherle, M. & Wahlgren, M. Molecular Aspects of Severe Malaria Molecular Aspects of Severe Malaria. *Clinical Microbiology Reviews* **13**, 439–450 (2000).

10. Griffith, K. S., Lewis, L. S., Mali, S. & Parise, M. E. Treatment of Malaria in the United States. A Systematic Review. *Journal of American Medical Association* **297**, 2264–2277 (2007).

11. Prudêncio, M., Rodriguez, A. & Mota, M. M. The silent path to thousands of merozoites: the Plasmodium liver stage. *Nature reviews. Microbiology* **4**, 849–56 (2006).

12. Mackinnon, M. J. & Marsh, K. The selection landscape of malaria parasites. *Science* **328**, 866–71 (2010).

13. Callaway, E. Malaria research should go to “basics”. *Nature* **449**, 266 (2007).

14. Portugal, S., Drakesmith, H. & Mota, M. M. Superinfection in malaria: Plasmodium shows its iron will. *EMBO Reports* **12**, 1233–42 (2011).

15. Cowman, A. F. & Crabb, B. S. Invasion of red blood cells by malaria parasites. *Cell* **124**, 755–66 (2006).

16. Zuccala, E. S. & Baum, J. Cytoskeletal and membrane remodelling during malaria parasite invasion of the human erythrocyte. *British Journal of Haematology* **154**, 680–689 (2011).

17. Hanssen, E., McMillan, P. J. & Tilley, L. Cellular architecture of Plasmodium falciparum-infected erythrocytes. *International Journal for Parasitology* **40**, 1127–35 (2010).

18. Rowe, a, Obeiro, J., Newbold, C. I. & Marsh, K. Plasmodium falciparum rosetting is associated with malaria severity in Kenya. *Infection and Immunity* **63**, 2323–6 (1995).

19. Juillerat, A. *et al.* Structure of a Plasmodium falciparum PfEMP1 rosetting domain reveals a role for the N-terminal segment in heparin-mediated rosette inhibition. *Proceedings of the National Academy of Sciences of the United States of America* **108**, 5243–8 (2011).

20. Scherf, a *et al.* Antigenic variation in malaria: in situ switching, relaxed and mutually exclusive transcription of var genes during intra-erythrocytic development in Plasmodium falciparum. *The EMBO Journal* **17**, 5418–26 (1998).

21. Voss, T. S. *et al.* A var gene promoter controls allelic exclusion of virulence genes in Plasmodium falciparum malaria. *Nature* **439**, 1004–8 (2006).

22. Recker, M., Arinaminpathy, N. & Buckee, C. O. The effects of a partitioned var gene repertoire of Plasmodium falciparum on antigenic diversity and the acquisition of clinical immunity. *Malaria Journal* **7**, 18 (2008).

23. Flick, K. & Chen, Q. var genes, PfEMP1 and the human host. *Molecular and Biochemical Parasitology* **134**, 3–9 (2004).

24. Valle-delgado, J. J., Urbán, P. & Fernàndez-Busquets, X. Demonstration of specific binding of heparin to Plasmodium falciparum-infected vs non-infected red blood cells by single-molecule force spectroscopy. *Nanoscale* **In press**, (2012).

25. Roll Back Malaria website. at <http://www.rbm.who.int/>

26. Breman, J. G. & Brandling-Bennett, a D. The challenge of malaria eradication in the twenty-first century: Research linked to operations is the key. *Vaccine* **29**, D97–D103 (2012).

27. Feachem, R. G. a, Phillips, A. a, Targett, G. a & Snow, R. W. Call to action: priorities for malaria elimination. *Lancet* **376**, 1517–21 (2010).

28. Hay, S. I., Guerra, C. a, Tatem, A. J., Noor, A. M. & Snow The global distribution and population at risk of malaria: past, present, and future. *Lancet Infectious Diseases* **4**, 327–336 (2004).

29. Nájera, J. a, González-Silva, M. & Alonso, P. L. Some lessons for the future from the Global Malaria Eradication Programme (1955-1969). *PLoS Medicine* **8**, e1000412 (2011).

30. Mills, A., Lubell, Y. & Hanson, K. Malaria eradication: the economic, financial and institutional challenge. *Malaria Journal* **7 Suppl 1**, S11 (2008).

31. Alonso, P. L. Malaria: deploying a candidate vaccine (RTS,S/AS02A) for an old scourge of humankind. *International Microbiology* **9**, 83–93 (2006).

32. Daily, J. P. Antimalarial drug therapy: the role of parasite biology and drug resistance. *Journal of Clinical Pharmacology* **46**, 1487–97 (2006).

33. Karunamoorthi, K. Vector control : a cornerstone in the malaria elimination campaign History of Malaria Control : Past Experience. *Clinical Microbiology and Infection* **17**, 1608–1616 (2011).

34. The malERA Consultative Group on Vector Control A research agenda for malaria eradication: vector control. *PLoS Medicine* **8**, e1000401 (2011).

35. WHO *Resistance of vectors and reservoirs of disease to pesticides. Tenth report of the WHO Expert Committee on Vector Biology and Control, Geneva. WHO Technical Report Series, No: 737.* (1986).

36. Yadouleton, A. W. *et al.* Insecticide resistance status in Anopheles gambiae in southern Benin. *Malaria Journal* **9**, 83 (2010).

37. Tham, W.-H., Healer, J. & Cowman, A. F. Erythrocyte and reticulocyte binding-like proteins of Plasmodium falciparum. *Trends in Parasitology* **28**, 23–30 (2012).

38. Hoffman, S. L. *et al.* Protection of humans against malaria by immunization with radiation-attenuated Plasmodium falciparum sporozoites. *The Journal of Infectious Diseases* **185**, 1155–64 (2002).

39. Baird, J. K. Host age as a determinant of naturally acquired immunity to Plasmodium falciparum. *Parasitology Today* **11**, 105–11 (1995).

40. Hviid, L. Naturally acquired immunity to Plasmodium falciparum malaria in Africa. *Acta Tropica* **95**, 270–5 (2005).

41. Matuschewski, K. & Mueller, A.-K. Vaccines against malaria - an update. *The FEBS Journal* **274**, 4680–7 (2007).

42. Nosten, F. *et al.* Randomised double-blind placebo-controlled trial of SPf66 malaria vaccine in children in northwestern Thailand. *Lancet* **348**, 701–707 (1996).

43. Valero, M. V *et al.* Evaluation of SPf66 malaria vaccine during a 22-month follow-up field trial in the Pacific coast of Colombia. *Vaccine* **14**, 1466–70 (1996).

44. Graves, P., Gelband, H. & Garner, P. The SPf66 Malaria Vaccine: What is the Evidence for Efficacy? *Parasitology Today* **14**, 218–20 (1998).

45. Acosta, C. J. *et al.* Evaluation of the SPf66 vaccine for malaria control when delivered through the EPI scheme in Tanzania. *Tropical Medicine & International Health* **4**, 368–76 (1999).

46. Bermúdez, A. *et al.* Synthetic vaccine update: applying lessons learned from recent SPf66 malarial vaccine physicochemical, structural and immunological characterization. *Vaccine* **25**, 4487–501 (2007).

47. Graves, P. & Gelband, H. Vaccines for preventing malaria (Review). *Cochrane. Database. Syst. Rev.CD000129* (2006).

48. Alonso, P. L. *et al.* Efficacy of the RTS,S/AS02A vaccine against Plasmodium falciparum infection and disease in young African children: randomised controlled trial. *Lancet* **364**, 1411–20 (2004).

49. Vaccines, T. malERA C. G. on A research agenda for malaria eradication: vaccines. *PLoS Medicine* **8**, e1000398 (2011).

50. WHO Guidelines for the treatment of malaria. *2nd edition* (2010).

51. Salako, L. a Toxicity and side-effects of antimalarials in Africa: a critical review. *Bulletin of the World Health Organization* **62 Suppl**, 63–8 (1984).

52. Davis, T. M., Syed, D. a, Ilett, K. F. & Barrett, P. H. R. Toxicity Related to Chloroquine Treatment of Resistant Vivax Malaria. *The Annals of Pharmacotherapy* **37**, 526–529 (2003).

53. Vangapandu, S. *et al.* Recent advances in antimalarial drug development. *Medicinal Research Reviews* **27**, 65–107 (2007).

54. J.K. Baird Effectiveness of antimalarial drugs. *The New England Journal of Medicine* **353**, 420–2; author reply 420–2 (2005).

55. Rosenthal, P. J. Artesunate for the treatment of severe falciparum malaria. *The New England Journal of Medicine* **358**, 1829–36 (2008).

56. Murambiwa, P., Masola, B., Govender, T., Mukaratirwa, S. & Musabayane, C. T. Anti-malarial drug formulations and novel delivery systems: a review. *Acta Tropica* **118**, 71–9 (2011).

57. Fitch, C. D. Ferriprotoporphyrin IX, phospholipids, and the antimalarial actions of quinoline drugs. *Life Sciences* **74**, 1957–72 (2004).

58. Musabayane, C. T., Windle, R. J., Forsling, M. L. & Balment, R. J. Arginine vasopressin mediates the chloroquine induced increase in renal sodium excretion. *Tropical Medicine & International Health* **1**, 542–50 (1996).

59. Fragasso, G. *et al.* Cardiotoxicity after low-dose chloroquine antimalarial therapy. *Heart and Vessels* **24**, 385–7 (2009).

60. Roos, J. M., Aubry, M.-C. & Edwards, W. D. Chloroquine cardiotoxicity: clinicopathologic features in three patients and comparison with three patients with Fabry disease. *Cardiovascular Pathology* **11**, 277–83 (2002).

61. Silman, A. & Shipley, M. Ophthalmological monitoring for hydroxychloroquine toxicity: a scientific review of available data. *British Journal of Rheumatology* **36**, 599–601 (1996).

62. Bray, P. G., Mungthin, M., Ridley, R. G. & Ward, S. a Access to hematin: the basis of chloroquine resistance. *Molecular Pharmacology* **54**, 170–9 (1998).

63. Bray, P. G. *et al.* Cellular uptake of chloroquine is dependent on binding to ferriprotoporphyrin IX and is independent of NHE activity in Plasmodium falciparum. *The Journal of Cell Biology* **145**, 363–76 (1999).

64. Hempelmann, E. Hemozoin biocrystallization in Plasmodium falciparum and the antimalarial activity of crystallization inhibitors. *Parasitology Research* **100**, 671–6 (2007).

65. Wernsdorfer, W. H. & Kouznetsov, R. L. Drug-resistant malaria--occurrence, control, and surveillance. *Bulletin of the World Health Organization* **58**, 341–52 (1980).

66. Biagini, G. a., O'Neill, P. M., Nzila, A., Ward, S. a. & Bray, P. G. Antimalarial chemotherapy: young guns or back to the future? *Trends in Parasitology* **19**, 479–487 (2003).

67. Wells, T. N. C., Burrows, J. N. & Baird, J. K. Targeting the hypnozoite reservoir of Plasmodium vivax: the hidden obstacle to malaria elimination. *Trends in Parasitology* **26**, 145–51 (2010).

68. Davidson, D. E. *et al.* New tissue schizontocidal antimalarial drugs. *Bulletin of the World Health Organization* **59**, 463–79 (1981).

69. Burgoine, K. L., Bancone, G. & Nosten, F. The reality of using primaquine. *Malaria Journal* **9**, 376 (2010).

70. Beutler, E. & Duparc, S. Glucose-6-phosphate dehydrogenase deficiency and antimalarial drug development. *The American Journal of Tropical Medicine and Hygiene* **77**, 779–89 (2007).

71. Chan, T. K., Todd, D. & Tso, S. C. Drug-induced haemolysis in glucose-6-phosphate dehydrogenase deficiency. *British Medical Journal* **2**, 1227–1229 (1976).

72. Sagara, I. *et al.* A randomized trial of artesunate-mefloquine versus artemether-lumefantrine for treatment of uncomplicated Plasmodium falciparum malaria in Mali. *The American Journal of Tropical Medicine and Hygiene* **79**, 655–61 (2008).

73. Evans, S. J. & Waller, P. C. Neurological, cardiovascular and metabolic effects of mefloquine in healthy volunteers: a double-blind, placebo-controlled trial. *British ournal of Clinical Pharmacology* **43**, 665 (1997).

74. Tran, T. M., Browning, J. & Dell, M. L. Psychosis with paranoid delusions after a therapeutic dose of mefloquine: a case report. *Malaria Journal* **5**, 74 (2006).

75. Winstanley, P. Mefloquine: the benefits outweigh the risks. *British ournal of Clinical Pharmacology* **42**, 411–3 (1996).

76. Price, R. *et al.* Adverse effects in patients with acute falciparum malaria treated with artemisinin derivatives. *The American Journal of Tropical Medicine and Hygiene* **60**, 547–55 (1999).

77. Alin, M. H., Ashton, M., Kihamia, C. M., Mtey, G. J. & Björkman, a Clinical efficacy and pharmacokinetics of artemisinin monotherapy and in combination with mefloquine in patients with falciparum malaria. *British ournal of Clinical Pharmacology* **41**, 587–92 (1996).

78. Kappe, S. H. I., Vaughan, A. M., Boddey, J. a & Cowman, A. F. That was then but this is now: malaria research in the time of an eradication agenda. *Science* **328**, 862–6 (2010).

79. Eckstein-Ludwig, U. *et al.* Artemisinins target the SERCA of Plasmodium falciparum. *Nature* **424**, 957–61 (2003).

80. Piero, O., K, H. R., Bernard, M. & Yongyuth, Y. Possible modes of action of the artemisin-type compounds. *Trends in Parasitology* **17**, 122–126 (2001).

81. Haynes, R. K. *et al.* A partial convergence in action of methylene blue and artemisinins: antagonism with chloroquine, a reversal with verapamil, and an insight into the antimalarial activity of chloroquine. *ChemMedChem* **6**, 1603–15 (2011).

82. Nosten, F. & White, N. J. Artemisinin-based combination treatment of falciparum malaria. *The American Journal of Tropical Medicine and Hygiene* **77**, 181–92 (2007).

83. Egan, T. J. & Kaschula, C. H. Strategies to reverse drug resistance in malaria. *Current Opinion in Infectious Diseases* **20**, 598–604 (2007).

84. Noedl, H. *et al.* Evidence of artemisinin-resistant malaria in western Cambodia. *The New England Journal of Medicine* **359**, 2619–20 (2008).

85. Bzik, D. J., Li, W. B., Horii, T. & Inselburg, J. Molecular cloning and sequence analysis of the Plasmodium falciparum dihydrofolate reductase-thymidylate

synthase gene. *Proceedings of the National Academy of Sciences of the United States of America* **84**, 8360–4 (1987).

86. Lu, F. *et al.* Mutations in the antifolate-resistance-associated genes dihydrofolate reductase and dihydropteroate synthase in Plasmodium vivax isolates from malaria-endemic countries. *The American Journal of Tropical Medicine and Hygiene* **83**, 474–9 (2010).

87. Cunha-Rodrigues, M., Prudêncio, M., Mota, M. M. & Haas, W. Antimalarial drugs - host targets (re)visited. *Biotechnology Journal* **1**, 321–32 (2006).

88. Milhous, W. K., Weatherly, N. F., Bowdre, J. H. & Desjardins, R. E. In Vitro Activities of and Mechanisms of Resistance to Antifol Antimalarial Drugs. *Antimicrobial Agents and Chemotherapy* **27**, 525–530 (1985).

89. Zhang, Y. U. N. & Meshnick, S. R. Inhibition of Plasmodium falciparum Dihydropteroate Synthetase and Growth In Vitro by Sulfa Drugs. *Antimicrobial Agents and Chemotherapy* **35**, 267–271 (1991).

90. Björkman, a & Phillips-Howard, P. a Adverse reactions to sulfa drugs: implications for malaria chemotherapy. *Bulletin of the World Health Organization* **69**, 297–304 (1991).

91. Looareesuwan, S. *et al.* Efficacy and safety of atovaquone/proguanil compared with mefloquine for treatment of acute Plasmodium falciparum malaria in Thailand. *The American Journal of Tropical Medicine and Hygiene* **60**, 526–32 (1999).

92. Baggish, A. L. & Hill, D. R. Antiparasitic Agent Atovaquone. *Antimicrobial Agents and Chemotherapy* **46**, 1163–1173 (2002).

93. Watt, G. *et al.* Quinine with tetracycline for the treatment of drug-resistant falciparum malaria in Thailand. *The American Journal of Tropical Medicine and Hygiene* **47**, 108–11 (1992).

94. Tan, K. R., Magill, A. J., Parise, M. E. & Arguin, P. M. Doxycycline for malaria chemoprophylaxis and treatment: report from the CDC expert meeting on malaria chemoprophylaxis. *The American Journal of Tropical Medicine and Hygiene* **84**, 517–31 (2011).

95. Pradines, B. *et al.* Antibiotics for prophylaxis of Plasmodium falciparum infections: in vitro activity of doxycycline against Senegalese isolates. *The American Journal of Tropical Medicine and Hygiene* **62**, 82–5 (2000).

96. Taylor, W. R. *et al.* Chloroquine/doxycycline combination versus chloroquine alone, and doxycycline alone for the treatment of Plasmodium falciparum and Plasmodium vivax malaria in northeastern Irian Jaya, Indonesia. *The American Journal of Tropical Medicine and Hygiene* **64**, 223–8 (2001).

97. Lell, B. & Kremsner, P. G. Clindamycin as an Antimalarial Drug : Review of Clinical Trials. *Antimicrobial Agents and Chemotherapy* **46**, 2315–2320 (2002).

98. Wiesner, J., Borrmann, S. & Jomaa, H. Fosmidomycin for the treatment of malaria. *Parasitology Research* **90 Suppl 2**, S71–6 (2003).

99. Borrmann, S. *et al.* Fosmidomycin plus clindamycin for treatment of pediatric patients aged 1 to 14 years with Plasmodium falciparum malaria. *Antimicrobial Agents and Chemotherapy* **50**, 2713–8 (2006).

100. Price, R. N. & Nosten, F. Drug resistance malaria:clinical consequences and strategies for prevention. *Drug Resistance Updates* **4**, 187–196 (2001).

101. Petersen, I., Eastman, R. & Lanzer, M. Drug-resistant malaria: molecular mechanisms and implications for public health. *FEBS Letters* **585**, 1551–62 (2011).

102. Hastings, I. M., Paget-McNicol, S. & Saul, A. Can mutation and selection explain virulence in human P. falciparum infections? *Malaria Journal* **3**, (2004).

103. White, N. J. Antimalarial drug resistance. *Journal of Clinical Investigation* **113**, 1084–1092 (2004).

104. Dondorp, A. M. *et al.* Artemisinin Resistance in. *The New England Journal of Medicine* **361**, 455–467 (2009).

105. Enserink, M. Malaria's Drug Miracle in Danger. *Science* **328**, 844–6 (2010).

106. Bonnet, M. *et al.* Varying efficacy of artesunate+amodiaquine and artesunate+sulphadoxine-pyrimethamine for the treatment of uncomplicated falciparum malaria in the Democratic Republic of Congo: a report of two in-vivo studies. *Malaria Journal* **8**, 192 (2009).

107. Andriantsoanirina, V. *et al.* Plasmodium falciparum drug resistance in Madagascar: facing the spread of unusual pfdhfr and pfmdr-1 haplotypes and the decrease of dihydroartemisinin susceptibility. *Antimicrobial Agents and Chemotherapy* **53**, 4588–97 (2009).

108. Sachs, J. & Malaney, P. The economic and social burden of malaria. *Nature* **415**, 680–5 (2002).

109. Fidock, D. a, Rosenthal, P. J., Croft, S. L., Brun, R. & Nwaka, S. Antimalarial drug discovery: efficacy models for compound screening. *Nature Reviews. Drug discovery* **3**, 1–9 (2004).

110. Wilson, M., Kannangara, K., Smith, G., Simmons, M. & Raguse, B. *Nanotechnology: Basic Science and Emerging Technologies. Taylor & Francis*. (2002).

111. Ramsden, J. *Nanotechnology: An Introduction. Elsevier*. (2011).

112. Vollath, D. *Nanomaterials. An introduction to synthesis, properties and applications. Willey-VCH*. (2008).

113. Service, R. F. Nanotechnology Grows Up. *Science* **304**, 1732–4 (2004).

114. Maynard, A. D., Warheit, D. B. & Philbert, M. a The new toxicology of sophisticated materials: nanotoxicology and beyond. *Toxicological Sciences* **120 Suppl**, S109–29 (2011).

115. European Science Fundation *Nanomedicine. An ESF-European Medical Research Council Forward Look Report*. **33**, (2005).

116. Langer, R. & Vacanti, J. P. Tissue engineering. *Science* **260**, 920–6 (1993).

117. Orive, G., Hernández, R. M., Gascón, A. R., Domínguez-Gil, A. & Pedraz, J. L. Drug delivery in biotechnology: present and future. *Current Opinion in Biotechnology* **14**, 659–664 (2003).

118. Beija, M., Salvayre, R., Lauth-de Viguerie, N. & Marty, J.-D. Colloidal systems for drug delivery: from design to therapy. *Trends in Biotechnology* **30**, 485–496 (2012).

119. Carino, G. & Mathiowitz, E. Oral insulin delivery. *Advanced Drug Delivery Reviews* **35**, 249–257 (1999).

120. Wong, T. W. Design of oral insulin delivery systems. *Journal of Drug Targeting* **18**, 79–92 (2010).

121. Katz, E. & Willner, I. Integrated nanoparticle-biomolecule hybrid systems: synthesis, properties, and applications. *Angewandte Chemie* **43**, 6042–108 (2004).

122. Panyam, J. & Labhasetwar, V. Biodegradable nanoparticles for drug and gene delivery to cells and tissue. *Advanced Drug Delivery Reviews* **55**, 329–347 (2003).

123. Hauck, T. S., Giri, S., Gao, Y. & Chan, W. C. W. Nanotechnology diagnostics for infectious diseases prevalent in developing countries. *Advanced Drug Delivery Reviews* **62**, 438–48 (2010).

124. Sultana, S., Khan, M. R., Kumar, M., Kumar, S. & Ali, M. Nanoparticles-mediated drug delivery approaches for cancer targeting: a review. *Journal of Drug Targeting* 1–19 (2012).doi:10.3109/1061186X.2012.712130

125. Lipid, N. P. *et al.* The targeted delivery of multicomponent cargos to cancer cells by nanoporous particle-supported lipid bilayers. *Nature Materials* **10**, 389–397 (2011).

126. Ghosh, P. *et al.* Intracellular Delivery of a Membrane-Impermeable Enzyme in Active Form using Functionalized Gold Nanoparticles. *Journal of American Chemical Society* **132**, 2642–2645 (2010).

127. Schaeublin, N. *et al.* Surface charge of gold nanoparticles mediates mechanism of toxicity. *Nanoscale* **3**, 410–420 (2011).

128. Torchilin, V. P. Multifunctional nanocarriers. *Advanced Drug Delivery Reviews* **58**, 1532–55 (2006).

129. Svenson, S. & Prud'homme, R. K. *Multifunctional Nanoparticles for Drug Delivery Applications: Imaging, Targeting and Delivery*. 9–29 (Springer US: 2012).doi:10.1007/978-1-4614-2305-8

130. Storm, G., Wilms, H. P. & Crommelin, D. J. Liposomes and biotherapeutics. *Biotherapy* **3**, 25–42 (1991).

131. Storm, G. & Crommelin, D. J. . Liposomes: quo vadis? *Pharmaceutical Science & Technology Today* **1**, 19–31 (1998).

132. Willis, M. & Forssen, E. Ligand-targeted liposomes. *Advanced Drug Delivery Reviews* **29**, 249–271 (1998).

133. Kajiwara, E. *et al.* Long-circulating liposome-encapsulated ganciclovir enhances the efficacy of HSV-TK suicide gene therapy. *Journal of controlled release* **120**, 104–10 (2007).

134. Blume, G. & Cevc, G. Liposomes for the sustained drug release in vivo. *Biochimica et Biophysica Acta* **1029**, 91–7. (1991).

135. Sharma, A. & Sharma, U. S. international journal of pharmaceutics. *International Journal of Pharmaceutics* **154**, 123–140 (1997).

136. Crommelin, D. J. a & Storm, G. Liposomes: from the bench to the bed. *Journal of Liposome Research* **13**, 33–6 (2003).

137. Al-Jamal, W. T. & Kostarelos, K. Construction of nanoscale multicompartment liposomes for combinatory drug delivery. *International Journal of Pharmaceutics* **331**, 182–5 (2007).

138. Chang, H.-I. & Yeh, M.-K. Clinical development of liposome-based drugs: formulation, characterization, and therapeutic efficacy. *International Journal of Nanomedicine* **7**, 49–60 (2012).

139. Kreuter, J. Nanoparticulate systems for brain delivery of drugs. *Advanced Drug Delivery Reviews* **47**, 65–81 (2001).

140. Soppimath, K. S., Aminabhavi, T. M., Kulkarni, a R. & Rudzinski, W. E. Biodegradable polymeric nanoparticles as drug delivery devices. *Journal of Controlled Release* **70**, 1–20 (2001).

141. Agnihotri, S. a, Mallikarjuna, N. N. & Aminabhavi, T. M. Recent advances on chitosan-based micro- and nanoparticles in drug delivery. *Journal of Controlled Release* **100**, 5–28 (2004).

142. Manfredi, a., Ranucci, E., Suardi, M. & Ferruti, P. Polymerization Kinetics of Poly(amidoamine)s in Different Solvents. *Journal of Bioactive and Compatible Polymers* **22**, 219–231 (2007).

143. Ranucci, E., Spagnoli, G., Ferruti, P., Sgouras, D. & Duncan, R. Poly(amidoamine)s with potential as drug carriers: degradation and cellular toxicity. *Journal of Biomaterials Science, Polymer Edition* **2**, 303–15 (1991).

144. Ferruti, P. *et al.* Amphoteric Linear Poly(amido-amine)s as Endosomolytic Polymers: Correlation between Physicochemical and Biological Properties. *Macromolecules* **33**, 7793–7800 (2000).

145. Pattrick, N. G., Richardson, S. C., Casolaro, M., Ferruti, P. & Duncan, R. Poly(amidoamine)-mediated intracytoplasmic delivery of ricin A-chain and gelonin. *Journal of Controlled Release* **77**, 225–32 (2001).

146. Richardson, S. C. W., Ferruti, P. & Duncan, R. Poly(amidoamine)s as Potential Endosomolytic Polymers: Evaluation In Vitro and Body Distribution in Normal and Tumor-Bearing Animals. *Journal of Drug Targeting* **6**, 391–404 (1999).

147. Ferruti, P., Marchisio, M. a. & Duncan, R. Poly(amido-amine)s: Biomedical Applications. *Macromolecular Rapid Communications* **23**, 332–355 (2002).

148. Franchini, J., Ranucci, E., Ferruti, P., Rossi, M. & Cavalli, R. Synthesis, physicochemical properties, and preliminary biological characterizations of a novel amphoteric agmatine-based poly(amidoamine) with RGD-like repeating units. *Biomacromolecules* **7**, 1215–22 (2006).

149. Lavignac, N. *et al.* Synthesis and endosomolytic properties of poly(amidoamine) block copolymers. *Macromolecular Bioscience* **4**, 922–9 (2004).

150. Richardson, S. C. W., Pattrick, N. G., Lavignac, N., Ferruti, P. & Duncan, R. Intracellular fate of bioresponsive poly(amidoamine)s in vitro and in vivo. *Journal of Controlled Release* **142**, 78–88 (2010).

151. Marchisio, M. A., Tongo, T. & Ferruti, P. A selective de-heparinizer filter made of new cross-linked polymers of a poly-amido-amine structure. *Experientia* **1**, 93–5 (1973).

152. Donghi, D. *et al.* Tricarbonyl-rhenium complexes of a thiol-functionalized amphoteric poly(amidoamine). *Biomacromolecules* **10**, 3273–82 (2009).

153. Ferruti, P., Danusso, F., Franchi, G., Polentarutti, N. & Garattini, S. Effects of a series of new synthetic high polymers on cancer metastases. *Journal of Drug Targeting* **16**, 496–9 (1973).

154. Ferruti, P. *et al.* Synthesis, characterisation and antitumour activity of platinum(II) complexes of novel functionalised poly(amido amine)s. *Macromolecular Chemistry and Physics* **200**, 1644–1654 (1999).

155. Andersson, L. *et al.* Poly(ethylene glycol)-poly(ester-carbonate) block copolymers carrying PEG-peptidyl-doxorubicin pendant side chains: synthesis and evaluation as anticancer conjugates. *Biomacromolecules* **6**, 914–26 (2005).

156. Lavignac, N., Nicholls, J. L., Ferruti, P. & Duncan, R. Poly(amidoamine) conjugates containing doxorubicin bound via an acid-sensitive linker. *Macromolecular Bioscience* **9**, 480–7 (2009).

157. Cavalli, R. *et al.* Amphoteric agmatine containing polyamidoamines as carriers for plasmid DNA in vitro and in vivo delivery. *Biomacromolecules* **11**, 2667–74 (2010).

158. Duncan, R. The dawning era of polymer therapeutics. *Nature reviews. Drug discovery* **2**, 347–60 (2003).

159. Nanjwade, B. K., Bechra, H. M., Derkar, G. K., Manvi, F. V & Nanjwade, V. K. Dendrimers: emerging polymers for drug-delivery systems. *European Journal of Pharmaceutical Sciences* **38**, 185–96 (2009).

160. Mintzer, M. A. & Grinstaff, M. W. Biomedical applications of dendrimers: a tutorial. *Chemical Society Reviews* **40**, 173–90 (2011).

161. Hirsch, L. R., Halas, N. J. & West, J. L. Whole-Blood Immunoassay Facilitated by Gold Nanoshell–Conjugate Antibodies. *Methods in Molecular Biology* **303**, 101–111 (2005).

162. Polpanich, D., Tangboriboonrat, P., Elaissari, A. & Udomsangpetch, R. Detection of malaria infection via latex agglutination assay. *Analytical chemistry* **79**, 4690–5 (2007).

163. Newman, D. M. *et al.* A magneto-optic route toward the in vivo diagnosis of malaria: preliminary results and preclinical trial data. *Biophysical Journal* **95**, 994–1000 (2008).

164. Rodrigues Ribeiro Teles, F. S., Pires de Távora Tavira, L. A. & Pina da Fonseca, L. J. Biosensors as rapid diagnostic tests for tropical diseases. *Critical Reviews in Clinical Laboratory Sciences* **47**, 139–69 (2010).

165. Bell, D., Wongsrichanalai, C. & Barnwell, J. W. Ensuring quality and access for malaria diagnosis: how can it be achieved? *Nature reviews. Microbiology* **4**, S7–20 (2006).

166. Nanomal Project. at <http://www.nanomal.org>

167. Sisquella, X. *et al.* A single-molecule force spectroscopy nanosensor for the identification of new antibiotics and antimalarials. *The FASEB Journal* **24**, 4203–17 (2010).

168. White, N. J. Assessment of the Pharmacodynamic Properties of Antimalarial Drugs In Vivo. *Antimicrobial Agents and Chemotherapy* **41**, 1413–1422 (1997).

169. Santos-Magalhães, N. S. & Mosqueira, V. C. F. Nanotechnology applied to the treatment of malaria. *Advanced Drug Delivery Reviews* **62**, 560–75 (2010).

170. Shillcock, J. C. & Lipowsky, R. Tension-induced fusion of bilayer membranes and vesicles. *Nature Materials* **4**, 225–8 (2005).

171. Singhal, a & Gupta, C. M. Antibody-mediated targeting of liposomes to red cells in vivo. *FEBS Letters* **201**, 321–6 (1986).

172. Gupta, Y., Jain, A. & Jain, S. K. Transferrin-conjugated solid lipid nanoparticles for enhanced delivery of quinine dihydrochloride to the brain. *The Journal of Pharmacy and Pharmacology* **59**, 935–40 (2007).

173. Owais, M., Varshney, G. C., Choudhury, A., Chandra, S. & Gupta, C. M. Chloroquine encapsulated in malaria-infected-erythrocyte-specific antibody-bearing liposomes effectively controls chloroquine-resistant Plasmodium berhei infections in mice. *Antimicrobial Agents and Chemotherapy* **39**, 180–184 (1995).

174. Dierling, A. M. & Cui, Z. Targeting primaquine into liver using chylomicron emulsions for potential vivax malaria therapy. *International Journal of Pharmaceutics* **303**, 143–52 (2005).

175. Postma, N. S., Hermsen, C. C., Zuidema, J. & Eling, W. M. Plasmodium vinckei: optimization of desferrioxamine B delivery in the treatment of murine malaria. *Experimental Parasitology* **89**, 323–30 (1998).

176. Postma, N. S., Crommelin, D. J., Eling, W. M. & Zuidema, J. Treatment with liposome-bound recombinant human tumor necrosis factor-alpha suppresses parasitemia and protects against Plasmodium berghei k173-induced experimental cerebral malaria in mice. *The Journal of Pharmacology and Experimental Therapeutics* **288**, 114–20 (1999).

177. Aricat, B. & Ozert, A. Characterization, in vitro and in vivo studies on primaquine diphosphate liposomes. *Journal of Microencapsulation* **12**, 469–485 (1995).

178. Green, M. D., D'Souza, M. J., Holbrook, J. M. & Wirtz, R. a In vitro and in vivo evaluation of albumin-encapsulated primaquine diphosphate prepared by nebulization into heated oil. *Journal of Microencapsulation* **21**, 433–44 (2004).

179. Stensrud, G., Sande, S. a, Kristensen, S. & Smistad, G. Formulation and characterisation of primaquine loaded liposomes prepared by a pH gradient using experimental design. *International Journal of Pharmaceutics* **198**, 213–28 (2000).

180. Longmuir, K. J., Robertson, R. T., Haynes, S. M., Baratta, J. L. & Waring, A. J. Effective targeting of liposomes to liver and hepatocytes in vivo by incorporation of a Plasmodium amino acid sequence. *Pharmaceutical Research* **23**, 759–69 (2006).

181. Robertson, R. T., Baratta, J. L., Haynes, S. M. & Longmuir, K. J. Liposomes Incorporating a Plasmodium Amino Acid Sequence Target Heparan Sulfate Binding Sites in Liver. *Journal of Pharmaceutical Sciences* **97**, 3257–3273 (2008).

182. Gabriëls, M. Physical and chemical evaluation of liposomes, containing artesunate. *Journal of Pharmaceutical and Biomedical Analysis* **31**, 655–667 (2003).

183. Chimanuka, B., Gabriëls, M., Detaevernier, M.-R. & Plaizier-Vercammen, J. a Preparation of beta-artemether liposomes, their HPLC-UV evaluation and relevance for clearing recrudescent parasitaemia in Plasmodium chabaudi malaria-infected mice. *Journal of Pharmaceutical and Biomedical Analysis* **28**, 13–22 (2002).

184. M.A.Bayomi, A.A.Al-Angary, M.A.Al-Mehsal & M.M.Al-Dardiri In vivo evaluation of arteether liposomes. *International Journal of Pharmaceutics* **175**, 1–7 (1998).

185. Vogel, G. The “do unto others” malaria vaccine. *Science* **328**, 847–8 (2010).

186. Memvanga, P. B. & Préat, V. Formulation design and in vivo antimalarial evaluation of lipid-based drug delivery systems for oral delivery of β-arteether. *European Journal of Pharmaceutics and Biopharmaceutics* **82**, 112–9 (2012).

187. Singh, K. K. & Vingkar, S. K. Formulation, antimalarial activity and biodistribution of oral lipid nanoemulsion of primaquine. *International Journal of Pharmaceutics* **347**, 136–43 (2008).

188. Shanmugam, S. *et al.* Physicochemical characterization and skin permeation of liposome formulations containing clindamycin phosphate. *Archives of Pharmacal Research* **32**, 1067–75 (2009).

189. Mosqueira, V. C. F. *et al.* Efficacy and Pharmacokinetics of Intravenous Nanocapsule Formulations of Halofantrine in Plasmodium berghei-Infected Mice. *Antimicrobial Agents and Chemotherapy* **48**, 1222–1228 (2004).

190. Bhadra, D., Bhadra, S. & Jain, N. K. Pegylated lysine based copolymeric dendritic micelles for solubilization and delivery of artemether. *Journal of Pharmacy & Pharmaceutical Sciences* **8**, 467–82 (2005).

191. Agrawal, P., Gupta, U. & Jain, N. K. Glycoconjugated peptide dendrimers-based nanoparticulate system for the delivery of chloroquine phosphate. *Biomaterials* **28**, 3349–59 (2007).

192. Föger, F. *et al.* Inhibition of malarial topoisomerase II in Plasmodium falciparum by antisense nanoparticles. *International Journal of Pharmaceutics* **319**, 139–46 (2006).

193. Goodyer, I. D., Pouvelle, B., Schneider, T. G., Trelka, D. P. & Taraschi, T. F. Characterization of macromolecular transport pathways in malaria-infected erythrocytes. *Molecular and Biochemical Parasitology* **87**, 13–28 (1997).

194. Akhtar, F., Rizvi, M. M. A. & Kar, S. K. Oral delivery of curcumin bound to chitosan nanoparticles cured Plasmodium yoelii infected mice. *Biotechnology Advances* **30**, 310–20 (2012).

195. Bhadra, D., Bhadra, S. & Jain, N. K. PEGylated peptide dendrimeric carriers for the delivery of antimalarial drug chloroquine phosphate. *Pharmaceutical Research* **23**, 623–33 (2006).

196. B.Saparia, A.Solanki & Murthy, R. S. R. Sustained release implants of chloroquine phosphate for possible use in chemoprophylaxis of malaria. *Indian Journal of Experimental Biology* **39**, 902–5 (2001).

197. Urbán, P., Estelrich, J., Adeva, A., Cortés, A. & Fernàndez-Busquets, X. Study of the efficacy of antimalarial drugs delivered inside targeted immunoliposomal nanovectors. *Nanoscale Research Letters* **6**, 620 (2011).

198. Angulo- Barturen, I. *et al.* A Murine Model of falciparum-Malaria by In Vivo Selection of Competent Strains in Non-Myelodepleted Mice Engrafted with Human Erythrocytes. *PloS One* **3**, e2252 (2008).

199. Urbán, P., Estelrich, J., Cortés, A. & Fernàndez-Busquets, X. A nanovector with complete discrimination for targeted delivery to Plasmodium falciparum-infected versus non-infected red blood cells in vitro. *Journal of Controlled Release* **151**, 202–11 (2011).

200. Lee, E. S. *et al.* Binary mixing of micelles using Pluronics for a nano-sized drug delivery system. *Colloids and surfaces. B:Biointerfaces* **82**, 190–5 (2011).

201. Pembouong, G. *et al.* A comprehensive study in triblock copolymer membrane interaction. *Journal of Controlled Release* **151**, 57–64 (2011).

202. Champion, J. A., Katare, Y. K. & Mitragotri, S. Particle shape: a new design parameter for micro- and nanoscale drug delivery carriers. *Journal of Controlled Release* **121**, 3–9 (2007).

203. Gratton, S. E. A. *et al.* The effect of particle design on cellular internalization pathways. *Proceedings of the National Academy of Sciences of the United States of America* **105**, 11613–8 (2008).

204. Winograd, E. & Sherman, I. W. Malaria infection induces a conformational change in erythrocyte band 3 protein. *Molecular and Biochemical Parasitology* **138**, 83–7 (2004).

205. Pouvelle, B. *et al.* Direct access to serum macromolecules by intraerythrocytic malaria parasites. *Nature* 73–75 (1991).

206. Lyon, J. A., Carter, J. M., Thomas, A. W. & Chulay, J. D. Merozoite surface protein-1 epitopes recognized by antibodies that inhibit Plasmodium falciparum merozoite dispersal. *Molecular and Biochemical Parasitology* **90**, 223–234 (1997).

207. Bergmann-Leitner, E. S., Duncan, E. H. & Angov, E. MSP-1p42-specific antibodies affect growth and development of intra-erythrocytic parasites of Plasmodium falciparum. *Malaria Journal* **8**, 183 (2009).

208. Rakestraw, S. L., R.G., T. & Yarmush, M. . Antibody-targeted photolysis: In vitro studies with Sn(IV) chlorin e6 covalently bound to monoclonal antibodies using a modified dextran carrier. *Proceedings of the National Academy of Sciences of the United States of America* **87**, 4217–4221 (1990).

209. Vogel, C.-W. Preparation of immunoconjugates using antibody oligosaccharide moieties. *Methods in Molecular Biology. Humana Press Inc* 87–108 (2004).

210. Becker, K. & Kirk, K. Of malaria, metabolism and membrane transport. *Trends in Parasitology* **20**, 590–6 (2004).

211. Martin, R. E. *et al.* Chloroquine transport via the malaria parasite's chloroquine resistance transporter. *Science* **325**, 1680–2 (2009).

212. Qiu, L., Jing, N. & Jin, Y. Preparation and in vitro evaluation of liposomal chloroquine diphosphate loaded by a transmembrane pH-gradient method. *International Journal of Pharmaceutics* **361**, 56–63 (2008).

213. Leite, E. A. *et al.* Cardiotoxicity reduction induced by halofantrine entrapped in nanocapsule devices. *Life Sciences* **80**, 1327–34 (2007).

214. David, P. H., Hommel, M., Miller, L. H., Udeinya, I. J. & Oligino, L. D. Parasite sequestration in Plasmodium falciparum malaria: spleen and antibody modulation of cytoadherence of infected erythrocytes. *Proceedings of the National Academy of Sciences of the United States of America* **80**, 5075–9 (1983).

215. Vogt, A. M. *et al.* Release of sequestered malaria parasites upon injection of a glycosaminoglycan. *PLoS pathogens* **2**, e100 (2006).

216. Paul, S. & Planque, S. Antibody engineering. *Encyclopedia of Life Sciences. John Wiley & Sons, Ltd. Chichester* (2005).

217. Ma, Z. *et al.* Targeting human epidermal growth factor receptor signaling with the neuregulin's heparin-binding domain. *The Journal of Biological Chemistry* **284**, 32108–15 (2009).

218. Famulok, M., Mayer, G. & Blind, M. Nucleic Acid Aptamers From Selection in Vitro to Applications in Vivo. *Accounts of Chemical Research* **33**, 591–599 (2000).

219. Fries, L. F. *et al.* Liposomal malaria vaccine in humans: a safe and potent adjuvant strategy. *Proceedings of the National Academy of Sciences of the United States of America* **89**, 358–62 (1992).

220. Agger, E. M. *et al.* Cationic liposomes formulated with synthetic mycobacterial cordfactor (CAF01): a versatile adjuvant for vaccines with different immunological requirements. *PloS one* **3**, e3116 (2008).

221. K.Agrawal, A. and C. M. G. Antibody-bearing liposomes as chloroquine vehicles in treatment of murine malaria. *Methods in Molecular Medicine* **25**, 227–239 (2000).

222. Bhadra, D., Yadav, a K., Bhadra, S. & Jain, N. K. Glycodendrimeric nanoparticulate carriers of primaquine phosphate for liver targeting. *International Journal of Pharmaceutics* **295**, 221–33 (2005).

ACKNOWLEDGEMENTS

Una etapa importante de mi vida está a punto de finalizar junto con esta tesis, y al echar la vista atrás me vienen en mente muchos momentos y personas que me han ayudado a llegar hasta aquí, sin vuestro apoyo y colaboración esta tesis no hubiera sido posible.

Volia agrair als meus directors de tesi la confiança que han dipositat en mi des del primer dia, deixant-me desenvolupar les meves pròpies idees i contribuint al meu desenvolupament científic i personal. Xavi, gràcies per l'oportunitat de formar part d'aquest projecte i per tenir sempre la porta del teu despatx oberta, no oblidaré les alegries que hem compartit amb cada experiment que sortia bé. Joan, gràcies pels teus consells i per cuidar sempre de la teva guapetona.

Quiero agradecer a Josep Samitier el apoyo que me ha dado como jefe del grupo de Nanobioengineering del IBEC, y a todos los miembros del Nanobiolab (a los que ya no están, y a los que siguen al pie del cañón) los buenos momentos que hemos compartido durante el día a día en el laboratorio. La ventaja de estar en un grupo tan grande y multidisciplinar es la cantidad y diversidad de personas que vamos conociendo, de todas podemos aprender siempre algo, tanto a nivel profesional como personal. Quiero agradecer también la ayuda del personal de los CCITUB y de administración del IBEC.

Alfred, gràcies per transmetre'm la teva passió per la malària, ensenyar-me a cultivar "paràsits contents" i per tots els dubtes que m'has resolt. Noelia, Núria, Val, habéis sido unas compis de cultivos estupendas, cuesta creer que en una sala tan pequeña quepan tantos buenos momentos y confidencias. No puedo olvidarme de las chicas de Kymos, gracias por esas conversaciones de pasillo y las comidas de tupper.

Voldria agrair als membres del Departament de Físicoquímica de Farmàcia la seva disponibilitat sempre que he anat a preparar liposomes, i en especial a la Maria Antònia per totes les xerrades que hem compartit i la seva ajuda y a Sonia por todos esos ratitos, dentro y fuera del labo.

Vorrei ringraziare la Prof. Ranucci dell' Università degli Studi di Milano per la possibilità che mi ha dato di fare uno stage presso il suo laboratorio, e anche il Prof. Ferruti e la dott.ssa Manfredi per il loro prezioso supporto. Grazie all'aiuto di tutti i ragazzi del

laboratorio sono riuscita a non combinare troppi casini! Grazie Ele per essermi sempre vicina.

Quiero agradecer también a Chema Bautista de la Universidad Complutense de Madrid el haberme acogido en su laboratorio con los brazos abiertos, a Amalia el hacer de “mami” y a Antonio su ayuda, ¡formáis un buen equipo! ¿Qué decir de las chicas (y Sergio) del labo? Ale, Isa, María, Patri (super teacher), Susi, no sé qué hubiera hecho sin vosotras. María Momo, Jesús, gracias por todo. Os echo de menos...

Després de Madrid, vaig tornar a BCN, però al CRESIB!. Volia agrair als meus companys de laboratori les estonetes tan divertides (i els moments de “teràpia tésica”) que hem compartit entre experiments, tuppers, picnics i balls. M’ho he passat molt bé aquests mesos!

Mis amigos de la uni también han soportado las alegrías y penas de esta tesis, va pasando el tiempo y cada uno va encontrando su camino, no nos vemos tanto como nos gustaría, pero siempre tendremos los recuerdos de lo que hemos vivido juntos.

A mis amigas de Tarragona, mis Marías, que han sabido sacarme una sonrisa cuando parecía imposible, apoyándome en todo momento. Gracias chicas, sois únicas.

A Lele, senza di te non ce l’avrei fatta. Insieme, sempre, fino alla luna. A Arduina, Stefy, Nadia e Lucio, per il prezioso sostegno e l’aiuto ricevuto. A Leonardo, per essere un angelo caduto dal cielo, e a Ginevra, per essere la mia migliore amica.

A mi familia, por su amor incondicional. A mi padre, por creer tanto en mí que está convencido de que mi granito de arena puede cambiar el mundo. A mi madre, por ser la mujer más extraordinaria que conozco. A mi hermano, porque sé que siempre está ahí. Y a mis primos Marc e Imanol, por su ayuda en esta etapa final de la tesis.

Esta tesis ha podido realizarse gracias a la concesión de una beca PFIS del ISCIII.